THE NOTCH SIGNALLING PATHWAY AND MESENCHYMAL CELL FATES DURING WOOL FOLLICLE INITIATION IN THE SHEEP.

Stephanie P. Xavier

Bachelor of Science in Agriculture (Honours)

Thesis submitted to the University of Sydney

for the degree of Doctor of Philosophy.

Research carried out at the School of Natural Sciences, The University of Western Sydney, Parramatta North Campus and The Faculty of Veterinary Science, The University of Sydney, Camden Campus.

November 2009.

DECLARATION

I declare that the work presented in this thesis represents my original research, except where duly acknowledged, and that none of the material presented here has been previously submitted for a higher degree to this or any other university or institution.

Stephanie P. Xavier

March 2009.

TABLE OF CONTENTS

LIST OF TABLES

LIST OF FIGURES

ABSTRACTS ARISING FROM THE RESEARCH

Xavier S.P., Tomkins L., Gordon-Thomson C., Moore G.P.M. and Wynn P.C. (2007). Notch and Delta are involved in wool follicle development. *The Faculty of Veterinary Science Postgraduate Conference.* The Veterinary Conference Centre, Sydney, November 2007, p 89.

Xavier S.P., Gordon-Thomson C., Tomkins L., Wynn P.C. and Moore G.P.M. Notch signalling and wool follicle initiation. COMBIO 2007, *Proceedings of the Australian Society for Biochemistry and Molecular Biology*, Vol. 39, Sydney, September 2007, p 97.

Xavier S.P., Tomkins L., Gordon-Thomson C., Moore G.P.M. and Wynn P.C. (2007). The Notch signaling pathway is involved in wool follicle development. *The Fifth International Congress of Hair Research.* Vancouver, Canada, June 2007, P-176, p 90.

Xavier S.P., Tomkins L., Gordon-Thomson C., Moore G.P.M. and Wynn P.C. (2006). The Notch signalling pathway in foetal sheep skin development. *The Faculty of Veterinary Science Postgraduate Conference.* Plant Breeding Institute, Cobbitty, p 86.

Xavier S.P., Tomkins L., Gordon-Thomson C., Moore G.P.M. and Wynn P.C. The Notch signalling pathway in foetal sheep skin development. COMBIO 2006, *Proceedings of the Australian Society for Biochemistry and Molecular Biology* Brisbane, Queensland, POS-WED-64, p 180.

Xavier S.P., Tomkins L., Gordon-Thomson C., Moore G.P.M. and Wynn P.C. (2006). Mesenchymal signalling in foetal sheep skin and follicle formation. *AWI Annual Postgraduate Conference.* Perth, WA, p 15.

Xavier S.P., Gordon-Thomson C., Moore G.P.M. and Wynn P.C. (2005). Morphogenesis of dermal papilla in foetal sheep skin. *Faculty of Veterinary Science Postgraduate Conference.* PBI, Cobbitty, p 16.

Xavier S.P., Gordon-Thomson C., Wynn P.C. and Moore G.P.M. (2005). Distribution of dermal papilla cells in foetal sheep skin; effects on wool follicle density and fibre quality. *AWI, Sheep CRC, Beef CRC Combined Conference.* Noosa, QLD, p 8.

Gordon-Thomson C., Xavier S.P., Botto S., Graham H.J., Moore G.P.M. and Wynn P.C. (2005). Wool follicle initiation: Identification of a founder cell population. *Mechanisms of Development*: **122** (supplement 1) 03-P036.

ACKNOWLEDGEMENTS

I wish to thank Professor Peter Wynn and Professor Philip Moore for their guidance, support and supervision for the duration of this project. I thank Professor Chris Moran for his supervision in the final stages of the project. I thank the staff and management of the School of Natural Sciences, The University of Western Sydney for allowing me access to their research facilities for the duration of the project, in conjunction with the Faculty of Veterinary Science, The University of Sydney.

I appreciate the assistance of Dr Clare Gordon-Thomson with probe production, *in situ* hybridisation, Northern hybridisation and immunohistochemistry, and assistance with editing abstracts, conference presentations and for her numerous constructive suggestions during the preparation of this thesis. I am indebted to Lisa Tomkins for her support, persistence with immunohistochemistry, and assistance with basic tissue culture procedures and in setting up and running the *in vitro* trials. I thank Associate Professor Peter Thomson for his guidance and assistance with the statistical procedures. Jim Watts kindly performed the S:P follicle counts and follicle diameter measurements. I wish to thank Elaine Chew and Karen Barnes of the Veterinary Anatomy and Pathology Laboratory, The University of Sydney, for processing, paraffin embedment of samples and their advice on sectioning procedures, as well as producing the tangential sections of adult sheep skin biopsies. I appreciate the assistance of Katrina Stewart, formerly CMRI, Westmead for kindly providing her *in situ* hybridisation protocol for riboprobes and advice for creating probes. Dr Mel McDowall kindly provided me with the protocol for the floating culture system that she had devised for growing embryonic mouse skin.

I appreciate the assistance of Craig Kristo, Sherry Catt and Kaylene Scrimgeour for anaesthetising and intubating the animals on days of surgery and surgeon Dr Peter McCullagh. I would like to thank Dave Palmer, Byron Biffin, Keith Tribe and Luke Chappel for maintaining, monitoring and co-ordinating reproduction of the flocks, and to Dr Jeff Downing for conducting LAI. Fine-woolled Merino ewes and semen were purchased from Charlie Massey and his Severn Park Merino Stud, Cooma, NSW. Tukidales were purchased from Sue Tracey. Merino ewes, provided by Dr Jeff Downing were used for the DAPT skin trials. I am grateful to Dr Nicole Spiegel for monitoring animals used for tissue collection for the DAPT skin trials, and Dr Ian Martin for the care, preparation and supply of pregnant mice for the preliminary studies. Frank Lovicu, Department of Anatomy, Faculty of Medicine, The

University of Sydney, kindly provided a rat from which whiskers were collected for preliminary papilla culture work.

The Delta-1 clone was kindly provided by Associate Professor Barry Powell, Women's & Children's Health Research Institute Incorporated, North Adelaide, SA, Australia. It originated from Achim Gossler, The Jackson Laboratory, Bar Harbor, ME, USA. The Delta-3 clone (SD61) was kindly provided by Associate Professor Sally Dunwoodie, The Victor Chang Cardiac Research Institute, Darlinghurst, NSW, Australia. Murine cDNA for Lunatic Fringe (accession number: NM008494), constructed by Randy Johnson, Department of Biochemistry and Molecular Biology, The University of Texas M.D. Anderson Cancer Centre Houston, Texas, was provided by Dr Gavin Chapman, The Victor Chang Cardiac Research Institute, NSW, Australia. Ovine sequences for Delta-1, Delta-3 and Lunatic Fringe were provided by Alan Pearson and Zhidong Yu, AgResearch Ltd, Hamilton, New Zealand.

This work was supported by a postgraduate scholarship from Australian Wool Innovation. I was the recipient of the Faculty of Veterinary Science Grants-in-Aid Scholarships; Sir Clunies Ross (2005 –2008) and the NHP Graham Scholarship (2006 and 2008). I received a travel award from the Australasian Wool and Hair Research Society (2007) that assisted in allowing me to present my work in Canada. I received an Australian and New Zealand Society for Cell and Developmental Biology student travel award (2006), allowing me to present my research at the Combined Biology Conference.

Finally I thank family and friends, namely Sam Busbridge, Prue Tompson, my parents (Penny and Rui) and my grandmother, Patricia Tompson, who have supported and encouraged me throughout the course of this work.

GLOSSARY OF ABBREVIATIONS

BMP:	Bone morphogenetic protein
BSA:	bovine serum albumin
CBF-1:	C promoter-binding protein 1
cDNA:	complementary DNA
CDS:	coding sequence
Co:	Company
Corp:	Corporation
CDP:	Chlorodiazepoxide hydrochloride
CRR:	Cysteine-rich region
CSL:	CBF-1/Suppressor of Hairless/Lag-1
d:	day
DAB:	3, 3'-Diaminobenzidine
DAPI:	4', 6-Diamidino-2-phenylindole
DAPT:	N-[N-(3,5-Difluorophenacetyl-L-alanyl)]-S-phenylglycine *t*-butyl ester
DEPC:	Diethyl pyrocarbonate
DIG:	Digoxygenin
DMEM:	Dulbecco's modified Eagle's medium
DMSO:	Dimethyl sulphoxide
DP:	dermal papilla
D-PBS:	Dulbecco's phosphate buffered saline
dpc:	days post coitus
DSL:	Delta/Serrate/Lag-2
DTT:	Dithiothreitol
EDTA.2H_20:	Ethylene-diaminetetra-acetic acid, disodium salt, dihydrate
EGF:	Epidermal growth factor
EST:	Expressed sequence tag
FGF:	Fibroblast growth factor
FBS:	foetal bovine serum
FITC:	Fluorescein-5-isothiocyanate
G:	guage
×*g*:	g-force

HES: Hairy/Enhancer of Split

hr: hour

IgG: Immunoglobulin G

Inc: Incorporated

IPTG: Isopropyl-β-D-thiogalactopyranoside

LAI: laparoscopic artificial insemination

LEF-1: Lymphocyte enhancer factor-1

LNG: Lin12/Notch/Glp-1

Milli-Q water: water produced by a Millipore filtration system

min: minute

mRNA: messenger RNA

NBT/BCIP: Nitro-blue tetrazolium chloride/5-bromo-4-chloro-3'-indolyphosphate p-toluidine salt

NICD: Notch intracellular domain

OCT: optimal cutting temperature

P: Passage of cells

PBS: Phosphate-buffered saline

PCR: polymerase chain reaction

pDNA: plasmid DNA

PEST: proline, glutamate, serine, threonine

Pty Ltd: Proprietary Limited

RAM: RBP-Jκ-associated molecule

REML: restricted maximum likelihood

rpm: revolutions per minute

sec: seconds

Shh: Sonic hedgehog

SOB medium: Hanahan's medium

SOC medium: Hanahan's medium with 0.02mM glucose added

SSC: Saline Sodium Citrate

S:P: Secondary to Primary follicle ratio

TACE: TNF-α-converting enzyme

TAD: transcriptional activator domain

TAE buffer: Tris-acetate-EDTA buffer

TBS: Tris-buffered saline

TE buffer:	Tris-EDTA buffer
Tris:	Tris(hydroxymethyl)aminomethane
tRNA:	transfer RNA
Tween 20:	Polyethylene–sorbitan monolaurate
yr:	year

GLOSSARY OF SOLUTIONS

Cell culture media (pH 7.4): DMEM (MultiCel™) with 10% heat inactivated FBS, 23mM Hepes buffer (MultiCel™), 10mM $NaHCO_3$, and 2% Penicillin/Streptomycin (MultiCel™) added.

0.1% DEPC-treated water: Within the fumehood, 1 ml of DEPC was dispensed into 1 L Milli-Q water. The solution was shaken for 16 hr at room temperature. Carbon dioxide gas was released and the solution autoclaved.

Detection buffer: 0.1M NaCl; 0.1M Trizma-HCl, pH 9.5; 5mM $MgCl_2$; 0.1% Tween 20.

Developer/replenisher: 25% developer A; 2.5% developer B; 2.5% developer C (Agfa-Gevaert Ltd).

Ficoll loading buffer: 0.25% bromophenol blue; 0.25% xylene cyanol FF; 15% Ficoll 400.

Freezing media: 20% FBS; 20% glycerol; 60% DMEM.

Heat inactivated foetal bovine serum (FBS): FBS (JRH Biosciences) was thawed, and 45 ml aliquots were measured before the tubes were heat inactivated by heating at 60°C for 1 hr. The tubes were stored at -20°C.

Hybridisation solution: 0.6M NaCl; 20mM Tris (pH 7.4); 20mM NaH_2PO_4 (pH 6.8); 10mM EDTA (pH 8.0); 0.4% Ficoll; 0.4% polyvinylpyrrolidone; 50mM DTT; 5% polyribonuclease A; 2.5% yeast transfer RNA (tRNA); 10% dextran sulphate; 50% formamide (deionised).

LB/ampicillin plates: 171mM NaCl; 1% tryptone (Oxoid Ltd); 0.5% yeast extract (Oxoid Ltd); 100 µg/ml ampicillin; 0.5% bacteriological agar (750-gel; Chem-Supply). The dishes were stored at 4°C for up to 1 month. To detect transformed bacterial colonies, 5 mg/ml X-galactosidase (Promega Corp) and 100 µl of 100mM IPTG were added and spread over the surface of the dish. The plates were stored at 4°C for at minimum of 1.5 hours before use.

LB medium (pH 7.0): 171mM NaCl; 1% tryptone (Oxoid Ltd); 0.5% yeast extract (Oxoid Ltd).

Maleic acid buffer (pH 7.5): 0.1M maleic acid; 0.15M NaCl.

4% Paraformaldehyde in PBS: Within a fumehood, paraformaldehyde (4%) was added to 1x PBS solution within a conical flask, placed in a waterbath and heated to 60°C with stirring. Concentrated NaOH was added drop-wise to the solution until the powder dissolved and the solution became transparent. The solution was cooled, dispensed into 30 ml specimen jars and stored at –20°C for up to 3 months.

PBS in 0.1% DEPC-Treated Water: Within 0.1% DEPC-treated water; 171mM sodium chloride (NaCl); 3.4mM potassium chloride (KCl); 10mM sodium phosphate, dibasic, anhydrous (Na_2HPO_4); 1.84mM potassium phosphate, monobasic, anhydrous (KH_2PO_4) were added. The pH was adjusted to 7.4 and the solution autoclaved.

1x PBS: 3.35mM KCl; 10mM Na_2HPO_4; 1.8mM KH_2PO_4; 8% (w/v) NaCl.

PCR mastermix: 1x DNA polymerase buffer; 0.2mM dNTP mix; 25pM T3 primer (Sigma® Genosys); 25pM T7 primer (Sigma® Genosys).

Rapid fixer: 20% fixative A; 5% fixative B (Agfa-Gevaert Ltd).

RNA dilution buffer: 5 parts 0.1% DEPC-treated water; 3 parts 20x SSC; 2 parts formaldehyde (37%).

SOB Medium (pH 7.0): 2% tryptone; 0.5% yeast extract; 117mM NaCl; 2.5mM KCl;10mM $MgCl_2$.

SOC medium: 2% tryptone; 0.5% yeast extract; 117mM NaCl; 2.5mM KCl; 10mM $MgCl_2$; 0.02mM glucose.

SSC: 10x: 1.5M NaCl; 150mM sodium citrate.

4x: 0.6M NaCl; 60mM sodium citrate.

2x: 3M NaCl; 30mM sodium citrate.

1x: 150mM NaCl; 15mM sodium citrate.

0.1x: 15mM NaCl; 1.5mM sodium citrate.

1x TAE buffer: 40mM Tris-acetate; 2mM Na_2EDTA.

TBS: 50mM Tris-HCl; 30mM NaCl.

TE Buffer (pH 7.6): 10mM Tris (pH 7.6) and 1mM EDTA (pH 8.0).

Trypsin solution: 0.02% EDTA.$2H_20$; 0.1% glucose; 0.04% KCl; 0.8% NaCl; 0.58% sodium bicarbonate; 0.1% trypsin.

Washing Buffer: 0.1M maleic acid; 0.15M NaCl; 0.3% Tween 20.

ABSTRACT

Wool follicle development is initiated during foetal life through signals exchanged between the mesenchyme and epithelium. Follicle primordia are initially visible as condensations of dermal prepapilla cells, and are associated with epithelial thickenings.

The dermal papilla is believed to secrete signalling molecules that direct the rate of cell division in surrounding bulb cells in the mature wool follicle. This determines the amount of fibre grown. It has been hypothesised that the dermal papilla cell population of the skin is finite and is determined at follicle initiation in the foetus. It is thought that this population defines the total quantity of fibre producing tissue in the mature sheep. The developmental mechanisms that specify this cell population and control their distribution in the growing follicle population is not known. There is however, evidence implicating the Notch signalling pathway in foetal skin development. Some Notch signalling pathway genes have been identified in ovine skin and other tissue, including the incomplete sequences of Notch-1, Jagged-1, Delta-1 and Delta-4.

This study reports on the roles of some key Notch genes prior to (d 56) and during (d 70) primary follicle initiation in Merino and Tukidale lines of sheep. Tukidale animals were chosen as a strong-woolled comparison to the fine-woolled Merino, due to their markedly different follicle densities and fibre characteristics.

Different experimental procedures were utilised to provide a more thorough understanding of the role of the Notch signalling pathway in wool follicle initiation in sheep. DIG-labelled riboprobes for Delta-1, Delta-3 and Lunatic Fringe were generated from murine cDNA sequences and a PCR-generated ovine cDNA probe for Notch-1 provided information on gene expression using *in situ* hybridisation studies. Transcripts were detected in sectioned foetal skin prior to and during follicle development. In skin sampled prior to follicle initiation, Delta-1 transcripts were detected throughout the epithelium and in some mesenchymal cells. Notch-1 was detected in the epithelium, particularly in the basal layer, and in some mesenchymal cells. In skin sampled during follicle initiation, Delta-1 was expressed in the epithlium, basal layer of the epithelium and in some mesenchymal cells. Some Notch-1 transcripts were detected in the epithelium, with staining appearing stronger in the basal layer. Notc-1 transcripts were also detected in a few cells within the epithelial plug, in some mesenchymal cells and in the dermal condensates in the cells around the periphery of this structure. Counts of Delta-1 and Notch-1 labelled mesenchymal and dermal condensate cells

were conducted. An interesting finding of this work was that no significant differences were detected between the numbers of cells labelled for Delta-1 or Notch-1 when the Merino and Tukidale skin samples were compared.

Antibodies were used for immunohistochemistry studies in sectioned foetal sheep skin collected from Merino and Tukidale foetuses. Delta-1, Notch-1 and activated Notch protein expression were detected in skin samples.

The behaviour of dermal papilla cells was investigated *in vitro*. An aggregating cell model whereby papilla cells were grown on the extracellular matrix complex Matrigel™ was developed. The cell cultures were shown to aggregate prior to reaching confluency, with the cells being observed over a 31 day period. A floating foetal sheep skin culture system was devised whereby skins were cultured on collagen-coated membranes for 4 days. Cell and skin cultures were examined in the presence and absence of the γ-secretase inhibitor DAPT, which was dissolved in DMSO and added to the culture media. Dermal papilla cell aggregation was abolished in all dermal papilla cell cultures in the presence of 50μM DAPT. The formation of new follicle buds within skin harvested on day 70 of foetal development and cultured for 4 days was hindered. An investigation in to the effect of treatment with 50μM DAPT on follicle diameter in day 70 Merino skin cultures suggested that DMSO and DAPT had some effect on follicle diameter, when compared to the untreated controls.

The results of this project have provided new insights into the mechanisms by which the wool follicle population is established in a foetus and suggest that some Notch signalling pathway genes are involved in the specification of prepapilla cell fate at follicle initiation.

CHAPTER 1: LITERATURE REVIEW

1.1 INTRODUCTION TO PROJECT

Morphogenesis of hair, wool and feather follicles is initiated in skin by molecular interactions between the epithelium and the underlying mesenchymal cells (Hardy, 1949; Hardy and Lyne, 1956). The molecular mechanisms involved in follicle initiation and the orchestration of the particular patterns, spacing and follicle characteristics are however not fully understood. The very complexity of this biological system dictates that many developmental genes and their products contribute to the establishment of the cell populations and the interactions involved in these processes. Notch pathway genes may play a role in follicle initiation and patterning as they are implicated in cell specification in various other organ systems, and transcripts for the Notch receptor and some of its ligands and modulators have been shown by others to be expressed in follicle primordia during morphogenesis (Crowe *et al.*, 1998; Powell *et al.*, 1998; Botto, 2000; Favier *et al.*, 2000; Gordon-Thomson *et al.*, 2008).

The focus of this study was to examine the expression patterns of the Notch receptor, and two of its ligands Delta-1 and Delta-3, and the effector, Lunatic Fringe prior to and during follicle initiation of wool follicles in foetal sheep skin, from strong- and fine-woolled breeds. This comparative approach was undertaken to determine whether the pattern of Notch pathway gene expression differed in the two breeds varying in wool follicle density and in the diameter of fibres produced. A role for Notch signalling in wool follicle initiation was also explored by blocking Notch receptor activation, using an inhibitor of gamma secretase in cultured isolated dermal papilla cell and skin explants cultures. This enzyme facilitates the activation of Notch in the cell membrane.

A comprehensive review of the literature in the following sections describes the current knowledge on the biology of skin and hair and wool follicles and the influence of genes on hair and wool development.

1.2 BIOLOGY OF SKIN

Skin is the largest organ of the body. Prior to its morphogenesis, various cellular interactions occur that specify the formation of dermal progenitor cells before future cutaneous appendage fields are established. These steps lead to the formation of an embryonic skin consisting of a thin epidermis overlying a dense dermis, followed by the initiation and

organisation of regular repetitive appendage primordia. In the case of hair or wool, organogenesis of the epidermal placode follows, producing a mature hair follicle or compound wool follicle (Hardy and Lyne, 1956; Olivera-Martinez *et al.*, 2004).

1.2.1 EPIDERMIS

The epidermis forms the outer protective layer of skin. It consists of multiple layers of keratinocytes that lie above the dermis, as illustrated in Figure 1.1. It has no direct blood supply or lymphatic system. Its role is to guard against infection, to prevent dehydration, and to undergo re-epithelialization after wound injuries. To accomplish these feats, the epidermis constantly replenishes itself (Lowell *et al.*, 2000; Fuchs, 2007).

The epidermis consists of a living and a dead component. The living component can be divided into 3 layers, the basal layer, the spinous layer (*Stratum spinosum*) and the granular layer (*Stratum granulosum*). The basal layer consists of mitotically active stem cells which have an unlimited self-renewal capacity and transit amplifying cells which have a low self-renewal capacity and high capability for differentiation (Lowell *et al.*, 2000; Zhou *et al.*, 2006). The basal layer is located at the junction of the epidermis and the dermis. It surrounds the entire hair follicle and is continuous with the epidermis (Roth, 1965). The basal layer adheres to an underlying basement membrane rich in extracellular matrix and growth factors (Fuchs, 2008). Laminin, nidogen, and entactin form defined complexes and type IV collagen and heparan sulphate proteoglycan cause these compounds to be incorporated into an insoluble gel-like structure (Kleinman *et al.*, 1986). The spinous layer consists of 3-6 layers of spinous cells, which possess bundles of keratin filaments within the suprabasal cytoplasm that connect to desmosomal plaques at the plasma membrane. These cells are transcriptionally active but are no longer dividing. The cells express keratin genes and gene products. The granular layer is made up of 1-3 layers of granular cells that produce and transiently store the components which constitute the lipid barrier (Fuchs, 2001). The dead component of the epidermis (*Stratum corneum*) is comprised of flattened, non-living cells (Lyne, 1966), held together by secreted lipids that protect the underlying cells from the external environment (Fuchs, 2001).

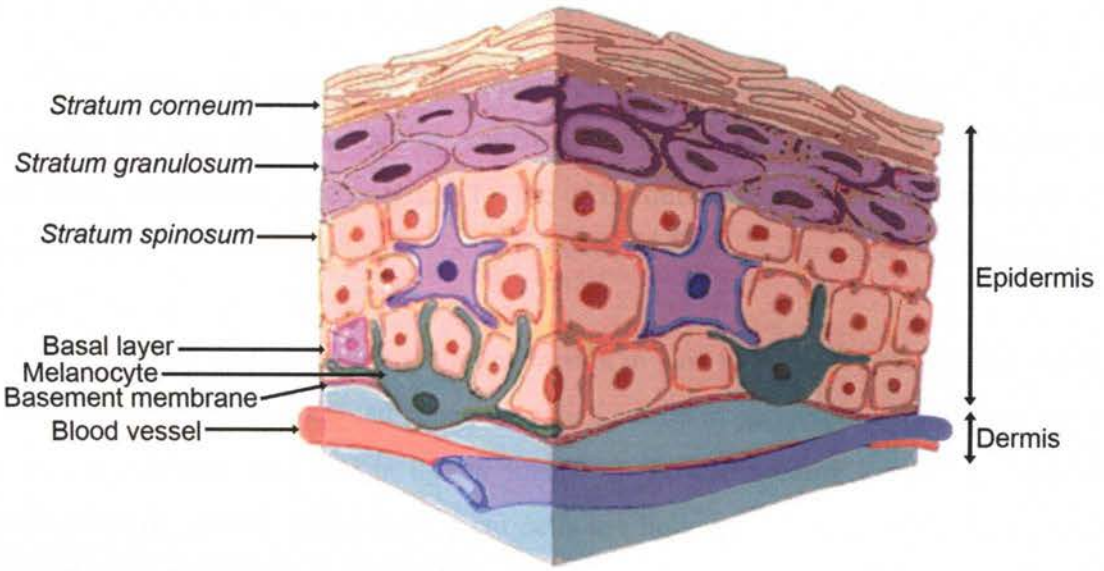

Figure 1.1: A schematic of the mammalian epidermis and its various layers. The epidermis consists of a dead component, known as the *stratum corneum*, as well as 3 living layers: *stratum granulosum*, *stratum spinosum* and the basal layer. Melanocytes can be seen within the epidermis. The dermis lies beneath the epidermis and basement membrane and contains blood vessels. Image adapted from site (found 04-10-2005). http://www.cs.stedwards.edu/chem/Chemistry/CHEM43/CHEM43/Photocarcino/

1.2.1.1 Epidermal stem cells

By definition, stem cells must be able to self-renew and produce differentiated progeny (Huelsken *et al.*, 2001; Tiede *et al.*, 2007). Stem cells are critical for replenishing and maintaining homeostasis within a tissue and for regenerating damaged tissue throughout the lifetime of an animal (Blanpain *et al.*, 2004; Ward *et al.*, 2006). Many stem cells divide symmetrically, allowing this cell population to increase in number (Tiede *et al.*, 2007): some cells remain as undifferentiated stem cells and others undergo terminal differentiation (Lewis, 1998).

The self-renewing capacity of the skin is dependent on proliferation of a subpopulation of keratinocytes known as epidermal stem cells, residing in the basal layer of the epidermis, in the hair follicle bulge and in the base of the sebaceous gland (Lavker *et al.*, 1993; Watt, 2001; Alonso and Fuchs, 2003; Fuchs, 2008). Epidermal stem cells can migrate, self-renew, proliferate outside the follicle bulb, and participate in the hair cycle (Claudinot *et al.*, 2005). Although normally slow cycling, they can be induced to proliferate in response to wounding and certain growth stimuli (Lavker *et al.*, 1993).

1.2.1.2 Melanocytes and pigmentation

Melanocytes are specialised pigmented cells that produce melanins, the pigments responsible for skin and hair colour. Cutaneous melanocytes originate from highly motile neural-crest progenitors that migrate to the skin during embryonic development (Gray-Schopfer *et al.*, 2007). Melanocytes reside in the basal layer of the epidermis (Figure 1.1) and in hair follicles (Figure 1.2).

Two discrete melanocytic populations reside in hair follicles. These are the melanocyte stem cells and their differentiated progeny, which reside in geographically distinct regions to comprise a follicular unit that is tightly linked to the surrounding keratinocyte population (Slominski *et al.*, 2004). Melanocyte stem cells are believed to reside in the bulge region of the hair follicle (Tiede *et al.*, 2007). Hair follicle melanocyte stem cells have important roles in normal hair pigmentation and senile hair greying, and specific genetic defects have shed further light on the survival properties of this cell population (Lin and Fisher, 2007).

In the case of Merino sheep, white wool is produced as a result of the failure of melanocytes to migrate to the skin at the time of wool follicle development (Fleet *et al.*, 2004), and their absence from the follicle usually persists in the adult (Rogers, 2006). This absence of pigmentation is a desirable trait in wool production.

1.2.2 DERMIS

The dermis is a dynamic structure. It is able to change in response to mechanical stresses, the different phases of the hair growth cycle and with swelling and shrinking of glands (Billingham and Silvers, 1965). The dermis extends from the basal layer of the epidermis to the smooth muscle. It consists of fibroblasts and connective tissue that surround the hair follicles and skin glands. Within the dermis, numerous blood vessels form a network of capillaries that lie in close proximity to the epidermis, around hair follicles and in the dermal papillae (Lyne, 1966). Networks of nerves are found throughout the dermis and around the hair follicles, and these form the majority of the sensory nerve tissue in hair-bearing regions of skin (Winkelman, 1965; Lumpkin and Caterina, 2007).

1.2.2.1 Dermal progenitor cells

Jahoda *et al.* (2003) found that dermal papilla and dermal sheath cells were able to differentiate spontaneously or in a directed fashion along other mesodermal lineages *in vitro*. They hypothesised that the hair follicle dermis is the main source of multipotent stem cell activity in the dermal compartment of the skin. It was thought that the expression of alkaline

phosphatase in dermal papilla and dermal sheath cells may reflect the broader stem cell capabilities of these populations (Jahoda, 2003).

1.2.3 MORPHOGENESIS OF THE HAIR AND WOOL FOLLICLE

Our knowledge of the molecular mechanisms involved in hair follicle morphogenesis has been provided by experimental manipulation, for example in transgenesis studies in mice. Cell fate decisions are involved in the morphogenesis of hair follicles, during foetal life. Follicles form at discrete body sites as the result of reciprocal interactions between the epidermis and dermis (Hardy and Lyne, 1956; Powell *et al.*, 1998; Jahoda *et al.*, 2001), and these interactions are maintained throughout adult life in order for the hair to continue to cycle (Williams *et al.*, 1994; Pispa and Thesleff, 2003).

Morphologically, the initiation of hair follicle development begins with "crowding" of epidermal keratinocytes, and the formation of placodes, followed by a condensation of fibroblasts in the underlying mesenchyme. The signalling cross-talk between the mesenchymal condensate and the epithelial placode drives proliferation in both structures, shaping the dermal condensate and initiating the down-growth of the ectodermal placode (Hardy, 1992; Schmidt-Ullrich and Paus, 2005). In the developing Merino foetus, a main antero-posterior gradient in the time of follicle morphogenesis was observed across the body (Carter and Hardy, 1947), so that follicle development occurred earlier in the head, neck and limbs than over the rest of the body. By conducting grafts where guinea pig epidermis and dermis from different areas of the body were transplanted and observed for a period of 100 d prior to histological examination, it was shown that mammalian dermis orchestrated changes in the cellular dynamics of the epidermis, which in turn determined the size of the dermal papilla associated with this interaction (Billingham and Silvers, 1965). The functional and structural relationships between the inner and outer root sheaths of follicles and dermal papilla were found to be essential for the growth processes that determine hair size and shape in the rabbit and guinea pig (Straile, 1965). Chimeric experiments where quail and duck epidermis and dermis were grafted onto each other in various combinations supported the theory that integumentary epithelium acts in a permissive way, and the dermis acts instructively to establish the timing and spacing of feather bud development (Eames and Schneider, 2005). Their studies involved taking orthotopic grafts of unilateral or bilateral populations of neural crest cells (from the midbrain and rostral hindbrain) at embryonic stage 9.5, and transplanting them from duck to quail and quail to duck.

Morphogenesis of the wool follicle will be described in more detail in Section 1.6.1.

1.3 BIOLOGY OF THE HAIR FOLLICLE

The mesenchymal tissues develop limb and then more specific ectopic appendages early in embryonic development. The hair follicle (Figure 1.2) is the most prominent mini-organ of the skin and one of the defining features of mammalian species. For its entire life-time, the hair follicle undergoes cyclic transformations (Schmidt-Ullrich and Paus, 2005). The mature hair follicle involutes and regenerates, with cyclically alternating periods of rapid growth, apoptosis-driven regression, and relative quiescence. The hair cycle is further discussed in Section 1.5.

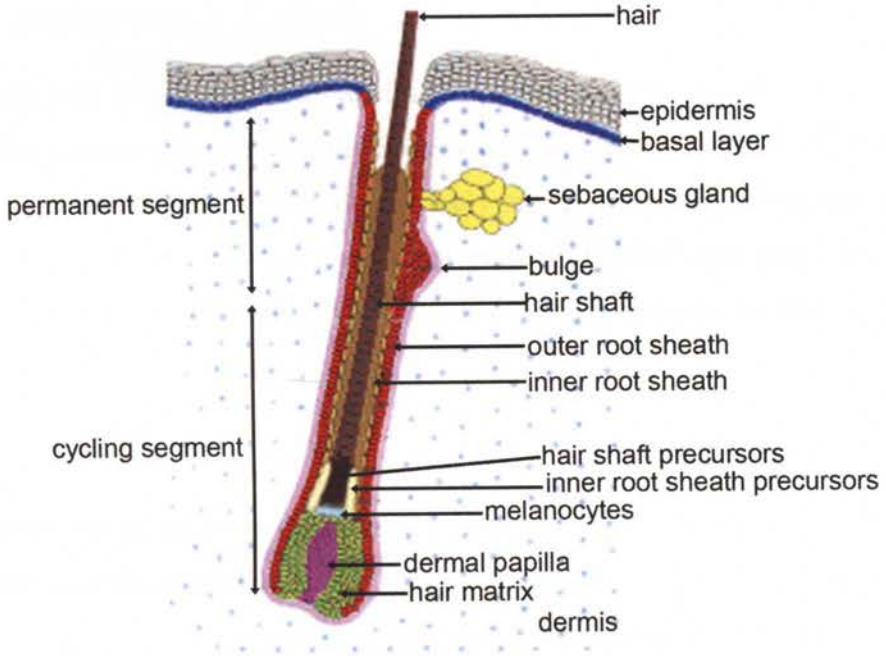

Figure 1.2: Schematic diagram of a mature hair follicle. The hair follicle consists of an upper permanent section, and a lower cycling section. The hair matrix consists of proliferating cells. The dermal papilla is encased within the matrix, in the base of the follicle. Upon differentiation, the hair matrix generates the hair shaft and inner root sheath cells. Melanocytes reside in the upper section of the matrix. The outer root sheath is continuous with the basal layer of the epidermis. The bulge, located below the sebaceous gland, contains follicular stem cells. Dermal fibroblasts are represented by blue dots. Figure adapted from (Gritli-Linde *et al.*, 2007).

1.3.1 THE DERMAL PAPILLA

Papilla cells are first visible in the focal aggregations of mesenchymal cells associated with the epidermal condensations at follicle initiation (Hardy and Lyne, 1956). In the later phases of follicle development, cells of the dermal condensate are incorporated into a pocket at the base of the follicle, to form the dermal papilla. These cells stay in close proximity to the proliferating cells of the hair bulb during hair growth (Figure 1.2), and play an important role in epithelial-mesenchymal interactions (Section 1.2.3).

The size of the papilla was found to correlate with the volume of its matrix and the diameter of the hair shaft formed. The number of mitoses that occur in the follicle matrix was found to be proportional to the activity of the dermal papilla and to its volume (Van Scott and Ekel, 1958), consistent with the finding that the size of the dermal papilla influenced the rate of hair production (Cohen, 1965). This phenomenon was found to be true for all rat and mouse follicles (Ibrahim and Wright, 1982). The dermal papilla was believed to be the origin of signals that regulate cell division within the hair bulb (Hardy and Lyne, 1956; Hardy, 1992), as follicles which did not possess a papilla did not grow fibres.

1.3.2 THE OUTER ROOT SHEATH

The outer root sheath can be divided into 3 major components, the upper external outer root sheath, the sebaceous gland and the lower external outer root sheath (Straile, 1965). It is thought that the external root sheath cells actively migrate upwards during hair growth in the mouse and Merino sheep, and that outward migration of these cells may play a role in the process of moving the hair cylinder and inner root sheath towards the skin surface (Straile, 1965).

1.3.2.1 The sebaceous gland

The sebaceous gland is an appendage of the hair follicle, located above the bulge and just below the hair shaft orifice at the skin surface, surrounded by the basal layer of the epithelium. Its main role is to generate terminally differentiated sebocytes, which produce lipids and sebum. When sebocytes disintegrate, they release their oils into the hair canal for lubrication and protection against bacterial infections. They also produce cytokines and growth factors which assist in maintaining the functional integrity of the skin. Sebaceous gland homeostasis necessitates a progenitor population of cells that give rise to a continual flux of proliferating, differentiating and dead cells that are lost through the hair canal (Fuchs, 2007).

Hair follicle development has been described in relation to the initiation and location of sebaceous glands (Mooney and Nagorcka, 1985) attached to the follicle by the Reaction-Diffusion theory, described in Section 1.7.2.

1.3.2.2 The sweat gland

The apocrine sweat or sudiferous gland is one of the major cutaneous appendages in the skin. These simple coiled tubular glands are located within the dermis (Jenkinson *et al.*, 1979), and a duct connects the gland to the hair canal. The functions of sweat glands are thermoregulation, excretion and protection which it achieves by secretion and excretion of water, salts and waste (Sato *et al.*, 1989).

Apocrine sweat glands develop as attachments to the primary follicles within the skin. The Reaction-Diffusion theory (Section 1.7.2) of follicle development explains the formation of sweat glands (Mooney and Nagorcka, 1985), in accordance with primary wool follicle development is illustrated in Figure 1.4.

1.3.3 THE INNER ROOT SHEATH

The inner root sheath is composed of 3 concentric layers; Henle's layer, Huxley's layer and the cuticle layer. Henle's layer and the cuticle layer are thin transitional surfaces that connect Huxley's layer with the rest of the hair follicle, as illustrated in Figure 1.3. In the sheep, Huxley's layer is 1 cell wide. Woods and Orwin (1982) have shown that the inner root sheath cuticle, that hardens first, imprints its cuticle pattern on the fibre cuticle cell layer, so that is the reason why the inner root sheath cuticle and fibre cuticle scales appear to be interlocking (c.f. Straile, 1965).

Near the base of the growing hair follicle, epidermal cells arise from a mass of rapidly proliferating tissue, known as the matrix. These cells differentiate to form a core of keratinised material composed of the hair and its surrounding inner root sheath. Throughout hair growth, this core passes upwards through the external root sheath (Straile, 1965).

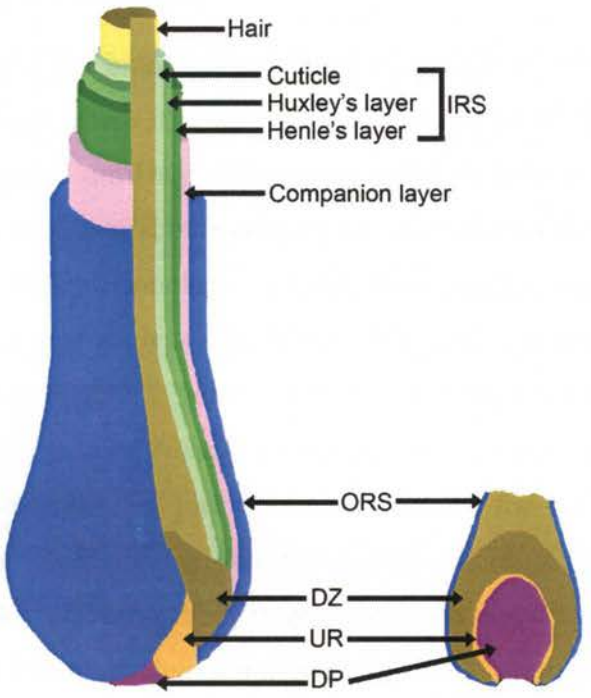

Figure 1.3. Schematic diagram of the inner root sheath (IRS) of a mature hair follicle. The hair fibre is surrounded by the three layers of the IRS: the cuticle, Huxley's layer and Henle's layer. The companion layer surrounds the IRS, which is in turn surrounded by the outer root sheath (ORS). The dermal papilla (DP) is enclosed in the base of the follicle, within an undifferentiated zone (UR) and differentiated zone (DZ), which together make up the hair matrix. Figure adapted from http://www.tfl.com/pdfs/others/stuctureofbovineskin.pdf (found 05-02-2009).

1.3.4 THE FOLLICLE BULGE

The follicle bulge located in the outer root sheath below the sebaceous gland in hair follicles is not morphologically evident in wool follicles. The absence of the bulge in the Merino wool follicle suggests that different cellular processes occur during the hair cycle in the sheep, compared to the mouse (Rogers, 2006). Alternatively, it may be a relatively small structure due to the continual growth of the wool fibre, in contrast to the cyclical growth of hair.

Follicle bulge formation in the mouse has been shown to be accompanied by internal movements and a reorganisation of the stem cell niche architecture. Whether the follicle bulge contains a number of layers of unipotent stem cells, or whether the stem cells within the bulge are multipotent and contribute to the interfollicular and follicular keratinocyte lineages remains unclear (Blanpain *et al.*, 2004). Recent research has provided evidence that follicle bulge cells are the stem cells for the interfollicular epithelium, and in some cases the follicular epithelium as well (Fuchs, 2007; Fuchs, 2008).

1.3.5 THE ARRECTOR PILI MUSCLE

The arrector pili muscle is a branched structure, comprised of smooth muscle, located on the side of the follicle from where it bifurcates around the duct of the sweat gland. Each arrector pili muscle is orientated similarly with respect to the follicle to which it is attached. Fine strands of elastic tissue also connect the primary and secondary follicles in the upper part of the dermis to provide a follicle orientation that flows more readily. Groups of follicles have the tendency to lie in rows at right angles to the average orientation of the muscles (Chapman, 1965). Sick *et al.* (2006) identified WNT and its inhibitor Dikkopf as the main determinants of hair follicle spacing in the mouse. Polarity of the hair follicle is thought to occur in two phases. Firstly, a Frizzled-6-dependent phase which orientates the follicles in response to anterior-posterior signalling. Secondly, a Frizzled-6-independent phase occurs where the follicles signal to one another allowing them to orientate with respect to their neighbouring follicles (Stark *et al.*, 2006). Hammerschmidt and Schlake (2007) found that the ectodysplasin pathway generates a polarised signal in the hair follicle.

1.3.6 THE CORTEX

The cortex consists of a solid cylinder of cells that surround the portion of the follicle which lies above the epidermis (Roth, 1965). Transmission electron microscopy highlighted that 3 types of cells exist within the cortex of wool and hair fibres; orthocortical, mesocortical and paracortical. The proportion of orthocortical cells was discovered to increase as fibre diameter increased, while the proportion of mesocortical and paracortical cells decreased, often with a partial substitute of paracortex by mesocortex (Plowman *et al.*, 2007).

1.4 VIBRISSA FOLLICLES

Vibrissae develop earlier than pelage follicles. They can be distinguished from pelage follicles by their large size, hour-glass shape, and dense dermal sheath surrounding the developing follicle (Kollar, 1966). Vibrissae function as specialised sensory organs. Structurally they consist of a large innervated follicle surrounded by an outer collagenous capsule (Williams *et al.*, 1994). They can be found bilaterally within the upper lip and cheek skin in 5 organised rows in the rat and mouse (Williams *et al.*, 1994). In sheep, they are randomly located in the upper lip, cheek and chin.

1.5 THE HAIR CYCLE

Mammalian hair goes through cycles of growth and rest. Cycling is a developmental process that occurs over the total lifetime of a mammal. To grow and cycle, the follicle requires recurring patterns of epithelial-mesenchymal interactions, involving both follicular epithelium and associated connective tissues (Stenn and Paus, 2001). A hair is produced during a period of active growth referred to as anagen, then passes through an intermediate phase known as catagen, and then to a resting phase referred to as telogen (Roth, 1965). The extended hair cycles seen in sheep wool, horse mane and tail, and human scalp represent special cycles in biology. These follicles cycle independently of the environment over a period of 2-6 years (Stenn and Paus, 2001).

1.5.1 ANAGEN

At the onset of anagen, the cycling portion of the follicle regenerates and undergoes a new round of hair growth. Epidermal stem cells located at the base of the follicle bulge receive signals from the dermal papilla and the stem cells proceed to regenerate the hair follicle and produce a new hair (Rendl *et al.*, 2005). The interactions which occur between the dermal papilla and proximal bulb region are required for fibre production (Pisansarakit and Moore, 1986). The connective tissue sheath is likely to be the source of a significant number of anagen dermal papilla cells. Migration of cells from the mitotically-active connective tissue sheath into the dermal papilla is responsible for much of the 2-fold increase in the number of dermal papilla cells during anagen development (Tobin *et al.*, 2003a). Tobin *et al.* (2003b) suggested the connective tissue sheath was the source of the specialised mesenchymal cells that migrate into the follicle papilla during anagen. Recent studies have suggested that FGF-7 induced and maintained hair growth during anagen (Fuchs, 2007), and that TGF-β was the principle modulator of the transition from the anagen phase to the catagen phase (Iino *et al.*, 2007).

1.5.2 CATAGEN

During catagen, the hair ceases to grow and the lower, epithelial part of the follicle enters a regressive phase, during which the hair follicle begins to lose its structural integrity. Shrinkage of the epithelium pulls the basement membrane (Rendl *et al.*, 2005) and the dermal papilla upward (Huelsken *et al.*, 2001).

1.5.3 TELOGEN

Although this stage of the hair cycle is considered to be the "resting phase", the hair follicle does not appear to be completely switched off. During telogen, the dermal papilla is smaller in size, mainly a result of its reduced volume of extracellular matrix (Montagna *et al.*, 1952). The dermal papilla cells are held in closer proximity to each other by intimate cell-cell contacts through the development of specialised structures in the cell membrane such as caveoli, although their role in this process require further clarification (Tobin *et al.*, 2003a). It has been suggested that the dermal papilla cells of the telogen follicle are recharging for the following anagen, based on significant inter-papilla cell communication and potentially distinct subpopulations of papilla cells observed (Tobin *et al.*, 2003b).

1.6 WOOL FOLLICLE BIOLOGY

The structure and morphogenesis of the compound wool follicle has been described in the earlier seminal work of Hardy and Lyne (1956) and others. The sheep fleece consists of primary, secondary original and secondary derived follicles, all of which are formed during successive waves of initiation along the skin during foetal skin development (Carter and Hardy, 1947). The complete follicle population is established before birth, by approximately day 150 of gestation (Moore *et al.*, 1989; Moore *et al.*, 1998). In the postnatal fleece, a typical follicular group is comprised of 3 primary follicles and a variable number of secondary follicles (Lyne, 1966).

The distribution of initiation points for primary and secondary original follicles is believed to constrain their density, as they develop from evenly spaced aggregates of cells. No such limits exist on the distribution of secondary derived follicles. The quantitative morphological analyses reported by Moore *et al.* (1996) suggested that when the majority of initiation sites in a foetal skin were used up, the initial stages of follicle branching commenced.

Variations in wool production between different body sites is controlled by variations in fibre density at the different sites, with fibre diameter and staple length being higher in the midbody region, and fibre diameter increasing as fibre density decreased from the anterior to posterior regions (Young and Chapman, 1958).

Environment has a significant effect on wool production with lambs up to 3 years of age born from underfed ewes possessing secondary to primary follicle ratios of up to 29% and 47% lower than the ratios observed in higher birth weight lambs obtained from fully fed ewes

(Kelly *et al.*, 1996). Twins are generally of a lower birth weight than singleton lambs, due to competition for nutrients during foetal life. Commonly, twin-born lambs produce 4% less wool that is up to 0.2 μm broader than that produced by their singleton counterparts (Turner, 1961; Brown *et al.*, 1966; Turner *et al.*, 1968; File, 1981). Strong wool Merinos produce more wool per follicle than that produced by fine wool Merinos, due to the presence of a higher volume of cortical cells, a higher rate of bulb cell mitosis and a more efficient incorporation of cortical cells into fibre (Hocking Edwards and Hynd, 1992).

1.6.1 PRIMARY FOLLICLE DEVELOPMENT

Primary follicle development (Figure 1.4) commences between days 54 and 63 of gestation, with follicles forming at regularly spaced intervals. Either this pattern is already determined, or each developing follicle becomes surrounded by a small zone where development of another follicle is inhibited (Hardy, 1949; Lyne, 1966). Primary follicles form on the head and limbs before migrating over the rest of the foetus (Carter and Hardy, 1947). Two lateral primary follicles develop subsequently in association with the earlier-forming central primary follicles to form a trio. An adult Merino follicle population is comprised of 5-10% primary follicles. (Stephenson, 1957). Primary follicles can be distinguished from secondary follicles by their associated sudiferous gland, large sebaceous gland and arrector pili muscle (Lyne, 1966; Moore *et al.*, 1989; Rogers, 2006).

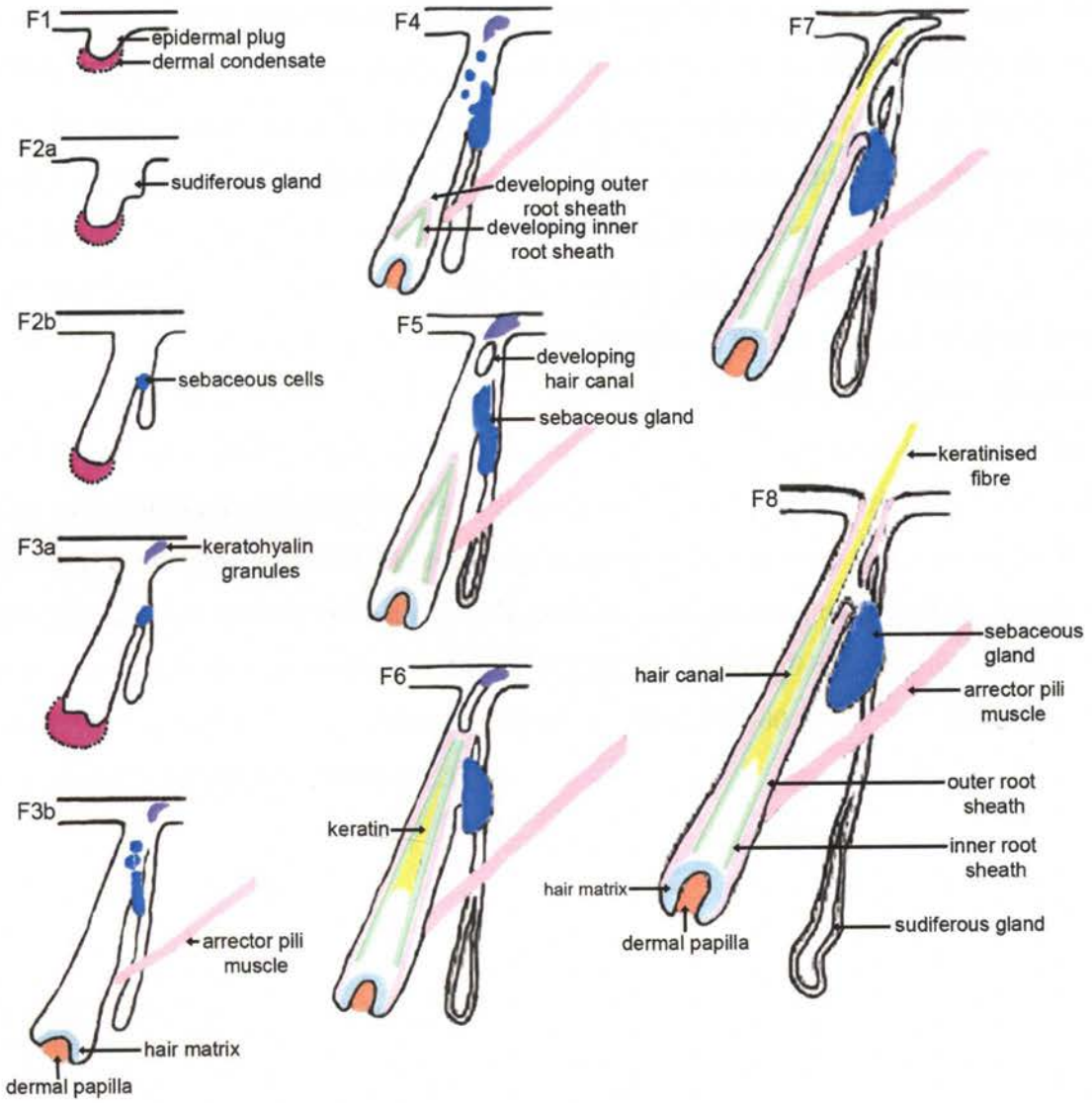

Figure 1.4: Schematic representation of the stages of primary wool follicle development. The first stage (F1) begins with the emergence of an aggregation of dermal cells beneath the epidermal plug. In the second stage (F2), the base of the epidermal plug is seen to become flattened, before a rudimentary form of the sudiferous gland appears as a solid bud ental to the developing follicle, and a bi-lobed sebaceous gland bud forms ental to the sudiferous gland. In the third stage (F3), changes to the size of the papilla are notable as the cells become encased in the base of the plug and the hair matrix. The arrector pili muscle and keratohyalin granules form during this stage. During the fourth stage (F4) the inner (Henley's layer) and outer root sheath begin formation. At the fifth stage (F5) the hair cone is in line with the base of the developed sebaceous gland, and the hair canal is visible. In addition, Huxley's layer, the developing hair cuticle and cortex are distinguishable. By the sixth stage (F6), the tip of the hair cone is solid, the hair canal is completely formed, and all layers within the follicle can be visualised. By stage 7 (F7), the tip of the wool fibre has emerged through the inner root sheath, in line with the epidermis. By stage 8 (F8), the hair has emerged through the periderm. Image adapted from Hardy and Lyne (1956).

1.6.2 SECONDARY FOLLICLE DEVELOPMENT

Secondary original follicles develop between the primary follicles at non-randomly distributed sites from days 80 to 90 of gestation in the Merino foetus (Moore *et al.*, 1996). The secondary derived follicles are the last to form (from approximately day 100 of

gestation), appearing at pre-existing initiation sites where they can be seen to branch from secondary original and other secondary derived follicles. Secondary follicle initiation ceases at least 10 days before birth in the Merino, with no significant change in the ratio of secondary to primary follicles detected after day 126 of gestation (Hocking Edwards, 1999). Secondary follicles emerge as a compound follicle from a common pilary canal (Hardy and Lyne, 1956). The stages of secondary follicle development are illustrated in Figure 1.5.

At follicle maturity, each compound follicle is made up of 1 secondary original follicle and a number of secondary derived follicles (Moore *et al.*, 1998). In Merino sheep, the secondary derived follicles make up the majority of a fleece. However, the population of follicles varies between different breeds of sheep (Rogers, 2006). The Tukidale was found to have a significantly lower ($p<0.001$) secondary to primary follicle ratio (S:P) compared to the Merino. The average relative primary follicle density, average secondary follicle density and average total follicle density were found to be (17.92 ± 1.21, 67.59 ± 5.06, and 16.13 ± 1.22 respectively) compared to the Merino (100.00 ± 7.64, 100.00 ± 14.94, 100.00 ± 7.92 respectively) (Champion and Robards, 2000).

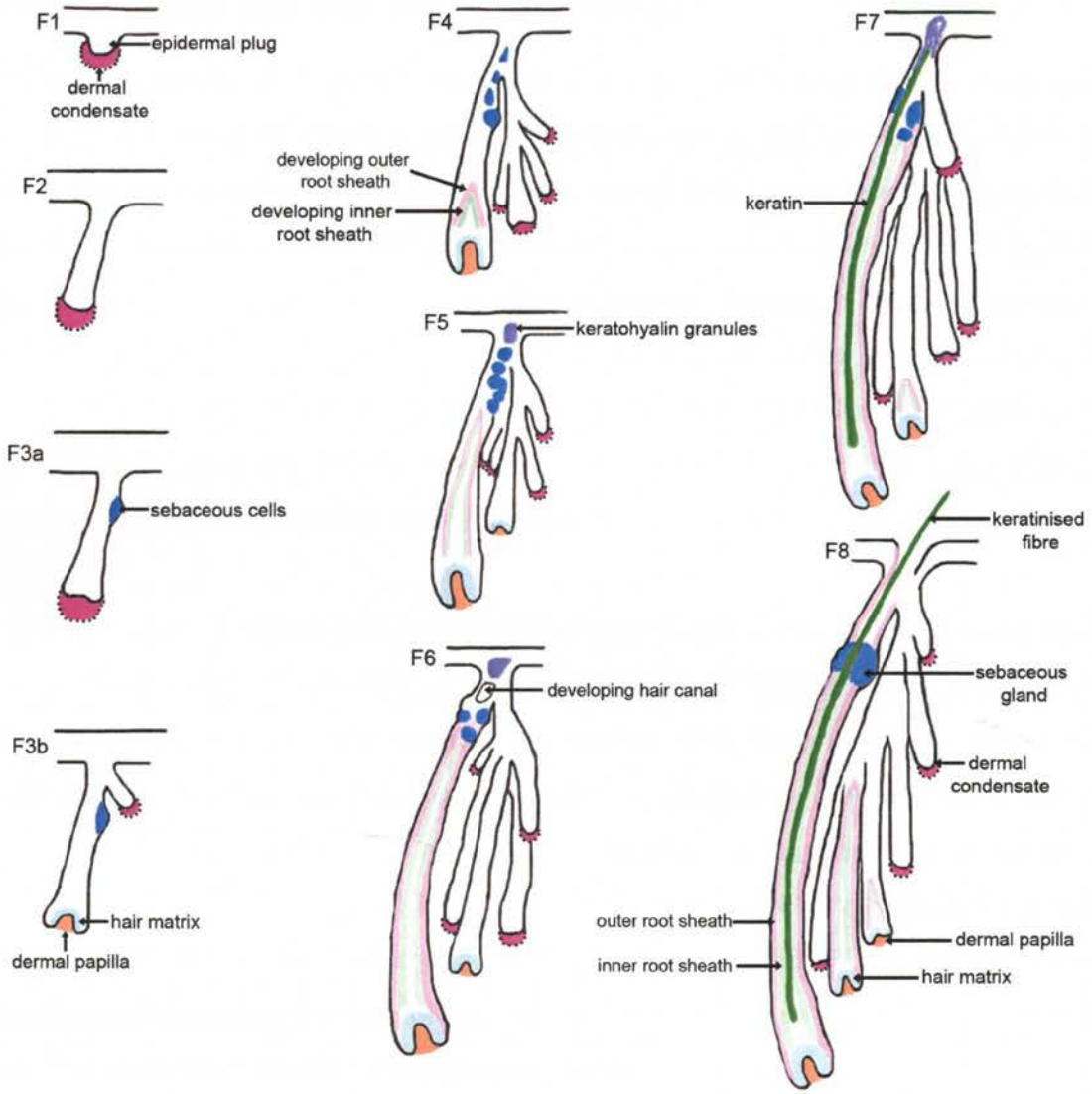

Figure 1.5: Diagrammatic representation of development of secondary wool follicles in the Merino, where secondary original and secondary derived follicles can be observed. During the first stage of development (F1) an aggregation of dermal cells is visible beneath the epidermal plug. The plug continues to elongate downward through the dermis to form the secondary original follicle. In stage 2 (F2), the follicle appears more elongated than a primary follicle, and the base of the epidermal plug begins to flatten. At stage 3 (F3) a rudimentary sebaceous gland is visible, the hair matrix is evident, and a secondary derived follicle can commonly be seen to form as a lateral branch off the side of the original follicle or pre-existing derived follicle. In stage 4 (F4), many differentiated sebaceous cells can be seen, the inner root sheath and outer root sheaths are visible in the more developed follicle, and many derived follicles may be observed as a number of branches extending from the existing follicles. By stage 5 (F5), the hair cone has reached the level of the sebaceous gland, formation of the epidermal hair canal begins in the upper region of the follicle, while the sebaceous cells are degenerating in the lower region of the follicle, and development of the already present derived follicles occurs in addition to formation of more of these follicles. At stage 6 (F6), a canal space in the lower region of the follicle is observable. During stage 7 (F7), the tip of the fibre has become keratinised and emerges through the inner root sheath, positioned in a common hair canal. At stage 8 (F8), the fibre has penetrated through the surface of the skin. Image adapted from Hardy and Lyne (1956).

1.6.3 FIBRE DIAMETER AND FOLLICLE DENSITY

A negative genetic correlation between fibre diameter and follicle density exists, and it may be possible to decrease fibre diameter by increasing follicle density (Hocking Edwards *et al.*, 1996). Data presented by Moore *et al.* (1989) showed that Merino skin produced more or less follicles as fibre diameter decreased or increased respectively. Selection aimed at altering one fleece trait has been shown to cause other undesired changes in fleece characteristics (Rendel and Nay, 1978). Animals selected for increased fibre diameter showed a decrease in follicle density, whereas those selected for finer fibres showed an increase in density. The number of papilla cells per follicle was found to be inversely related to follicle density, indicating that papilla cell number shared a positive relationship with fibre diameter (Moore *et al.*, 1998).

The processes of follicle initiation and fibre specification were believed to be distinct from one another with both occurring at, or before follicle initiation. It was concluded that no specific instructions in foetal skin program the number of follicles that form, so that wool fibre dimensions must be specified during follicle morphogenesis (Moore *et al.*, 1996), and the number of follicles and fibre size must be a consequence of the manner in which the cell population is utilised (Moore *et al.*, 1989; Moore *et al.*, 1998). Selective breeding has reduced the difference in size between primary and secondary derived follicles and greatly increased the abundance of secondary derived follicles in the skin, resulting in fleeces of finer and more uniform fibre diameter in Merino sheep (Rogers, 2006).

1.7 THE THEORIES OF FOLLICLE DEVELOPMENT

Relatively simple mathematical techniques have been used to reveal the underlying principles governing complex signalling pathways and cellular behaviours that generate biological patterns (Stark *et al.*, 2007).

1.7.1 THE FOUNDER CELL THEORY

Moore *et al.* (1996) hypothesised that the negative correlation between fibre diameter and follicle density was a function of the size of the prepapilla, and that the number of mesenchymal cells in each prepapilla aggregate determined fibre diameter and therefore the final number of follicles in the adult sheep. It was further proposed that the number of mesenchymal cells recruited to form each follicle at initiation determined the diameter of the fibre produced (Moore *et al.*, 1998). Each initiation event was thought to deplete the original

mesenchymal cell population, with follicle formation ceasing when the committed prepapilla cells were utilised (as illustrated in Figure 1.6).

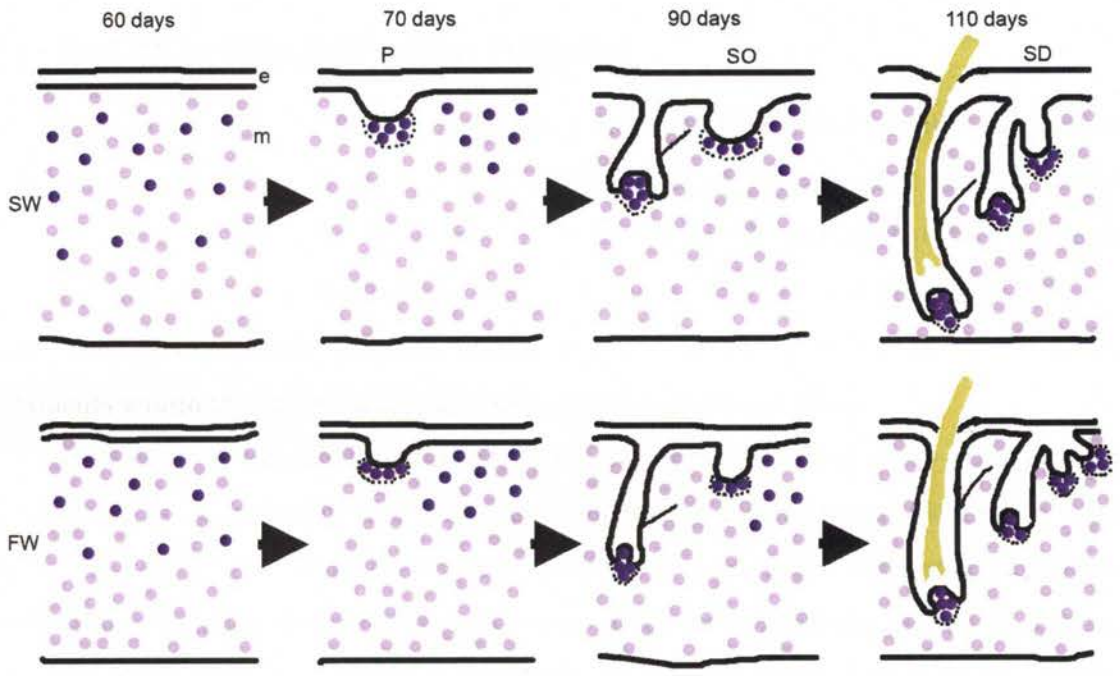

Figure 1.6: Schematic of the Founder Cell Theory of follicle development. The theory proposes that a population of committed mesenchymal cells (purple circles) among other mesenchymal cells (mauve circles) exists within the foetal mesenchyme (m) which is depleted during successive waves of follicle development, where these cells aggregate below the epidermal thickening, forming the dermal prepapilla (outlined). Follicle development occurs in successive waves from an undifferentiated epithelium (e) at d 60, to the formation of primary follicles at d 70, secondary original (SO) follicles on at d 90, and secondary derived (SD) follicles at d 110. By the end of follicle development, no committed cells remain in the m. Further, the theory proposes that more of these committed cells are incorporated into each prepapilla in a strong-woolled (SW) than in a fine-woolled (FW) line, thereby fewer follicles which produce larger fibres form in a SW line compared to a higher number of follicles and smaller prepapilla size in the FW line. Figure adapted from Moore *et al.* (1998).

The even spacing of primary follicles seen during follicle initiation is believed to be a result of pre-patterning. This may occur as a result of follicle spacing being determined prior to initiation or alternatively, each developing follicle may be surrounded by a zone of inhibition (Hardy, 1949; Lyne, 1966). In the case of pre-patterning, a sub-population of mesenchymal cells may become committed to a dermal condensate fate long before follicle initiation occurs. It is thought that mesenchymal cells are likely to be equipotent prior to the up-regulation of genes in some cells that decide the fate of those cells and possibly prevent other cells from taking on that same fate. The Notch signalling pathway is one such mechanism that may be involved in controlling the fate of mesenchymal cells at follicle initiation, through local cell-to-cell interactions (Artavanis-Tsakonis *et al.*, 1999). It was theorised that Notch signalling may act through lateral inhibition within the sheep

mesenchyme, a means by which some mesenchymal cells would signal to their neighbouring cells, due to up-regulated signalling in those cells, instructing their neighbours not to take on the same follicular fate (Bray, 1998).

1.7.2 THE REACTION-DIFFUSION THEORY

The reaction-diffusion theory, based on a biochemical reaction, is able to account for the initiation and development of wool follicles. The theory accounts for the initiation, development and alignment of trios of primary follicles, and predicts that the orientation of the trios is determined by the location of sweat glands (Mooney and Nagorcka, 1985). The system can spontaneously produce spatial patterns in the distribution of its chemical components within the epithelium (Nagorcka, 1986; Nagorcka, 1995a).

The theory was extended to account for the development of secondary original follicles. The pre-patterns generated by the theory account for the loss of sweat glands in secondary follicles, as well as the tendency of these follicles to form linear trio groups between the already-formed primary follicles, with each new generation of follicles arising in response to pre-pattern changes in the epidermis caused by the growth of existing follicles (Nagorcka, 1995b).

In common with the founder cell theory, the reaction diffusion theory states that the initial size of the dermal prepapilla is a major factor determining the size of the dermal papilla in the mature follicle bulb and, hence, fibre diameter and fibre length growth rate (Nagorcka, 1995b).

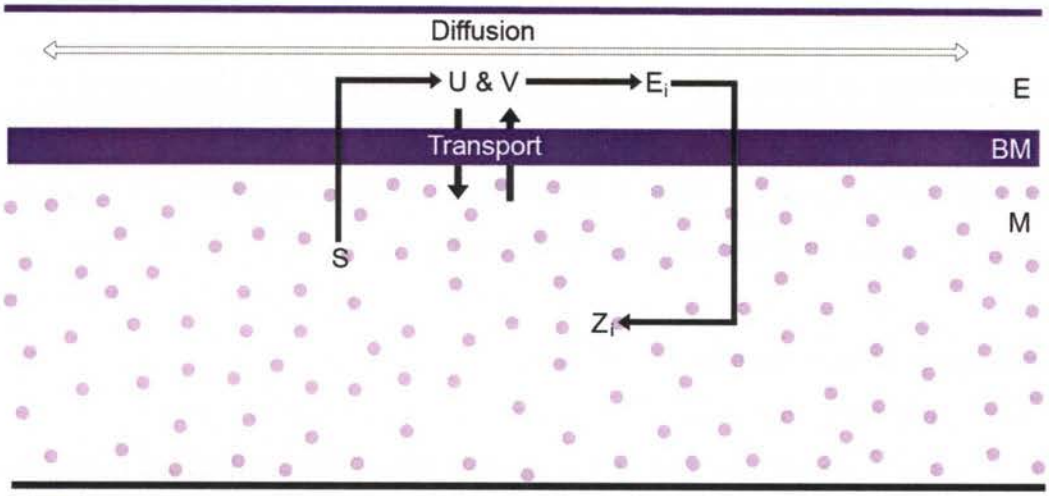

Figure 1.7: Schematic of the Reaction-Diffusion Theory of follicle development. The essential components of the pre-pattern mechanism are the chemicals (U and V) that diffuse through the epithelium (E), through the basement membrane (BM) and react with each other in a reaction-diffusion system, denoted as U & V. A mesenchymal (M) signal (S) is required to alter the reaction or diffusion rates of U and or V, so as to produce spatial patterns in the distribution of U and V. Localised high concentrations of U give rise to the epithelial factor (E_i) and mesenchymal factor (Z_i) which regulate mitotic activity of the epithelial and mesenchymal cells in a localised region (Nagorcka, 1986; Nagorcka, 1995a). Figure adapted from Nagorcka (1995a).

1.7.3 THEORY THAT FIBRE DIAMETER & FOLLICLE DENSITY ARE NOT SPECIFIED SIMULTANEOUSLY

Adelson *et al.* (1992) found the number of cells in the dermal condensates of wool follicles approximately doubled by the time the wool follicle reached maturity. They believed that the cell proliferation observed in the dermal condensate was able to account for the increase in cell number. Cell proliferation was thought to be consistent with the Reaction-Diffusion Theory (Section 1.7.2) of follicle initiation and morphogenesis.

In later work, whether the predicted inverse relationship between follicle density and fibre diameter was established at the time of wool follicle initiation was of interest (Adelson *et al.*, 2002). The amount of cell division which occurred during periods of increasing cell number was found to be sufficient to explain the observed increase in cell number within the dermal condensate. Their results suggested that local factors acting on the dermal condensate are important in regulating the ultimate size of the follicle and fibre diameter. They also found that the diameter of the wool follicle rudiment at follicle initiation was not a good predictor of the adult fibre diameter, indicating that the genes which determine fibre diameter are primarily expressed after follicle initiation has occurred (Adelson *et al.*, 2002). Thereby, the theory that wool follicle density and fibre diameter are separately during follicle development was in disagreement with the Founder Cell (Section 1.7.1) and Reaction Diffusion (Section 1.7.2) theories of wool follicle development.

1.8 GENE EXPRESSION DURING FOLLICLE DEVELOPMENT

As a consequence of the progressive process of commitment to particular pathways through cell-type specific gene expression in an embryo, differing cell populations arise and organise themselves in space (Arias *et al.*, 2002). It is likely that several signalling pathways are acting in parallel, in synergy, or in succession with one another, leading to hair follicle development (Schmidt-Ullrich and Paus, 2005).

Research into the development of hair and other ectodermal organs using mice, chick and other experimental models, has allowed for the mechanisms underlying wool follicle development to be studied. The Notch signalling pathway was shown to have a number of roles in skin and hair follicle development. Notch is thought of as the gate keeper of the commitment of epidermal cells in the basal layer to terminally differentiate (Fuchs, 2008), to be necessary for postnatal hair follicle development and maintenance (Vauclair *et al.*, 2005), and to be expressed in keratinocytes of developing human epidermis (Lowell *et al.*, 2000). Notch-2, Delta-1 and Lunatic Fringe are likely candidates for dermal papilla formation in mice (Favier *et al.*, 2000). Studies in sheep have highlighted that Notch signalling pathway genes are active during wool follicle initiation (Botto, 2000; Gordon-Thomson *et al.*, 2008). Notch and the transforming growth factor-β signalling pathways are thought to work together as tumour suppressors (Niimi *et al.*, 2007). The WNT signalling pathway is thought to act downstream of the first dermal message as a promoter of formation of the epithelial placode (Pispa and Thesleff, 2003). It has been proposed that the fibroblast growth factor, bone morphogenetic protein and epidermal growth factor signalling pathways act downstream from WNT to mediate and modulate the WNT signal, thereby contributing to the stabilisation and refinement of the patterning process of hair follicles (Sick *et al.*, 2006). Sonic hedgehog is thought to play an essential role in maintaining the integrity of hair follicles (Gritli-Linde *et al.*, 2007).

1.8.1 THE NOTCH SIGNALLING PATHWAY

The Notch signalling pathway is an evolutionarily conserved mechanism, used by metazoans, that controls the fates of various cells through local cell interactions, providing an essential intercellular communication system in a huge range of organisms, as divergent as nematodes and humans (Artavanis-Tsakonis *et al.*, 1999; Kanwar and Fortini, 2004). There is a generalisation that Notch tends to maintain cells in an "undifferentiated state" (Arias *et al.*, 2002).

In mammals, a wide variety of cells use the Notch signalling system for embryonic development and, in adults, maintenance of homeostasis. During embryonic development in mammals Notch genes are widely expressed, suggesting Notch regulates the differentiation of many different cell types (Lindsell *et al.*, 1996). The pathway also influences cell fate decisions including cell differentiation, survival/apoptosis, and cell cycling in physiologic and pathologic contexts, particularly in conjunction with stem cell behaviour (Chiba, 2006). Functional studies of Notch pathway genes in fish, frog, chick and mouse embryos have shown Notch signalling to be involved in the development of almost every organ system within the vertebrate body (Weinmaster and Kintner, 2003). Notch signalling has been found to play a role in long-term survival, growth and stem cell maintenance, and tumour suppression in mice (Pan *et al.*, 2004). At this point in time, Notch signalling is believed to play an important role in the transition between basal and suprabasal epidermal cells, functioning as the gatekeeper of commitment of basal epidermal cells to terminally differentiate (Fuchs, 2008).

Only a few target genes downstream of Notch are known. These are members of the HES (Hairy/Enhancer of Split) family of basic helix-loop-helix transcriptional regulators and were identified through neurogenesis studies in mammals (Miele and Osborne, 1999; Kopan, 2002).

1.8.1.1 The Notch receptors

The 4 mammalian Notch receptors, Notch-1 to -4, are type I transmembrane proteins comprised of a series of characteristic structural motifs, illustrated in Figure 1.8. Notch receptors consist of an extracellular domain, a transmembrane domain, and an intracellular domain. The extracellular region consists of a number of epidermal growth factor (EGF)-like-tandem repeats, a juxta-membrane negative regulatory region that consists of 3 membrane-proximal Lin12/Notch/Glp-1 (LNG) repeats (Rebay *et al.*, 1991), and a heterodimerisation domain that is important in maintaining Notch receptors in the 'off' state (Roy *et al.*, 2007). Notch-1 and Notch-2 contain 36 EGF-like repeats, Notch-3 contains 34, and Notch-4 contains 29. Some of these repeats serve as a ligand-binding site (Chiba, 2006), binding to the DSL family of transmembrane ligands. For example, in *Drosophila* EGF-repeats 11 and 12 on Notch are required for binding to Delta and Serrate on adjacent cells (Baron *et al.*, 2002). Interspecies sequence comparisons have shown that 3 areas of homology exist within EGF-repeats 11-13, 23-27 and 31-34 of *Drosophila* Notch. These similarities suggest that these regions may form functional subdivisions of the Notch extracellular domain (Wesley, 1999).

The intracellular domain consists of 4 distinct regions, the RBP- Jκ–associated molecule (RAM) domain, ankyrin repeats (7), a transcriptional activator domain (TAD) and C-terminal proline, glutamate, serine, threonine (PEST) sequence (Baron, 2003). The PEST domain contains a structural motif that targets the Notch protein for recognition by cellular degradation machinery (Roy *et al.*, 2007).

Optimal activation of Notch is achieved via integration of the ankyrin and TAD (Notch-1 and -2 only) domains with a specific enhancer sequence (Ong *et al.*, 2006). The RAM domain associates with CBF-1/Supressor of Hairless/Lag-1 (CSL) protein, the ankyrin repeat region associates with proteins to form a complex. PEST negatively regulates the half-life of Notch proteins. The heterodimerisation domains in the extracellular and transmembrane regions of Notch consist of 103 and 65 amino acids respectively (Chiba, 2006). C promoter-binding protein-1 (CBF-1) is the transcription factor activated by Notch. It is also known as Suppressor of Hairless in the fly, Lag-1 in the worm, and RBP-Jκ in mammalian cells (Buono *et al.*, 2006; Roy *et al.*, 2007). RBP-Jκ-mediated Notch signalling was proposed to regulate cell fate specification of hair follicle stem cells at the bulge region, and results have suggested that Notch-1 signalling is essential for postnatal hair follicle development and homeostasis (Vauclair *et al.*, 2005).

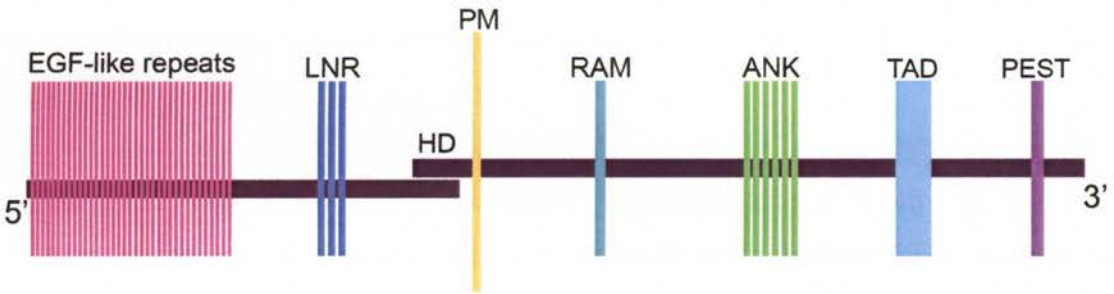

Figure 1.8: The protein structure of the Notch-1 receptor. The receptor is bound to the plasma membrane (PM) of a cell. It is comprised of 36 epidermal growth factor (EGF)-like-repeats; 7 ankyrin repeats (ANK); a heterodimerisation domain (HD); 3 Lin-Notch repeats (LNR); a PEST domain (PEST); a RBP-Jk-associated molecule (RAM) domain; trans-activation domain (TAD). Figure modified from Botto (2000) and Chiba (2006).

The phenotype observed in conditional Notch-1 knockout transgene expression driven by the keratin 14 promoter in keratinocytes in (N1KO-K14Cre) mice suggested that Notch-1 function is dispensable for placode formation but necessary for postnatal hair follicle development during the first growth cycle (Vauclair *et al.*, 2005).

Research has demonstrated the divergent roles of the Notch receptors during development in mice. Mice homozygous for targeted mutations of Notch-1 (Swiatek *et al.*, 1994) and Notch-2 (Hamada *et al.*, 1999) genes died during embryogenesis. The Notch-3

gene was found to be non-essential for embryonic development and fertility in mice (Krebs *et al.*, 2003). Notch-4-deficient mice were fertile and viable as homozygotes (Krebs *et al.*, 2000).

1.8.1.1.1 Proteolytic processing of Notch

Although the Notch signalling pathway appears to be generally activated through cell-cell interactions, proteolytic cleavage of both receptors and ligands has been shown to be important for signalling (Six *et al.*, 2003).

1.8.1.1.1.1 Site 1 cleavage

Notch is synthesised in the endoplasmic reticulum of a cell, before the receptor is transported through the secretory pathway to the trans-Golgi Network, where it is constitutively cleaved at the extracellular site (RXR/KR) by a Furin-like protease (Le Borgne and Schweisguth, 2003), known as site 1 (S1) cleavage, yielding an 180kDA fragment (Kopan, 2002). The resulting halves of Notch, the ligand-binding and transmembrane subunits (Roy *et al.*, 2007), are non-covalently bound together by a calcium-dependent interaction in the heterodimerisation domain (Rand *et al.*, 2000). Notch is then transported to the cell surface (Hansson *et al.*, 2004). Following the series of proteolytic cleavages, the Notch gene encodes a 300 kDa transmembrane receptor (Bianchi *et al.*, 2006).

1.8.1.1.1.2 Site 2 cleavage

Site 2 (S2) cleavage occurs at the plasma membrane after a Notch receptor on a cell binds to a ligand on an adjacent cell, through their DSL domains. The receptor-ligand interaction, causes cleavage by TNF-α-converting enzyme (TACE), also known as ADAM17 (Bray, 2006). The extracellular domain of Notch is shed (Chitnis, 2006), releasing the membrane-tethered intracellular domain of Notch, an event thought to be dependent on a member of the ADAM metalloprotease family, such as Kuzbanian (Baron, 2003), also known as ADAM10 (Bray, 2006).

Interestingly, studies have demonstrated that Notch and its ligands undergo the same ectodomain processing, by the same molecular machinery and suggest that the regulated intramembrane proteolysis of both receptor and ligand may play important, potentially competitive roles in cell signalling (LaVoie and Selkoe, 2003).

1.8.1.1.1.3 Site 3 cleavage

Site 3 (S3) cleavage is a constitutive intramembranous cleavage event, mediated by Presenilin-dependent γ-secretase activity (Baron *et al.*, 2002), which releases the soluble intracellular domain of Notch. Cleavage of the extracellular domain of Notch is not believed to be a regulated process (Schweisguth, 2004). In mammals, the homologous proteins Presenilin-1 and Presenilin-2 (Geling *et al.*, 2002) are associated with a large complex of proteins which make up γ-secretase activity. These proteins cleave the amyloid precursor protein within the transmembrane domain (Baron, 2003). Presenilin-1 is required for efficient processing of Notch-1 to produce the Notch intracellular domain, and is inhibited by γ-secretase inhibitors (De Strooper *et al.*, 1999). Crumbs reduces the activity of the γ-secretase complex, which mediates the proteolytic intracellular processing of Notch (Herranz *et al.*, 2006).

The intracellular domain of Notch translocates to the cells nucleus where it acts as a transcriptional regulator, binding via its RAM domain and ankyrin repeats to activate CSL proteins. Binding displaces a histone deacetylase, allowing the recruitment of acetylases and Mastermind, which together activate Notch transcription (Weinmaster and Kintner, 2003; Chitnis, 2006; Roy *et al.*, 2007).

1.8.1.1.1.4 Site 4 Cleavage

The recently identified cleavage site 4 (S4) is located in the centre of 4 sequential alanine residues. Valine is dispensable for determining the cleavage site of Notch-1, and affects its cleavage precision. Valine residues are important in substrate recognition of the γ-secretase complex and constitution of the enzyme-substrate complex (Tanii *et al.*, 2006).

1.8.1.2 Ligands of the Notch pathway

Signalling by the Notch receptor is activated by DSL ligands (Fleming, 1998) through direct cell-to-cell interactions. They have been characterised by sharp boundaries formed between cells expressing one or the other. The ligands were expressed in a punctate manner, in which individual cells expressed different levels of these ligands, suggesting their expression may have a role in establishing, defining and maintaining regionalisation within tissues in the developing embryo (Lindsell *et al.*, 1996). For example, Delta-1 provides a positive signal for haematopoietic development into the plasmacytoid dendritic cell lineage by augmenting the proportions and absolute numbers of plasmacytoid dendritic cells produced from the progenitor cells (Olivier *et al.*, 2008).

These ligands are modified through ubiquitination, with important consequences for signalling (Le Borgne and Schweisguth, 2003).

The Notch family of ligands, like their receptors, are all cell-surface type I transmembrane proteins (Schweisguth, 2004). Notch and Delta interact with each other through their repeated EGF-like domains. As illustrated in Figure 1.9, there are differences in the size and structure of the DSL ligands within and between species. Delta and Jagged signal in vertebrates, whereas Serrate (the invertebrate form of Jagged) is found in *Drosophila.* Jagged and Serrate contain a cysteine-rich region (CRR) following the EGF-like repeats. These domains do not share significant homology (Lindsell *et al.*, 1995). Regardless of structural differences, the ligands share functional similarities that are evident in their ability to substitute for each other when mutations occur (Fleming, 1998). Expressed sequence tags (ESTs) for Delta-1 have been isolated from ovine skin and these have been compared to the known human Delta-1 sequence (Figure 1.10).

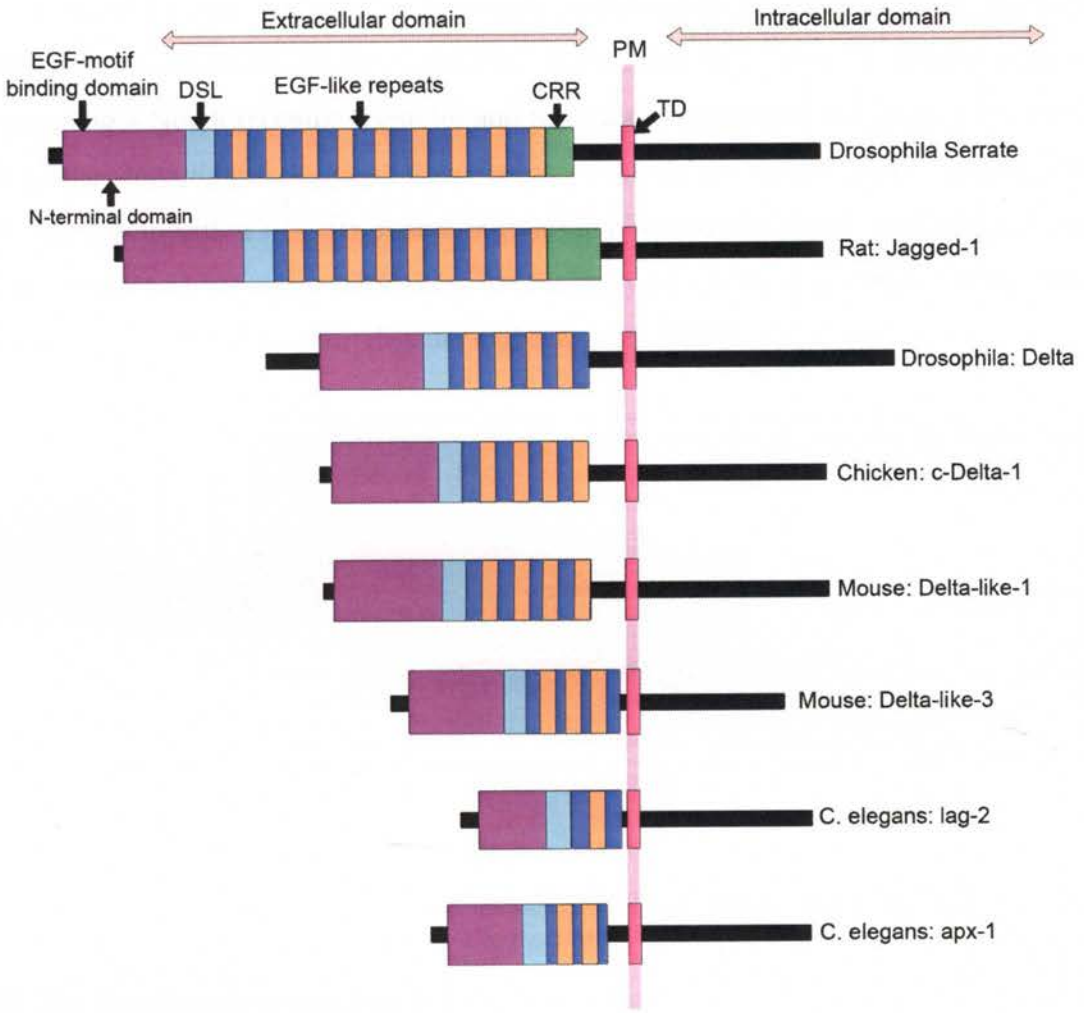

Figure 1.9: Conserved domains of the Delta/Serrate/Lag-2 (DSL) ligands in different species. Within the extracellular domain, the EGF-motif binding region consists of the N-terminal domain and the DSL domain. The cysteine-rich region (CRR) is unique to Serrate-like homologs. The ligands are all bound to the plasma membrane (PM) of a cell and therefore all have a transmembrane domain (TD). The intracellular domain of the ligands is highly variable in sequence and length amongst the homologs. Figure adapted from Fleming (1998).

Figure 1.10: Comparison of human and ovine Delta -1 sequences. The human Delta-1 sequence (hDll1) is 3158 nucleotides long with coding sequences (CDS) located in positions 318-2490. Two ovine ESTs homologous to the human sequence have been identified. They are 857 and 614 nucleotides long and are located on either the 5' or 3' end of the human homologue. The numbers above the diagram show the stop and start positions of high sequence similarity. The blue area signifies an area with no significant homology, the green areas illustrate some homology, the pink areas signify areas of high homology. Diagram courtesy of Zhidong Yu and Alan Pearson, AgResearch, New Zealand.

The Delta ligands contain 6-8 EGF repeats, whereas the Jagged ligands contain 16 (Weinmaster and Kintner, 2003). Notch signalling is important in all tissues and the beneficial

effects of Notch ligands may involve responses in cells of the vascular, immune and nervous systems. Delta is a transmembrane ligand that only affects the activity of adjacent cells which are expressing a Notch receptor (Heitzler and Simpson, 1991), refer to Figure 1.11. The DSL region on the Delta ligand (Figure 1.9) serves as a binding site for the Notch receptor (Chiba, 2006). The juxtaposition of cells expressing varying amounts of ligand and receptor suggest that a cell is able to become a "signalling" cell simply by expressing a higher level of ligand relative to its neighbouring cells (Heitzler and Simpson, 1991).

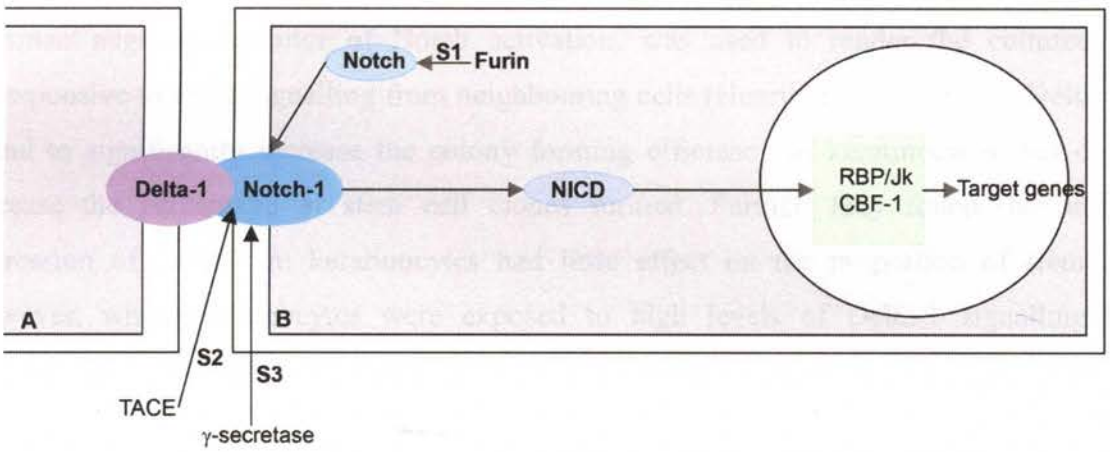

Figure 1.11: Schematic of a simplified version of the Notch signalling pathway. The Notch receptor is processed in the Golgi apparatus of cell B and undergoes Furin-mediated S1 cleavage before the receptor is made available on the cell surface. The Delta-1 ligand on the surface of cell A then binds to the Notch-1 receptor on adjacent cell B. This ligand-receptor binding triggers the S2 and S3 cleavages of Notch, before the Notch intracellular domain (NICD) translocates to the cell nucleus (cell B) and the downstream target genes are activated.

1.8.1.2.1 Processing of Delta

Delta-1 is constitutively cleaved, first by an ADAM metalloprotease at a site 10 amino acids N-terminal to the transmembrane region. Impairment of ADAM cleavage prevents the appearance of the intracellular domain. Delta-1 is then cleaved by a γ-secretase-like protease that releases the intracellular part of the molecule, which translocates to the nucleus. The location of the γ-secretase cleavage site has not been determined, but it is of interest that a conserved Val residue is present 4 amino acids N-terminal to the end of the transmembrane region of Delta orthologs, a position identical to the Val residue recognised by γ-secretase during Notch cleavage (Six *et al.*, 2003), as discussed in Section 1.8.1.1.1.4.

1.8.1.3 Expression of Notch pathway genes in skin

Notch-1 was found to be expressed in all living layers of keratinocytes in the developing human epidermis (Lowell *et al.*, 2000). Botto (2000) showed that Notch pathway

genes were active during wool follicle initiation and development in sheep foetuses, and appeared confined to the epidermis and cells derived from the epidermis. Expression of Jagged-1 and Jagged-2 was primarily detected in the epidermis.

Notch signalling during epidermal differentiation appeared to promote cell differentiation. Notch expression in keratinocytes stimulated the expression of differentiation markers, and activated Notch-1 reduced cellular proliferation. The levels of Delta-1 expression were lower in keratinocytes in the epidermal basal layer where stem cells reside, but elevated levels of Delta promoted the stem cell phenotype (Lowell *et al.*, 2000). Delta^{T}, a dominant-negative inhibitor of Notch activation, was used to render the cultured cells unresponsive to Delta signalling from neighbouring cells (Henrique *et al.*, 1997). Delta^{T} was found to significantly increase the colony forming efficiency of keratinocytes, but did not increase the percentage of stem cell clones formed. Further, they found that uniform expression of Delta-1 in keratinocytes had little effect on the proportion of stem cells. However, when keratinocytes were exposed to high levels of Delta-1 signalling from neighbouring cells, their proliferative potential was strongly reduced (Lowell *et al.*, 2000).

1.8.1.4 Expression of Notch pathway genes in hair and wool formation

Both Jagged-1 and Jagged-2 were found to be expressed in the embryonic epidermis and in the epidermal component of the developing hair follicles in vertebrates (Powell *et al.*, 1998). It is possible that Notch signals promote the selection of hair formation in bulge stem cells (Chiba, 2006). Use of a Cre-lox system in mice demonstrated that Notch signalling inhibited stem cells in the hair follicle bulge from differentiating into epidermal cells, instead promoting hair formation (Yamamoto *et al.*, 2003).

The investigations of Favier *et al.* (2000) found that during mouse embryogenesis Notch-2, Delta-1 and Lunatic Fringe genes were likely required for dermal papilla formation. Delta-1 expression was localised in the early dermal condensation. Lunatic Fringe and Notch-1 expression were also found in the dermal condensation, while Notch-2 was found in the mesenchyme. Notch-1, Jagged-2 and Lunatic Fringe may have a role in the patterning of epidermal cells, and forming the hair placode. Delta-1 was an indicator of mesenchymal cell segregation between the dermal condensation and the interfollicular dermis, the latter expressing Notch-2. In the epidermal compartment of the hair follicle, Notch-1 was localised to the inner placode cells and Jagged-2 to the outer placode cells. The receptor–ligand interactions occurring were believed to be Notch-2 and Delta-1 in the dermis, and Notch-1 and Jagged-2 in the epidermis (Favier *et al.*, 2000).

In advanced hair placodes, Jagged-1 expression parallelled Notch-1 expression in the inner placode cells. In contrast, Jagged-2 was expressed in the presumptive outer root sheath cells, the basal cells and the inner placode cells (Powell *et al.*, 1998).

During wool follicle development, similarities in localisation of expression patterns of Notch-1 and Jagged-1 in skin, with samples ranging from d 60 of gestation to adult skin, were taken to suggest a functional receptor-ligand relationship (Gordon-Thomson *et al.*, 2008). On d 70 of development in wool follicle primordia, Notch, Jagged and CBF-1 transcripts were localised to the cells located at the end of the distal tip of the epidermal plug (Botto, 2000; Gordon-Thomson *et al.*, 2008).

1.8.1.5 Expression of Notch pathway genes in feather development

The embryonic chick feather buds are hexagonally arranged and arise progressively in tracts. This pattern is thought to be set up from signals in the dermis which influence the epidermis. Furthermore, feather development is dependent on reciprocal interactions between the dermis and the epidermis (Crowe *et al.*, 1998).

Notch-1 and Notch-2 mRNAs are expressed in the skin in a localised pattern prior to the initiation of the feather bud. In the early stages of feather bud development, Delta-1 and Notch-1 were transcribed in the dermis where they localised to the forming feather buds (Favier *et al.*, 2000). Notch-2 expression was excluded from the bud. A precise patterning of Delta-1 expression in chick dermal cells precedes and coexists with the early stages of feather morphogenesis. A disruption of this patterning leads to inhibition of feather morphogenesis (Viallet *et al.*, 1998). As the feather bud elongates through the dermis, the expression levels of Delta-1 decreased, whereas Notch-1 and Serrate-2 were expressed in stripes orientated from the feather base to tip (Crowe *et al.*, 1998).

1.8.1.6 Mechanisms of Notch signalling

The existence of different modes of Notch signalling implies that the ligands can act by activating or blocking Notch signalling, depending on whether the cells express the ligand and receptor or one cell expresses the ligand and another the receptor (Pourquié, 2000). Different cell types express unique tissue-specific components that are capable of modulating the Notch receptor signal from a neighbouring cell, suggesting that a number of pathways which regulate Notch activity by potentiating or restricting the cells response may be involved (Fleming, 1998). For example, Delta prefers to bind to Fringe-modified Notch, whereas Jagged prefers to bind to the unmodified form of Notch. Fringe acts within the Golgi

apparatus as an N-acetylglucosaminyltransferase and adds GlcNAc groups to O-linked fucose attached to specific EGF-like repeats in the Notch extracellular domain (Bruckner *et al.*, 2000), glycosylating the extracellular EGF-like repeats of Notch, thereby enabling Notch to be activated by Delta (Peterson and McClay, 2005). It has been suggested that Fringe modulates Notch signalling by enzymatically modifying Notch receptors, Notch ligands, or some essential accessory factor (Panin and Irvine, 1998), and may specifically target EGF-12 on the Notch receptor (Lei *et al.*, 2003). The preferences for ligand binding to modified or unmodified Notch receptors provides the basis for Notch hyper-activation at boundaries between Fringe-expressing and non-expressing cells (Kopan, 2002). In many cases it is the distribution of Fringe glycosyltransferases rather than of Notch receptors or their ligands, that is the key determinant of where Notch signalling will be active (Haines and Irvine, 2003). Notch signalling is involved in cell fate specification in developing tissues for which three different patterning mechanisms are utilised, as discussed below.

1.8.1.6.1 THE ROLE OF NOTCH SIGNALLING IN CELL FATE SPECIFICATION AND PATTERNING

1.8.1.6.1.1 Lateral inhibition

In the context of lateral inhibition, illustrated in Figure 1.12, Notch signalling facilitates competitive interactions between cells. Notch signalling is dependant on DSL ligand-regulated binding of the extracellular domain of Notch (Chitnis, 2006). All cells within the group initially express the same ligand and receptor and have the ability to signal to one another. With time, one cell signals to the other signal-receiving cells, inhibiting them from adopting the same fate, so that adjacent cells adopt different cell fates because of negative regulation. Thus, adjacent cells with similar potential adopt different fates, regulating cell diversity in a developing tissue (Bray, 1998; Lewis, 1998; Simpson, 1998; Chitnis, 2006). This signalling mechanism is utilised in the development of epithelial cells into neural cells in *Drosophila*, by preventing neighbouring cells from developing the same (Myat *et al.*, 1996). They showed that Delta-Notch signalling prevented proliferating neuroepithelial cells from differentiating prematurely, acting as a negative feedback loop to limit the rate of conversion of proliferative precursor cells into non-proliferative differentiating cells, allowing neurogenesis in the chick to continue for days. It was also suggested that the gene products of Neuralized and Snail may participate in the regulation of Delta endocytosis during lateral

inhibition, thereby promoting activation of Notch in neighbouring cells (Morel and Le Borgne, 2003).

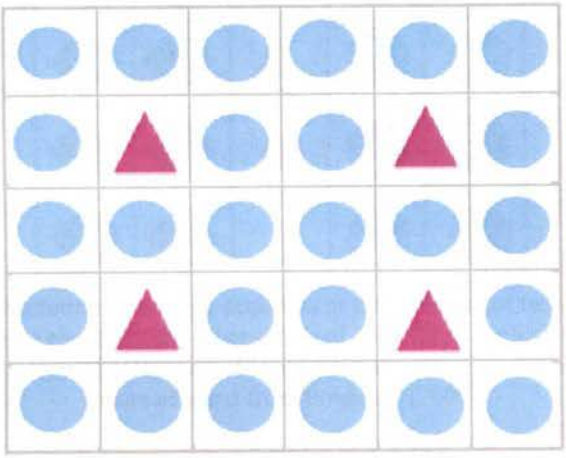

Figure 1.12: Schematic representation of lateral inhibition in a group of cells during Notch signalling. Cells expressing high levels of a Notch ligand (Delta; pink triangles) stimulate activation of the Notch receptor in the surrounding cells (blue circles), so that only the Delta-bearing cells are able to differentiate. Image adapted from Pourquié (2000).

1.8.1.6.1.2 Lineage decisions

Lineage decisions, illustrated in Figure 1.13, involve specific responses at the interface of two different cell populations. This mechanism involves the interaction of two cell populations that use different ligands from each other (for example Delta-1 and Jagged-1) and additional molecules (such as Lunatic Fringe) that make the cells insensitive to the ligand produced by like cells. Up-regulation of the ligand is caused by activation of the Notch receptor. All the cells within a group of cells cooperatively make cell fate choices, and the cells undergo an all-or-none formation along the sharply defined boundaries of gene expression (Lewis, 1998). This type of signalling is observed along the wing margin of *Drosophila* (Simpson, 1998).

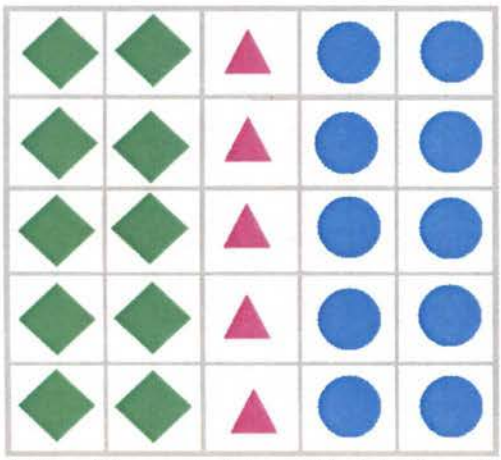

Figure 1.13: Schematic representation of lineage decisions at the interface of two distinct groups of cells. One cell population (green diamonds) signals to the other group of cells (blue circles), resulting in the formation of a differentiated group of cells (pink diamonds) at the interface of the two groups.
Image adapted from Pourquié (2000).

1.8.1.6.1.3 Boundary definition

In the case of boundary definition, illustrated in Figure 1.14, Notch activation works using positive feedback. Cells that receive a Notch signal produce the Notch ligand and activate the cells on the opposite side of the boundary, keeping the two populations of cells distinct from each other (Bray, 1998). Activation occurs in those cells not expressing the ligand, located at the periphery of the cell cluster (Pourquié, 2000). This form of signalling can be observed during establishment of the dorsal-ventral boundary in the wing imaginal disk (Irvine, 1999) and in the development of the hindgut (Fuβ and Hoch, 2002) in *Drosophila*. For this mechanism to work, the dorsal cells use Fringe to create an asymmetry between the two cell populations and to promote activation of Notch in the cells at the cell boundaries (Kim *et al.*, 1995; Panin *et al.*, 1997). Fringe contributes to the spatial and temporal patterns of Notch activation signals by determining where each ligand is able to activate Notch (Peterson and McClay, 2005). Notch is hyper-activated when Fringe-expressing and Fringe-non-expressing territories lie adjacent to one another, forming a boundary (Irvine and Rauskolb, 2001).

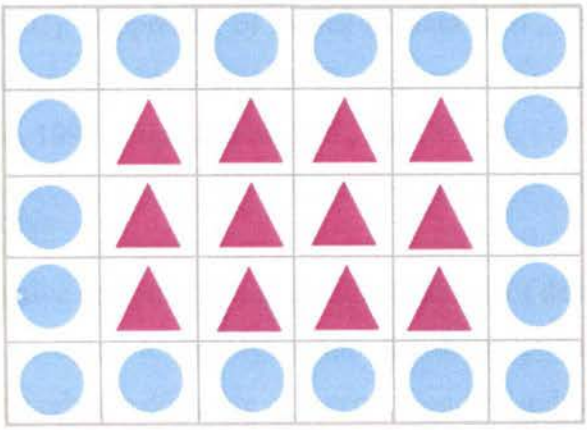

Figure 1.14: Schematic representation of boundary formation during Notch signalling. Notch activation is prevented in clusters of cells that express the Notch ligand (pink triangles). Activation occurs in cells not expressing the ligands, located at the periphery of the cell cluster (blue circles). Adapted from Pourquié (2000).

1.8.1.8 Methods of regulating Notch signalling

1.8.1.8.1 Ubiquitination

Ubiquitin has been identified as a tag for proteins that are destined for degradation, providing a signal for endocytosis (Bonifacino and Weissman, 1998). Ubiquitination of proteins serves to regulate protein function by targeting the ubiquitinated substrates to specific cell organelles (Hershko and Ciechanover, 1998). Notch internalisation appears to modulate pathway activity by controlling steady-state levels of Notch at the cell surface and preventing its inappropriate activation in the absence of ligand binding (Kanwar and Fortini, 2004).

Ubiquitination also serves as a signal for the internalisation of DSL gene products. Endocytosis of the DSL ligands activates Notch, most likely by assisting to remove the extracellular domain of Notch. The recycling of DSL ligands is also critical for their functioning. Factors that regulate DSL ligand and Notch endocytosis, recycling, and degradation play a critical role in biasing the outcome of Notch signalling (Chitnis, 2007). Neuralized ubiquitinates Delta, promoting its endocytosis and potentiating its ability to activate Notch (Boulianne *et al.*, 1993; Le Borgne and Schweisguth, 2003).

Following binding of Delta to Notch, Neuralized adds ubiquitin to the intracellular domain of Delta and triggers Epsin-dependent endocytosis of the ligand, triggering a conformational change in Notch that allows S2 cleavage of the receptor to occur, and the extracellular domain is trans-endocytosed to the ligand-expressing cell, allowing Presenilin to perform S3 cleavage of Notch (Kopan, 2002; Kanwar and Fortini, 2004). Other proteins that mark Notch for ubiquitination include Deltex, a positive regulator of the Notch signalling

pathway (Baron *et al.*, 2002), Suppressor of Deltex (Sakata *et al.*, 2004; Wilkin *et al.*, 2004), and Sel-10 which was originally identified in *C. elegans* as a negative regulator of Notch signalling (Hubbard *et al.*, 1997; Gupta-Rossi *et al.*, 2001).

1.8.1.8.2 Endocytosis

Internalisation of active receptors is a known mechanism of desensitisation that involves transporting the active receptor to the lysosome for degradation. The Notch signalling pathway is sensitive to the relative dose rate of receptors and ligands at the cell surface (Baron *et al.*, 2002) and it is believed that endocytosis of Delta facilitates Notch activation, a possible requirement for signal transduction (Le Borgne and Schweisguth, 2003).

Endocytosis and recycling may serve as a mechanism for returning unbound Delta to the cell surface, a common strategy for re-sensitising receptors following interaction with agonists (Chitnis, 2006). Eventually, the regulation of endocytosis and the recycling of DSL ligands contribute to the effective delivery of a signal to neighbouring cells. The factors that regulate these trafficking events may influence the outcome of Notch signalling (Chitnis, 2007).

Endocytosis and signalling of Delta are mediated by Epsin (Kanwar and Fortini, 2004; Chitnis, 2007), Mindbomb (Le Borgne and Schweisguth, 2003; Weinmaster and Kintner, 2003; Herranz *et al.*, 2006) and Shibire (Baron *et al.*, 2002). Endocytosis of Notch was believed to be caused by Numb (Guo *et al.*, 1996; Baron *et al.*, 2002; Roegiers and Jan, 2004) to promote asymmetric cell division and the responsiveness of neighbouring cells to Notch (Heitzler and Simpson, 1991; Carson *et al.*, 2006). Similarly, Sanpodo is required for Notch signalling during asymmetric cell division (Skeath and Doe, 1998). Sanpodo positively regulates Notch signalling at the plasma membrane, with regard to Numb-regulated cell fate decisions (O'Connor-Giles and Skeath, 2003; Hansson *et al.*, 2004).

1.8.1.9 The Notch signalling pathway and disease

Each Notch family member has been implicated in a clinical disorder (Nakazawa *et al.*, 2001). Mammalian Notch-1 was originally identified in oncogenes responsible for acute T cell lymphoblastic leukaemia (Ellisen *et al.*, 1991), caused by a breakage on human chromosome 9, where a translocation within a Notch-1 intron occurs. This finding suggested a role for Notch-1 in the differentiation of T-cell lymphocytes (Joutel and Tournier-Lasserve, 1998). The product of feline leukaemia virus/Notch-2 recombinant provirus caused thymic lymphoma in infected cats (Rohn *et al.*, 1996). Mutations in Notch-3 are associated with the

inherited stroke and dementia syndrome cerebral autosomal-dominant arteriopathy with subcortical infarcts and leukoencephalopathy (CADASIL) (Joutel *et al.*, 1996). Notch-4 is up-regulated in mouse mammary tumour virus, which induces breast cancer (Robbins *et al.*, 1992). Other known disorders include Tetralogy of Fallot, Alagille Syndrome, an autosomal dominant condition that is a common genetic cause of childhood chronic liver disease believed to be caused by a defective Jagged-1 gene (Joutel and Tournier-Lasserve, 1998), and spondylocostal dysostosis in humans which is thought to be caused by mutations in Delta-3, Mesp-2 or Lunatic Fringe (Dunwoodie *et al.*, 2002; Sparrow *et al.*, 2006).

1.8.2 INTERACTIONS BETWEEN NOTCH AND OTHER SIGNALLING PATHWAYS

By working together with other signalling systems that can bias the outcome of cell fate decisions, Notch signalling can facilitate the specification of the unique fates to cells with single-cell precision in a distribution that could not have been reliably achieved by either Notch signalling or the biasing mechanism alone (Chitnis, 2007). Notch has been found to cooperate with the fibroblast growth factor (FGF), Ras/MAP kinase, transforming growth factor-β/bone morphogenetic protein (TGF-β/BMP) and Wnt pathways (Hansson *et al.*, 2004).

The formation of epithelial placodes in response to the first dermal signal involves activation of EDA/EDAR signalling in the epithelium, followed by epithelial Wnt signalling, and subsequent activation of BMP signalling (Millar, 2002). The actions of EDA/EDAR and Wnt promote placode formation, whereas BMP signalling represses placode fate in adjacent skin. FGF signalling was also found to promote placode fate, and regulate expression of Delta-1 (Millar, 2002). Research has provided evidence of a direct interaction between Notch and BMP signalling pathways, and indicate that Notch has a crucial role in the execution of certain aspects of BMP-mediated differentiation control (Dahlqvist *et al.*, 2003).

1.8.3 THE WNT SIGNALLING PATHWAY

The Wnt protein family, regulate many developmental processes. Ligands, such as Wingless, activate Frizzled receptors and, through Dishevelled, induce an increase in cytoplasmic β–catenin by preventing its degradation in proteosomes (Barker *et al.*, 2000). Thereby, Wnt signalling regulates β-catenin at the level of protein stability (Wodarz and Nusse, 1998). Wnt signalling blocks Notch directly via the Abruptex domain (Wesley and Saez, 2000) or, indirectly acts by stimulating Dishevelled to block glycogen-synthase kinase 3

(GSK-3), or to circumvent the Deltex/Notch interaction (Kopan, 2002). GSK3β-mediated phosphorylation appears to stabilise the Notch Intracellular Domain and to potentiate its activity in the cell nucleus (Schweisguth, 2004).

Evidence suggests that Wnt paracrine signalling molecules act early in the process of follicle formation to promote placode fate. Wnt and platelet-derived growth factor-A molecules are strong candidates as components of the first epithelial signal inducing formation of the dermal condensate. Wnt signalling appears to act downstream of the first dermal message as a promoter of placode formation (Pispa and Thesleff, 2003). It was proposed that the FGF, BMP and EGF pathways, which appear to act downstream of Wnt, mainly mediate and modulate Wnt signals, thereby contributing to the stabilisation and refinement of the hair follicle patterning process (Sick *et al.*, 2006). Wnt signalling was recently found to be required in epidermal keratinocytes for hair follicle regeneration following wounding in mice (Ito *et al.*, 2007). Wnt signalling is thought likely to be required for induction of the dermal condensate. Whereas, Shh acts later in follicle morphogenesis, is dependent on Wnt signalling and is required for proliferation of follicular epithelium and development of the dermal condensate into a dermal papilla (Millar, 2002). Activation of the Wnt signalling pathway may be required for generation of the first dermal message in chick dorsum, for initiation of formation of vibrissa follicles, and for development in the early stages of the majority of pelage follicles. Wnt proteins are also required in the formation of tooth and mammary gland buds (Andl *et al.*, 2002). The canonical Wnt pathway is required at the induction stage and in mature murine hair follicles to yield the normal complement of different hair types. Further, Wnt and ectodysplasin signalling affects the molecular asymmetry of the hair bulb in all murine hair (Hammerschmidt and Schlake, 2007).

A number of Wnt family members are expressed in distinct patterns and stages in the developing skin of mammals and birds. These include Wnt3, Wnt3a, Wnt4, Wnt5a, Wnt7a, Wnt10a and Wnt10b. Specific Wnts maintain anagen gene expression *in vitro* and mediate hair inductive activity in organ culture (Kishimoto *et al.*, 2000). It is known that Wnt1, Wnt3a and Wnt5a are expressed in feather primordia, while Wnt11 is expressed in the inter-bud dermis region. The expression patterns of these genes are believed to play a role in controlling the shape of the feather bud. Wnt7a is involved in the anterior-posterior orientation of the feather primordia, during outgrowth of the feather bud (Chang *et al.*, 2004). Wnt1 from the dorsal neural tube has been shown to induce the specification of dermal progenitors from the dorsal dermomyotome. The dermal precursors express Wnt11, which may be implicated in their migration to the sub-ectodermal space (Olivera-Martinez *et al.*, 2004).

There is a direct interaction between Smad7 and the Wnt/β-catenin pathway via recruitment of Smurf2 for β-catenin degradation, which affects hair follicle and sebaceous gland morphogenesis. The maintenance of low levels of Smad7 in the skin is required to allow the balanced signalling between Wnt/β-catenin and hedgehog pathways for normal hair follicle and sebaceous gland development and regeneration (Han *et al.*, 2006).

There is a possibility that Shh and Wnt pathways play distinct, and perhaps interwoven functions, in hair follicle morphogenesis, cycling, and/or patterning in mammalian skin (Gat *et al.*, 1998).

1.8.3.1 β-Catenin

β–catenin activity was discovered to act genetically downstream of Tabby and Downless during placode formation in mice. BMP and Shh were found to act downstream of β–catenin (Huelsken *et al.*, 2001).

Nuclear localisation of β-catenin has been observed in the dermis, underlying the chick feather tract 2 days before feather placodes were visible (Noramly *et al.*, 1999).

Transient β-catenin stabilisation may be a key player in the long-sought epidermal signal leading to hair development and implicate aberrant β-catenin activation in hair tumours (Gat *et al.*, 1998).

β-catenin played a double role in hair follicle formation in the mouse; it is essential during the formation of hair placodes during embryogenesis and is required for the differentiation of skin stem cells in the adult (Huelsken *et al.*, 2001).

T-cell factor/lymphoid enhancer factor (Tcf/Lef) are a group of closely related transcription factors that are the functional effectors of the Wnt pathway (Roy *et al.*, 2007). Tcf-3, like Lef-1 is a downstream mediator involved in the Wnt signalling pathway (Pispa and Thesleff, 2003).

1.8.3.2 Lymphocyte enhancer factor-1 (LEF-1)

Lef-1 is an architectural protein chaperoning a number of distinct factors controlling transcription of target genes (Boras-Granic *et al.*, 2006). It is useful as a hair germ marker (Yi *et al.*, 2006). In the context of the canonical Wnt-signalling cascade, complexes of Lef-1 and the transcriptional repressors, such as Groucho, are replaced by Lef1-β-catenin containing complexes, resulting in activated transcription of Wnt-target genes (Behrens *et al.*, 1996). Lef-1 is a downstream mediator in the Wnt signalling pathway. Wnt signalling, mediated by Lef-1, is likely to regulate the expression of the hair keratins as the hair keratin promoters

contain Lef-1 binding sites and Lef-1 is expressed within the hair matrix (Pispa and Thesleff, 2003). Lef-1-mediated Wnt signalling is thought to lie upstream of the Hedgehog-signalling pathway (Boras-Granic *et al.*, 2006).

The expression pattern of Lef-1 suggest it may have a positive role in early hair follicle morphogenesis (Fuchs, 2001), with its mRNA detected in the ectodermal placodes at the sites of follicle morphogenesis (Zhou *et al.*, 1995). In addition, mice lacking Lef-1 failed to grow whiskers and had a reduced number of pelage hairs (van Genderen *et al.*, 1994). Whisker follicle development required both epithelial and mesenchymal Lef-1 activity (Boras-Granic *et al.*, 2006). Lef-1 was expressed in the mesenchyme and was not required for the initiation of pelage follicles. In the epithelium, Lef-1 was required to complete vibrissa follicle development and for the early stages of pelage hair development in mice (Kratochwil *et al.*, 1996).

The Wnt signalling pathway is antagonised by a number of extracellular inhibitors, including Dickkopf1 (Dkk1) (Wu *et al.*, 2000). Dkk1 acts upstream of Dishevelled, in the Wnt pathway, to prevent the initiation and development of vibrissae and pelage hair follicles. Ectopic expression of Dkk1 blocks localised expression of known placode markers, indicating that canonical Wnt signals are required for the process of follicle initiation. Endogenous expression of Dkk1 in mesenchymal cells surrounding developing follicles may be regulated by BMPs expressed in the placode and dermal condensate, and may mediate some of the placode-repressing functions of the BMPs (Andl *et al.*, 2002). It has been speculated that Dkk1 is responsible for concentrating Wnt activity to the placode and dermal condensate, where Wnt has to overcome the hair follicle-inhibitory Dkk1 action (Schmidt-Ullrich and Paus, 2005).

1.8.4 THE BONE MORPHOGENETIC PROTEINS (BMPs)

BMPs have been implicated in feather morphogenesis. BMP2 expression was detected in emerging epidermal placodes and dermal condensations during feather development in the chick (Eames and Schneider, 2005). The BMP antagonists gremlin and follistatin were also expressed, with gremlin detected in the dermis and follistatin in the epidermis (Noramly and Morgan, 1998). During patterning of the feather bud patterning, BMP2, BMP4 and BMP7, as well as BMP antagonists (excluding gremlin) were detected in feather primordia (Olivera-Martinez *et al.*, 2004; Eames and Schneider, 2005). It has also been proposed that BMP signalling plays a key role in maintaining hair follicle stem cell quiescence (Fuchs, 2008).

1.8.5 THE FIBROBLAST GROWTH FACTORS (FGFs)

FGFs promote placode growth, are expressed during the early stages of follicle development, promoting placode fate and follicle formation (Millar, 2002). FGF molecules have been shown to induce the formation of ectopic follicles in chick embryos and to lead to the formation of feather buds in chick embryos that would otherwise fail to develop feathers due to the ectodermal defect *scaleless* (Chuong *et al.*, 1996; Song *et al.*, 1996; Widelitz *et al.*, 1996). FGF-10 appears to act as a promoter for epithelial budding, and has been implicated in the development of hair and feather development along with FGF receptor 2b (Pispa and Thesleff, 2003). It was thought likely that FGFs acting within the mesenchyme were required for development of the ectodermal organs within an organism (Celli *et al.*, 1998; De Moerlooze *et al.*, 2000; Ohuchi *et al.*, 2000).

1.8.6 SONIC HEDGEHOG (Shh)

Shh is involved in activating cell proliferation in the epidermis and dermis, and is believed to function as a general growth activator of cutaneous appendages (Olivera-Martinez *et al.*, 2004). Shh is normally expressed in the proximal tip of the in-growing epithelium of the hair follicle, but is not believed to be required for hair placode formation or penetration of the epithelial plug down through the dermis. However, it seemed to be essential for morphogenesis of the hair shaft (St-Jacques *et al.*, 1998). There is an essential function for Shh in maintaining the integrity of the hair follicle, which is necessary for generation and organisation of the inner root sheath and shaft cells and their precursors, as well as for specifying and/or maintaining the identity of the outer root sheath (Gritli-Linde *et al.*, 2007). Further, ablation of epithelial Shh signalling has been shown to result in the follicular outer root sheath taking on an epidermal character and loss of some hair follicles, highlighting an intrinsic requirement for Shh activity within the epithelium of hair follicles (Gritli-Linde *et al.*, 2007). Shh acts by binding to its receptor Patched, which triggers the activation of members of the Gli family proteins. Data demonstrates that Gli-2 plays a key role in Shh signalling in follicle development during embryogenesis (Mill *et al.*, 2003). Shh induces dermal Wnt5a and transcription factor Gli-1, both required for normal dermal papilla proliferation. At the same time, the dermal papilla begins to express Versican, hepatocyte growth factor (HGF) and neural cell adhesion molecule (NCAM) and up-regulates its alkaline phosphatase activity, indicators of its increasing inductive power (Kaplan and Holbrook, 1994; Muller-Rover *et al.*, 1998; Lindner *et al.*, 2000; Schmidt-Ullrich and Paus, 2005).

Shh is also a well characterised marker of the feather bud. Shh expression has been isolated to the epithelial placode during chick feather development (Eames and Schneider, 2005).

1.8.7 TRANSFORMING GROWTH FACTOR-β (TGF- β)

It was previously thought that the TGF-β and Notch signalling pathways acted independently and in parallel of each other. However, Notch is suspected of playing a role in the regulation of epithelial-to-mesenchymal transitions, to modulate TGF-β signalling and cellular adhesion in cardiac development and this can occur during embryogenesis and during Notch-mediated transformation *in vitro* (Timmerman *et al.*, 2004). It has also been observed that the cell cycle inhibitory effects of TGF-β in cultured cells could be overridden by the intracellular domain of Notch (Rao and Kadesch, 2003).

TGF-β and Notch act as tumour suppressors by inhibiting epithelial cell proliferation. TGF-β1 was found to induce the expression of endogenous Notch ligands in keratinocytes and mammary epithelial cells, whereas the regulation of Notch receptors was complex and dependent on the tissue. The epithelial cell cycle stopped when TGF-β signalling induced Jagged-1 production, leading to activation of the Notch receptor and further signalling via CSL which in turn regulated the cell cycle inhibitors p15 and p21(Niimi *et al.*, 2007).

Worldwide research investigating the development of hair follicles and other ectodermal organs, and the genes and proteins involved, has sparked an interest in the processes by which morphogenesis of wool follicles in sheep occur. By building on research conducted using mice, chicken, and other experimental models, the mechanisms underlying wool follicle development can be studied to further our knowledge of the processes underlying the morphogenesis of wool follicles and to ultimately improve wool production, benefiting the wool industry.

1.9 THE AUSTRALIAN WOOL INDUSTRY

Research into wool growth and follicle biology has been driven by the demands of the wool industry to improve both the efficiency and quantity by which farmers can produce wool. Wool follicle density is a strongly heritable trait, and is one of the most important components of fleece structure. In the Merino, the total number of primary follicles remains fairly constant throughout the life of an animal and between different individuals. However, the total number of secondary follicles differs enormously between different breeds and

individuals within a breed (Hardy and Lyne, 1956). It was suggested that when most of the follicle initiation sites have been occupied, follicle branching starts (Moore *et al.*, 1996).

Wool studies in Merino sheep have found that follicle density is negatively correlated with follicle diameter. This finding has practical implications for the wool industry as selective breeding programs could be established to alter fibre diameter characteristics in a desired direction within a given flock. By selecting sheep for increased follicle branching, a reduction in fibre diameter would be observed. Production of fibre by the skin of a sheep uses a finite cellular and molecular resource and there is no guarantee that larger number of follicles will produce more wool.

Large differences in follicle densities have been recorded in different Merino lines selected for high or low fibre diameter, or for long or short staple length (Moore *et al.*, 1998). Primary and secondary original follicle numbers are relatively constant in different sheep lines. Differences in follicle densities are due to secondary derived follicles (Moore *et al.*, 1995). Merino sheep skin contains up to 60 follicles per square millimetre and 10-100 million follicles in the entire skin. The follicles have an extended period of anagen, producing ~15 cm long fibres annually, of ~20 micron (Rogers, 2006). Fibre growth is relatively consistent throughout the year. Wool output is a result of the productivity of individual follicles and the total number of follicles in the skin of an animal. The more follicles, the more wool will be produced (Moore *et al.*, 1989). The amount of wool a sheep produces depends on the size of the animal, follicle density and the volume of fibre per follicle produced in a period of time. To maximise wool production it would be desirable to select large-sized animals with high follicle densities, low fibre diameter and a fast fibre growth rate (Adelson *et al.*, 2004).

A relationship between staple length and crimp has been discovered. The longer the length of a staple of wool, the lower the crimp frequency (Rogers, 2006). Merino wool fibres appear highly crimped. The angle of fibre emergence was found to change in a cyclical manner with time, the contemporaneous angles of emergence of adjacent fibres formed a sequence across the surface of the skin, as time progressed this sequence migrated across the skin surface, so that staple crimp emerged at an angle from the skin, and approximately three-quarters of a staple crimp was found to form in 9 days (Chapman, 1965).

The genotype of a breed of sheep is only partly responsible for the follicle population and fleece type characteristic of a given breed. Other, non-heritable, factors also contribute to the wool producing capabilities of an individual. For example, inadequate maternal nutrition or stress when secondary follicle development is occurring would have a detrimental effect on

the number of follicles initiated in the foetus (Hocking Edwards *et al.*, 1996; Hocking Edwards, 1999).

Comparing the Australian Merino with other breeds showed huge discrepancies in follicle ratios. The Merino possessed much higher secondary to primary follicle ratios compared to the British long-wool, short-wool and carpet-wool fleece types, with the Merino found to be distinct from all other sheep genotypes due to the increased number of secondary follicles (Carter and Clarke, 1957). Other research compared wool follicle development in Drysdale, Merino, Merino × Romney, Romney and Wiltshire breeds. Primary follicle density developed similarly across all 5 genotypes. The main differences in secondary follicle populations between the different breeds were associated with an extended follicle initiation period and more rapid rate of follicle initiation in the Merino, likely due to the tendency of secondary derived follicles to bud from already existing secondary follicles, a phenomenon that is relatively insignificant in all breeds apart from the Merino (Hocking Edwards *et al.*, 1996).

1.9.1 AUSTRALIAN WOOL INNOVATION (AWI) AND SHEEP GENOMICS

In October 2007, AWI changed dramatically following the integration of the Woolmark Company into AWI. This allowed AWI to make the transition from a research and development organization, into an international fibre research and marketing company. AWI has 3 main goals: to increase the worldwide demand for Australian Merino wool, to improve and sustain profitability for Merino wool producers, and to improve the technology available to in turn increase productivity and decrease on-farm costs (AWI Strategic Plan 2008/09 – 2010/11).

Sheep Genomics is a joint initiative of AWI and Meat and Livestock Australia (MLA). Sheep Genomics invests in research aimed to speed up the progress in breeding sheep with specific fleece yield and micron characteristics. Their research is concentrated on the initiation of wool follicles in a sheep foetus, and manipulation of follicle-forming genes at critical times with the aim to alter the number, shape, size and activity of wool follicles. By conducting such investigations, it is hoped that tools enabling faster improvement in wool quality than that which is achieved by selective breeding alone will be discovered. The aim is to develop genetic markers for certain desirable fleece traits and therapeutic treatments to enhance fibre traits and wool production (http://www.sheepgenomics.com).

Wool traits that are economically important are moderately or highly heritable and are generally easy and inexpensive to measure to a level sufficiently precise for animal evaluation

(Purvis and Franklin, 2005). The practical potential of gene discovery in wool research is the provision of molecular markers for selective breeding and for altering wool growth and the structure of wool by altering other biological pathways that could lead to the development of novel properties of wool (Rogers, 2006).

1.10 AIMS AND OBJECTIVES OF THIS PROJECT

The purpose of this project was to study the process of primary follicle initiation in foetal sheep skin and to investigate the involvement of the Notch signalling pathway in this process. It was hypothesised that prior to follicle initiation, a sub-population of mesenchymal cells would express genes that differentiated them from the rest of the mesenchymal cell population, and that the Notch signalling pathway was involved in such mesenchymal cell fate decisions.

In line with the Founder Cell Theory, mesenchymal cells that were to aggregate and form the dermal condensate at follicle initiation would be labelled with Notch pathway gene transcripts or express protein prior to and during follicle initiation. To test this theory, investigations into whether the Notch signalling pathway is involved in the process of follicle initiation in foetal sheep skin were conducted using *in situ* hybridisation and immunohistochemistry studies in skin sampled prior to (day 56) and during (day 70) primary follicle initiation. Cell culture techniques were employed to observe the behaviour of dermal papilla cells collected from whiskers in culture and the development of follicle buds in cultured foetal skin samples. The effect of blocking the Notch signalling pathway *in vitro* was investigated using a known inhibitor of Notch activation, namely the γ-secretase inhibitor known as DAPT.

For these studies, skin was sampled from fine woolled Merinos and strong woolled Tukidales. The Tukidale was used as a comparison to the Merino to allow us to investigate the process of primary follicle initiation in two breeds with markedly different follicle density and fibre diameter characteristics. The comparison of two such divergent breeds would allow for agreement or disagreement with the Founder Cell Theory, as well as to determine if there were differences in the process of primary follicle initiation or Notch signalling pathway transcript or protein expression in these markedly different breeds.

CHAPTER 2: MATERIALS AND METHODS

2.1 MATERIALS

2.1.1 ANIMALS

2.1.1.1 Mice

Preliminary *in situ* hybridisation and immunohistochemistry experiments were carried out on embryonic mouse skin. Inbred Quackenbush-Swiss line 5 (QSi5) and Advanced Intercross Line (AIL) animals were kindly provided by Dr Ian Martin and Prof Chris Moran from the Faculty of Veterinary Science, University of Sydney, Camperdown Campus, NSW.

2.1.1.2 Sheep

Merinos and Tukidales were used for all experiments. The Merinos were fine-woolled animals obtained from different sources, 4-7 yrs of age, as described in each chapter. Tukidales were strong-woolled, 4 yrs of age, from a single property.

2.1.2 EQUIPMENT

All laboratory work was conducted wearing SensiClean® powder-free latex gloves (Ansell International, Richmond, VIC, Australia). Schott bottles (SCHOTT Australia Pty Ltd, Frenchs Forest, NSW, Australia) were used to contain solutions. Pyroneg powder (Johnson Diversey, WI, USA) was used to clean glassware. Equipment and solutions were autoclaved before use (Atherton Centenary Series, VIC, Australia) unless otherwise stated.

Milli-Q water (ZAWQ05001; Milli-Pore Australia Pty Ltd, North Ryde, NSW, Australia) was used to make up all solutions, unless otherwise specified. The pH of solutions was measured using a pH meter Φ340 pH/Temp meter (Beckman Coulter Inc^{TM}, CA, USA). Reagents and solutions were stored at the recommended temperatures, between 4°C and –80°C, the latter using an ULT2186-5-W14 freezer (GS Laboratory Equipment, NC, USA). Chemicals were handled within a fumehood (FC-I; Fisher Hamilton, NSW, Australia) where indicated by their material safety data sheet (MSDS).

Solutions were delivered using Pipetman® pipettors (Gilson Inc, WI, USA) and MAXYMum Recovery^{TM} pipette tips (Axygen Scientific Inc, CA, USA) or serological pipettes (Cellstar®; Greiner Bio-One Ltd, Stonehouse, Great Britain, UK) used in conjunction with a manual pipettor (Bel-Art Products, NJ, USA).

All syringes and needles used were produced by Terumo® Medical Corp (NJ, USA).

Other general lab equipment included the following: a vortex for mixing solutions (MS2 minishaker; IKA® Works Inc, NC, USA), a capsulefuge (Tomy PMC-060; Tomy Kogyo Co Ltd, Tokyo, Japan) or microfuge® 18 centrifuge (367161; Beckman Coulter Inc^{TM}) for condensing solutions, a refrigerated microcentrifuge (5417R; Eppendorf South Pacific Pty Ltd, North Ryde, NSW, Australia), a balance (BP310S; Sartorius AG, Göttingen, Germany), a heat and stirring block (CH2092-001; Industrial Equipment and Control Pty Ltd, Thornbury, VIC, Australia), a single dry block heater (Ratek Instruments Pty Ltd, Boronia, VIC, Australia) or Thermoline Australia dry block heater (DB3; Thermoline Scientific Equipment Pty Ltd, Wetherill Park, NSW, Australia), an ice machine (Ice Queen 135 Air; Industria Tecnica Valenciana S.A., Valencia, Spain), liquid nitrogen Dewar (Taylor-Wharton Australia Pty Ltd, Albury, NSW, Australia), a platform shaker (IKA-Vibrax-VXR; Janke and Kunkel GmbH and Co K.G., Staufen, Germany), a shaking incubator (OIA-S; Labec Laboratory Equipment, Marrickville, NSW, Australia) for growing bacterial cultures.

2.1.3 REAGENTS

Reagents were purchased from Sigma-Aldrich Inc (MI, USA) unless otherwise stated. The reagents were of either analytical reagent (AR) or molecular biology grade, depending on their use.

2.2 METHODS

2.2.1 MOUSE HUSBANDRY

Mature Quackenbush Swiss Line 5 (QSi5) females were mated with males of the same strain. The resulting embryos were used to study the development of pelage and whisker follicles. Laboratory Animal Services of Sydney University provided standard husbandry in accordance with the Australian Code of Practice for the Care and Use of Animals for Scientific Purposes, 7th Edition (2004), freely available from http://www.nhmrc.gov.au/publications/synopses/_files/ea16.pdf. The mice were subject to a relatively constant environment: 12 hr light, 12 hr dark, average temperature 22°C. All mice were supplied with clean newspaper-based litter, tissues and cardboard.

2.2.1.1 Diet

Mice were provided with rat and mouse cubes (Glen Forrest Stockfeeders, Glen Forrest, WA, Australia) and water *ad libitum*.

2.2.1.2 Mating procedures

Females were housed in open cages, alternating with male cages for two weeks before mating, to encourage oestrus cyclicity. Mature females were housed with males from approximately 1600h and examined for copulatory plugs for the next 5 d. The presence of a plug was designated as 0 days post coitus (dpc). Those females were separated from the males and checked every second day for weight increases.

2.2.1.3 Sampling embryos

Pregnant mice were sacrificed from 13-17 dpc using carbon dioxide gas. These stages encompassed whisker and pelage hair follicle initiation and early development (Table 2.1).

Table 2.1: Characterised development of the mouse embryo from 13-19 days post coitus (dpc). Adapted from The Edinburgh Mouse Atlas Staging Criteria, http://genex.hgu.mrc.ac.uk/Databases/Anatomy/MAstaging.html.

dpc	Stage of Development
13	Five rows of whiskers
14	Hair follicles in pectoral, pelvic and trunk regions
15	Hair follicles also in cephalic region
17	Wrinkled skin
18	Long whiskers
19	Newborn mouse

The abdominal fur of the pregnant animal was moistened with 70% ethanol [absolute ethanol (A.J.P. Scientific Inc, NJ, USA) in Milli-Q water] and an incision made along the ventral midline from the hind limbs to the sternum. Using fine scissors and watchmaker's forceps, the uterus was excised and placed in a 90 mm bacteriological dish (Greiner Bio-One Ltd) containing phosphate buffered saline (PBS) [171mM NaCl; 3.4mM KCl; 10mM Na_2HPO_4; 1.84mM KH_2PO_4] prepared in RNase-free water (0.1% diethyl pyrocarbonate (DEPC)-treated water). Individual embryos were transferred to a 30 ml specimen jar (Techno-Plas Pty Ltd, St Marys, SA, Australia) and fixed overnight in 4% paraformaldehyde in PBS at 4°C.

2.2.2 SHEEP HUSBANDRY

Ewes were maintained under field conditions at the University of Sydney Sheep Reproduction Unit, Cobbitty, NSW. Animals used for the project had attained a fat score of 2 to 3 [refer toWhite and Holst, (2006). Fat scoring sheep and lambs. Prime Fact 302, NSW Department of Primary Industries (Orange, NSW)].

2.2.2.1 Oestrus synchronisation

Animals were mated within the natural breeding season to maximise conceptions. Oestrus synchronisation was achieved in each flock by inserting Ova-Gest® intravaginal progestagen-impregnated sponges (Bioniche Animal Health Australasia Pty Ltd, Armidale, NSW, Australia). The sponges were removed after 12 d and the ewes received 400 U/ml Pregnecol® pregnant mare serum gonadotropin (PMSG; Bioniche Animal Health) intramuscularly. Fifty-four hours later, ewes were either artificially inseminated or penned with a ram. In the latter case, a ram of the same bloodline was fitted with a Sire-sine® harness (Hortico Limited, Laverton North, VIC, Australia) and marking crayon so that mounted ewes could be identified. The ram was left with the ewes for 48 hr.

2.2.2.2 Laparoscopic artificial insemination (LAI)

Merino ewes aged 5-7 yr, were obtained from Severn Park Merino Stud, Cooma, NSW. Frozen semen from a fine woolled (~19 μm) ram of the same stud, was purchased from Allstock Pty Ltd (Narromine, NSW, Australia) in 0.25 ml straws. The ram chosen produced sperm with 70% motility. The straws were stored in liquid nitrogen within a Dewar (750-RS; Taylor-Wharton) before use. Following oestrus synchronisation (Section 2.2.2.1) ewes were housed without food or water for 18 hr prior to insemination.

Straws were thawed in a 37°C water bath (Unistat II NB7; Thermoline Scientific Equipment Pty Ltd) and the semen transferred to sterile test tubes stored within a 30°C incubator (Labmaster; Shree Ganesh Electrical System, Ambala Cantt, India). Sperm motility was estimated to be 60% after thawing.

The semen was delivered directly to the uterine horns of each ewe by abdominal puncture. To effect this, animals first received intramuscular injections of 4.05 mg acepromazine maleate (ACP; Delvet Pty Ltd, Seven Hills, NSW, Australia) and 100 mg Ketamine® (Troy Laboratories Pty Ltd, Smithfield, NSW, Australia) before being securely clamped in a laparotomy cradle. The abdominal region was clipped using Oster® animal clippers (Golden A5®, two-speed; Oster®, TN, USA). Each ewe was injected subcutaneously

with 20 mg of Lignocaine® (Troy Laboratories) on either side of the abdomen, 5-7 cm anterior to the udder and 3-4 cm on either side of the mid-ventral line, at the site of abdominal puncture. The designated puncture sites were sterilised by spraying with a 5% solution of hibitane (chlorohexidine gluconate 5% w/v, isopropyl alcohol 4% w/v; Pharmaceuticals Pty Ltd, Melbourne, VIC, Australia) in 70% ethanol.

The cradle was tilted to 45 degrees and a trocar-cannula was used to pierce each side of the abdomen. The trocar was removed and a fibre optic cable and (7 mm) telescope with gas line attachment and two-way gas tap was inserted. The abdomen was briefly inflated with carbon dioxide to locate the uterus. Thawed semen (0.1 ml) was injected into the lumen of each uterine horn, half way between the uterine bifurcation and the utero-tubal junction, using a glass inseminating pipette (internal diameter of 2 mm, external diameter 4.5 mm, 30 cm long) attached to a 1.0 ml syringe for drawing up and expulsion of the semen. At least 20 million motile spermatozoa were administered to each ewe. After semen deposition, the pipette and telescope were withdrawn before the two cannulae were removed and the abdomen was allowed to deflate. The abdominal wounds were sprayed with Cetrigen® (Virbac Pty Ltd, Milperra, NSW, Australia).

Between each insemination, the surgical instruments were sterilised in alcoholic hibitane and the insemination pipettes rinsed in a 0.9% sodium chloride (NaCl) solution. The animals were returned to field conditions following LAI.

2.2.3 SAMPLING FOETAL SHEEP TISSUE

2.2.3.1 Prior to surgery

At least one week before surgery, all ewes were transported to the Shute Building Animal House, The University of Sydney, Camden Campus. At this time the ewes were examined using a real-time ultrasound scanner (SDL-32C; Apscan, Camperdown, NSW, Australia) to determine whether they were pregnant and whether they were bearing a single foetus or twins. Animals not pregnant were returned to field conditions, while those pregnant were housed within the Animal House for foetal skin sampling. Animal work was approved by animal ethics (N00/1-2004/3/3870).

2.2.3.2 Ovine diet

All animals were fed a standard diet (approximately 1.2 kg per animal each day) of lucerne chaff and lupins (60:40, w/w), with water available *ad libitum*. A molasses block was provided for environmental enrichment.

Food was withheld for 24 hr preceding surgery.

2.2.3.3 Repeated sampling of foetal ovine skin

Skin was harvested from each sheep foetus on two occasions, the first at d 56 of gestation, prior to the appearance of wool follicles, and the second at d 70, corresponding to the first wave of primary follicle initiation. These sampling points were chosen so that the events involved in the process of wool follicle development could be investigated.

2.2.3.3.1 Foetal skin collection prior to follicle initiation

2.2.3.3.1.1 Pre-operative care

Prior to surgery, wool was clipped from the neck and abdomen of each ewe. General anaesthesia was induced by intravenous injection of 50-100 mg thiopentone sodium (Thiobarb powder; Jurox Pty Ltd, Rutherford, NSW, Australia), dissolved in sterile water for injection (Cattlekare Animal Health Products, Dandenong South, VIC, Australia).

The anaesthetised animal was fitted orally with a Lo-Contour™ Murphy tracheal tube (8, 0 oral/nasal 10, 9 27 mm diameter; Mallinckrodt Medical Inc, MO, USA) with the aid of a 20 cm Miller blade laryngoscope, before she was secured in a prostrate position to a surgical table in an operating theatre. The tracheal tube was connected to a Midget 3 anaesthetic apparatus (Commonwealth and Industrial Gases Pty Ltd, Sydney, NSW, Australia) fitted with a Fluotec-3 halothane compartment (Cyprane Keighley, England). The ewe received medical EP grade oxygen gas (Air Liquide Healthcare, Alexandria, NSW, Australia) at a rate of 1.5-2.0 L/min. Anaesthesia was maintained with Halothane BP (Laser Animal Health, Salisbury, SA, Australia) in oxygen dosed to effect, typically requiring a vaporiser setting of 1.5-2.0%. Indicating soda lime was used to absorb exhaled carbon dioxide and other acidic gases (Vivalyme; Ohmed Medical Inc, Leeds, UK). The abdominal operative field was scrubbed with PVP iodine (7.5 mg/ml povidon-iodine; Apex Laboratories Pty Ltd, Somersby, NSW, Australia) followed by alcoholic hibitane, with the aid of cotton wool (Dove, NJ, USA).

2.2.3.3.1.2 During surgery

A surgeon experienced in foetal manipulation conducted all procedures and standard aseptic conditions were maintained. Gammex medical surgical gloves (Ansell International), a surgical gown and fenestrated drape (Multigate® Medical Products Pty Ltd, Wetherill Park, NSW, Australia) were worn in theatre. Drapes were placed over the animal and clamped in place using mosquito forceps, leaving the operative field uncovered. A diathermy plate (Downs Surgical Ltd, England) along with cotton wool soaked in alcoholic hibitane was secured under the right foreleg, against the ewe's chest.

A 15 cm incision was made parallel to the ventral midline, with a scalpel blade (number 22; Swann-Morton®, England) and the uterus was exteriorised and placed inside a 280 by 325 mm plastic bag (Defries Industries Pty Ltd, Keysborough, VIC, Australia) (Figure 2.1; A). Viaflex® Plasma-Lyte® solution (148 REP electrolyte solution; Baxter Healthcare, Old Toongabbie, NSW, Australia), warmed to 37°C within an incubator (Labmaster), was added to prevent drying

A 5 cm incision was made in the uterus using a Downs Diadon 450 P2 diathermy machine (Downs Surgical Ltd). The uterus was secured to the drapes using forceps (Figure 2.1; B). The allantoic bubble was used to manipulate the amnion so the hindquarters of the foetus were pointing outwards (Figure 2.1; C). Amniotic fluid was collected from the bubble (Figure 2.1; D) using a 60 ml syringe and 19G needle, dispensed into a 250 ml bottle and reserved at 37°C. The amnion and allantois were opened using a scalpel.

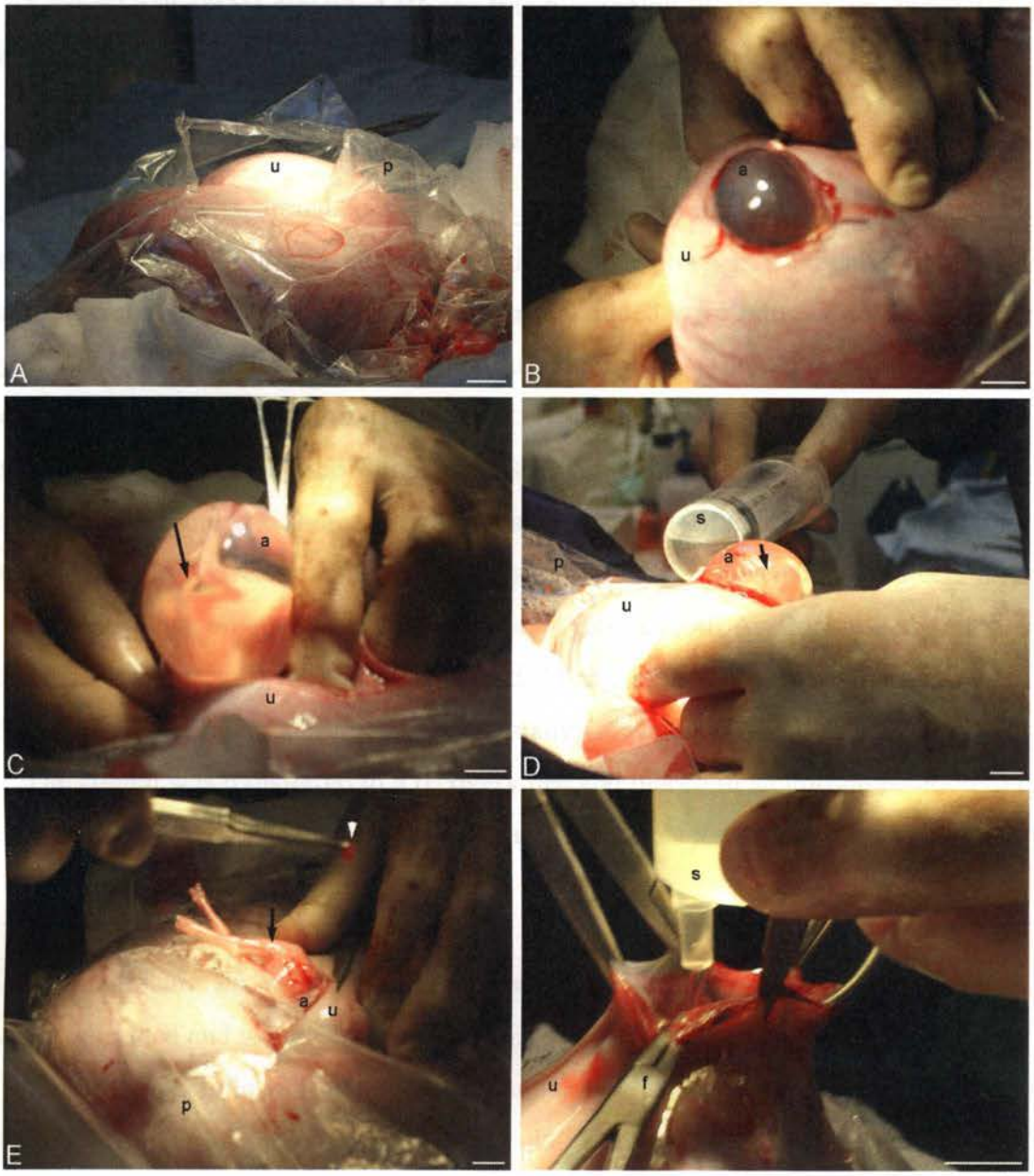

Figure 2.1: Surgery to collect foetal skin biopsies at d 56 gestation. A; the exteriorised uterus (u) contained within a plastic bag (p). B; an incision was made in the uterus (u) and through the chorion to expose the amniotic sac (a) so that the foetus could be located. C; the foetus (black arrow) was manipulated so that the posterior end was facing out of the amnion (a). D; amniotic fluid was collected with a syringe (s). E; a skin biopsy (white triangle-make more obvious) was excised from the gluteal region of the foetus. F; the foetus was returned to the uterus, the artery forceps (f) were held up so that the amniotic fluid could be returned to the uterus. Scales represent 1 cm.

2.2.3.3.1.3 Foetal skin biopsy collection

RNase-free fine scissors and scalpel blades were used to make an incision in the gluteal region of the foetus on one side of its rump. A 7 mm square of skin was excised (Figure 2.1; E) and transferred to 4% paraformaldehyde in PBS at 4°C for 4 hr.

Surgical equipment remained RNase-free by dipping in 10% sodium dodecyl sulphate (SDS) and absolute ethanol.

2.2.3.3.1.4 Returning the foetus to the uterus

The foetus was returned to the uterus and the aspirated amniotic fluid and Plasma-Lyte® solution with ~600 mg benzylpenicillin sodium powder (BenPen®; Commonwealth Serum Laboratories Ltd, Parkville, VIC, Australia) added were returned to the uterine cavity (Figure 2.1; F). The uterine incision was closed tightly using non-absorbable Dysilk sutures (metric 7, USP 5; Dynek Pty Ltd, Hendon, SA, Australia) and a round-bodied suturing needle (number 5; Surgical Indent and Supplies, NSW, Australia). The uterus was returned to the abdominal cavity and the abdomen was sutured using absorbable Prolene needles for skin (metric 4, Astraloc* eyeless; Ethicon, Livingston, UK). The ewe received injections of 600 mg oxytetracycline broad-spectrum antibiotic (Tetravet 200LA; Bomac Laboratories Ltd, Auckland, New Zealand) intramuscularly and 25 mg of Meloxicam analgesic (Metacam®; Boehringer Ingelheim GmbH, Ingelheim, Germany) subcutaneously.

The animal was transferred to a recovery pen and placed in an upright position to ensure patency of her airways. The tracheal tube was removed once jaw tension was exhibited.

2.2.3.3.1.5 Post-operative care

Once all animals were mobile, they were herded back to the Animal House and provided with feed and water (Section 2.2.3.2).

The morning following surgery, all animals were thoroughly examined for signs of wound breakdown or discomfort. All animals received follow-up injections of 25 mg meloxicam and 600 mg oxytetracycline (administered for a minimum of 3 d). The animals were monitored daily.

2.2.3.3.2 Foetal skin collection during follicle initiation

On d 70 of gestation, the ewes were herded to a holding pen and euthanased with 3.6 g pentobarbitone (Valabarb®; Jurox) delivered intravenously. Death was confirmed by lack of eye reflexes and heart beat.

Each animal was lifted onto a surgical table, the abdomen opened and the uterus exteriorised. The uterus was carefully opened in close proximity to the sutures to expose the amniotic sac. Amniotic fluid was collected in a sterile 250 ml bottle by piercing the uterus with the tip of a scalpel blade. The foetus was located and transferred into an RNase-free

container. The umbilical cord was clamped with a pair of artery forceps and severed before the foetus was euthanased by cervical dislocation. The reserved amniotic fluid was poured over the foetus to keep the skin moist.

Watchmaker's forceps and fine scissors were used to excise a skin biopsy (10 mm square) from the gluteal region of the unsampled side. Samples were placed directly into 4% paraformaldehyde in PBS and stored at 4°C for 4 hr.

2.2.3.3.2.1 Estimating day of gestation

Once the tissue samples were collected the foetus was weighed and the crown-rump length was measured (Figure 2.2). These measurements were analysed using a linear mixed model analysis (Figure A1.1; Tables A1.1 and A1.2). A multivariate restricted maximum likelihood (REML) analysis was attempted but was not used due to computational difficulties estimating the variance component associated with fitting the desired model.

Minor effects, as a result of repeated sampling, on the rate of development were not important as all samples included in the count studies (Chapters 3 and 4) were sampled both prior to and during follicle initiation. Upon histological comparison of samples collected on d 70 after earlier sampling and those sampled for the first time on d 70, no differences were observed in the stage of follicle initiation between samples.

Figure 2.2: Measuring foetal crown-rump length using a piece of string. The measurement was taken from the crown (C) of the head to the base of the tail, or rump (R). Scale represents 1 cm.

2.2.3.3.2.2 Adult skin biopsies

Right midside skin samples were also collected, from a shaved area, from each mother using a 8mm trephine (Acuderm Inc, FL, USA). The tissue was placed into 4% paraformaldehyde in PBS at 4°C overnight.

2.2.3.3.2.2.1 Investigating adult skin and wool follicle characteristics

Secondary to primary follicle ratios (S:P) as well as fibre diameters (for primary and secondary follicles) were estimated from tangential skin sections cut at the level of the sebaceous glands. Counts were performed on Merino and Tukidale samples, with 16 sections per sample used. These measurements were analysed and the data are presented in Figure A2.1 and Table A2.1 (S:P follicle ratios) and Figure A3.1 and Table A3.1 (fibre diameters).

2.2.4 HISTOLOGICAL PROCESSING OF TISSUES

2.2.4.1 Processing samples for wax embedding

Mouse embryos and foetal sheep skins were processed through a graded series of ethanol concentrations made up in 0.1% DEPC-treated water at 4°C: twice in 50% for 30 min and twice in 70% for 1 hr. Adult biopsies were washed twice in 50% and twice in 70% ethanol for 1 hr at 4°C. Each sample was placed into a sterile 90 mm bacteriological dish and examined under a stereomicroscope (SMZ645/660; Nikon Corp, Kanagawa, Japan). Ovine skin samples were placed within a folded sponge before all samples were placed within CliniPure Tissue Embedding Cassettes (HD Scientific Supplies Pty Ltd, Wetherill Park, NSW, Australia). Samples were processed at the Veterinary Pathology and Diagnostic Services, Faculty of Veterinary Science, The University of Sydney, Camperdown Campus, where they were loaded into a Shandon Excelsior™ Tissue Processor (Thermo Fisher Scientific Inc, MA, USA). The samples were dehydrated in absolute ethanol at room temperature for 30 min, cleared in xylene (Chem-Supply, Gillman, SA, Australia) with a 30 min and 1 hr wash at 30°C, immersed in molten paraplast tissue embedding medium (M°Cormick Scientific, MO, USA) at 60°C twice for 30 min and once for 1 hr. A Shandon Histocentre 3 embedding machine (Thermo Fisher Scientific) was used to embed the samples. The blocks were stored at room temperature within a Histosette™ paraffin block storage container (Anatomical Pathology Unit, Thermo Electron Corp, ON, USA).

2.2.4.2 Processing samples for OCT embedding

Following fixation the embryos and foetal sheep skin biopsies were washed thrice in PBS for 30 min. Soaking the samples in 10% sucrose for 1 hr and 30% sucrose overnight was conducted prior to cryopreserving the tissue. The samples were processed through 1/3 Tissue-Tek® optimal cutting temperature medium (OCT) compound (Sakura Finetek USA Inc, CA, USA), 2/3 OCT and pure OCT, for 30 minutes on a platform shaker. The embryos were placed into a Tissue-Tek® cryomold® (10 x 10 x 5 mm) treated with Tissue-Tek® mould release, containing OCT before being frozen in liquid nitrogen, wrapped in aluminium foil and stored at –80°C.

2.2.5 SECTIONING TISSUE BLOCKS

2.2.5.1 Sectioning wax-embedded tissue

A floatation bath (Labec Laboratory Equipment Pty Ltd Limited, Marrickville, NSW, Australia) was sprayed with RNaseZAP® and wiped out using Kimwipes® (Kimberley-Clark Australia Pty Ltd, Macquarie Park, NSW, Australia) followed by 70% ethanol, and allowed to dry. For *in situ* hybridisation studies, all surfaces of the microtome (Leica RM2135; Leica Microsystems Pty Ltd, Gladesville, NSW, Australia) were wiped to remove any RNases. Milli-Q water was poured into the floatation bath and heated to 45°C.

Tissue blocks were chilled to –20°C, within a plastic bag, for 10 min before sectioning to harden the paraffin wax and ensure good histology was maintained.

Samples were sectioned 5 µm thick using a Leica 819 low profile microtome blade (Leica Microsystems Pty Ltd), at an angle of 6 degrees. Ribbons of sections were separated so that two serial sections were allocated to each slide. Sections were briefly floated on the surface of the water before being mounted on a SuperFrost *Ultra* Plus® slide (Menzel-Gläser®, Menzel GmbH and Co KG, Braunschweig, Germany). The slides were labelled with a HB pencil and air-dried in a fumehood for 10 min. Air bubbles were pierced with a B-D® Ultra-Fine™ needle (29G, 0.5 ml insulin syringe; Becton Dickinson and Co, NJ, USA) before drying at 60°C in an oven (I-N601; Nedtex Co Ltd, Taipei, Taiwan) for 1 hr, followed by further drying at 37°C in an oven (BE 600/T1 + I; Memmert GmbH and Co KG, Schwabach, West Germany) overnight and then stored within a slide box (Tissue-Tek®) at 4°C.

2.2.5.2 Sectioning OCT-embedded tissue

Before use, the cryotome (77210164GB; Life Sciences International, England) was defrosted to remove any built-up ice. The blade and working areas within the machine were sprayed with RNaseZAP®, 70% ethanol and wiped out with Kimwipes®. The working temperature was set at –20°C and the cryobar at –42°C.

The sample was placed in the cryotome and left to warm to working temperature (15 min). Excess OCT medium was trimmed before a large drop of OCT medium was dispensed onto a clean chuck and the block was placed so that it was orientated for cutting longitudinal sections. The blade apparatus was set to an angle of 5 degrees before 10 µm sections were cut. SuperFrost *Ultra* Plus® or silane coated (ProSciTech, Thurwingowa, QLD, Australia) slides (at room temperature) were used to mount sections. The tissue was fixed by immersing the slide in pre-chilled methanol for 30 sec. The slides were air dried within the cryotome, placed in a slide box (Tissue-Tek®) and stored at –20°C.

2.2.6 STAINING

Paraffin-embedded sections required de-waxing and rehydration: twice in xylene for 10 min, twice in absolute ethanol for 5 min, in 90%, 70% and 50% ethanol for 2 min, and rinsed in Milli-Q water.

Sections were stained with Mayer's haematoxylin (Sigma Diagnostics®) for 15 sec, rinsed in Milli-Q water, dipped three times in acidic ethanol [1% hydrochloric acid (Fronine Laboratory Supplies, Riverstone, NSW, Australia) in absolute ethanol], rinsed, dipped five times in 2% sodium bicarbonate aqueous solution, and rinsed. The slides were placed in 50% and 70% ethanol for 1 min and counterstained using alcoholic Eosin Y solution, with phloxine (Sigma Diagnostics®) for 15 sec. The tissue was immersed in two 5 min washes each of 95% and absolute ethanol, cleared in two 10 min washes of xylene, and mounted with a mixture of Distyrene, a plasticiser, and xylene (DPX) mountant for histology (Fluka; a division of Sigma-Aldrich Inc) and coverslips (ProSciTech). The slides were left to dry in the fumehood.

2.2.7 MICROSCOPY

Slides were examined with a Leica fluorescence DMRBE Microscope (Leica Microsystems Pty Ltd). Images were recorded using the parameters specified in Table A4.1, using a SPOT RT Slider camera (2.3.1; Diagnostics Instruments Inc, MI, USA) attached to

the microscope and stored in a computer with SPOT Advanced Software (version 3.4) as jpeg files.

2.2.8 *IN SITU HYBRIDISATION*

All reagents used prior to hybridisation were of molecular biology grade and solutions were made up with 0.1% DEPC-treated water. Equipment was treated with RNaseZAP®. Slides were processed in a slide rack (Tissue-Tek®) within 250 ml plastic slide staining dishes (Tissue-Tek®) for all hybridisation steps.

2.2.8.1 De-waxing and rehydration of paraffin-embedded sections

Slides were scored around the sections using a glass knife before the sections were deparaffinised and rehydrated as described (Section 2.2.8.1). The slides were transferred to 0.9% NaCl for 5 min.

The sections were rinsed in PBS for 5 min, fixed with 10% neutral buffered formalin (Sigma Diagnostics®) for 20 min and washed twice in PBS for 5 min. Protein digestion was carried out for 5 min in TE buffer (pH 7.6) [10mM Trizma-HCl; 1mM EDTA] supplemented with 1mM Proteinase K. The slides were rinsed again in PBS for 5 min and re-fixed in 10% neutral buffered formalin (20 min).

Acetylation was carried out for 10 min in 3mM triethanolamine (TEA; pH 8.0) in 0.1% DEPC-treated water, supplemented with 6.2µM acetic anhydride. The sections were washed in PBS, followed by 0.9% NaCl, for 5 min. The sections were dehydrated (2 min in 50% and 70% ethanol, 5 min in 90% and two 5 min washes in absolute ethanol) and air-dried.

2.2.8.2 Pre-hybridisation of tissue

The hybridisation mixture without probe [0.6M NaCl; 20mM Tris (pH 7.4); 20mM NaH_2PO_4 (pH 6.8); 10mM EDTA (pH 8.0); 0.4% Ficoll; 0.4% polyvinylpyrrolidone; 50mM dithiothrietol (DTT; Promega Corp, WI, USA); 5% polyribonuclease A (Roche Diagnostics GmbH, Basel, Switzerland); 2.5% yeast tRNA; 10% dextran sulphate (Fluka); 50% formamide (deionised)] was incubated at 95°C for 2 min. Whatman® filter paper (Whatman Laboratory Division, England, UK) wet with 4x SSC [0.6M NaCl; 60mM sodium citrate] and 50% formamide was placed in the bottom of a hybridisation chamber to prevent the tissue from drying. Approximately 200 µl of hybridisation mix was added to each slide, using a glass Pasteur pipette (Volac International Ltd, England). The hybridisation chamber was

placed in a 55°C water bath for 1 hr (Mini Unistat; Australasian Scientific Marketing Group, Australian Scientific, Kotara, NSW, Australia).

2.2.8.3 Hybridisation of probe with tissue

The hybridisation mixture was incubated at 95°C with the probe transcripts for 2 min. The sense and antisense riboprobes were used at a working concentration of 200 µg RNA per ml of hybridisation mix. Approximately 100 µl of the probe mixture was added to each slide. The slides were incubated in the hybridisation chamber overnight at 55°C within the water bath.

2.2.8.4 Post-hybridisation washes

The sections were subject to a number of post-hybridisation washes of increasing stringency within the 55°C water bath, to remove non-specific binding. These included: two 20 min in 4 x SSC [0.6M NaCl; 60mM sodium citrate], one 20 min in 2x SSC [0.3M NaCl; 30mM sodium citrate], one 20 min in 1x SSC [150mM NaCl; 15mM sodium citrate], and finally two 20 min in 0.1x SSC [15mM NaCl; 1.5mM sodium citrate] at 65°C (Unistat II; Thermoline Scientific Equipment Pty Ltd). The slides were allowed to cool to room temperature (20 min) before being placed in 0.1x SSC for 5 min, at room temperature.

2.2.8.5 Immunohistochemistry for detection of probe-cell hybrids

Non-specific antibody binding was blocked using the following procedure. Slides were initially washed for 5 min in 1x maleic acid buffer (pH 7.5) [0.1M maleic acid; 0.15M NaCl]. Approximately 200 µl blocking solution (DIG Wash and Block Buffer Set; Roche Diagnostics GmbH) diluted in 1x maleic acid buffer, with 20% heat-inactivated sheep serum (Thermo Electron Corp), was added to the sections and incubated for 45 min in a humidified chamber at room temperature.

Anti-Digoxigenin-AP antibody (Fab fragments) (Roche Diagnostics GmbH) was centrifuged at 10,000 ×*g* for 5 min at 4°C before use. The antibody was used at a dilution of 1 in 500, in blocking solution. Approximately 100 µl antibody diluted 1 in 500 with blocking solution, was added to each section and incubated for 1 hr at room temperature. The antibody was drained from the sections and the slides were rinsed in washing buffer [0.1M maleic acid; 0.15M NaCl; 0.3% Tween 20] for 10 min. They were then placed in detection buffer [0.1M NaCl; 0.1M Trizma-HCl (pH 9.5); 5mM $MgCl_2$; 0.1% Tween 20] for 10 min.

The colour substrate, nitro-blue tetrazolium chloride/5-bromo-4-chloro-3'-indolyphosphate p-toluidine salt (NBT/BCIP; Roche Diagnostics GmbH) [10% in detection buffer containing 1% polyvinyl alcohol (70 – 1,000 kD)] was pipetted onto the sections. The slides were incubated at 37°C until colour was detected (30-120 min) by microscopic examination. The reaction (Figure 2.3) was stopped with three 10 min washes in warm Milli-Q water.

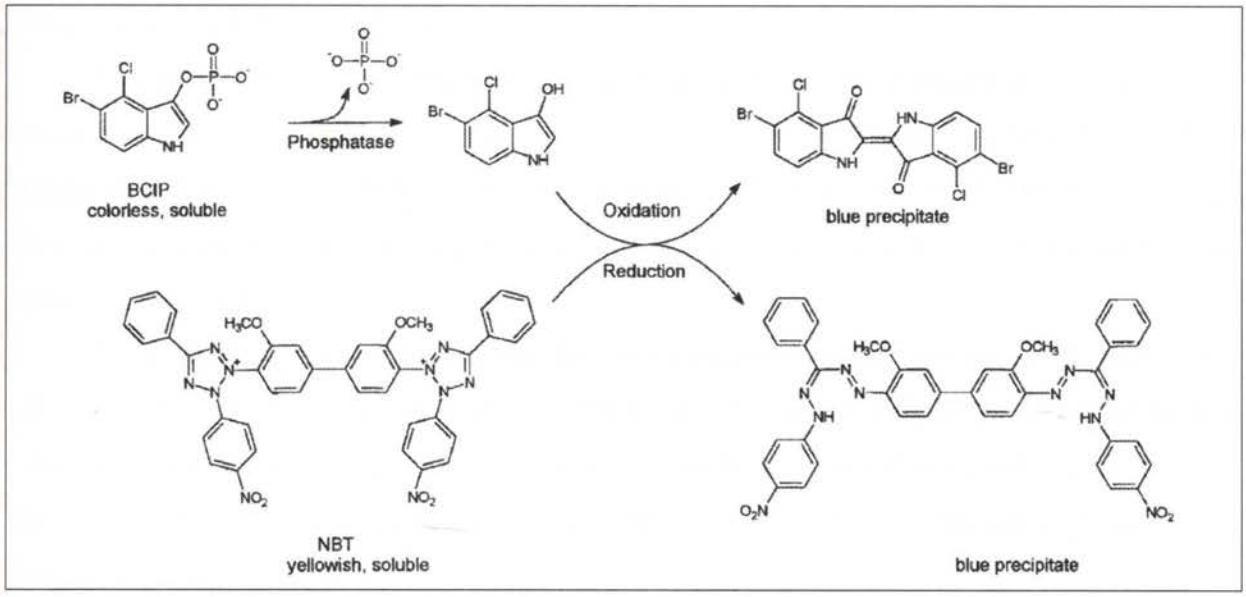

Figure 2.3: The oxidation-reduction reaction that occurs with the use of NBT/BCIP, causing cells to turn purple in the presence of alkaline phosphatase (AP). BCIP is the AP-substrate that reacts following dephosphorylation and oxidation to produce a blue precipitate. NBT serves as the oxidant, producing a blue precipitate and intensifying the colour of the reaction. Information adapted from the product specification sheet from Roche Diagnostics GmbH.

The sections were mounted under coverslips using UltraCruz™ fluorescence mounting medium with 4', 6-Diamidino-2-phenylindole (DAPI) (Santa Cruz Biotechnology Inc, CA, USA) and examined with a Leica fluorescence DMRBE Microscope. Gene transcript localisation, marked by the purple alkaline phosphatase-labelled cells, was detected using bright field imagery. DAPI fluorescence (350 nm) was observed using a suitable filter (excitation/emission; 330/385 nm) to locate the cell nucleus, to permit counting of mesenchymal cells (refer to Chapters 3 and 4). Bright field and DAPI fluorescence images were recorded and stored using the SPOT camera (Section 2.2.7).

2.2.8.6 Experimental design, cell counts and statistical analysis

A random number table was generated in Microsoft® Office Excel 2003 (Microsoft Corp, WA, USA) to provide an unbiased method for allocating fields of view from sections used in the *in situ* hybridisation studies of foetal sheep skin to be investigated further. Counts

of labelled and unlabelled mesenchymal cells of skin were collected on d 56 and d 70 of gestation. In total, 7 Merinos and 5 Tukidales from these two time points, with 3 sections and 3 fields of view were investigated.

Once the fields to be counted were identified, the bright field and DAPI images were merged using Adobe Photoshop (Creative Suite 2; Adobe Systems Inc, CA, USA) with sufficient transparency so that the labelled and unlabelled cells were visible. The combined image was saved (as a jpeg file).

Cell counts were performed with the aid of ImageJ from NIH Image (Rasband, W. S.; ImageJ, US National Institutes of Health, Bethesda, Maryland, USA, http://rsb.info.nih.gov/ij/, 1997-2008), which was freely available to download from the Internet, and the cell counter plug-in was installed. The data generated were collated in an Excel spreadsheet.

Once counting was complete, the data were analysed using GenStat for Windows 9th Edition (VSN International Ltd, Hemel Hempstead, UK). A generalised linear mixed model was used to analyse the count data. However, in situations where this model did not work a linear mixed model with log-transformed counts was used. Given that most counts were reasonably large this approach was justified.

2.2.9 IMMUNOHISTOCHEMISTRY

Sections were brought to room temperature within their slide box. A circle was scored around the sections with a glass knife. Sections were de-waxed if paraffin-embedded samples were used, as previously described (Section 2.2.6).

2.2.9.1 Fluorescence method

After being washed in 50% ethanol for 1 min, the slides were immersed in 0.9% NaCl for 5 min followed by 5 min in 1x PBS [3.35mM KCl; 10mM HNa_2O_4P (AnalaR®, BDH Chemicals Australia Pty Ltd, Kilsyth, VIC, Australia); 1.8mM KH_2PO_4; 8% (w/v) NaCl]. The slides were placed in a humidified chamber. Approximately 200 µl of blocking reagent [3% normal donkey serum in 1x PBS with 0.1% bovine serum albumin (BSA; fraction V)] was added to each slide before they were incubated for 1 hr at room temperature.

The blocking reagent was removed and replaced with approximately 100 µl of a goat polyclonal antibody to human Delta (H-20) (Santa Cruz Biotechnology) in the blocking reagent at a concentration of 0.0002 µg/ml. For the control slides the antiserum was replaced with normal goat serum at the same concentration. Alternatively a 10 molar excess of the

Delta (H-20) peptide was incubated overnight with the antibody before use. The slides were incubated at 4°C overnight, within a humidified chamber. They were then drained and washed three times in 1x PBS with 0.1% BSA, for 10 min.

The secondary antibody, donkey anti-goat IgG conjugated to fluorescein-5-isothiocyanate (FITC) (Santa Cruz Biotechnology) was diluted at a concentration of 0.00132 µg/ml in 1x PBS with 0.1% BSA. Approximately 100 µl of the solution was added to each slide and the slides were incubated for 1 hr at room temperature. The primary antibody was drained from the slides, before they were washed three times in 1x PBS with 0.1% BSA, for 10 min.

The solution was drained from the sections and the slides mounted with coverslips and UltraCruz™ fluorescence mounting medium with DAPI. The slides were examined using fluorescence microscopy on the same day with DAPI and FITC (200-300 nm and 400-500 nm respectively) filters.

CHAPTER 3: THE EXPRESSION OF TWO DELTA LIGANDS AND A NOTCH MODULATOR IN OVINE SKIN

3.1 INTRODUCTION

The gene expression patterns of the Notch pathway ligands Delta-1, Delta-3 and modulator Lunatic Fringe were investigated using *in situ* hybridisation. Previous studies have shown these genes to be expressed in developing hair follicles in both mice and humans, and during feather formation in chickens.

In mouse embryos, Delta-1 was found to be expressed early in initiation, in dermal condensate cells of follicle primordia (Powell *et al.*, 1998; Favier *et al.*, 2000). In developing human epidermis, Delta-1 was confined to the basal layer of the epidermis, with the highest level of expression detected in clusters of cells that co-localised with keratinocyte stem cells (Lowell *et al.*, 2000). It is interesting that the expression patterns of Delta-1 differ between human and mouse skin considering that they both produce hair follicles. In the developing chick, Delta-1 was localised within the dermis (Eames and Schneider, 2005), with transcripts detected in the mesenchyme underlying epithelial placodes during feather initiation (Crowe *et al.*, 1998).

Over expression of Delta-1 in early chicken embryos using a replication competent retrovirus was shown to cause feather bud loss (Crowe *et al.*, 1998), suggesting Delta-1 may have a role in directing cells to either a smooth skin or feather fate. Such over expression of Delta-1 was thought to cause an irreversible block to feather initiation by inhibiting the formation of the feather bud.

Delta-1 expressed sequence tags (ESTs) have been isolated from ovine skin (refer to Figure 1.9). In the developing mouse embryo, Delta-3 and Delta-1 were believed to cooperate in the formation of somite boundaries during segmentation of the paraxial mesoderm. It was noted that Delta-3 and Delta-1 were both extensively expressed during neurogenesis in overlapping and distinct domains (Dunwoodie *et al.*, 1997). Later, loss of Delta-3 function mutations in mouse embryos were shown to result in severe axial skeletal defects consisting of highly disorganised vertebral and costal defects (Dunwoodie *et al.*, 2002). Delta-3 was capable of functioning like other Notch pathway ligands as a strong Notch signalling inhibitor when expressed in responding cells (Weinmaster and Kintner, 2003). Cells expressing both the Notch receptor and Delta-3 ligand were inhibited from producing a signal during

somitogenesis. This may be a result of there being an abundance of Delta-3 ligand on the cell surface, in comparison to Notch: the Delta-3 molecules may bind to one another rather than forming receptor-ligand associations. Delta-3 was found to be unable to activate Notch signalling in adjacent cells in the presomitic mesoderm (Weinmaster and Kintner, 2003). Thus, the Delta-3 ligand and Notch-1 receptor on adjacent cells do not bind with one another to produce a signal to downstream target genes.

The Golgi-localised, glycosyltransferase Fringe proteins have been shown to play an essential role in the spatial regulation of Notch signalling at many developmental boundaries during pattern formation (Baron *et al.*, 2002). Fringe contributes to the spatial and temporal patterns of Notch activation signals by determining where each ligand can activate Notch (Peterson and McClay, 2005).

Fringe proteins are not usually needed for Notch signalling to occur. Instead, they seem to function mainly during inductive signalling events where Notch is activated along the borders between distinct cell populations. Fringe is believed to specifically influence Notch receptor-ligand binding (Panin and Irvine, 1998). Using a co-culture myoblast assay it was demonstrated that mammalian Lunatic Fringe inhibits Jagged-1-mediated signalling and potentiates Delta-1-mediated signalling through Notch-1 (Hicks *et al.*, 2000). Fringe potentiates Delta-1 binding, proteolytic processing, nuclear translocation of the Notch intracellular domain, and CSL activation (Weinmaster and Kintner, 2003). Where Fringe is expressed, there is an inhibition of Jagged-dependent Notch signalling and a potentiation of Delta-dependent signalling (Fleming *et al.*, 1997).

Fringe appeared to be a requirement for a Notch-Delta signal for secondary mesenchymal cell specification and later for endoderm specification prior to morphogenesis in the sea urchin (Peterson and McClay, 2005). Lunatic Fringe expression was detected in the dermal condensates of embryonic mouse skin, along with Notch-1 and Delta-1 (Favier *et al.*, 2000). Experiments using mouse embryos null for Lunatic Fringe found that these embryos had a reduced viability compared to wild type embryos (Sparrow *et al.*, 2006). In the developing chick, misexpression of Lunatic Fringe abolished cyclic gene expression in the caudal presomitic mesoderm and severely perturbed positioning of somite boundaries. These findings suggested that rhythmic oscillations of Lunatic Fringe protein are essential for co-ordinating boundary positioning and that Lunatic Fringe works in a negative feedback loop on Notch signalling in the chick segmentation clock (Dale *et al.*, 2003).

The highly conserved structure of these Notch pathway genes between species (Fleming, 1998) meant that murine probes could be used to detect expression of the same

genes in ovine tissue. Sequence alignments of known murine sequences with ovine ESTs revealed homologies of 80 – 83% for Delta-1, 79% for Delta-3 and 85% for Lunatic Fringe (refer to Appendix 5.5). The present study focused on the localisation of gene transcripts belonging to the Delta-1 and Delta-3 ligands and their modulator, Lunatic Fringe in foetal sheep skin prior to and during follicle initiation. These genes were studied to determine whether they could be used as markers for identifying the founder cells of the dermal papilla cell population within foetal sheep skin prior to and during follicle initiation. It was hoped that these genes could be used to identify the founder cells prior to and during follicle initiation. Following the founder cell theory, this would mean that on d 56 mesenchymal cells destined to form the dermal condensates, and later the dermal papilla, would be expressing a Notch ligand. On d 70, the mesenchymal cells previously expressing the ligand would have migrated to common points below the basal layer of the epidermis to form the dermal condensates. Some mesenchymal cells would remain in the mesenchymal cell population for later waves of follicle initiation. This would enable the follicle-producing ability of a skin to be deduced. The Founder Cell Theory, based on the principle that the skin produces more or less follicles of lower or higher diameter respectively (Moore *et al.*, 1989), proposed that the formation and quantity of fibre-producing follicular tissue was controlled by a population of dermal cells giving rise to the dermal papilla and that these cells became committed to a follicle lineage at or prior to follicle initiation (Moore *et al.*, 1998).

3.2 MATERIALS AND METHODS

3.2.1 ANIMALS

Mouse embryos were used to test the specificity of the murine cDNA-generated Delta-1 riboprobe. All sheep underwent oestrous synchronisation (Section 2.2.2.1), with Merinos impregnated by LAI (Section 2.2.2.2) and Tukidales by natural mating.

Skin was collected from the gluteal region of Merino and Tukidale foetuses at d 56 and d 70 of gestation. These samples were processed in to paraffin wax (Section 2.2.4.1), sectioned (Section 2.2.5.1) and stained with haematoxylin and eosin (Section 2.2.6). Microscopic examination confirmed that the skin sampling times coincided with events surrounding the first wave of primary follicle initiation in both lines.

3.2.2 RIBOPROBE CREATION

Riboprobes to be used for *in situ* hybridisation studies were created for Delta-1, Delta-3 and Lunatic Fringe. Murine complementary DNA (cDNA) was used as a template for these probes, as the murine forms of these genes had been sequenced, and the sequences were available in GenBank. Riboprobes were produced following the method described in de Iongh *et al.* (2001) and the instructions in the Roche Applied Science DIG-Application Manual for Non-Radioactive *In Situ* Hybridisation (2002).

The murine Delta-1 cDNA (2.1 kb; X80903) had been cloned into pBluescript II SK(-) phagemid (accession number X52330; Stratagene, CA, USA). The murine Delta-3 cDNA (2.1 kb; BC052002) had been cloned into pBluescript II SK (+) (accession number X52328; Stratagene). Murine Lunatic Fringe cDNA (2.2 kb; accession number AF015768) had been ligated into pBluescript II SK (+). The structure of the pBluescript plasmid is illustrated in Figure A0.1.

3.2.2.1 Transformation of *E.coli* for pDNA amplification

3.2.2.1.1 Recovering the plasmid DNA

The cDNA was kindly supplied on Whatman filter paper (Delta-1 from Barry Powell; Delta-3 from Sally Dunwoodie; Lunatic Fringe from Gavin Chapman). The paper containing plasmid DNA (pDNA) was removed from the sealed bag, placed in a sterile 1.5 ml microfuge tube (Greiner Bio-One) with 50 µl 1mM Tris (pH 7.6), vortexed, and incubated for 5 min to rehydrate the DNA. The DNA was centrifuged briefly at room temperature at 20,800 ×*g*. The paper was removed from the tube, the concentration of pDNA quantified with an 8.5 mm (light beam height) BioPhotometer (613101006; Eppendorf), the pDNA diluted to ≤10 ng/µl with 1mM Tris (pH 7.6) and stored at –20°C.

3.2.2.1.2 Chemical transformation of competent cells

To chemically transform XL1-Blue cells (Promega Corp) for Delta-3, or JM109 (Promega Corp) cells for Delta-1 and Lunatic Fringe, 500 µl of the suspension was thawed on ice, mixed, and dispensed into 5 pre-cooled microfuge tubes. XL1-Blue cells required the addition of 1.7% β-mercaptoethanol and incubation on ice for 10 min, with regular mixing.

The pDNA (5 ng/µl), containing the gene insert was added to two of the cell suspensions so that they contained 10 ng and 50 ng of pDNA. The pDNA control cells received 2 µl of the plasmid without the gene insert. As a method control, the fifth tube

received 2 µl of the untransformed cell suspension. The tubes were mixed by tapping and stored on ice for 10 min: those to be transformed with XL1-Blue were stored for 30 min.

Heat-shock was used to incorporate the pDNA into the cells. The cells were heated to 42°C for 45 sec then placed on ice for 2 min. To the JM109 cells, 900 µl cold SOC medium [2% tryptone; 0.5% yeast extract; 117mM NaCl; 0.02mM glucose] was added, to XL1-Blue cells pre-warmed medium (37°C) was added, and the tubes were incubated at 37°C for 1 hr, with shaking at 250 rpm. The cells were condensed by centrifugation at 12,857 ×*g* and the supernatant discarded. The remaining cells were diluted 10-fold and 100-fold.

Aseptically, 100 µl of transformed cells with the plasmid were plated on LB/ampicillin plates [171mM NaCl; 1% tryptone (Oxoid Ltd, Hampshire, England); 0.5% yeast extract (Oxoid Ltd); 100 µg/ml ampicillin; 0.5% bacteriological agar (750-gel; Chem-Supply, Gillman, SA, Australia)] treated with 5 mg/ml X-galactosidase (Promega Corp) and 100 µl of 100mM IPTG, so that recombinant colonies could be detected. Control plates received 100 µl of the untransformed cells. Five different concentrations of cells and pDNA were tested:

i. 100 µl untransformed competent cells
ii. 100 µl cells transformed with 100 µl of 10ng pDNA
iii. 100 µl cells transformed with 200 µl of 10 ng pDNA
iv. 100 µl cells transformed with 100 µl of 50 ng pDNA
v. 100 µl cells transformed with 200 µl of 50 ng pDNA

All plates were incubated at 37°C for 16-24 hr. If the transformation was successful the cells that received the plasmid were the only cells that formed colonies. Transformed cells that contained the plasmid without the gene insert were non-recombinant and appeared blue due to the LacZ plasmid gene remaining active, allowing the cells to utilise the X-galactosidase. The recombinant colonies appeared white due to the LacZ gene being inactivated by the gene insert.

3.2.2.1.3 PCR screen of chemically-transformed E.coli

For each transformation, a number of single white colonies were chosen, removed from the plate and the cells were transferred to a numbered square of a grid drawn on a new LB/ampicillin plate treated with 5 mg/ml X-galactosidase and 100 µl of 100mM IPTG and incubated at 37°C overnight. At the same time, each colony was inoculated into 70 µl of PCR master mix [1x DNA polymerase buffer; 0.2mM dNTP mix; 25pM T3 primer (5'AAT TAA CCC TCA CTA AAG GG 3'; Sigma® Genosys); 25pM T7 primer (5' GTA ATA CGA CTC ACT ATA GGG C 3'; Sigma® Genosys)] in the corresponding PCR tube (Greiner Bio-One)

and vortexed. The control tubes received 10 µl pDNA but no enzyme, and enzyme but no DNA. All tubes, except for the positive control, received 1.4U SuperTaq Plus™ polymerase (Enzyme Technologies Ltd, Ambion Inc, The RNA Company, TX, USA). The tubes were mixed, spun down and loaded into a thermocycler (PCR Sprint; Hybaid Ltd, Hampshire, UK). The polymerase chain reaction (PCR) consisted of 30 cycles of denaturing at 95°C for 1 min, annealing at 51°C for 1 min, extension at 72°C for 2 min. The final extension ran at 72°C for 5 min, after which the samples were stored at 4°C.

A DNA ladder (Hyperladder I; Bioline (Australia) Pty Ltd, Alexandria, NSW, Australia) was loaded along with 10 µl of the PCR products, mixed with 3 µl Ficoll loading buffer [0.25% bromophenol blue; 0.25% xylene cyanol FF; 15% Ficoll 400], into a 1% agarose gel (agarose MP; Roche Diagnostics) in 1x TAE buffer [40mM Tris-acetate; 2mM Na_2EDTA], with 0.2% ethidium bromide. The gel was immersed in 1x TAE buffer and electrophoresed at 100 V for 40 min. The gel bands were visualized with UV trans-illumination within a Geldoc XR (BioRad Laboratories).

3.2.2.2 Amplification of recombinant cell colonies

One white colony was chosen, based on the size and strength of the band visualised on the gel, and inoculated into a 10 ml LB broth starter culture containing 100 µg/ml ampicillin. The culture was incubated at 37°C with shaking at 250 rpm, until the OD_{600} reached 0.6 (~3 hr). Approximately 5 ml of the starter culture was inoculated into a 250 ml LB culture, in a 1 L conical flask (Pyrex®, Corning Australia, Lindfield, NSW, Australia) and incubated for 12-16 hr at 37°C, with shaking at 200 rpm.

3.2.2.3 Preparation of cell glycerol stocks

To prepare stocks of the amplified colony, 850 µl of the overnight culture and 150 µl glycerol were mixed within a 2 ml cryovial and stored at –80°C.

3.2.2.4 Purification of plasmid DNA from broth cultures

The pDNA was purified using an EndoFree® Plasmid Maxi Kit (Qiagen Pty Ltd, Doncaster, VIC, Australia), following the manufacturer's instructions.

The bacterial cells were harvested by centrifugation (580R; Eppendorf), using a fixed-angle rotor (F-34-6-38; Eppendorf), for 15 min at 4°C at 6,000 ×*g*, and the supernatant discarded. The cells were resuspended in 10 ml of Buffer P1 [50mM Tris·Cl, pH 8.0; 10mM EDTA; 100 µg/ml RNase A], before 10 ml of Buffer P2 [200mM NaOH; 1% SDS] was added

and the solution mixed by inversion and incubated at room temperature for 5 min. To the viscous lysate, 10 ml of chilled Buffer P3 [3M potassium acetate, pH 5.5] was added and mixed by inversion, at which time a white precipitate formed. The lysate was immediately transferred to the barrel of a QIAfilter maxi cartridge and incubated at room temperature for 10 min. The cap from the outlet nozzle was removed and the plunger was inserted into the cartridge. The lysate was filtered through the cartridge filter, trapping the plasmid. At this stage, 120 µl of the filtered lysate was saved for an analytical gel (sample 1). To the lysate, 2.5 ml Buffer ER [proprietary formulation] was added and mixed by inversion, prior to incubation on ice for 30 min.

A Qiagen-tip 500 was equilibrated with 10 ml Buffer QBT [750mM NaCl; 50mM MOPS, pH 7; 15% isopropanol; 0.15% Triton®] and allowed to empty. The filtered lysate was added to the tip and allowed to flow through the resin. A sample was taken from the flow through and saved for a gel (sample 2). The tip was washed twice with 30 ml of Buffer QC [1M NaCl; 50mM MOPS, pH 7; 15% isopropanol] by allowing it to flow through the tip. A sample was taken from the first wash and saved for a gel (sample 3).

The DNA was eluted from the resin within the Qiagen-tip using 15 ml Buffer QN [1.6M NaCl; 50mM MOPS, pH 7; 15% isopropanol] and collected. A sample of the eluate was reserved for a gel (sample 4). The DNA was precipitated from the eluate by adding 70% volume isopropanol, mixed and centrifuged at 4°C for 1 hr at 5,000 ×*g*. The supernatant was discarded and the glassy DNA pellet washed with 5 ml of 70% ethanol before centrifugation. The DNA pellet was air dried for 10 min, before being dissolved in 100 µl Buffer TE [10mM Tris, pH 8; 1mM EDTA].

The DNA yielded was quantified by biophotometer. If the yield was low, the 4 samples collected during the procedure were electrophoresed on a 1% agarose gel to determine where the problem occurred.

3.2.2.5 DNA purification by phenol: chloroform extraction

The DNA was transferred to a microfuge tube and the volume increased to 300 µl with TE buffer. An equal amount of phenol: chloroform: isoamyl alcohol (25:24:1, pH 7.8–8.0) was added, the solution vortexed to form an emulsion before the sample was centrifuged for 1 min at room temperature, at 10,600 ×*g*. The aqueous phase was transferred to a clean tube and an equal amount of chloroform was added before the sample was vortexed and centrifuged. The aqueous phase was transferred to a clean tube before 30 µl of 3M sodium acetate and 660 µl ice-cold 100% ethanol were added. The sample was mixed and stored at –80°C for 30 min

to facilitate DNA precipitation. The DNA was centrifuged for 15 min at 4°C, at 20,800 ×*g*. The supernatant was aspirated from the pellet before 600 µl of 80% ethanol was added and the sample centrifuged; this step was repeated. The supernatant was discarded and the pellet was air dried (~15 min) at room temperature. The pellet was redissolved in 50 µl TE buffer (pH 8.0) and the DNA concentration quantified using the biophotometer.

3.2.2.6 Analysis of the pDNA by restriction enzyme digest and DNA sequencing

The purified pDNA was linearised with the appropriate restriction enzymes to be used for linearisation of the pDNA for the antisense and sense probes. Delta-1 was digested with SmaI (sense) and KpnI (antisense) at 37°C for 5 hr. Delta-3 was digested with NotI (sense) and KpnI (antisense) at 37°C for 3½ hr. Lunatic Fringe was digested with XbaI (sense) and HindIII (antisense) at 37°C for 2 hr. The inserts were also isolated in digests with the EcoR1 enzyme, which isolated the pDNA insert from the multiple cloning site of pBluescript (refer to Figure A0.1). Samples of each of the digests and intact pDNA were electrophoresed and analysed on 1% agarose gels.

For sequencing, samples were set up in 0.2 ml PCR tubes and contained 0.27pM of T3 or T7 primers and 200 ng of intact pDNA. The samples were sequenced by Westmead DNA, Westmead Millennium Institute, Westmead, NSW, Australia. The sequencing results for Delta-1, Delta-3 and Lunatic Fringe are shown in Appendix 5, parts 1, 2 and 3 respectively, and were highly homologous with the known murine sequences deposited in GenBank. The known sequences of ovine ESTs isolated from ovine skin were compared with human Delta-1, and regions of high homology were identified. These mapped to the N- and C- termini of the human Delta-1 sequence (Figure 1.10), providing evidence that Delta-1 is expressed in ovine skin and that the ovine ESTs are highly homologous with the coding sequence in human mRNA. Sequence alignments of murine Delta-1 mRNA with ovine ESTs highlighted a 80 – 83% sequence identity at the nucleotide level (Section A5.5.1), allowing a murine riboprobe to Delta-1 to be used for detection of Delta-1 in ovine tissue.

3.2.2.7 Preparation of template for transcription

The pDNA was linearised to permit transcription of the inserted gene. For each digest, two microfuge tubes were set up on ice, for the labeled antisense and sense probes. Each tube contained 1 x restriction enzyme buffer, 0.2 µg acetylated BSA, 5 µg purified pDNA, and 25 U of restriction enzyme (refer to Table 3.1). The tubes were incubated at 37°C (SmaI was

incubated at 25°C) for 1-4 hr. Placing the tubes on ice stopped the reaction. The DNA strands produced are illustrated in Figure 3.1. The samples were electrophoresed on a 1% agarose gel in 1x TAE buffer to ensure the samples were entirely digested.

Table 3.1: The restriction enzymes used for linearising Delta-1, Delta-3 and Lunatic Fringe pDNA and their recognition sequences. Information from Promega Corporation Technical Notes.

pDNA	Restriction Enzymes	Recognition Sequence (Antisense)	Restriction Enzymes	Recognition Sequence (Sense)
murine Delta-1	KpnI	GC/GGCCGC	SmaI	CCC/GGG
murine Delta-3	KpnI	GC/GGCCGC	NotI	GGTAC/C
murine Lunatic Fringe	HindIII	A/AGCTT	XbaI	T/CTAGA

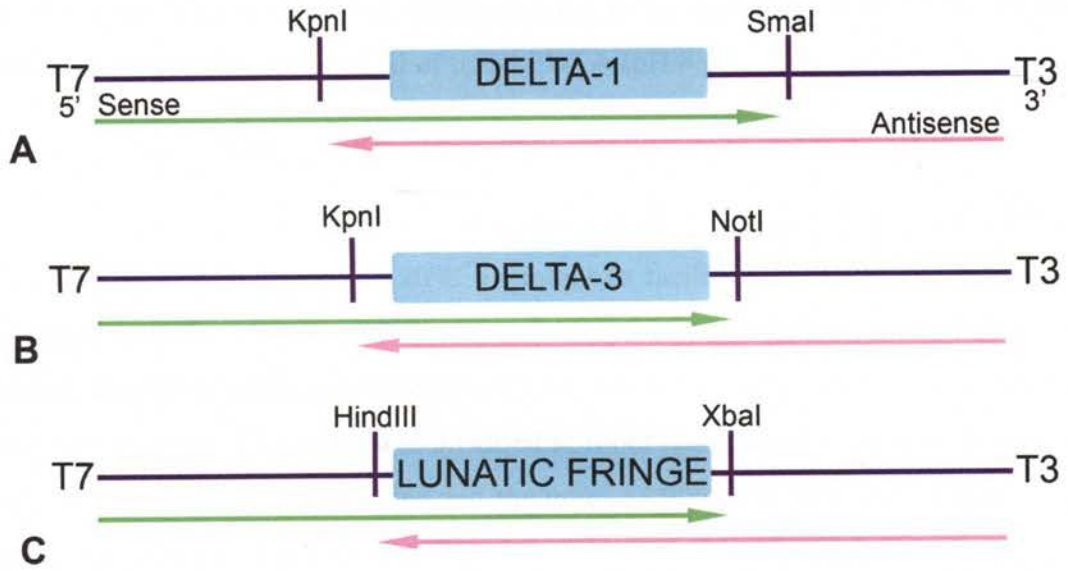

Figure 3.1: Transcription of the Delta-1, Delta-3 and Lunatic Fringe gene inserts for sequencing. A; Delta-1 (2.1 kb) antisense was read from the T3 promoter site to the restriction enzyme KpnI recognition sequence (GC/GGCCGC), sense read from the T7 promoter to the restriction enzyme SmaI recognition sequence (CCC/GGG). B; Delta-3 (2.1 kb) antisense strand was read from the T3 promoter to the restriction enzyme KpnI recognition sequence, sense strand was read from the T7 promoter to the restriction enzyme NotI recognition sequence (GGTAC/C). C; Lunatic Fringe (~2.2 kb) antisense strand was read from T3 promoter to the restriction enzyme HindIII recognition sequence (A/AGCTT) the sense strand was read from T7 promoter to the restriction enzyme XbaI recognition sequence (T/CTAGA).

3.2.2.8 Purification of linearised DNA

The linearised pDNA was purified by phenol: chloroform extraction, as described in Section 3.2.2.5.

3.2.3 TRANSCRIPTIONAL LABELLING OF DIG-RNA PROBES

3.2.3.1 Riboprobe preparation

A DIG Northern Starter Kit (Roche Diagnostics) was used for riboprobe production, following the kit instructions. It was estimated that from 1 µg of pDNA, approximately 20 µg of messenger RNA (mRNA) would be transcribed.

Three microfuge tubes were set up on ice for preparation of the antisense, sense (labelled) and sense (unlabelled) riboprobes. Each tube contained 20 µl; ~1 µg linearised pDNA, 40 U RNaseIn® (Roche Diagnostics), 4 µl (5x) DIG-NTP labelling mix (unlabelled NTP mix was substituted for the unlabelled sense probe), 4 µl (5x) transcription buffer and 1mM RNA polymerase (Promega Corp) [T3 for antisense, T7 for sense]. The contents of the tubes were mixed and spun down before incubation at 37°C for 2 hr. To each tube, 2 µl of DNase I (Roche Diagnostics) was added and the tubes incubated at 37°C for 15 min. The reaction was stopped by adding 2 µl of 0.2M EDTA (pH 8.0).

3.2.3.2 Probe precipitation

To each tube, 2.5 µl of 4M lithium chloride and 75 µl ice-cold 100% ethanol were added. The tubes were stored at –20°C overnight to facilitate RNA precipitation. The tubes were centrifuged for 15 min at 4°C with a force of 13,100 ×*g*, before the supernatant was discarded. The RNA pellet was washed with 50 µl ice-cold 80% ethanol, centrifuged and the supernatant removed. The pellet was air-dried at room temperature (~30 min) before 50 µl of 0.1% DEPC-treated water was added and the tubes incubated at 37°C for 30 min, to dissolve the RNA. The probe was stored at –20°C.

3.2.3.3 Probe quantification using the direct detection method

To estimate the amount of probe produced, a series of dilutions ranging from 10 ng/µl to 0.1 pg/µl were made up for the DIG-labelled probes and DIG-labelled actin RNA (positive control; Roche Diagnostics) in RNA dilution buffer [5 parts 0.1% DEPC-treated water; 3 parts 20x SSC; 2 parts formaldehyde (37%)].

A dry, positively-charged nylon membrane (Hybond–N^+; Amersham Pharmacia Biotech, England) was placed in a glass Petri dish and marked for orientation before 1 µl spots of each tube dilution were applied. The RNA was cross-linked to the membrane using UV trans-illumination for 3 min on each side. The membrane was washed in 1x washing buffer for 2 min with shaking, blocked for 30 min in 1x blocking solution made up in 1 x

maleic acid buffer, incubated with a 1:10,000 dilution of an antibody to Anti-Digoxigenin conjugated to alkaline phosphatase in 1x blocking solution, washed twice in 1x washing buffer for 15 min, and equilibrated in 1x detection buffer for 5 min.

The membrane was transferred to a hybridisation bag (Roche Diagnostics) before ~1 ml CDP-star (Roche Diagnostics) was added to the upper surface, the substrate spread evenly over the blot, and a bag sealer (CJ1; Taiwan) used to seal the bag. The membrane was incubated for 5 min at room temperature.

Within the dark room, the blot was exposed to Kodak Scientific Imaging film (X-Omat™, Blue XB-1; Kodak, NY, USA) within a Kodak Biomax MS Screen (20 x 25 cm) for 1-10 min. The film was placed in developer/replenisher [25% developer A; 2.5% developer B; 2.5% developer C (Agfa-Gevaert Ltd, Nunawading, VIC, Australia)] for 1 min, rinsed, placed in rapid fixer [20% fixative A; 5% fixative B (Agfa-Gevaert Ltd)] for 1 min, rinsed, and air-dried. The spot intensities of the riboprobes were compared to known concentrations of the actin riboprobe standard (Figure 3.2). As illustrated, when the probe detected a signal at a concentration of 0.1 pg/µl, it was deemed highly sensitive. This signified that the labelling reaction produced the expected (800 ng/µl) amount of RNA, as mentioned in Techniques for DIG-labelling of hybridisation probes (Roche Diagnostics). For this specificity of probe, 200 ng of probe was added to each ml of hybridisation solution.

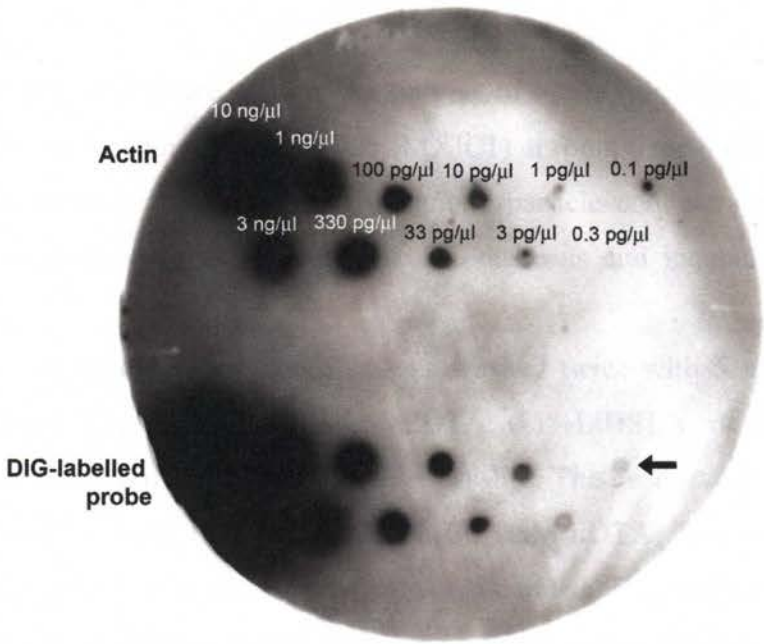

Figure 3.2: Quantification of a DIG-labelled riboprobe produced by transcription. The concentrations of the DIG-labelled riboprobe were compared with the DIG-labelled actin RNA standard. The probe produced was highly sensitive, with a signal detected at the 0.1 pg/µl concentration (arrow).

3.2.4 NORTHERN BLOTTING

3.2.4.1 Extraction of mRNA from foetal Merino sheep skin

A Dynabeads® messenger RNA (mRNA) Direct™ Kit (Dynal® Biotech ASA, Oslo, Norway) was used and the kit instructions followed to isolate mRNA from foetal sheep skin.

An unfixed, snap frozen in liquid nitrogen, d 70 foetal Merino midside skin sample, stored at (–80°C) was weighed whilst frozen and powdered under liquid nitrogen using a mortar and pestle. Approximately 200 mg was transferred to a pre-cooled Dounce homogeniser with 5 ml Lysis/Binding buffer supplied in the kit [100mM Tris-HCl, pH 7.5; 500mM LiCl; 10mM EDTA, pH 8; 1% lithium dodecylsulphate (LiDS); 5mM dithiothreitol (DTT)] and homogenised. The lysate was then dispensed into five microfuge tubes. The DNA was sheared by aspiration with a 21 G needle and syringe. The samples were centrifuged at 4°C for 1 min with a force of 1,500 ×*g*, before the lysate was pooled into a 15 ml tube, quantified and stored at –80°C.

3.2.4.2 mRNA extraction using Dynabeads

Dynabeads® Oligo $(dT)_{25}$ were re-suspended by vortexing, and 5 mg (1 ml) of the solution was dispensed into two microfuge tubes. The tubes were placed in a Dynal MPC®-E-1 magnetic particle concentrator. Once cleared, the supernatant was aspirated from the beads, the tube removed from the magnet. The beads were washed twice by re-suspension in 1 ml Lysis/Binding buffer.

The tissue lysate was thawed before the first set of beads was added. The solution was mixed and incubated on a Dynal sample mixer (MXIC1) at room temperature for 15 min. The tube was then placed in a Dynal MPC®-L magnetic particle concentrator for 2 min. The supernatant was transferred to the second set of Dynabeads and incubated on the sample mixer for 10 min.

The first set of beads/mRNA complex was washed twice with 5 ml Wash buffer A [10mM Tris-HCl, pH 7.5; 0.15M LiCl; 1mM EDTA; 0.1%LiDS], vortexed, and incubated with the magnet, with the buffer removed between washes. The beads were washed with 5 ml Wash buffer B [10mM Tris-HCl, pH 7.5; 0.15M LiCl; 1mM EDTA]. The magnet was used to collect the beads before ~4 ml of the supernatant was aspirated. The beads were re-suspended, transferred to a microfuge tube, collected with a magnet and the supernatant discarded. To the beads, 50 µl formaldehyde load dye (Ambion Inc) was added. The beads were re-suspended and incubated at 70°C for 15 min. The tube was placed on ice with the magnet. Once the

beads were concentrated, the supernatant, containing mRNA, was transferred to a microfuge tube and kept on ice. The process was repeated with the second set of beads. The eluted mRNA samples were stored on ice until they were loaded into a gel. Unused samples were stored at –20°C.

3.2.4.3 Fractionating mRNA in hot agarose gel

A 1.2% agarose (agarose MP; Roche Diagnostics) gel was prepared in 1x TAE buffer. The molten gel was equilibrated in a 50°C waterbath, poured into a gel-casting tray (Bio-Rad Laboratories), to a thickness of 0.6 cm, and left to set for 1 hr.

Microfuge tubes were set up as shown in Table 3.2. RNA Millennium marker (Ambion Inc) and RNA molecular weight marker III, DIG-labelled (Roche Diagnostics) were used. The tubes were vortexed and spun down. Tube 1 was incubated at 80°C and tubes 2-7 at 70°C, for 15 min. All tubes were condensed before 0.75 µg ethidium bromide was added to tubes 1 and 7.

Table 3.2: From d 70 Merino skin, mRNA samples were to be fractionated in a 1.2% agarose gel. RNA Millennium and RNA Molecular Weight Markers were used as size standards. Different concentrations of the high copy RNA (from the first set of Dynabeads) were run in addition to the low copy RNA sample (from the second set of Dynabeads). Formaldehyde load dye (Ambion Inc) and formamide were added to the mRNA samples.

Tube	1	2	3	4	5	6	7
RNA	RNA Millennium Marker	RNA Molecular Weight Marker	Low copy RNA	High copy RNA	High copy RNA	High copy RNA	High copy RNA
ng RNA	2	0.01	2-10				
µl sample	2	10	10	4	8	10	10
Formaldehyde load dye (µl)	6	4	–	6	2	–	–
60% formamide (µl)	7	1	5	5	5	5	5

The gel was placed in the electrophoresis equipment (Bio-Rad Laboratories) before 1 x TAE, heated to 60°C, was poured into the gel tank in line with the top of the gel, so that the upper surface of the gel was not wet. Once the buffer cooled to 50°C, the gel was pre-electrophoresed at 140 mA/150 V for 15 min. The denatured mRNA samples were loaded into their respective lanes in the gel and electrophoresed for 5 min, allowing the RNA to enter the gel matrix. The gel tank was filled with 1 x TAE (60°C), submerging the gel before electrophoresis was carried out at 113 mA/91 V for 20 min, maintaining the temperature of the gel at 50°C ± 2°C.

The gel was removed from the casting tray, placed in a square Petri dish and washed in 30 ml of 0.1% DEPC-treated water for 1 min, with shaking. The gel was trimmed using a scalpel blade, so that the top of the lanes and top right corner were removed. The gel was photographed with UV trans-illumination within the Gel Doc (Bio-Rad Laboratories), then washed twice in 40 ml 10 x SSC for 15 min, with shaking.

3.2.4.4 Capillary transfer of mRNA by downward flow

A BrightStar™-Plus positively charged nylon membrane (Ambion Inc) was cut slightly larger than the gel, the top right corner was cut for orientation and the bottom labelled. The membrane was pre-equilibrated by floating it on 0.1% DEPC-treated water until it had soaked through, and incubated in 30 ml of 10 x SSC for 5 min. Within a square Petri dish the wick (made out of Whatman paper) and four squares of Whatman paper were soaked in 10 x SSC.

The transfer apparatus was set up, with all paper the size of the membrane, as follows: a glass plate, 18 pieces dry QuickDraw™ blotting paper, 8 pieces dry Whatman paper, 2 pieces Whatman paper soaked in 10 x SSC, pre-wet BrightStar membrane (10 x SSC was added to flood the surface), agarose gel placed in the same orientation as the membrane (air bubbles squeezed out and the surface flooded with 10 x SSC), 2 pieces of wet Whatman (air bubbles removed), pre-soaked wick with either end submerged in 10 x SSC. A gel-casting tray was used to weigh down the blot. Capillary transfer was carried out for 2½ hr. Once complete, the apparatus was carefully disassembled. The wells of the gel were marked on the membrane before the membrane was transferred to a square Petri dish and rinsed twice in 2 x SSC for 5 min. The RNA was cross-linked to the membrane with UV trans-illumination for 3 min and rinsed briefly in 0.1% DEPC-treated water.

3.2.4.5 Pre-hybridisation

ULTRAhyb™ Ultra Sensitive hybridisation buffer (Ambion Inc) was pre-heated to 68°C in a water bath to dissolve the precipitate before two, 6 ml aliquots were taken.

The membrane was placed in a hybridisation bag (Roche Diagnostics), 6 ml of hybridisation buffer was added and the bag sealed. The membrane was incubated at 68°C within a hybridisation oven (Shake 'n' Stack; Hybaid Ltd) for 60 min, with shaking.

3.2.4.6 Hybridisation

The Delta-1 antisense riboprobe was diluted in 50 µl of 0.1% DEPC-treated water and denatured at 100°C for 10 min, cooled on ice and spun down before it was added to 6 ml hybridisation buffer (heated to 68°C) to give a final concentration of 100 ng/ml.

The pre-hybridisation solution was discarded, the membrane transferred to a fresh hybridisation bag, and the pre-warmed hybridisation buffer containing the probe was added before the bag was sealed. The membrane was incubated overnight at 68°C, with shaking.

3.2.4.7 Post-hybridisation

The hybridisation solution was discarded and the membrane transferred to a large glass Petri dish, covered with 100 ml of pre-heated 2 x SSC with 0.1% SDS and washed twice for 5 min within the 68°C oven. The membrane was then washed twice in 100 ml high stringency buffer [0.1 x SSC; 0.1% SDS] at 68°C for 15 min.

3.2.4.8 Immunological detection

The membrane was processed on a shaking platform at room temperature, first in 50 ml 1 x maleic acid buffer for 5 min, blocked in 30 ml of 1x blocking solution for 30 min, and incubated with Anti-DIG-AP antibody diluted in 1 x blocking solution (1:10,000) for 30 min. It was then transferred to a clean dish and washed twice in 30 ml of 1 x washing buffer for 15 min, before equilibration in 30 ml of 1 x detection buffer [0.1M Tris-HCl, pH 9.5; 0.1M NaCl; 50mM $MgCl_2$] for 5 min.

The membrane was placed in a hybridisation bag before 1 ml of CDP-Star, ready-to-use solution (Roche) was added and evenly spread over the membrane's surface. The membrane was covered, air bubbles pressed out and the bag heat-sealed. After 5 min, in the dark room, the membrane was placed within a Kodak Biomax MS Screen (20 x 25 cm; Kodak, NY, USA) and exposed to Kodak Blue XB-1 Scientific Imaging Film for 6 min. The film was processed through developer/replenisher and rapid fixer as described in Section 3.2.3.3.

3.2.5 IN SITU HYBRIDISATION

Samples were wax-embedded for these studies (Section 2.2.4.1) and 5 µm sections cut with a microtome (Section 2.2.5.1). The *in situ* hybridisation method described in Section 2.2.8 was followed. For the three probes tested, all tissues were incubated with riboprobe at a concentration of 200 ng/ml. The probes used to detect Delta-1, Delta-3 and Lunatic Fringe

transcripts were found to be highly specific (Section 3.2.3.3), detecting 0.1 pg/µl RNA or DNA.

3.2.5.1 Cell counts

Cell counts for Delta-1 labelled and unlabelled mesenchymal cells were performed on foetal sheep skin samples. The methodology previously described (Section 2.2.8.6) was followed. Briefly, 3 fields of view (290 x 220 µm) were investigated for 3 non-serial sections cut from skin samples collected from 7 Merino and 5 Tukidale foetuses sampled on d 56 and d 70 of gestation. The count data were analysed using a Genstat linear mixed model.

3.3 RESULTS

3.3.1 HISTOLOGY OF FOETAL SHEEP SKIN SAMPLES

Microscopic examination of the foetal skin samples confirmed that the collection times corresponded to the first phase of follicle initiation (Figure 3.3). Prior to follicle initiation (d 56), in both Merino and Tukidale samples, an undifferentiated epithelium and mesenchyme were observed. During follicle initiation (d 70), both breeds displayed some degree of primary follicle development. The epithelium had become more stratified, with epithelial thickenings or plugs also visible, below which mesenchymal cells had aggregated to form the dermal condensate.

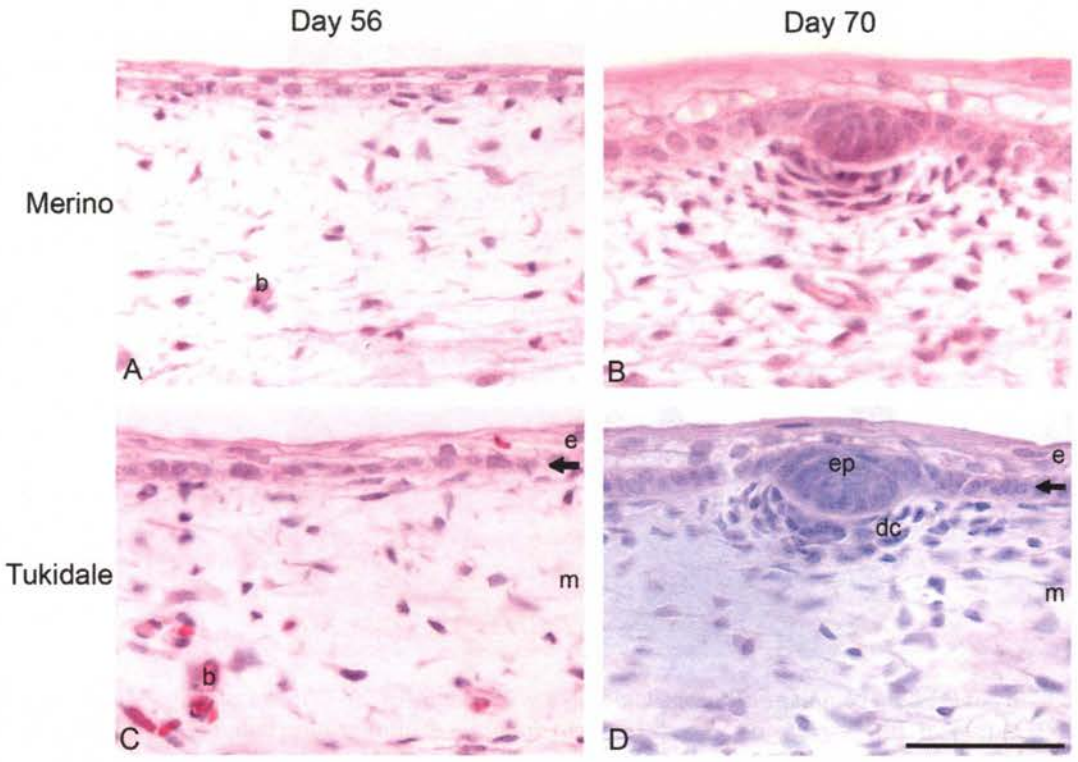

Figure 3.3: Histology of foetal Merino (A, B) and Tukidale (C, D) skin samples. A and C sampled at d 56. Undifferentiated epithelium (e) and mesenchyme (m), basal layer of the epidermis represented by arrows, b refers to blood vessels. B and D sampled at d 70. An epithelial plug (ep) and dermal condensate (dc) had formed. Sections stained with H&E. Image D stained differently to the other panels due to procedural differences, likely a result of a longer period in blueing solution. Scale represents 50 μm.

3.3.2 ALKALINE PHOSPHATASE ACTIVITY IN SHEEP SKIN

The dermal papilla is a structure known to possess a high level of endogenous alkaline phosphatase activity (Handjiski *et al.*, 1994). This high level of activity was confirmed in the foetal sheep skin sampled during follicle initiation (Figure 3.4).

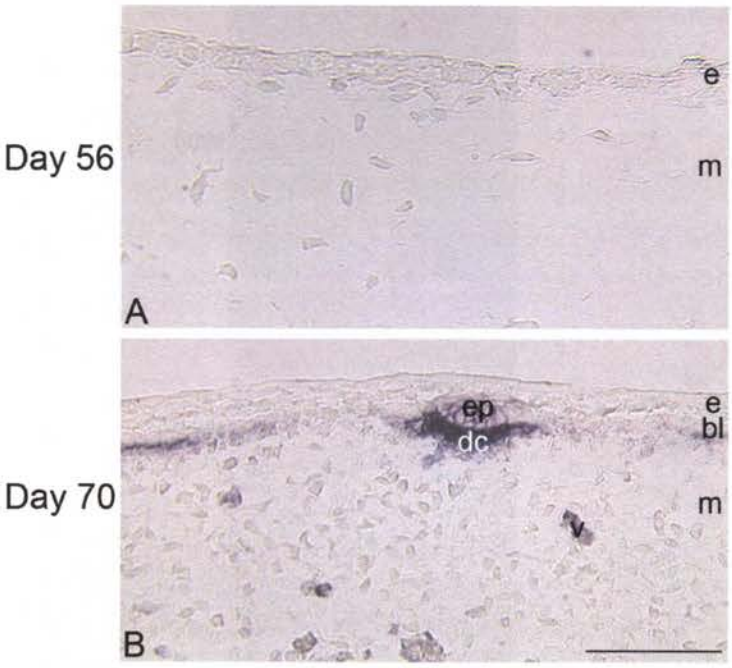

Figure 3.4: Endogenous alkaline phosphatase activity in foetal sheep skin sampled on d 56 and d 70 of development. Tissue sampled prior to follicle initiation (day 56) showed no activity, with no purple staining detected in the epithelium (e) or mesenchyme (m). Tissue sampled during follicle initiation (day 70) showed alkaline phosphatase activity in some cells. No activity was detected in the epithelium (e) or generally throughout the mesenchyme (m). A high level of activity was detected in the dermal condensate (dc) and developing blood vessels (v). Some activity was detected in the basal layer (bl), between the developing follicles, and in the epithelial plug (ep). Scale represents 50 μm.

To conduct *in situ* hybridisation on the foetal skin, using a colorimetric method of detection that utilises alkaline phosphatase as a means of detection, it was necessary to block endogenous activity. This was achieved by conducting titrations in which the sectioned foetal skin samples were subjected to varying concentrations of levamisole (Figure 3.5), a known inhibitor of alkaline phosphatase (Handjiski *et al.*, 1994). Titration confirmed that a concentration of 30mM levamisole was sufficient to minimise endogenous activity levels. No alkaline phosphatase activity was detected in skin sampled on d 56 of foetal development (Figure 3.4; A).

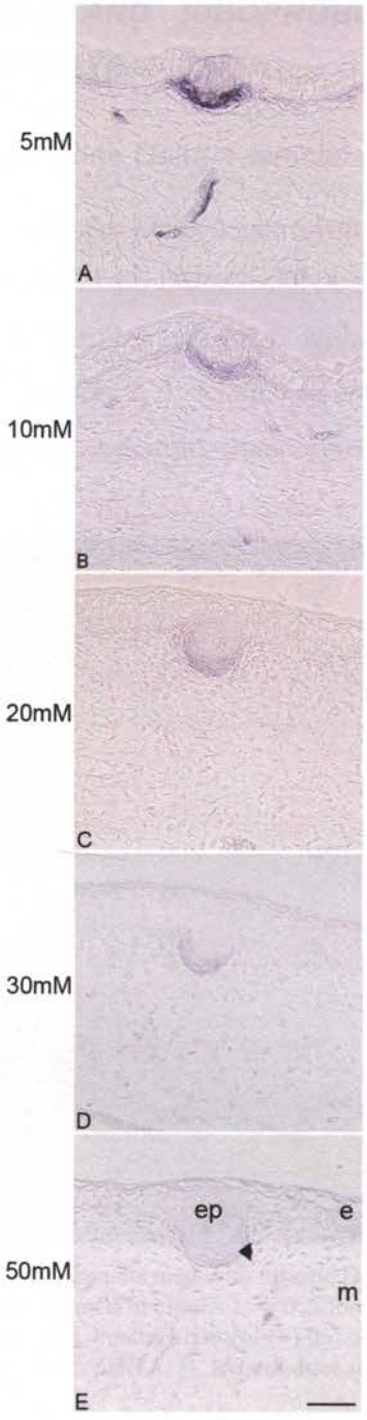

Figure 3.5: A titration of levamisole was tested on d 70 foetal sheep skin samples. A high level of endogenous activity was seen with the recommended 5mM concentration at d 70 (A). As the concentration increased, the level of activity diminished (B, C, D, E) so that minimal levels of staining were detected in the dermal condensate (black triangle). No stain was detected in the epithelium (e), mesenchyme (m) or epithelial plug (ep). The 30mM concentration sufficiently blocked endogenous activity. Scale represents 50 μm.

3.3.2 DELTA-1 TEMPLATE AND RIBOPROBE ANALYSIS AND IN SITU HYBRIDISATION RESULTS

3.3.2.1 Analysis of the murine Delta-1 template

The clones transformed with the Delta-1 gene were screened by PCR and clones that contained the expected size for the 2.1 kb Delta-1 cDNA insert. The correct-sized insert (2-2.5 kb; Figure 3.6) was visualised in samples 1, 4 and 6, with clone 4 chosen for further work due to the strong band produced. Samples 2, 3, 5 and 7 failed to produce a band, suggesting that these white colonies had not been successfully transformed, or the insert was not present.

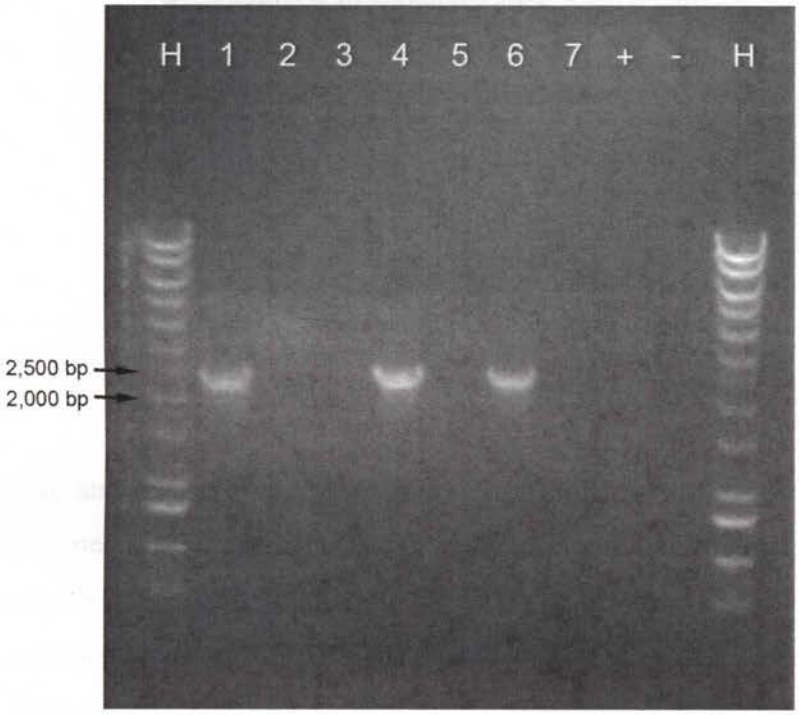

Figure 3.6: PCR screen of JM109 clones transformed with murine Delta-1 were amplified by PCR with T7 and T3 primers. The insert (2-2.5 kb) was isolated in clones 1, 4, 6. Clones 2, 3, 5, 7 did not contain insert. Clone 2 produced a non-specific band (~4,000 bp). Positive control (+) did not produce a band; negative control (-) did not contain pDNA. H; hyperladder size marker.

The transformed cells from clone 4 were amplified and the pDNA purified. The purified pDNA was subjected to a restriction enzyme digest and run on an agarose gel to ensure the purified plasmid contained the gene insert and that it was the correct size (2-2.5 kb). The pDNA was digested with EcoR1 (Figure 3.7; lane 1) to isolate the insert from the rest of the plasmid, by cutting at the same sites used to clone the gene insert into the multiple cloning site (Figure A0.1). Figure 3.7; lanes 2 and 3 contained pDNA linearised with SmaI and KpnI respectively, producing a single band. Lane 4 demonstrated that SmaI and KpnI, when used collectively cut the insert from the rest of the plasmid, having the same effect as EcoR1. Lane

5, containing the undigested Delta-1 pDNA positive control travelled relatively faster through the gel matrix compared to the linearised samples in lanes 2 and 3.

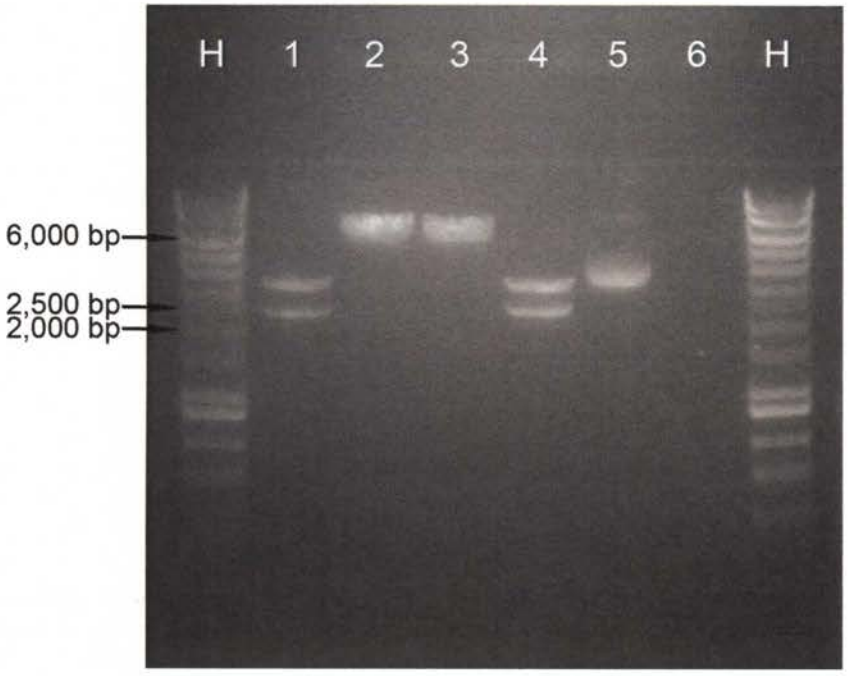

Figure 3.7: Restriction enzyme digest to isolate Delta-1 pDNA from pBluescript DNA. Lane 1 pDNA digested with EcoR1; 2 with SmaI; 3 with KpnI; 4 with SmaI and KpnI; 5 undigested Delta-1 pDNA positive control; 6 no DNA negative control. H; hyperladder size marker.

Sequencing analysis of the pDNA insert (Appendix 5.1) antisense and sense strands confirmed the gene as Delta-1. The query sequence was significantly similar (E=0) to GenBank sequences (accession number: BC065063) *M.musculus* Delta-like 1 (Drosophila), mRNA, and (accession number: BC057400) *M.musculus* Delta-like 1 (Drosophila), mRNA. A search of the database of ovine EST sequences in Ovita (Ovita® Ltd, Dunedin, New Zealand, available at http://www.ovita.co.nz), kindly provided by Alan Pearson and Zhidong Yu, AgResearch, New Zealand, revealed a contig map of 2 EST clones that matched the C- and N-terminals of the human Delta-like-1 sequence (accession number: NM_005618.3) with high homology, as illustrated in Figure 1.10. Further Blastn analysis using BioManager (available at http://www.angis.org.au) showed that the murine Delta-like-1 mRNA sequence (accession number: X80903.1) was highly homologous (83%, 88% and 80%) with ovine EST sequences (EE862149.1, EE749368.1 and EE853192.1 respectively) (Appendix 5.5.1).

In preparation of Delta-1 pDNA for transcription (Section 3.2.3), the DNA was linearised by restriction enzyme digestion (Figure 3.8), using KpnI for the antisense riboprobe and SmaI for the sense probe. The DIG-labelled riboprobes produced by transcription, were

highly sensitive, with a signal detected at the 0.1 pg/µl concentration in both sense and anti-sense probes.

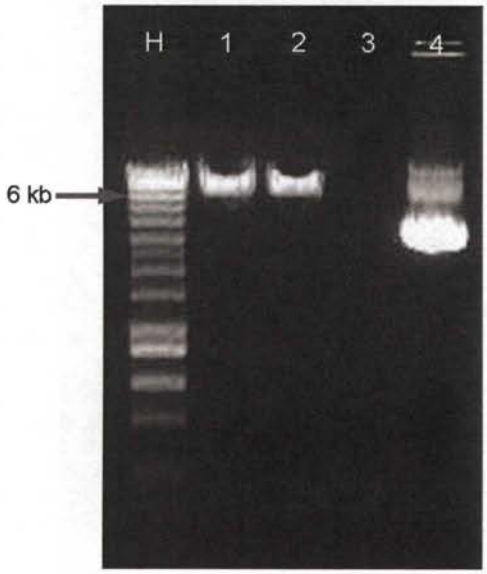

Figure 3.8: Restriction enzyme digest of Delta-1 pDNA for generating the Delta-1 riboprobe. Lane 1, pDNA linearised with KpnI; 3, pDNA linearised with SmaI; 3, negative control containing no DNA; 4, positive control containing undigested Delta-1 pDNA. H; hyperladder size marker.

3.3.2.2 Northern Blotting analysis of the Delta-1 riboprobe

Extraction of mRNA, using Dynabeads® Oligo $(dT)_{25}$, was carried out using d 70 Merino midside skin. Merino skin was used as more samples were available and the localisation of gene transcripts to Delta-1 appeared similar in the Merino and Tukidale skin. Further, d 70 skin was used due to its higher cell density compared to d 56 samples. After fractionation, the bands that were visualised under UV trans-illumination were the Millennium markers and no rRNA bands were seen (Figure 3.9; A), confirming that the samples did not contain rRNA. A strong band of the expected size of the mammalian Delta-1 mRNA (3.1 kb) was detected in the blot after hybridisation with the Delta1 riboprobe (Figure 3.9; B). A second, fainter band (2.5-3 kb) was visualised in all samples, suggesting an unknown derivative of Delta-1 was contained in the skin and detected by the riboprobe.

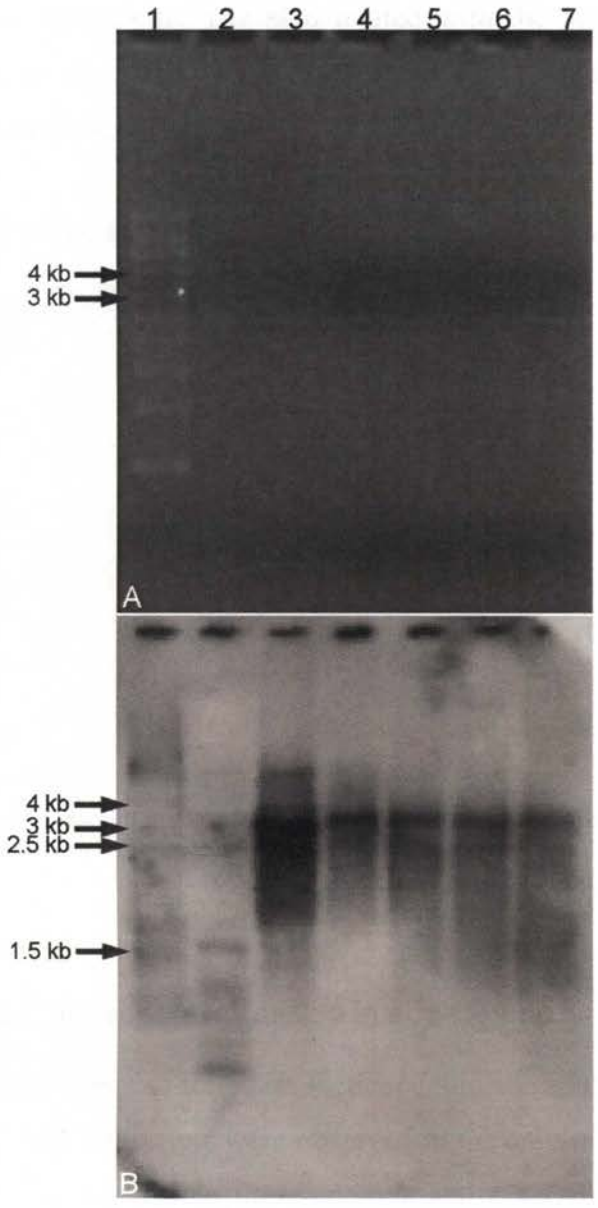

Figure 3.9: Northern blot of isolated mRNA (from day 70 Merino skin) for Delta-1. (A); fractionation of RNA in agarose gel. The Millennium marker stained with ethidium bromide showed clear bands, no band was visualised in lane 7 (ethidium bromide added to sample). B; Northern hybridisation membrane of RNA. Bands were visualised in all lanes. Lane 1; Millennium marker; 2, molecular weight marker; 3, low copy RNA from second set of Dynabeads; 4 – 7 high copy RNA from first set of Dynabeads using 4, 8, 10 and 10 µl (with ethidium bromide) respectively. The main band visualised in all samples was 3-4 kb, with a second fainter band of 2.5-3 kb visualised.

3.3.2.3 Delta-1 transcript expression in embryonic mouse skin

The Delta-1 (2.1 kb) probe was initially tested on sectioned embryonic mouse skin. Skin sampled at 15 dpc, treated with the antisense probe (Figure 3.10; A), showed gene transcripts in the epithelium, where staining was strongest. By contrast, staining in the epithelial plug was low. The mesenchyme possessed a scattered staining pattern, with some labelling in the

region of the dermal condensate. The skin treated with the sense probe (Figure 3.10; B) showed no staining in any cells within the tissue. This probe was thus used in further experiments with sheep skin.

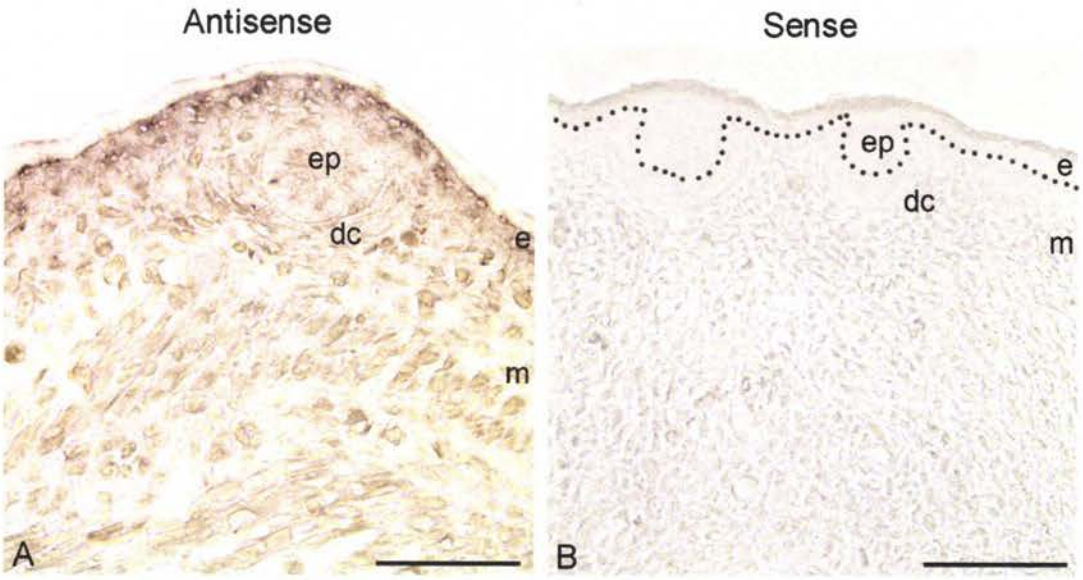

Figure 3.10: Delta-1 gene transcript in mouse skin collected at 15 dpc. A; staining was strong in the epithelium (e), scattered expression was seen in the mesenchyme (m), some staining was detected in the epithelial plug (ep) and dermal condensate (dc) with the antisense probe. B; no staining was visualised in the sense-labelled tissue. Dotted line indicates the position of the epithelial-mesenchymal junction. Scale represents 30 μm.

3.3.2.4 Delta-1 transcript expression in adult sheep skin

The Delta-1 probe was also tested on sectioned midside adult skin samples from Merino and Tukidale ewes. Gene transcripts were observed in the antisense sections (Figure 3.11; A, C). Strong staining was detected in the epidermis and outer root sheath cells, with lower levels of transcripts detected throughout the dermis. The Tukidale (Figure 3.11; C) appeared to have a stronger level of expression, compared to the Merino (Figure 3.11; A). Staining was observed in the dermal papilla in Merino and Tukidale samples. No colour had developed in the sense-treated tissue.

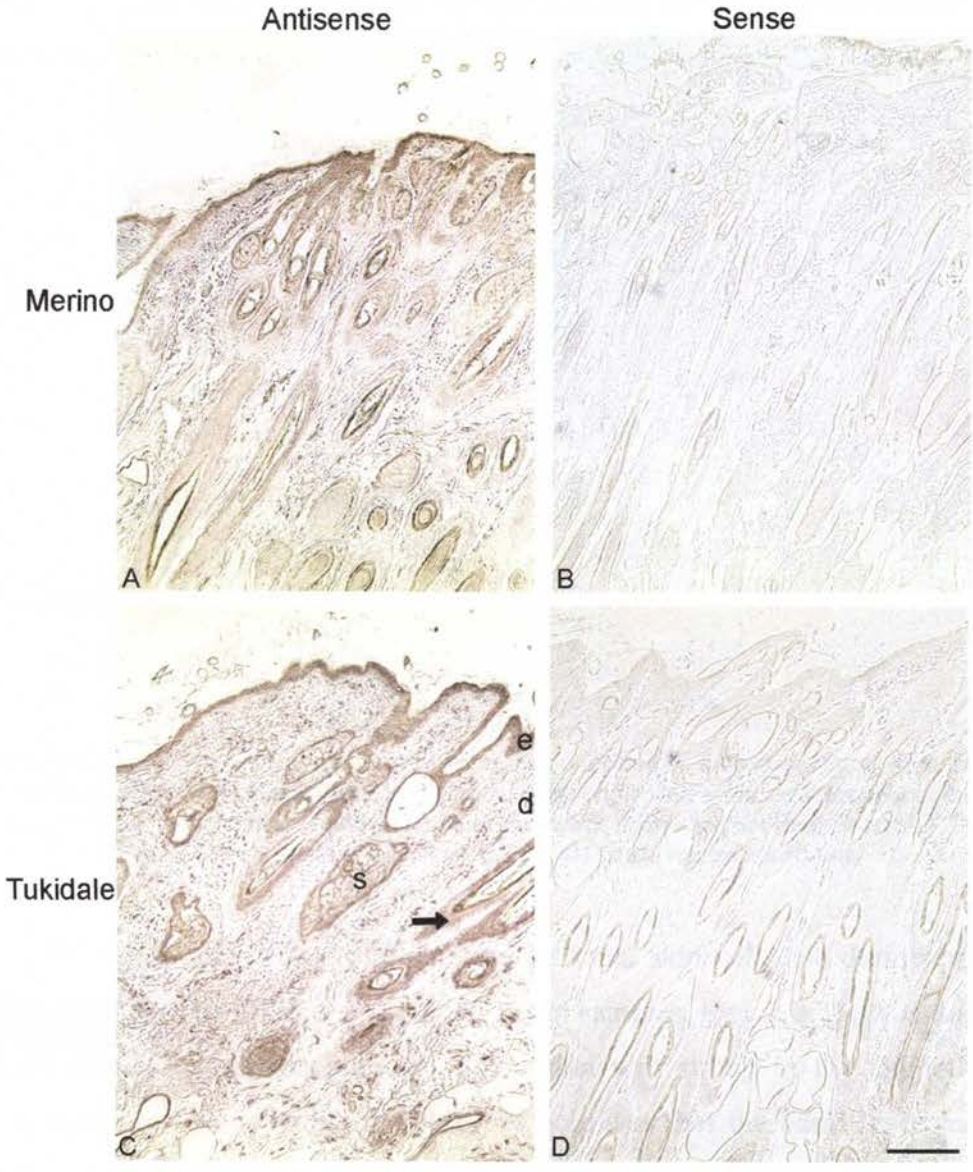

Figure 3.11: Delta-1 gene expression in adult sheep skin. In the sections incubated with the antisense probe (A, C) transcripts were detected in the epidermis (e) and outer root sheath (arrow). Minimal levels of expression were detected in the dermis (d) and sebaceous gland (s). No staining was visualised in the sense-treated tissue (B, D). Scale represents 200 μm.

3.3.2.5 Delta-1 transcript expression in foetal sheep skin

Delta-1 gene expression was investigated in foetal sheep skin collected at d 56 and d 70 of gestation, from fine-woolled Merino and strong-woolled Tukidale animals. Prior to follicle initiation, transcripts were strongly expressed in the epithelium of both breeds (Figure 3.12; A, C), with the basal layer in the Tukidale (Figure 3.12; C) appearing particularly strong. The mesenchyme in both breeds showed differential staining, with the fibroblasts exhibiting varying degrees of colour development. The blood vessels and muscle also expressed Delta-1.

The sense-labelled negative controls (Figure 3.12; B, D) showed no colour development, indicating the specificity of the probe.

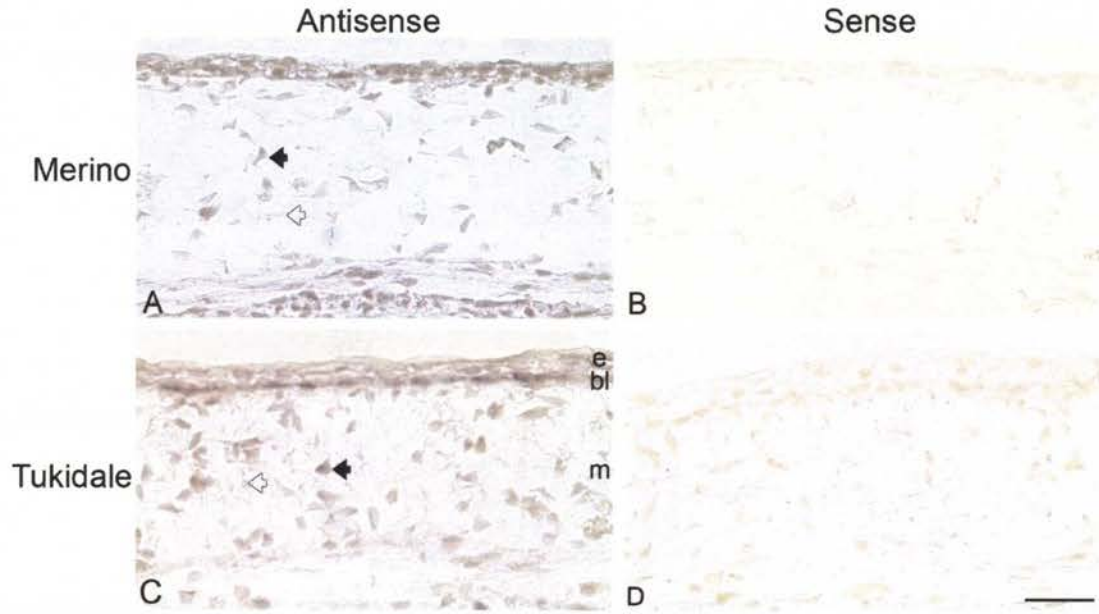

Figure 3.12: Delta-1 gene expression in foetal sheep skin collected on d 56 of gestation. Skin from Merino (A) and Tukidale (C) showed similar staining localisation. Transcripts were expressed throughout the epithelium (e). In the mesenchyme, some cells had stained (solid arrow) while others had not (hollow arrow). The sense-treated sections showed no staining (B, D). Scale represents 50 μm.

Delta-1 gene transcripts were detected in foetal skin collected during primary follicle initiation, at d 70. The Merino and Tukidale skin samples, Figure 3.13; A and B respectively displayed similar expression patterns. Expression was strong in the epithelium, with the interfollicular basal layer staining darkly. Of note was that the basal layer surrounding the developing follicles did not show any expression. The epithelial plug did not appear to express Delta-1 in the Merino, with low expression detected in the Tukidale. The mesenchyme was differentially stained, as was observed prior to follicle initiation. The dermal condensate appeared to show higher levels of gene expression than the general fibroblast population in the mesenchyme, an observation that was consistent in both breeds. Tissue treated with the labelled sense probe exhibited no colour development.

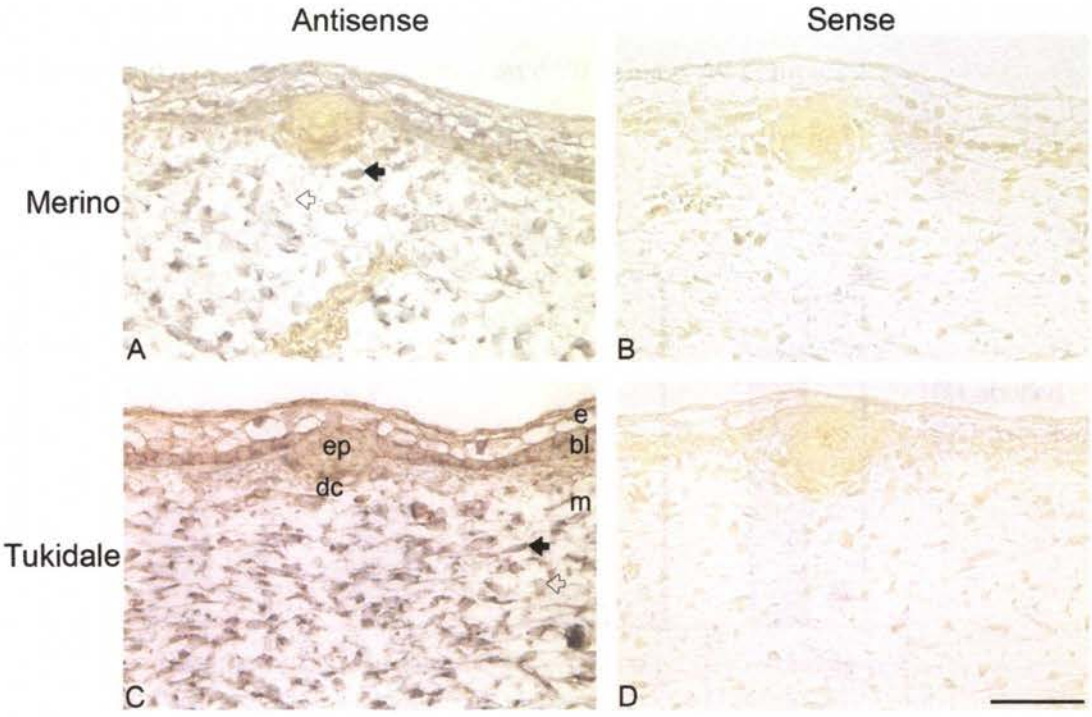

Figure 3.13: Delta-1 gene expression in foetal sheep skin collected on d 70 of gestation. Expression was investigated in Merino (A) and Tukidale (C) skin samples. Transcripts were detected in the epithelium (e), the basal layer (bl), and the dermal condensate (dc). Within the mesenchyme, transcripts were detected in some cells (solid arrow) and not in others (hollow arrow). Transcripts were detected in the epithelial plug of Tukidale but not in Merino (ep). No staining was observed in the sense-treated sections (B, D). Scale represents 50 μm.

3.3.2.6 Analysis of the Delta-1 bearing cell population

The sizes of the subpopulations of mesenchymal cells expressing the gene transcript for Delta-1 were quantified in both breeds of sheep by cell counting using image analysis (Image J). A linear mixed model analysis was performed on the log transformed count data. Breed, foetal age and labelling/no labelling with Delta-1 produced a highly significant 3-way interaction ($p<0.001$). This interaction was of biological interest and further investigated (Table A6.1). The back transformed means were graphed (Figure 3.14). Significantly fewer Delta-1 labelled mesenchymal cells were counted compared to those that remained unlabelled (in the d 56 and d 70 samples) in the Merino and Tukidale skins, suggesting Delta-1 was used as a mechanism for differentiating some cells from the rest of the population. The numbers of unlabelled and Delta-1 labelled mesenchymal cells increased significantly from d 56 to d 70 in the Merino and Tukidale samples (excluding cells within the dermal condensate). Significantly fewer unlabelled cells were counted in the d 56 Merino skin compared to the Tukidale at the same gestational age. No significant differences in cell number were detected for the numbers of labelled cells at d 56 when the Merino and Tukidale were compared.

Similarly, no significant differences were found when numbers of unlabelled or labelled cells from Merino and Tukidale skins collected on d 70 skins were compared.

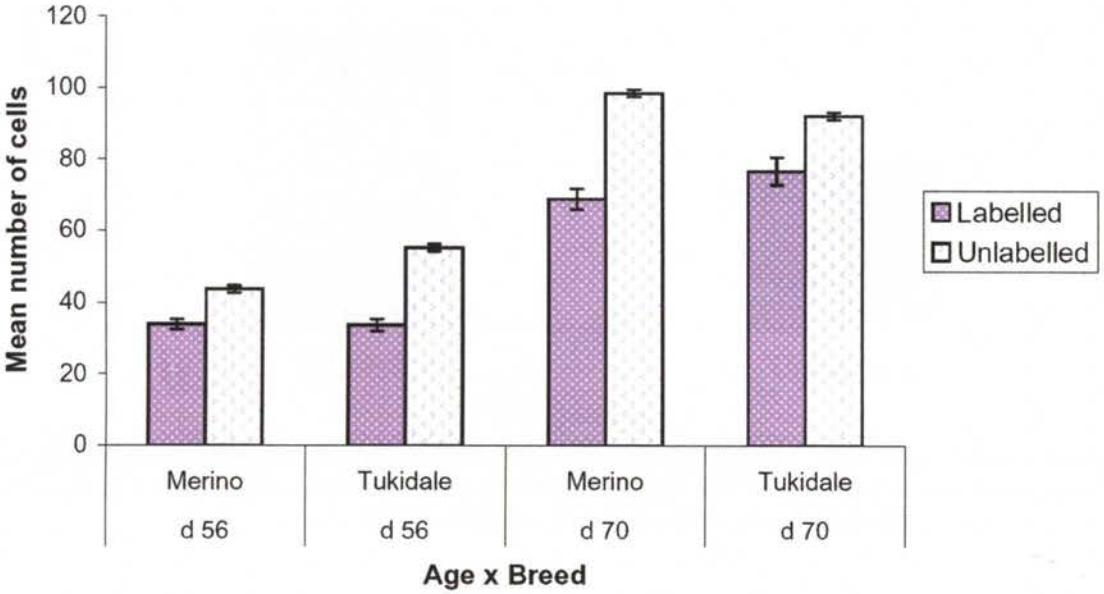

Figure 3.14: The 3-way interaction of foetal age, breed and labelling for Delta-1 in mesenchymal cells. The number of unlabelled cells was significantly higher than the number of Delta-1 labelled cells at both d 56 and d 70 for each breed. The numbers of Delta-1 labelled and unlabelled cells were significantly higher in the d 70 skins compared to the d 56 skins, in both the Merino and Tukidale samples. On d 56, the Tukidale samples contained significantly more Delta-1 unlabelled cells than the Merino samples. No significant difference in labelled cells was detected between the Merino and Tukidale samples on d 56. No significant differences were detected in cell numbers for labelled or unlabelled cells in the d 70 skins between the 2 breeds. Error bars represent standard error of the mean.

The numbers of Delta-labelled and unlabelled cells in the dermal condensate were counted within d 70, sectioned skin from Merino and Tukidale foetuses. The data were analysed on the log scale using a linear mixed model. No significant 3-way interaction (breed × labelling × number of dermal condensates (no_dc), p-value=0.530) was found, and no significant 2-way interactions were found (labelling × no_dc, p-value=0.769; breed × no_dc, p-value=0.908; breed × labelling, p-value=0.650) allowing these interactions to be dropped from the model so that the main effects could be investigated. Breed was found to have no significant effect on the number of cells (Delta-1 labelled and unlabelled) in the dermal condensate (p=0.440) at follicle initiation and was dropped from the model. The number of dermal condensates in a field of view had a significant effect on the number of cells counted in the section ($p<0.001$), but was of no interest. Whether the cells in the dermal condensate were labelled for Delta-1 or unlabelled was highly significant ($p<0.001$) and the back transformed means were graphed (Figure 3.15) to allow further investigation. The number of

cells labelled with Delta-1 was significantly higher than the number of unlabelled cells within the dermal condensate (Table A6. 2).

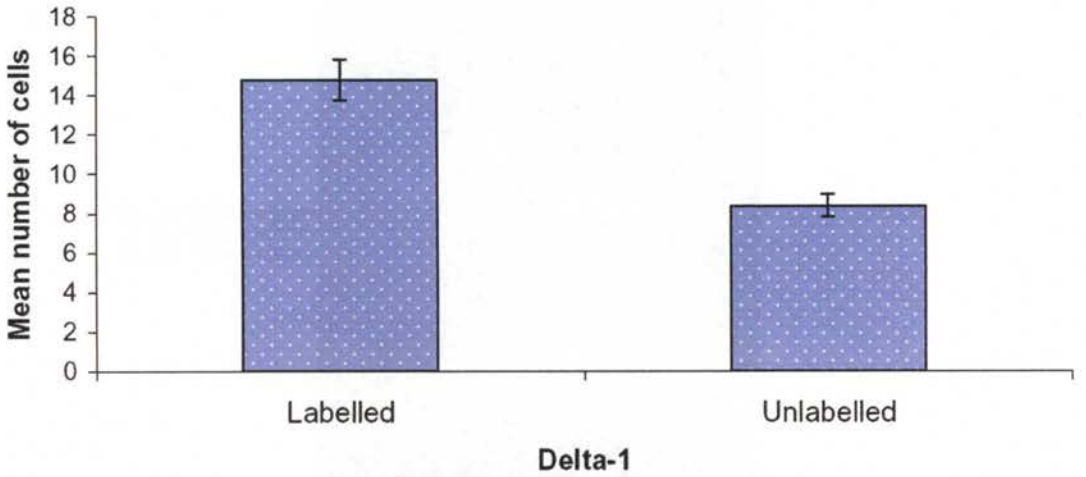

Figure 3.15: Delta-1 labelling has a significant effect ($p<0.001$) on the number of cells counted within the dermal condensate of d 70 foetal skin. Significantly more Delta-1 labelled than unlabelled cells were found to exist within this structure. Error bars represent standard error of the mean.

3.3.3 ANALYSIS OF THE DELTA-3 TEMPLATE

Linearisation of the Delta-3 pDNA with restriction enzymes NotI and KpnI, when analysed on a gel showed that the undigested pDNA (Figure 3.16; lane 1) migrated more rapidly through the gel matrix when compared to its linearised counterpart (Figure 3.16; lane 2). The presence of more than one band suggested some degradation of the sample and possible RNA and/or protein contamination. The pDNA digested with EcoR1 (Figure 3.16; lane 3) demonstrated that the enzyme was cutting the Delta-3 insert (2.1 kb) within the multiple cloning site from the rest of the pDNA (Figure A0.1) at 2 sites. The pDNA digested with KpnI and NotI (Figure 3.16; lane 4) also produced this result. The band in lane 2 shows that the NotI enzyme cut the pDNA at one site only, so that the pDNA was linearised but the DNA insert was not isolated.

Figure 3.16: Restriction enzyme digest of Delta-3 pDNA. Lane 1, pDNA positive control; 2, pDNA digested with NotI; 3, pDNA digested with NotI and EcoR1; 4,digested with EcoR1; 5, undigested 8 ng/µl pDNA. H, hyperladder size marker.

Sequencing the gene insert confirmed it to be Delta-3 when the sequence was run against all other sequences in GenBank using a Blastn search (Appendix 5.2). The sequenced insert shared a high homology with other mammalian Delta-3 sequences in the GenBank database. The sequences were a significant match (E-value=0) in GenBank with the *Mus musculus* sequences: (accession number: BC052002) mRNA for Delta-like 3, (accession number: AB013440) mRNA for Delta-like 3 protein, and (accession number: Y11895) mRNA for the M-Delta-like 3 gene. The sequence read from the T7 promoter site, the antisense strand, was also similar (E-value=0) to (accession number: AF084576) *Rattus norvegicus* Delta-3 mRNA. A search of the database of ovine EST sequences in Ovita, kindly provided by AgResearch, found an EST clone (EE835675.1) that shared a 79% sequence identity with the murine Delta-like-3 mRNA sequence (NM_007866.2) (Section A5.5.2).

Before transcription the pDNA was digested with the restriction enzymes NotI (for antisense probe) and KpnI (for sense probe) (Figure 3.17). The sense strand was read from the T7 promoter site to the NotI restriction and the antisense strand from the T3 promoter site to the KpnI restriction site.

The linearised pDNA samples were DIG-labelled by transcription (Section 3.2.3) to create the RNA probes. The probe was quantified (Section 3.2.3.3) and found to be highly sensitive, with signal detected at concentrations as low as 0.1 pg/µl.

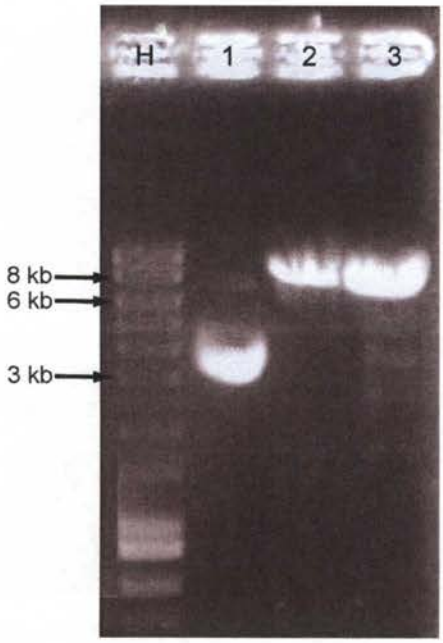

Figure 3.17: Linearisation of Delta-3 pDNA by restriction enzyme digestion prior to sequencing. Lane 1; undigested pDNA control. Lane 2; pDNA digested with NotI. Lane 3; pDNA digested with KpnI. H; hyperladder size marker.

3.3.3.1 Delta-3 transcript expression in foetal sheep skin

The Delta-3 antisense and sense (DIG-labelled) probes were tested on foetal Merino skin. The tissue treated with the antisense probe at d 56 and d 70 showed some scattered staining within the mesenchyme and at d 70, in the dermal condensate (Figure 3.18). The tissue treated with the labelled sense probe stained darkly. The sense staining was reduced by increasing the stringency of the post-hybridisation washes but not eliminated. This was an undesirable result and the probe was not used for the cell count analysis.

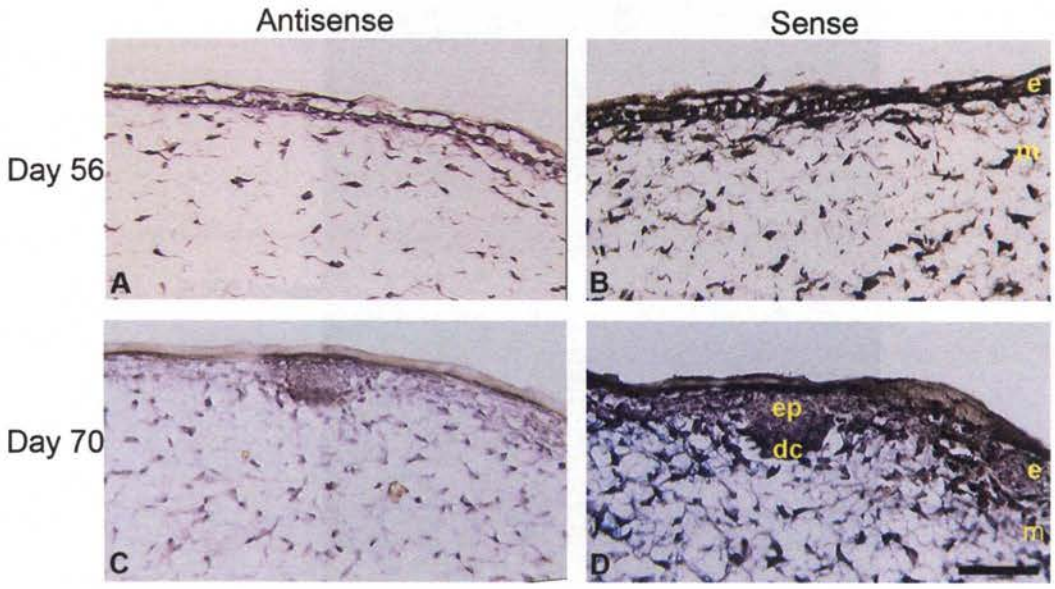

Figure 3.18: Delta-3 gene transcripts in foetal Merino skin sampled on d 56 and d 70 of development. Expression was stronger in skin prior to follicle initiation (d 56; A) than during follicle initiation (d 70; C). In d 56 skin (A), transcripts were detected in the epithelium (e) and strongly in some cells within the mesenchyme (m). In d 70 skin (C), transcripts were detected in some cells in the mesenchyme (m) and dermal condensate (dc). Minimal staining was detected in the epithelium (e) and epithelial plug (ep). Sense treated sections (d 56, B; d 70, D) showed strong non-specific staining. All sections were counterstained with Mayer's haematoxylin. Scale represents 50 μm.

3.3.4 ANALYSIS OF MURINE LUNATIC FRINGE TEMPLATE

After chemical transformation of JM109 cells with Lunatic Fringe pDNA, 7 single white colonies from a selective plate were screened for containing the gene insert by PCR (Figure 3.19). From the gel, it appeared that clones 1-4 did not contain significant levels of the insert. This may have been a result of the pDNA from these inserts not being successfully amplified. An alternative explanation is that these clones should have appeared as blue colonies. Clones 5-7 did contain an insert of the expected size (~2.5 kb). A strong band was produced by clone 7, and this clone was chosen for amplification. The positive control (lane 8) used was Lunatic Fringe pDNA. The numerous bands produced by the pDNA suggested the sample had degraded and was contaminated with RNA and/or protein. The negative control (Figure 3.19; lane 9) produced no band, as expected.

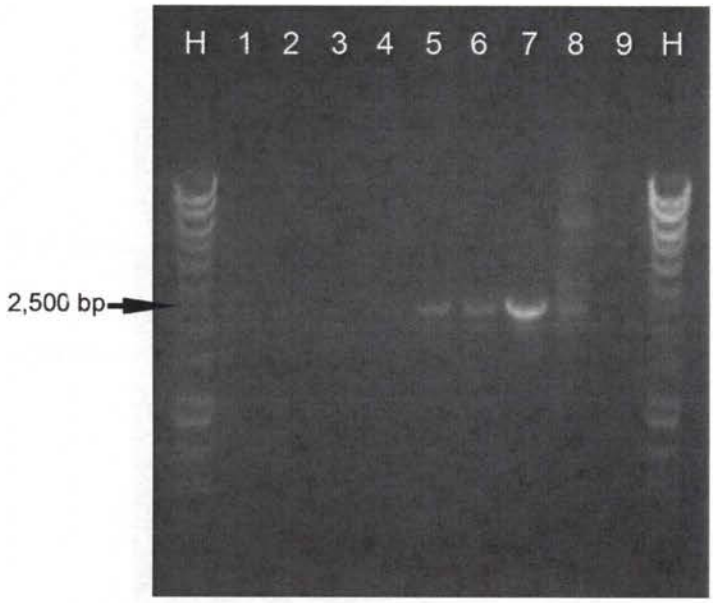

Figure 3.19: PCR screen of Lunatic Fringe pDNA from chemically transformed JM109 clones. Clones 1-4 did not appear to carry the insert. The amplified product (~2,500 bp) was isolated in clones 5, 6 and 7. Lane 8 contained Lunatic Fringe pDNA. Lane 9 contained no DNA. Clone 7 was used for further work. H; hyperladder size marker.

Lunatic Fringe pDNA digested with the restriction enzyme EcoR1 isolated the (2.2 kb) gene insert from the rest of the pDNA (Figure 3.20; lane 1). Restriction enzymes HindIII (lane 2) and XbaI (lane 3) each cut the pDNA once in the multiple cloning site. When HindIII and XbaI were used together (lane 4) Lunatic Fringe was isolated from the plasmid, giving the same result as when the pDNA was digested with EcoR1. The circular pDNA (lane 5) ran at a faster rate through the gel matrix than the linearised samples.

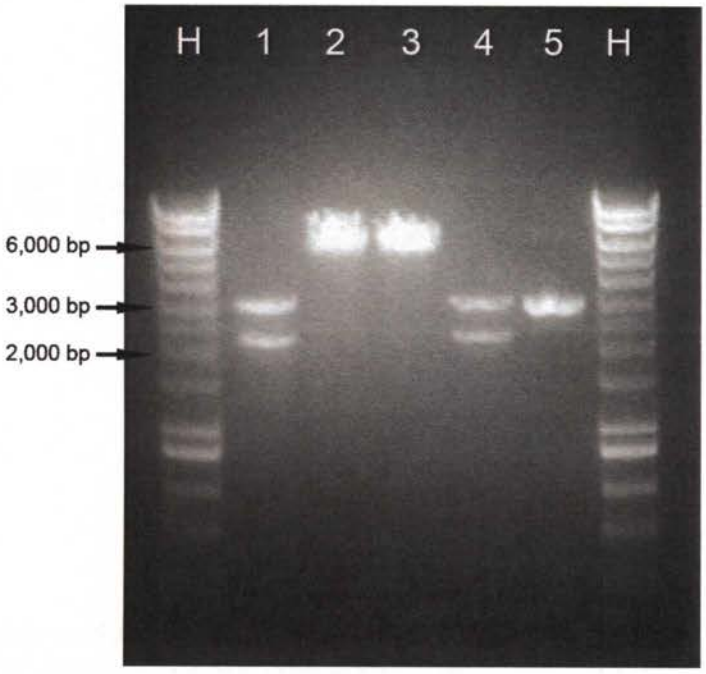

Figure 3.20: Restriction enzyme digest of murine Lunatic Fringe pDNA. Lane 1, EcoR1; 2, HindIII; 3, Xba1; 4, HindIII and XbaI; 5, undigested pDNA control. H; hyperladder size marker.

A murine Lunatic Fringe cDNA sequence was used as the template for the *in situ* hybridisation studies that matched the sequences of a contig map of ovine EST clones in the Ovita databank. The ovine ESTs kindly provided by AgResearch, when aligned in Blastn were found to share an 85% sequence identity (Section A5.5.3) with the murine homolog (NM_008494.3).

Sequence analysis of the gene insert confirmed it to be murine Lunatic Fringe when the sequence was compared against other sequences in GenBank, using a Blastn search (Appendix 5.3). The sequence generated from the T7 primer (the sense strand) was significantly similar (E=0) to *M. musculus* sequences: (accession number: MMU94351) Lunatic Fringe precursor mRNA, (accession number: AF015768) Lunatic Fringe mRNA, (accession number: AY124581) Lunatic Fringe gene, exon 1, partial, and (accession number: AC110253) chromosome 5, clone RP23-270N2, complete sequence. The sequence generated from the T3 primer (the antisense strand) was not significantly similar to any other sequences, and there was no fake match to other sequences (E-value>0.001).

The Lunatic Fringe pDNA was digested with restriction enzymes to allow for transcription (Figure 3.21). To cut the pDNA to produce the antisense probe HindIII was used. XbaI was used to cut the pDNA to produce the sense probe. The enzymes successfully linearised the pDNA, cutting in only one location (lanes 1 and 2).

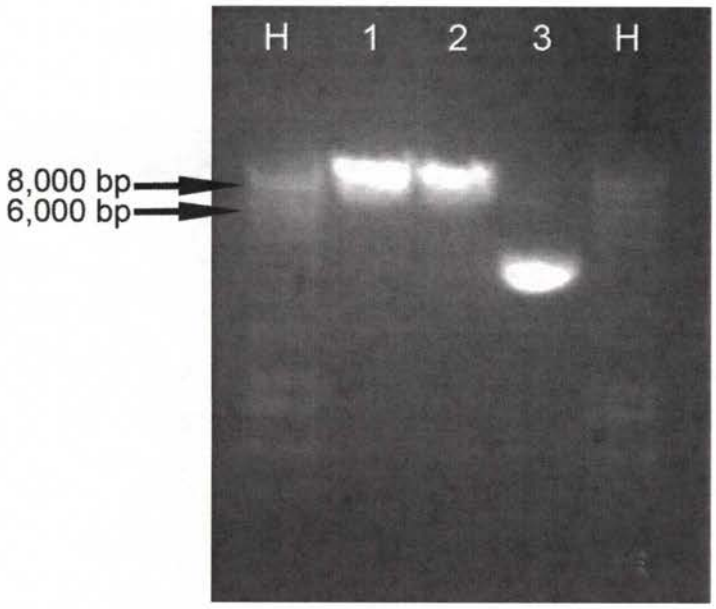

Figure 3.21: Overnight restriction enzyme digest of Lunatic Fringe pDNA. Lane 1, pDNA linearised with HindIII; lane 2, pDNA linearised with Xba1; lane 3, undigested Lunatic Fringe pDNA. H; hyperladder size marker.

The specificity of the antisense and DIG-labelled sense probes when tested by quantification on a blot (Section 3.2.3.3), were highly sensitive as a consequence of the 0.1 pg/µl dilution being clearly visible after a 2 min exposure time.

3.3.4.1 Lunatic Fringe transcript expression in foetal sheep skin

The murine Lunatic Fringe riboprobes were tested on foetal Merino skin samples. The antisense probe showed a consistently strong level of staining throughout the mesenchyme and epidermis at d 56 (Figure 3.22; A). At d 70, staining was scattered throughout the mesenchyme, being particularly strong in some isolated mesenchymal cells and the periderm (Figure 3.22; C). Staining was minimal in the epithelial plug and dermal condensate. The sense controls demonstrated a strong, non-specific staining throughout the tissue (Figure 3.22; B, D). Staining in the sense-treated tissue was reduced by increasing the stringency of the post-hybridisation washes. However, it was not eliminated so this probe was not persevered with.

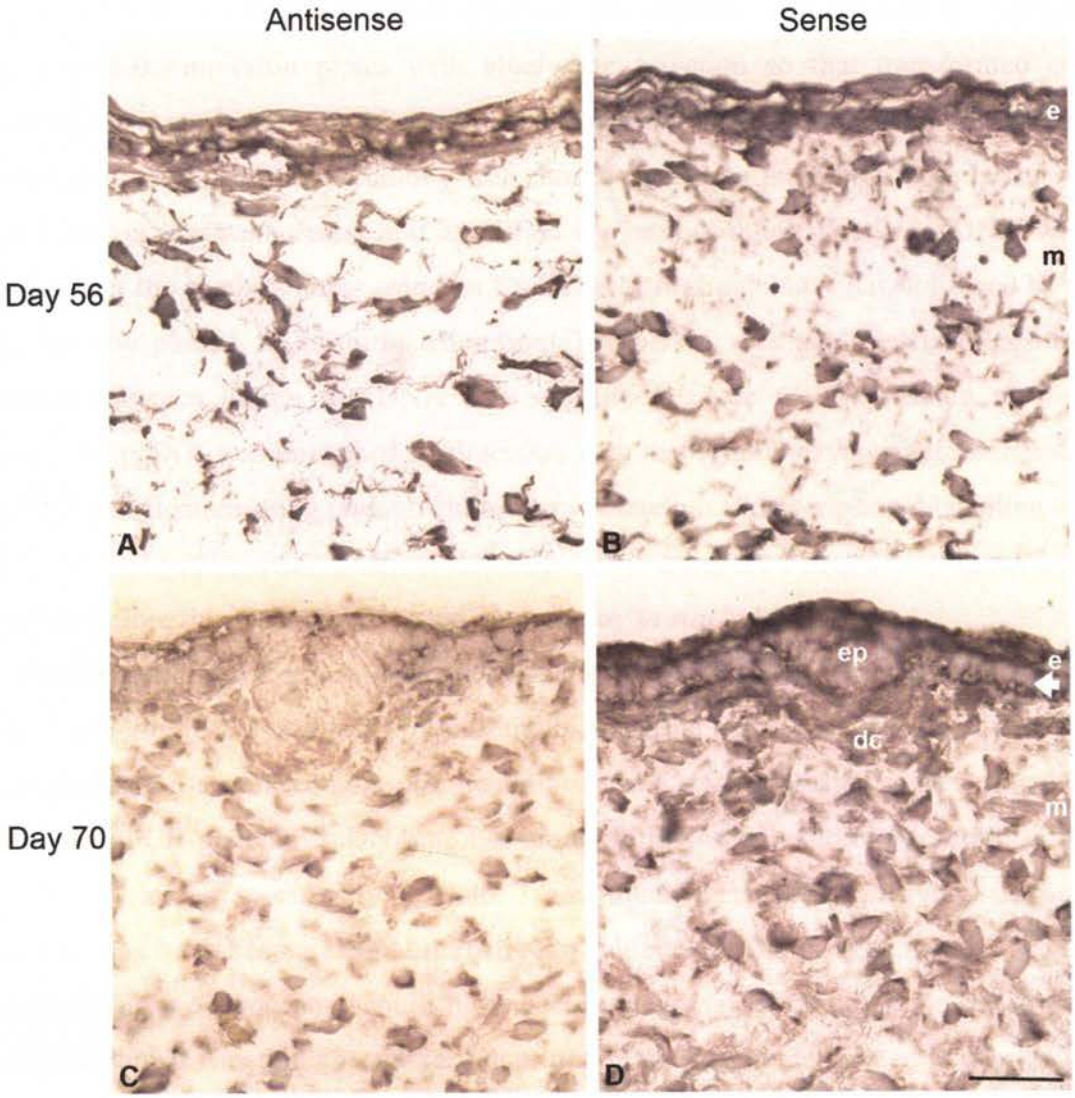

Figure 3.22: Gene transcripts for Lunatic Fringe in foetal Merino skin at day 56 and day 70 of development. In d 56 skin (A), a consistently strong level of staining was detected in the epithelium (e) and mesenchyme (m). In d 70 skin (C), staining was detected in some cells within the mesenchyme and the upper layers of the epithelium. Minimal levels of stain were detected in the epithelial plug (ep) and dermal condensate (dc). Strong non-specific staining was detected in sense-treated tissue (d 56, B; d 70, D). Scale represents 30 μm.

3.4 DISCUSSION

Riboprobes for *in situ* hybridisation experiments were created for Delta-1, Delta-3 and Lunatic Fringe from murine cDNA sequences. The riboprobes used in this study were created using murine cDNA as template for the probes, as these sequences were available in Genbank. The murine sequences used for the riboprobes shared high sequence identities with the ovine ESTs (79-88%; refer to Appendix 5.5). The cDNA was kindly supplied from other laboratories, cloned into pBluescript. The pDNA was amplified using chemical transformation of competent bacteria (JM109 was used for Delta-1 and Lunatic Fringe, XL1-

blue was used for Delta-3). Transformation of the bacteria was checked by growing the bacteria on LB/Ampicillin plates with blue/white selection so that transformed colonies containing the gene insert could be selected. A number of transformed colonies were then screened using PCR before one colony was chosen (based on that colony producing a clear, strong band on electrophoresis) and amplified by broth culture. Purified pDNA was then obtained from the broth cultures using an EndoFree® Plasmid Maxi Kit, followed by pDNA purification by phenol: chloroform extraction. The pDNA was analysed by digestion with restriction enzymes before the DNA was sequenced. Once the sequencing results were obtained, the pDNA was linearised by digestion with restriction enzymes before transcription and pDNA purification using phenol: chloroform extraction. Transcriptional labelling of DIG-riboprobes followed by quantification of the riboprobe using the direct detection method were carried out before the probes were tested on tissue by *in situ* hybridisation.

Non-specific staining was detected with the sense riboprobes for Delta-3 and Lunatic Fringe. The large probe size (~3 kb) and highly sensitive nature (0.1 pg/µl) of these probes did not hinder non-specific binding of the antibody to the DIG-labelled sense probes. Further studies using PCR-generated cDNA probes along with Northern blotting to confirm that the probes were binding specifically to Delta-3 and Lunatic Fringe respectively, in the foetal sheep skin may have been a useful alternative to achieve the aims if the chapter. The Delta-3 and Lunatic Fringe riboprobes could have been contaminated during probe construction or characterisation. It was thought unlikely that the pDNA was contaminated at any stage prior to sequencing as no sign of contamination was evident in the sequencing results. It was possible that the riboprobes were contaminated during transcriptional labelling. However, this was thought unlikely as remaking the riboprobes did not alter the *in situ* hybridisation results or reduce the non-specific staining in the sense controls.

The Delta-1 riboprobe was chosen for the analysis of the labelled mesenchymal cell populations at d 56 and d 70. Northern blotting confirmed that the Delta-1 probe was binding to a 3.1 kb mRNA band in sheep skin that corresponded to the size of other mammalian Delta-1 mRNA homologs.

The antisense riboprobe for Delta-1 proved highly specific and showed differential staining in the mesenchyme prior to and during follicle initiation, and in adult, Merino and Tukidale skin samples. On d 56 of development, Delta-1 transcripts were strongly expressed throughout the epithelium, with the basal layer in the Tukidale samples appearing particularly strong. Differential staining was seen in cells throughout the mesenchyme. A significantly lower proportion of mesenchymal cells expressed the Delta-1 transcript, compared to those

cells than remained unlabelled in the Merino and Tukidale samples. On d 70 of development, Delta-1 transcripts were strongly expressed in the epithelium, with the interfollicular basal layer staining particularly dark. Delta-1 transcripts were absent from the basal layer surrounding the developing wool follicles. Minimal expression was detected in the epithelial plug. The work of Lowell *et al.* (2000) showed that Delta-1 was differentially stained in the basal layer of the epithelium with localised expression in stem cells. They found that all keratinocytes expressed Delta-1, yet stronger expression was seen within the basal layer, an area enriched for stem cells.

It was noted that tissue cellularity (the numbers of mesenchymal cells counted in a 290 × 220 μm field) in the skin samples had significantly increased (approximately two-fold) from d 56 to d 70 for both breeds. The dermal condensate appeared to express higher levels of Delta-1 transcript compared to the residual mesenchymal cell population. No differences in transcript expression in the condensate were detected between Merino and Tukidale samples. However, a significantly larger proportion of cells within the dermal condensate were found to express Delta-1 transcript compared to those cells that remained unlabelled suggesting that the condensate was a focus for accumulation of these cells. If Delta-1 was used within the tissue as a distinguishing marker for founder or follicle primordial cells relative to the rest of the cell population, the follicle producing ability of a skin could potentially be deduced from foetal skin samples (Moore *et al.*, 1989; Moore *et al.*, 1998). Since not all cells were Delta-1 positive, clearly expression of this gene is not the sole determinant of this unique specialised cell population. Alternatively, the specification of mesenchymal cells destined to form the prepapillae may be determined by transient expression of Delta-1. Thus the determination of this cell population would require a longitudinal analysis of Delta-1 expression, which is not possible using the techniques adopted for this study. Thus, the findings from this study were unable to define the finite population of cells that are recruited within the dermis for the induction of the wool follicle population.

No significant differences in the proportions of Delta-1 positive cells within the dermal condensate were found between Merino and Tukidale samples in this study. These findings agreed with those obtained by Adelson *et al.* (2002) who found no correlation between foetal wool follicle rudiment diameter (measured at d 81) and adult wool fibre diameter. Thus, Delta-1 was not an ideal marker for the dermal condensate cell population as it failed to detect differences in this cell population between fine wool and strong wool breeds, during follicle initiation.

However, the present study suggests that Delta-1 may have a role in selecting cells within the mesenchyme, helping to specify some cells for recruitment to form a follicle. In addition, Delta-1 may have a role in keeping the cells within the condensate in close proximity with each other through Delta-Delta associations and to distinguish the cells within the condensate from the rest of the mesenchymal cell population. Whether Delta-1 bearing cells within the mesenchyme were able to migrate up towards the epithelium and form the dermal condensate was not investigated. It is known that Delta-1 bearing cells can form aggregations with one another (Pourquié, 2000), possibly providing a mechanism in which the prepapilla cells are kept in contact. Dermal papilla cells have a number of distinguishing characteristics. The cells normally show very low proliferative activity (Pierard and De La Brassinne, 1975) are flat and polygonal in shape (Messenger *et al.*, 1986), have a tendency to form papilla-like aggregations with one another (Pierard and De La Brassinne, 1975) and have the inductive ability to grow follicles when transplanted in contact with epidermal cells (Jahoda and Oliver, 1984; Jahoda *et al.*, 2001).

Morphologically, the initiation of hair follicles begins with "crowding" of epidermal keratinocytes, to form hair placodes. Placode formation is followed by the formation of a condensation of mesenchymal fibroblasts with inductive properties. The signalling cross-talk between the mesenchymal condensate and the epithelial placode drives proliferation of cells in both structures, shaping the dermal papilla and starting the down-growth of the epithelial plug (Schmidt-Ullrich and Paus, 2005).

The primary follicles in mice, as in other mammals, are regularly spaced, and later follicles appear in positions related to them. This pattern is either already laid down, or each developing follicle becomes surrounded by a small zone where development is inhibited (Hardy, 1949). Studies conducted by Jahoda *et al.* (2001) illustrated that dermal papillae share common features and signals across different species. They elegantly showed that human dermal papilla had hair-inducing capabilities that were conserved and recognised in other species, such as mice.

The cells within a dermal condensate are a kind of dermal fibroblast, which may be attracted to chemotactic factors from hair placode cells (Matsuzaki and Yoshizato, 1998). Epithelial-mesenchymal interactions are essential for the formation and integrity of follicles. These interactions have also been found to be bi-directional (Jahoda *et al.*, 2001). If transplanted papilla cells did not remain in contact with epidermal cells and therefore have no interaction with them, then no follicle formed. Other studies using dissociated cells have shown that epithelial cells quickly cluster and remodel themselves to generate a structure

reminiscent of a primitive epidermis with its placode and hair follicle with an infundibulum. This study suggested that the earliest phase of a developing epithelial-mesenchymal system requires an epithelial platform (Zheng *et al.*, 2005). Hair follicles maintain these epithelial-mesenchymal interactions in adult life to enable them to undergo cyclical growth and shaft production (Williams *et al.*, 1994). Delta-1 signalling is maintained in the epithelium of the adult skin and the outer root sheath. The adult epithelium may continue to signal using Delta-1 in the epithelial stem cells (Lowell *et al.*, 2000) which are responsible for regeneration of new epithelium and wound healing. The outer root sheath may express Delta-1 as it remains mitotically active during follicle growth (Straile, 1965).

It is thought that once the hair follicle pattern is established within a skin, the hair follicle precursor cells invade the underlying dermis in a controlled manner and gradually differentiate to produce a hair shaft and its surrounding root sheaths (Stark *et al.*, 2007).

The Notch signalling pathway is thought to be responsible for modulating the ability of cells to respond to Notch gene signals (Artavanis-Tsakonas *et al.*, 1995). Signalling between adjacent cells occurs when the extracellular domain of Delta binds specifically to the extracellular domain of Notch in a competitive manner with respect to Delta (Qi *et al.*, 1999). Cells expressing Notch do not bind to one another, whereas cells expressing Delta do aggregate homotypically, suggesting a competitive interaction between Notch and Delta for binding to Delta at the cell surface (Artavanis-Tsakonas and Simpson, 1991).

The response a zebrafish retinal cell makes when the function of one component of the Notch-Delta signalling cascade is altered depends on its context within the neighbouring pool of cells and the state of activation of Notch and Delta signalling cascades in those cells (Bernardos *et al.*, 2005). Similarly, it is believed that the context of Notch signalling in foetal sheep skin would affect the outcome of signalling. Due to the elevated level of Delta seen in the epithelium, it was assumed that Delta was expressed in epithelial stem cells within the basal layer. In addition, Delta-1 in the epithelium may have been signalling to the mesenchyme, instructing the mesenchymal fibroblasts to aggregate at certain intervals. It was interesting that during follicle initiation, Delta-1 was not expressed in the areas of the epithelium directly above a forming follicle. This suggested that prior to follicle initiation, Delta-1 may have a role in establishing the pattern of follicle development in the skin but that once the initiation sites had been established signalling was no longer required, suggesting that Delta-1 may signal in a negative feedback loop where the epithelium and mesenchyme communicate with one another. Within the mesenchyme, it was thought that the cells which were expressing Delta-1 were signalling to other cells not to take on the same dermal

condensate cell fate, in a manner akin to lateral inhibition (Pourquié, 2000; Chitnis, 2006). Delta-1 expressing cells were thought to be attracted to each other and to migrate to a common point, that being the site of follicle initiation, where they became clustered together in the dermal condensate. This would explain the significantly larger proportion of Delta-1 expressing cells found in the dermal condensate, in comparison with the rest of the mesenchymal cell population. Delta-1 may provide the cells in the condensate with a means to remain tightly packed together as a separate entity from the mesenchyme and to enable them to activate downstream target signals to allow follicle development to continue. Mesenchymal cells expressing Delta-1 during primary follicle initiation may be beginning the process of lateral inhibition in preparation for the waves of secondary follicle initiation.

In conclusion, this study demonstrated that Delta-1 transcripts were expressed in Merino and Tukidale skin collected prior to and during follicle initiation. It appeared that Delta-1 had a role in foetal sheep mesenchyme. It was believed that Delta-1 expression in a sub-population of cells allowed those cells to communicate with their neighbouring cells, possibly through lateral inhibition, as a means of establishing the dermal prepapilla cell population. As no significant differences were detected in the proportion of labelled and unlabelled cells within the dermal condensates of Merino and Tukidale samples, it was thought that Delta-1 may assist in maintaining these differentiated cells in close proximity to each other and in distinguishing them from the remaining mesenchymal cell population.

CHAPTER 4: NOTCH-1 GENE EXPRESSION IN SHEEP SKIN

4.1. INTRODUCTION

The Notch gene encodes a single loop transmembrane protein receptor of approximately 300 kD (Larsson *et al.*, 1994). The Notch signalling pathway allows neighbouring cells to communicate with one another through expression of Notch receptors and the ligands Delta, Jagged and Serrate on their cell surfaces. During development, the Notch signalling pathway plays a role in cell fate decisions in a diverse range of invertebrate and vertebrate species (Baron, 2003). The pathway is believed to control cell fate choices involving proliferation, differentiation, and apoptosis (Miele and Osborne, 1999). The regulation of spatial patterning, timing and outcomes of cell fate decisions by Notch signalling, has been proposed to be via one of a number of mechanisms, such as lateral inhibition and boundary definition (Bray, 1998), described in Section 1.8.1.6.1.1 and Section 1.8.1.6.1.3.

Notch-1 signalling has been studied in developing follicles in mouse (Powell *et al.*, 1998) and sheep (Botto, 2000; Gordon-Thomson *et al.*, 2008), and in developing chick feathers (Crowe *et al.*, 1998). In the developing murine hair follicle, Notch-1 transcripts have been detected in the epithelium and the epithelial plug. In advanced epithelial plugs, Notch-1 was primarily expressed in the inner root sheath cells, but not in the outer root sheath. Notch-1 was not expressed in the mesenchyme (Powell *et al.*, 1998). Conversely, Notch-1 and Notch-2 were expressed in chick skin prior to formation of the epidermal placode (Crowe *et al.*, 1998). In the early stages of vibrissae during mouse development, Notch-1 was transcribed in the dermis, and localised to the forming vibrissae follicles (Favier *et al.*, 2000). Earlier studies using foetal sheep skin found Notch-1 transcripts in the basal cells of the epidermis at d 60 of gestation, in a subpopulation of mesenchymal cells at d 60 and d 70. At d 70, transcripts were detected in small groups of cells at the basal layer bordering the epidermal plug and in a subpopulation of mesenchymal cells in the deeper layers of the dermis (Botto, 2000; Gordon-Thomson *et al.*, 2008). These studies have shown that Notch-1 signalling is present in skin prior to and during follicle development. The localisation of Notch-1 in the tissue of mice, sheep and chick prior to and during the formation of an epidermal appendage, suggests that Notch-1 may be involved in the formation of these

structures. It was thought that Notch-1 might play a role in determining which cells are to become papilla cells and which cells are to remain as mesenchymal cells.

In sheep, it is accepted that fibre diameter is negatively correlated with follicle number (Moore *et al.*, 1989). The Founder Cell Theory is based on the principle that the skin produces greater or lesser numbers of follicles as fibre diameter decreases or increases during selection (Moore *et al.*, 1989). It was proposed that the formation and quantity of fibre-producing follicular tissue was controlled by a population of dermal cells giving rise to the dermal papilla and that these cells became committed to a follicle lineage at or prior to follicle initiation (Moore *et al.*, 1998). A partial ovine Notch-1 cDNA isolated from sheep skin (GenBank accession number EF999923; Figure 4.1) showed a high level of homology (84-96%) with *Mus musculus, Rattus norvegicus, Homo sapiens* and *Bos taurus* (Gordon-Thomson *et al.*, 2008). It was thought that prepapilla (founder) cells could be identified using Notch expression *in situ* (Botto, 2000) as Notch-1 gene transcripts were localised in prepapilla cells by *in situ* hybridisation. If Notch-1 could be used to identify the mesenchymal cells within the skin prior to and during follicle initiation that would identify founder cells, the follicle-producing ability of a skin could be deduced. This would serve as a means of determining the numbers of follicles that would form within a skin, and the size of the fibres they would produce.

The focus of this study was to investigate the expression patterns of Notch-1 gene transcripts in foetal sheep skin collected prior to and during follicle initiation using *in situ* hybridisation. In particular we were interested in examining the distribution of Notch transcripts in mesenchymal cells prior to and during follicle initiation in two breeds with very different wool follicle characteristics to determine if differences in Notch-1 expression between the breeds could be detected. To achieve this (7) Merino and (5) Tukidale foetuses were included in this study. The expression of Notch-1 in adult skin samples was also investigated in these two breeds to determine if Notch-1 had a role in follicle maintenance in adult skin.

4.2. MATERIALS AND METHODS

4.2.1 ANIMALS

Skin was collected from the gluteal region of Merino and Tukidale foetuses at d 56 and d 70 of gestation, processed in to paraffin wax (Section 2.2.4.1) and sectioned (Section

2.2.5.1). The 7 Merino and 5 Tukidale foetuses investigated in Chapter 3 were also utilised in these studies.

4.2.2 PROBE PRODUCTION

The ovine Notch-1 cDNA sequence (Figure 4.1) was previously generated by Dr Stephen Botto using oligonucleotide primers R5 and RC13 that he developed from the known rat Notch-1 sequence. Primer R5 (5' CCC TTT CTA CCG CTG TCT ATG CCC TGC CAA 3') was located in EGF-like repeat 36 and primer RC13 (5' ATC TTC TTC TTC CTC ACT GTT GTT GCC TGT CTC 3') was located in ankyrin repeat 1. The DNA region selected was a GC-rich, 1.517kb sequence spanning the last EGF-like repeat in the extracellular domain to the first ankyrin repeat in the intracellular region (Appendix 5.4.1).

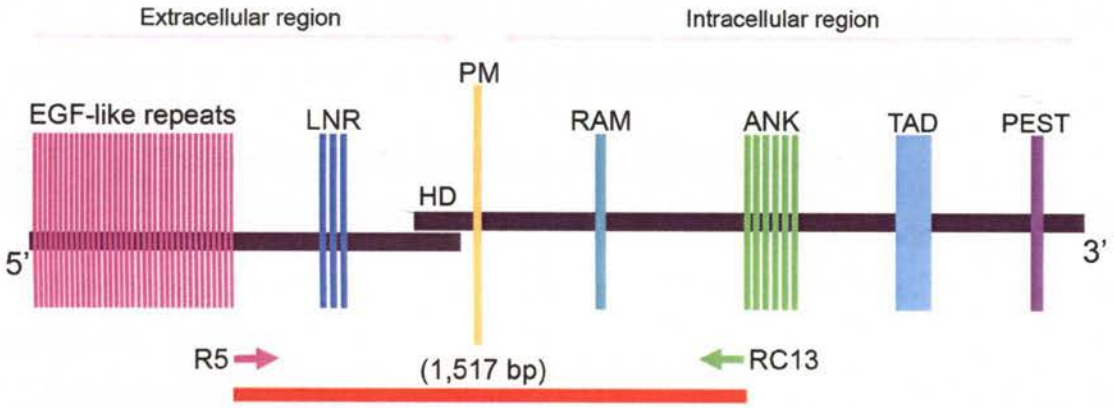

Figure 4.1: The protein structure of the Notch-1 receptor. The partial ovine Notch-1 sequence (red bar; 1,517 bp) mapped to the known rat sequence. EGF-like-repeat 36 to ankyrin repeat 1, in some of the extracellular, transmembrane and intracellular regions of Notch-1. ANK, ankyrin repeats; EGF, epidermal growth factor; HD, heterodimerisation domain; LNR, Lin-Notch repeat; PEST, PEST domain; PM, plasma membrane; RAM, RBP-Jk-associated molecule; TAD, trans-activation domain. Figure modified from Botto (2000) and Chiba (2006).

The partial ovine Notch-1 cDNA (GenBank accession number: EF999923) cloned in the pGEM®-T vector (Figure A0.2) was kindly provided by Dr Steven Botto (Appendix 5.4.1).

4.2.2.1 Amplifying Notch-1 transformed cells and pDNA

4.2.2.1.1 Amplification of recombinant cell colonies

A glycerol stock of transformed JM109 cells containing the pGEM®-T vector and Notch-1 insert was thawed. Within the laminar flow cabinet, a loop of transformed cells was inoculated into two 50 ml LB broth starter cultures containing 100 µg/ml ampicillin. The cultures were incubated at 37°C with agitation at 200 rpm, until the OD_{600} reached 0.6 (~8 hr). Approximately 1 ml of the starter cultures was inoculated into two 250 ml overnight LB

cultures, containing 100 µg/ml ampicillin, in 1 L conical flasks (Pyrex®, Corning Australia, Lindfield, NSW, Australia) and incubated for ~14 hr at 37°C, with shaking at 200 rpm.

4.2.2.1.2 Preparation of cell glycerol stocks

Glycerol stocks of the amplified Notch-1 transformed bacteria were prepared as described in Section 3.2.2.3.

4.2.2.1.3 Purification of plasmid DNA from broth cultures

The Notch-1 pDNA was purified from the broth cultures using an EndoFree® Plasmid Maxi Kit (Qiagen Pty Ltd) following the method described in Section 3.2.2.4.

4.2.2.2 Preparation of DNA for sequencing

Notch-1 pDNA samples purified from the broth cultures were linearised by restriction enzyme digestion and prepared for sequencing as described in Section 3.2.2.6.

4.2.2.3 Production of DIG-labelled cDNA probes using PCR

PCR was employed as an alternative method (to riboprobe production) to generate DIG-labelled and unlabelled cDNA probes. An unlabelled Notch-1 probe was used as a negative control in these studies.

The cDNA probes were produced using a DIG probe synthesis kit (Roche Diagnostics), following the PCR DIG labelling reaction for highly labelled probes containing unique sequences method in the Roche Applied Science DIG-Application Manual for Non-Radioactive *In Situ* Hybridisation (2002).

To produce 50 µl of probe solution, 0.2 ml PCR tubes (Scientific Specialities Inc., CA, USA) were set up on ice and the reagents were added as specified in Table 4.1. Primers R5 and RC13, described in Section 4.2.2, were synthesised by Sigma®-Genosys. Reaction volumes were made up to 50 µl with sterile Milli-Q water and stored at room temperature before the samples were mixed, spun down and loaded into a thermocycler. The DNA was initially denatured at 95°C for 1 min before the PCR of 35 cycles of denaturing at 95°C for 1 min, annealing at 55°C for 1 min, extension at 72°C for 2 min. The final extension ran at 72°C for 5 min, after which the samples were stored at 4°C for 50 min for elongation.

Table 4.1: Components required for producing cDNA probes for the *in situ* hybridisation studies. As the Notch-1 fragment to be amplified was >1 kb, the optimal ratio of DIG-dUTP:dTTP was 1.6. The human tissue plasminogen activator (tPA) kit standard (isolated from genomic DNA) was <1 kb and the optimal ratio of DIG-dUTP:dTTP was 1.3 (Roche, 2002).

Reagent	DIG-labelled Notch	Unlabelled Notch	tPA Kit Standard
PCR buffer with $MgCl_2$	1 x Expand High Fidelity reaction buffer with 1.5mM $MgCl_2$		
PCR DIG probe synthesis mix	100 µm dATP, dCTP, dGTP; 75 µm dTTP; 35 µm DIG-dUTP	x	200 µm dATP, dCTP, dGTP; 130 µm dTTP; 70 µm DIG-dUTP
dNTP stock solution	x	200 µm each dNTP	x
R5 upstream primer	0.5 µM	0.5 µM	x
RC13 downstream primer	0.5 µM	0.5 µM	x
Control PCR primer mix	x	x	0.5 µM
Notch-1 pDNA template	100 pg	100 pg	x
Control (kit) DNA template	x	x	100 pg
Expand high fidelity enzyme mix	2.6 U	2.6 U	2.6 U

4.2.2.3.1 Quantification of probes by gel electrophoresis

To check the efficiency of each DIG-labelling reaction, the reaction products were loaded into a 1% agarose gel. A DNA ladder (Hyperladder I) was loaded along with 4 µl of the PCR products, mixed with 3 µl Ficoll loading buffer and 3 µl sterile Milli-Q water, into an agarose gel in 1x TAE buffer, with 2% ethidium bromide. The gel was immersed in 1x TAE buffer and electrophoresed at 100 V for 30 min. The gel bands were visualized with UV trans-illumination within a Geldoc XR. The remaining reaction products were stored at 4°C.

4.2.2.3.2 Ethanol precipitation and purification of probes

The procedures described in the Roche Applied Science DIG-Application Manual for Non-Radioactive *In Situ* Hybridisation (2002) were followed for ethanol precipitation and purification of the cDNA probes.

The probes were transferred to 1.5 ml microfuge tubes. To each tube, 5 µl of 4M LiCl and 150 µl absolute ethanol (chilled to –20°C) were added. The tubes were vortexed, spun down and incubated at –80°C for 30 min for DNA precipitation. The tubes were centrifuged at 4°C for 15 min with a force of 13,100 ×*g*. The supernatant was discarded and the DNA pellet air-dried (1 hr). The pellet was dissolved in 50 µl TE buffer (pH 8.0; 10 mM Tris, 1mM EDTA) and the probes stored at –20°C for up to 1 yr.

4.2.2.3.3 *Probe quantification using the direct detection method*

To quantify the specificity of the cDNA probes produced by PCR, the direct detection method (Section 3.2.3.3) was followed. The probe was found to be highly sensitive, detecting 0.1 pg/µl of DNA. The Roche Applied Science DIG-Application Manual for Non-Radioactive *In Situ* Hybridisation (2002) recommended that successfully labelled probes be used at a concentration of 2 µl of probe per ml of hybridisation solution. Based on the intensity of the unlabelled Notch-1 probe compared to the bands produced by the Hyperladder (Figure 4.3) it was deduced that the DIG-labelled Notch-1 probe had a concentration of ~80 ng/µl.

4.2.2.4 *In situ* hybridisation

Initial *in situ* hybridisation experiments followed the two protocols suggested by Roche and that used by Botto (2000). Tissue was treated with 200mM hydrochloric acid (HCl) for 20 min at 37°C following rehydration, to increase permeability of the tissue to macromolecular reagents and to encourage protein extraction and partial hydrolysis of the target sequences to improve the signal-to-noise ratio. Pre-hybridisation was carried out using a solution of 50% formamide, 2x SSC and 5 µg/ml sonicated calf thymus DNA as a blocking agent. The tissue was hybridised using a solution comprised of 50% formamide, 4x SSC, 50 µg/ml yeast tRNA, 1 x Denhardt's solution [1 g/L Ficoll, 1 g/L polyvinylpyrrolidone, 1 g/L fraction bovine serum albumin] and 10% dextran sulphate.

The DNA *in situ* hybridisation protocol was unsuccessful, possibly because HCl treatment did not allow the probe to permeate into the cells or pre-hybridisation blocked the probe attachment sites, preventing the probe from binding.

The protocol used for the *in situ* hybridisation with riboprobes (Section 2.2.8) was followed, with modifications, as a riboprobe protocol was previously found to be successful in detecting Notch-1 expression in ovine tissue using PCR generated cDNA probes (Botto, 2000). The pre-hybridisation solution and hybridisation solution (containing the probe) were incubated at 95°C for 2 min prior to adding to the tissue to increase the accessibility of the tissue to the probe and to denature the DNA probe. The tissue was hybridised with the probe at 65°C. The post-hybridisation washes were carried out at a 55°C, with a final wash concentration of 1x SSC used.

By estimating the concentration of DNA probe produced using the biophotometer and performing a titration it was determined that the optimal concentration of probe DNA was 2.6

µg DIG-labelled Notch-1 and 4.3 µg DIG-labelled tissue Plasminogen Activator (tPA) control for each ml of hybridisation solution.

4.2.2.5 Experimental design, cell counts and analysis

The Notch-1 labelled and unlabelled mesenchymal cells within sectioned Merino and Tukidale foetal skin collected on d 56 and d 70 of gestation were counted and the data analysed as described in Section 2.2.8.6. Briefly, 3 fields of view (290 × 220 µm) were investigated for each of 3 non-serial sections for each sample point (d 56 and d 70) and foetus (7 Merino and 5 Tukidale). For the d 70 samples, the numbers of Notch-1 labelled and unlabelled cells within the dermal condensate were also counted. The count data were analysed within Genstat using a linear mixed model.

4.3 RESULTS

4.3.1 RIBOPROBES

A number of riboprobes to Notch-1 were generated and tested on sectioned foetal sheep skin. Each probe was tested at different concentrations, using different hybridisation temperatures and post-hybridisation wash temperatures. However, both the antisense and sense probes produced a signal. The sense staining was reduced by increasing the stringency of the post-hybridisation washes but not eliminated. A possible cause of this was the presence of the sticky Not1 site in the pGEM®-T vector (Botto, 2000).

The *in situ* hybridisation studies therefore concentrated on the application of DIG-labelled cDNA probes produced by PCR, used previously by Botto (2000).

4.3.2 PCR-GENERATED PROBES

The PCR generated probes were electrophoresed on agarose gels, which confirmed that DIG had been incorporated into the DNA. DIG-labelling increased the size of the probes. The intensity of the DIG-labelled probe was less when stained with ethidium bromide, compared to the unlabelled probe. The unlabelled Notch-1 probe (Figure 4.2; lane 2) was noticeably smaller in size (1,517 bp) compared to the DIG-labelled Notch-1 probe (~2 kb) (Figure 4.2; lane 1), due to high density labelling with DIG (1:6 ratio of DIG-dUTP). The tPA standard DNA supplied with the kit should have had an apparent size of 500-550 bp when run on the gel. The size of the unlabelled tPA fragment was 442 bp. It remained unclear as to why the

DIG-labelled tPA probe had an apparent size of 800 –1,000 kb on the gel (lane 3). However, this result was repeated in further PCR experiments.

The specificity of the Notch-1 probe used in this study had been determined previously. It was shown to hybridise with a mRNA band of the expected size for Notch (~9 kb) in sheep skin samples by Northern blotting (Gordon-Thomson *et al.*, 2008).

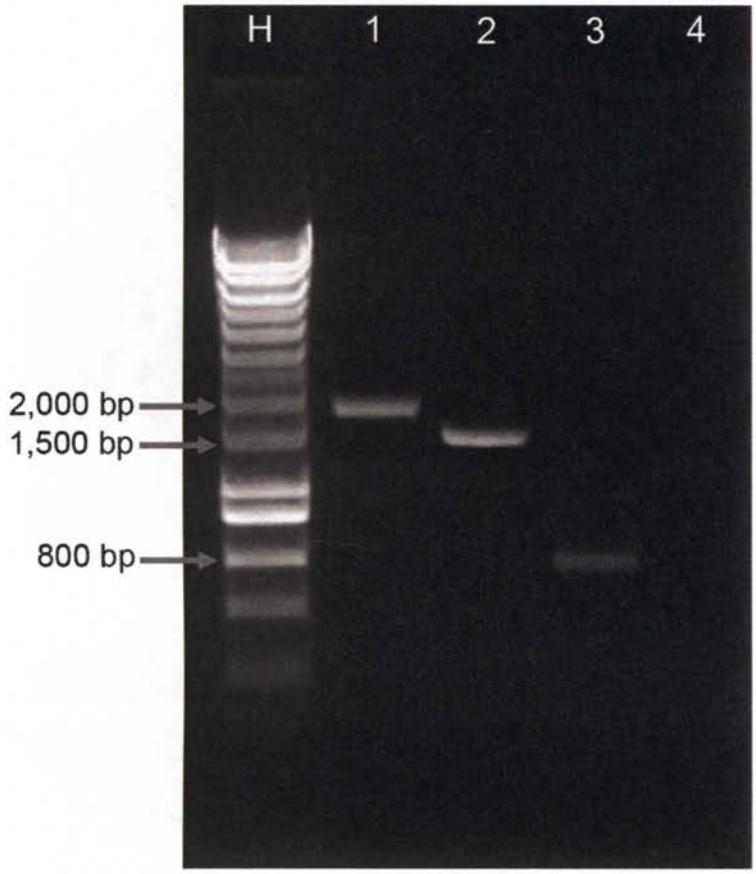

Figure 4.2: Gel analysis of DIG-labelled PCR probes for ovine Notch-1 cDNA. The probes were checked by gel electrophoresis to ensure DIG had been incorporated by PCR. It was evident that DIG-labelling increased the size of the DNA fragments, slowing the rate these samples passed through the gel matrix. H, hyperladder size marker; 1, DIG-labelled Notch-1 probe; 2, unlabelled Notch-1 probe; 3, DIG-labelled tPA kit standard; 4, negative control containing no DNA.

4.3.3 NOTCH-1 IN SITU HYBRIDISATION RESULTS

4.3.3.1 Notch-1 expression in adult sheep skin

Once the DNA probes were working consistently in sectioned foetal skin, Notch-1 expression in adult skin was investigated (Figure 4.3). Expression appeared similar in the Merino and Tukidale samples. Transcripts were detected throughout the dermis, with staining being particularly strong in the outer root sheath. A few cells within the sebaceous gland also

expressed Notch-1. No transcripts were detected in the epithelium or inner root sheath. No colour developed in the keratinised fibre. The Merino skin appeared darker than the Tukidale skin, a result of the high number of follicles within the Merino skin compared to the Tukidale. No colour developed in sectioned skin treated with the Notch-1 unlabelled probe. Investigating the expression of Notch-1 in mature sheep skin tested the consistency of the Notch-1 probe, with the results confirming previous observations (Botto, 2000).

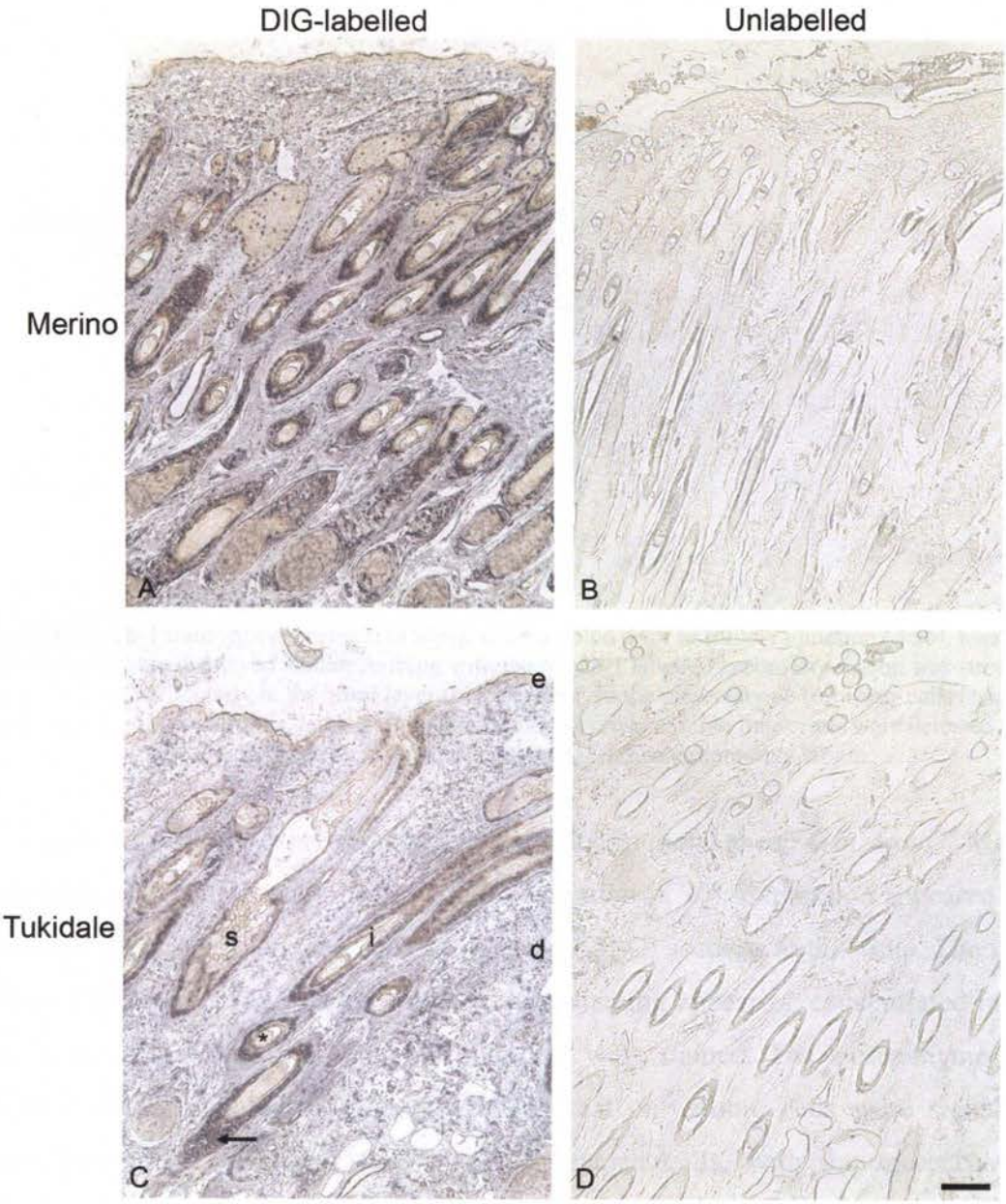

Figure 4.3: Notch-1 gene expression in adult Merino and Tukidale skin. Notch-1 expression was strong in both breeds (A, C). No staining was detected in the epithelium (e). The dermis (d) stained consistently. Staining was strong in the outer root sheath (black arrow). A few cells stained within the sebaceous gland (s); no staining was detected in the inner root sheath (i) or the keratinised fibre (*). Skin treated with the unlabelled probe showed no colour development (B, D). Scale represents 100 μm.

4.3.3.2 Notch-1 expression in foetal sheep skin

Notch-1 expression was investigated in foetal sheep skin sampled prior to follicle initiation. Skin from Merino (A) and Tukidale (C) foetuses sampled on d 56 of gestation showed similar transcript expression (Figure 4.4). Notch-1 was detected throughout the epithelium, it being particularly strong in the basal layer. Within the mesenchyme differential staining was seen, the fibroblasts exhibiting varying degrees of colour development. No staining was detected in skin treated with the Notch-1 unlabelled probe (Figure 4.4; B, D).

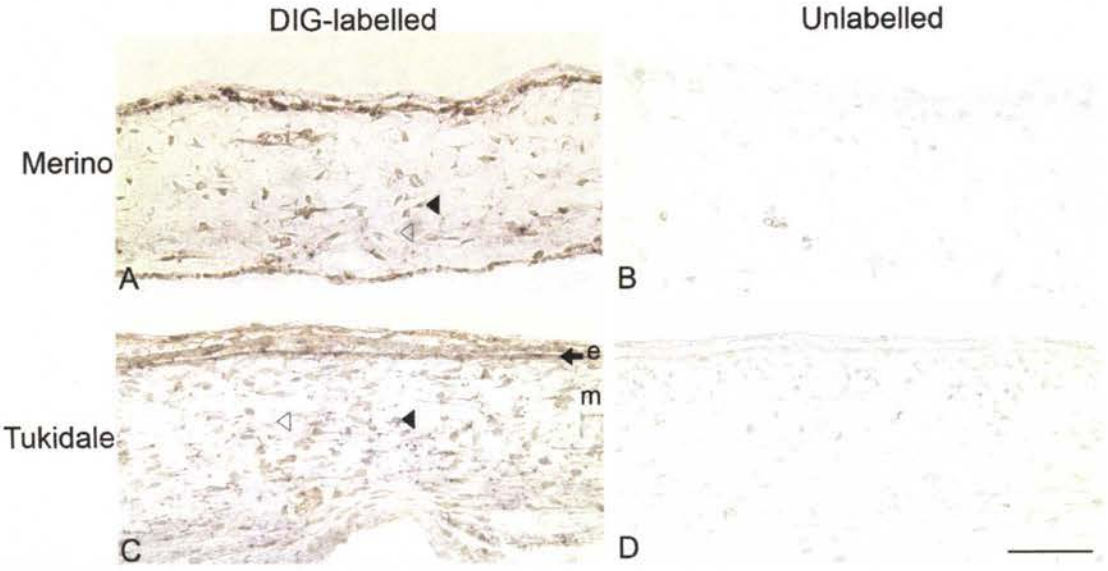

Figure 4.4: Notch-1 transcript expression in sheep skin sampled prior to follicle initiation (d 56). Merino (A) and Tukidale (C) skin displayed similar staining with the Notch-1 labelled probe. Expression was strong in the epithelium (e), particularly in the basal layer (black arrow). In the mesenchyme (m) some cells stained (solid arrowhead), but no stain was detected in others (hollow arrowhead). No transcripts were detected in tissue treated with the unlabelled probe (B, D). Scale represents 50 µm.

Notch-1 transcript expression was investigated in foetal sheep skin, from 7 Merinos and 5 Tukidales, collected during primary follicle initiation (d 70). Expression appeared similar in the Merino (Figure 4.5; A) and Tukidale (Figure 4.5; C) sections at this time. The epithelium was found to consistently express Notch-1, with staining appearing concentrated in the basal layer. Some cells within the epithelial plug also were stained. The mesenchyme contained both labelled and unlabelled cells, suggesting that only some cells were signalling. The dermal condensate contained stained and un-stained cells, with the mesenchymal cells bordering this structure appearing darker, suggesting a possible role for Notch-1 in distinguishing the condensate from the surrounding mesenchymal cells. The sections treated with the unlabelled probe demonstrated no colour development.

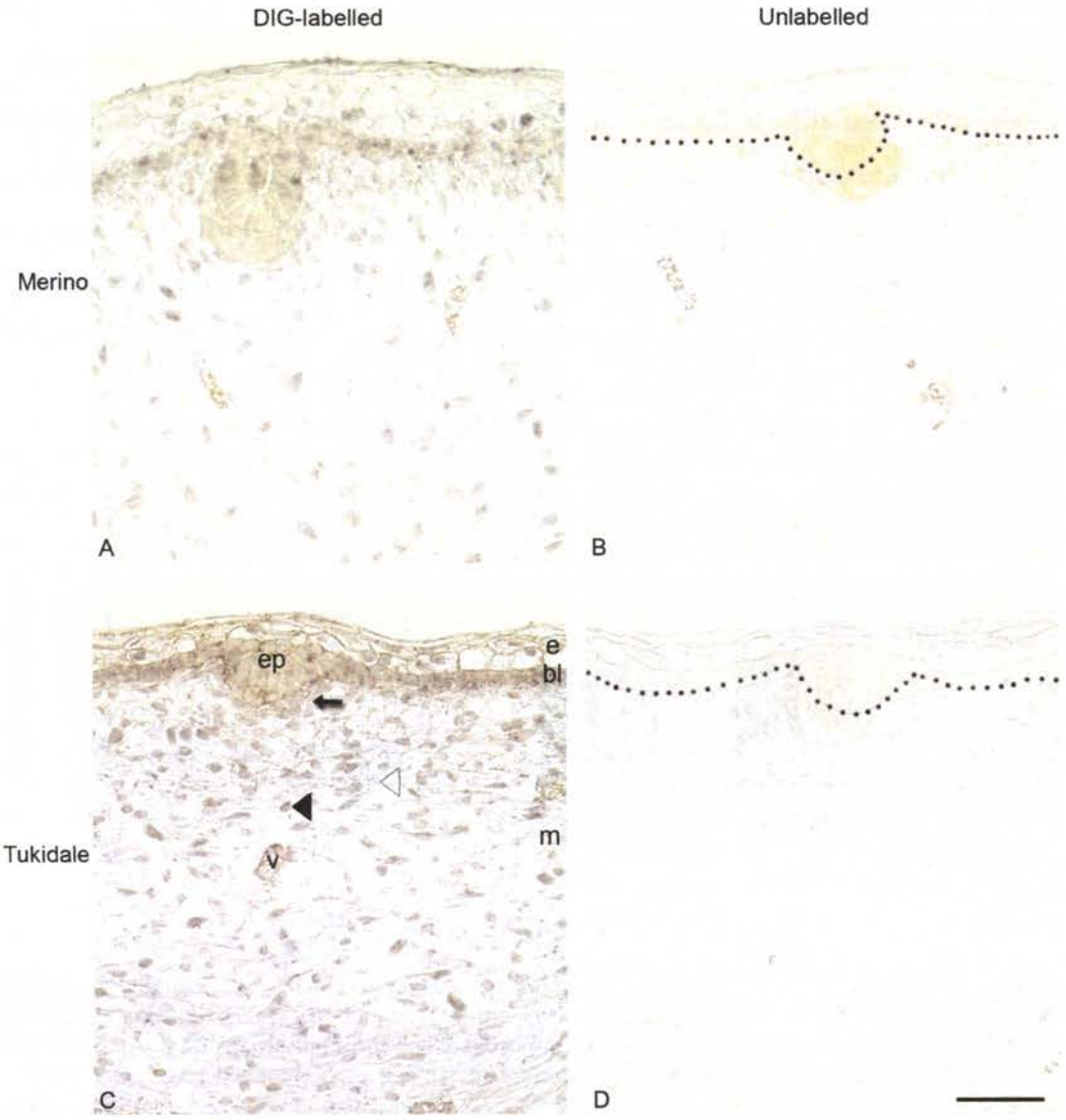

Figure 4.5: Notch-1 transcript expression in sheep skin during primary follicle initiation (d 70). Staining appeared similar in the Merino (A) and Tukidale (C). Skin treated with the DIG-labelled probe showed some staining in the epithelium (e), being concentrated in the basal layer (bl). Some staining was detected in the epithelial plug (ep). Within the mesenchyme (m) some cells had stained (solid arrowhead) whilst others had not (hollow arrowhead). Staining was detected in the dermal condensate (black arrow), with the cells around the periphery of this structure appearing stronger. No staining was detected in the unlabelled controls (B, Merino; D, Tukidale). Dotted line indicates position of the epithelial-mesenchymal junction. Blood vessel (v). Scale represents 50 μm.

4.3.3.3 Analysis of Notch-1 bearing cell population

The numbers of Notch-labelled and unlabelled mesenchymal cells were counted in the d 56 and d 70 sections. The data were analysed in Genstat, on the log scale, using a linear mixed model. The 3-way interaction between age, breed and Notch labelling had a highly significant ($p=0.001$) effect on mesenchymal cell number (Figure 4.6), and was investigated further (Table A7.1). The number of Notch-1 labelled and unlabelled cells was significantly

higher on d 70 compared to d 56 in the Merinos and Tukidales. Significantly more unlabelled cells than Notch labelled cells were counted at d 56 and d 70, within each breed. No significant differences were found in the number of unlabelled cells counted in the Merino compared to the Tukidale at d 56 or d 70. On d 56, the Merino skins contained significantly higher numbers of Notch-1 labelled cells than the Tukidale skins. In contrast, the d 70 Tukidale skins contained significantly higher numbers of Notch-1 labelled cells than the Merino skins.

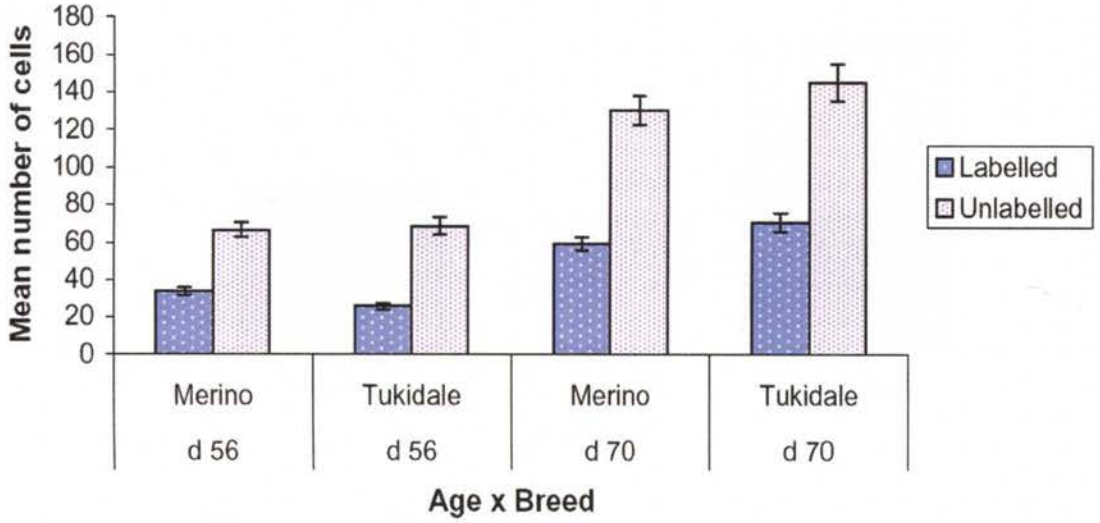

Figure 4.6: The significant (p=0.001) 3-way interaction of age x breed x Notch-1 labelled mesenchymal cells. The number of unlabelled cells was significantly higher than the number of labelled cells at both d 56 and d 70 for each breed. At d 56 the Merino skins contained significantly higher numbers of Notch-1 labelled cells than the Tukidale. At d 70 the Tukidale skins possessed significantly more labelled cells than the Merino. There were no significant differences between the numbers of unlabelled cells in the Merino and Tukidale at d 56 and d 70. The numbers of labelled and unlabelled cells was significantly higher in the d 70 skins than in the d 56 skins within each breed. Error bars represent standard error of the mean.

The numbers of Notch-labelled and unlabelled dermal condensate cells were counted within d 70 skin sections from Merino and Tukidale foetuses. The data were analysed on the log scale using a linear mixed model. No significant 3-way interaction (breed × labelling × number of dermal condensates per field of view; p-value=0.57) was found, and no significant 2-way interactions existed (labelling × number of dermal condensates per field of view, p-value=0.427; breed × number of dermal condensates per field of view, p-value=0.311; breed × labelling, p-value=0.927) allowing these interactions to be dropped from the model so that the main effects could be investigated. Breed was found to have no significant effect (p=0.959) on the number of cells labelled for Notch-1 in the dermal condensate and was not investigated further. The number of dermal condensates within a section was significant

($p<0.001$), but was removed from the model, as it was understood that more cells were found within a section that contained 2 condensates than a section containing only 1. Therefore the only term of interest was whether the cells within the dermal condensate were labelled for Notch-1 or remained unlabelled. Labelling for Notch-1 was highly significant ($p<0.001$; Figure 4.7). The number of unlabelled cells was significantly higher than the number of Notch-1 labelled cells within the dermal condensate (Table A7. 2).

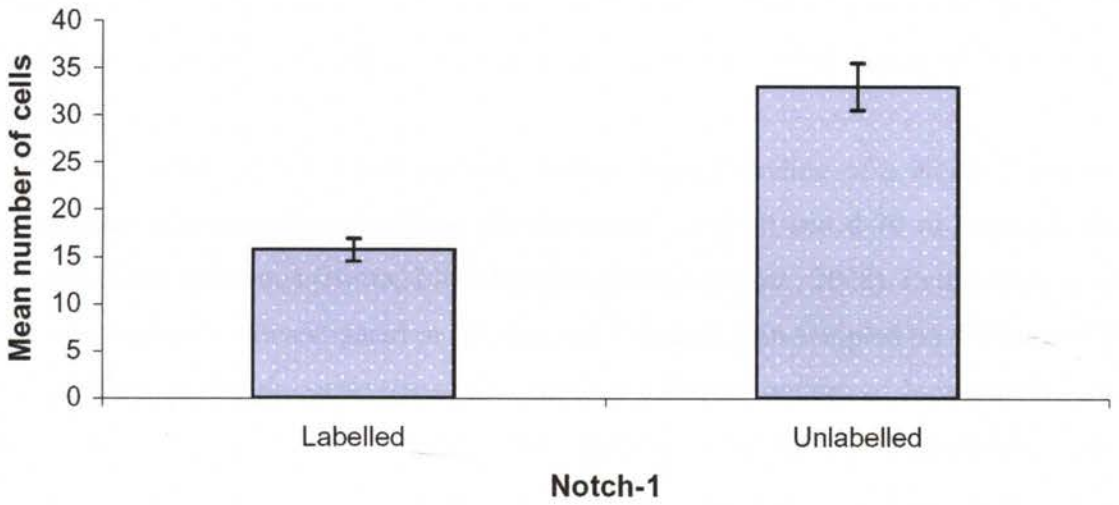

Figure 4.7: Notch-1 labelling in dermal condensate cells had a significant effect ($p<0.001$) on the number of cells counted within the d 70 foetal skin samples. Significantly more unlabelled than Notch-1 labelled cells were found to exist within this structure. Error bars represent standard error of the mean.

4.4 DISCUSSION

A number of riboprobes for Notch-1 were generated from ovine Notch-1 cDNA and tested using *in situ* hybridisations on sectioned foetal sheep skin. Strong non-specific staining was encountered with the DIG-labelled sense probes. Increased hybridisation temperatures, post-hybridisation wash temperatures and stringencies were tested but failed to eliminate the non-specific staining. A possible cause of the non-specific staining was the presence of a sticky Not1 restriction enzyme site in the pGEM-T® vector, as described by Botto (2000). It was unlikely that the non-specific staining was caused by steric hindrance as the probe was binding to the DIG-antibody and a clear band was produced on Northern blotting (Gordon-Thomson *et al.*, 2008). In future, this problem may be able to be rectified by using a different plasmid vector. A technical issue with the anomaly of the tPA DIG-labelled control probe was encountered. However, this result was repeated in each PCR. In this study, a PCR-generated

cDNA probe was used. This provided a way around the issue of the Not1 restriction enzyme site and differential staining was observed in the tissue.

A DIG-labelled ovine Notch-1 cDNA probe was produced by PCR. This method of probe production had a number of advantages: only a small amount of un-purified cloned pDNA was required (10 pg) to produce a high yield of very sensitive probe (able to detect 0.1-0.03 pg of DNA), less optimisation was required than for riboprobe production, and the template DNA could be impure. The length and nature of the probe was primer dependent and many copies of the unique labelled DNA were created. Thus, these PCR-labelled DNA probes were equally as sensitive as riboprobes in hybridising with RNA transcripts in the tissue (Roche, 2002).

Earlier studies in foetal Merino skin showed strong binding of a Notch-1 probe to a subpopulation of mesenchymal cells in skin collected on d 60 and d 70 of gestation and in basal cells of the epidermis (Botto, 2000; Gordon-Thomson *et al.*, 2008). In this study, Notch-1 gene expression was investigated in Merino and Tukidale skin sampled on d 56 and d 70 of gestation. Staining for the gene transcripts showed a similar pattern of localisation in these breeds, which was interesting considering their different wool follicle characteristics. In skin collected prior to follicle initiation, Notch-1 was detected throughout the epithelium, but binding was particularly strong in the basal layer. Differential staining was seen throughout the mesenchyme. A significantly lower proportion of cells within the mesenchymal cell population expressed the Notch-1 transcript when compared to those that remained unlabelled, in the Merino and Tukidale. The density of cells within the mesenchyme increased significantly from d 56 to d 70, but the proportion labelled with Notch-1 did not change with foetal age.

From this study it appeared that Notch-1 was signalling in randomly distributed cells within the mesenchyme of foetal sheep skin, with a signal detected in a relatively low proportion of mesenchymal cells. The random distribution of Notch-1 transcript expression in the mesenchymal cells may have been a result of the Notch signalling mechanism of lateral inhibition being responsible for the up-regulation of the Notch signal in a small number of cells within the mesenchyme prior to and during follicle initiation. It was possible that the Notch-1 signal was enriched in these mesenchymal cells as a result of Delta-1 signalling in other mesenchymal cells, so that the receptor and ligand-bearing cells were communicating with each other. The communication between the Notch-1 receptor and Delta-1 ligand would then presumably result in the formation of aggregations between neighbouring mesenchymal

cells, possibly serving as a mechanism by which dermal condensates form during follicle initiation.

In skin collected during follicle initiation, Notch-1 transcripts were detected throughout the epithelium, appearing particularly strong in the basal layer. Some staining was detected in the epithelial plug. Within the mesenchyme, differential staining was observed. The dermal condensate contained a significantly higher proportion of unlabelled cells than Notch-1 labelled cells. The cells on the periphery of the dermal condensate appeared to be expressing elevated levels of Notch-1 transcript, in relation to the rest of the condensate, particularly in the Tukidale, suggesting a possible role for Notch-1 in distinguishing the condensate from the surrounding mesenchymal cells. This was an interesting finding and suggested that Notch signalling in these cells may have been acting by boundary definition. In the establishment of the dorsal-ventral boundary in the wing imaginal disk in *Drosophila,* Notch is activated in the cells located at the interface between the dorsal and ventral fields of cells where it is involved in keeping these two cell populations distinct from one another (Pourquié, 2000). In the case of the dermal condensate-mesenchymal junction, it was thought that an elevated level of Notch-1 expression might have a role in distinguishing cells that have aggregated to form the condensate. It was theorised that Notch-1 gene transcripts were transiently expressed in the mesenchyme as a mechanism by which the mesenchymal cells that were to be incorporated into the dermal condensate could be differentiated from the general mesenchymal cell population. It was thought that once follicle initiation had occurred and the dermal condensate had formed, Notch-1 signalling may no longer have been required. Notch-1 may have a role in specifying a single round of cell division in the selected prepapilla cell population, and it is possible that the activated downstream targets of Notch-1 have a role in the development of the condensate from an aggregation of cells, into a fully developed follicle. The relatively low level of Notch-1 labelling in the dermal condensate may have been a result of the Notch-1 signalling mechanism having already affected these cells and therefore has subsequently diminished: in these studies it was not possible to investigate more than two time points in the developmental spectrum and therefore the time course of signalling intensity can only be speculated upon. An alternative explanation for a low proportion of cells in the condensate being labelled with Notch-1 was that the cells were aggregating using Delta-Delta associations and these relationships allowed the cells to be held in close proximity to one another.

The Founder Cell Theory postulated a developmental mechanism that controlled both follicle diameter and fibre size, viewed as an expression of the requirement that a select

subpopulation of mesenchymal cells participate in follicle formation, with each event gradually depleting the population of follicle-forming cells (Moore *et al.*, 1989). As fibre diameter and follicle density in the mature skin are highly and negatively correlated, it was proposed that fibre dimensions were specified during follicle morphogenesis (Moore *et al.*, 1996). In the present study, the numbers of cells in the dermal condensate were counted during primary follicle initiation in the d 70 skins for Merino and Tukidale samples. A significantly higher proportion of unlabelled cells than Notch-1 labelled cells were located in the dermal condensate. However, breed did not have a significant effect on the number of cells within the dermal condensate. Therefore, Notch-1 was not an ideal marker for the dermal condensate cell population as it failed to detect differences within this cell population between fine wool and strong wool breeds at this single time point, during follicle initiation. It has been demonstrated that the rate of cell division in the dermal condensate contributes to the observed increase in cell number during development, suggesting local factors acting on the condensate were important in regulating follicle size and fibre diameter (Adelson *et al.*, 2002). Therefore, it was assumed that the dermal condensate in the Tukidale had a higher rate of proliferation compared to the Merino and that suitable genetic markers for detecting differences between these breeds would be related to genes involved in influencing the mitotic potential of these specialised cells. Although these results explain in part the attainment of the ultimate size of the dermal papillae, they do not provide any evidence for a mechanism to explain the patterning of condensates that ultimately form the wool follicle population in the skin. Nor do they provide any evidence to suggest that the Notch family of genes specify a distinctive population of cells determined to form dermal papillae.

Previous studies by Moore *et al.* (1998) suggested the number of committed cells per follicle was inversely related to follicle density and indicated a direct relationship with fibre diameter. It has been shown that while the initial formation of the dermal condensate may involve cell migration and aggregation, the approximately two-fold increase in cell number during dermal papilla growth could be explained solely on the basis of cell proliferation (Adelson *et al.*, 1992). The results from this study suggest that factors expressed after follicle initiation influence the size of the fibre produced in the adult animal. No differences were detected between the size of the dermal condensate (at follicle initiation) in the Merino and Tukidale, and if the mitotic potential in the dermal condensate of these breeds were the same, the dermal papilla in adult skin, and therefore fibre diameter would be similar. However the differences in the follicle population in mature animals suggest that either the proliferative potential of these cells between breeds must be different, or additional cells from the putative

specified founder cell population are continuously incorporated selectively in the Tukidale foetal skin during their formation.

These results neither prove nor disprove the Founder Cell Theory which states that follicle number and fibre size are determined at or prior to follicle initiation (Moore *et al.*, 1989). However, this theory of cell proliferation within the dermal condensate is consistent with the predictions of the Reaction-Diffusion Theory of follicle morphogenesis (Nagorcka, 1986; Nagorcka, 1995a). These findings suggest that wool follicle initiation occurs in a similar manner in sheep breeds with markedly different follicle characteristics. Therefore, it is proposed that during follicle initiation, a number of cells aggregate to form the dermal condensate. However, the mitotic potential of the cells within the condensate of the different breeds differ, with the dermal condensate in the Tukidale having a much higher level of proliferative potential compared to the Merino. An alternative explanation is that the dermal condensate recruits cells from the mesenchymal population into the prepapilla following initiation and that this migration of cells into the condensate occurs at a higher rate in the Tukidale compared to the Merino. The theory however does not dismiss the likelihood of an initial founder cell population that is rate limiting for the number of prepapillae formed. The proliferative potential may simply be higher in the Tukidale. To provide confirmatory evidence for any mechanism ideally the number and distribution of prepapillae should have been determined by preparing longitudinal sections for each of the skin samples used in this study.

In conclusion, this study demonstrated that Notch-1 transcripts were expressed in Merino and Tukidale skin collected prior to and during follicle initiation. It appeared that Notch-1 had a role in the mesenchyme of foetal skin and was likely communicating with cells that were expressing the Delta-1 ligand, using the mechanism of lateral inhibition to allow neighbouring cells to communicate and establish the dermal prepapilla. Once the condensate had formed, it appeared that Notch-1 expression was transient. However, Notch-1 may have a role in maintaining the dermal condensate as a separate structure and distinguishing it from the remaining mesenchymal cell population. Future experiments to further investigate Notch-1 signalling in foetal sheep skin would be beneficial. It would be advantageous to ligate the ovine Notch-1 cDNA into a different plasmid vector and to then conduct *in situ* hybridisation experiments using antisense and sense DIG-labelled riboprobes. This would allow for different restriction enzymes to be utilised in order to construct different Notch-1 probes. It may also be of interest to investigate the role of Notch-1 at different times during follicle

development as well as to investigate the roles of other Notch receptors during follicle initiation in foetal sheep skin.

CHAPTER 5: DELTA-1 AND NOTCH-1 PROTEIN EXPRESSION IN SKIN

5.1 INTRODUCTION

The Notch signalling pathway is utilised by many species of animals to initiate and consolidate molecular differences between adjacent cells during development and growth in many tissues. The development of the hair follicle and formation of a hair fibre involve the coordinated differentiation of several different types of cells, within which Notch is thought to have a role (Crowe *et al.*, 1998).

When a Notch receptor on one cell is activated by a Delta ligand on an adjacent cell, an intracellular protease cleaves off the cytoplasmic tail of Notch, and the released Notch intracellular domain (NICD) is translocated into the cell's nucleus to activate transcription of a set of Notch-response genes (Fleming, 1998; Alberts *et al.*, 2002; Kopan, 2002; Roy *et al.*, 2007). Although the Notch pathway seems to be activated mainly through cell-cell interactions, proteolytic cleavage of both receptors and ligands has been shown to be important for signalling (Six *et al.*, 2003). The process of proteolytic cleavage of Notch is irreversible: each Notch-1 receptor molecule is able to signal only once. Therefore, the intensity and duration of the signal cannot be regulated through desensitisation of the receptor (Schweisguth, 2004). The intensity of the Notch signal would be proportional to the number of receptor molecules signalling at that time. The duration of a signal would be dependent on how quickly new receptors were synthesised and the turnover rate of receptor binding to ligand, and processing of the complex: and this would be influenced by the amount of ligand being expressed on adjacent cells. Therefore, the context in which Delta and Notch are being expressed and their interactions with one another (and with itself in the case of Delta) would influence the outcome of signalling. The intensity of the Delta and Notch signals within foetal sheep skin may influence the morphogenesis of follicles within the tissue.

In these immunohistochemical studies, the expression of Delta-1, Notch-1 and activated Notch protein were investigated. Delta-1 protein expression was investigated in foetal and adult sheep skin using immunofluorescence techniques. Notch-1 protein expression was studied, using an antibody generated to the ovine sequence, in foetal and adult sheep skin collected from Merino and Tukidale animals. Activated Notch expression was examined in foetal Merino skin collected during follicle initiation.

5.2 MATERIALS AND METHODS

5.2.1 ANIMALS

Mouse embryos at 15 dpc, collected as described in Section 2.2.1.3, were used in preliminary immunohistochemistry experiments to test the specificity of the Delta-1 antibody.

Skin was collected from the gluteal region of Merino and Tukidale foetuses on d 56 and d 70 of gestation. The animals used in these studies were euthanased at d 70 using 3.6 g pentobarbitone delivered intravenously on the day of sampling before the foetus was collected and a 10 mm skin biopsy was collected from either side of the foetus, as described in Section 2.2.3.3.2. The skin samples were processed into paraffin wax (Section 2.2.4.1) or OCT (Section 2.2.4.2) and sectioned using a microtome for the wax embedded tissue (Section 2.2.5.1), or cryotome for frozen tissue embedded in OCT (Section 2.2.5.2).

For the immunohistochemistry studies reported in this chapter, protein expression was investigated in 4 Merino and 4 Tukidale foetuses on d 56 and d 70 of foetal development. The results reported for each time point are based on the observation of 3 sections from each foetus. The adult skin studies used 3 skin collected from Merino and Tukidale ewes.

5.2.2 IMMUNOHISTOCHEMISTRY

Sections were brought to room temperature within their slide box, circled with a glass knife and de-waxed (if paraffin-embedded samples were used) as described in Section 2.2.6.

Two different antibodies to Notch-1 were tested in this study. Firstly, an affinity purified rabbit polyclonal antibody directed to a peptide sequence of ovine Notch-1, designed in the laboratory using the program PREDITOP by Dr Clare Gordon-Thomson, was generated. The peptide was synthesised by Mimitopes (Clayton, VIC, Australia) and an antiserum generated in rabbits by the Institute of Medical and Veterinary Research (Adelaide, SA, Australia). An intracellular epitope was chosen, mapping to a region between the transmembrane region of Notch-1 to the first ankyrin repeat (Figure 4.1), spanning ~18 amino acids with the sequence LMDDNQNEWGDEGLE. The antibody detected both the uncleaved Notch-1 receptor as well as the activated Notch-1 fragment that forms after S3 cleavage has occurred. The amino acid sequence of the peptide used was 100% homologous to the predicted amino acid sequence of the ovine Notch-1 cDNA (accession number: EF999923).

A rabbit polyclonal antibody to activated Notch-1 was purchased from Abcam Inc. (Cambridge, MA, USA). The peptide, designed from human and mouse Notch-1, with the sequence VLLSRKRRRQHGQC, corresponded to amino acids 1755-1767 of human Notch-1

protein (accession number: P46531) and nucleotides 998-1203 of ovine Notch-1 cDNA. The antibody recognised the cleaved intracellular (activated) form of Notch-1, produced after S3 cleavage of the receptor. The antibody was initially tested at 200 µg/ml, but further investigations were conducted using concentrations ranging between 20 and 80 µg/ml as a signal was detected at these concentrations using the colourimetric method (Section 5.2.2.2), and the non-specific staining detected in the control samples was minimised at these lower concentrations.

5.2.2.1 Fluorescence staining

The method described in Section 2.2.9.1 was followed, using a goat polyclonal antibody to Human Delta.

5.2.2.2 Vectastain method

Sections of paraformaldehyde-fixed tissues embedded in wax were incubated in 1x target retrieval solution (pH 6.0; Dako Australia Pty Ltd, Kingsgrove, NSW, Australia) for 20 min at 100°C in a water bath, within a fumehood. The solution was cooled to room temperature before the slides were washed thrice in Milli-Q water for 5 min.

Endogenous peroxidases were removed by immersing the slides in 0.3% hydrogen peroxide (AnalaR®) for 30 min. The slides were then washed three times in Tris-buffered saline (TBS: 50mM Tris-HCl; 30mM NaCl) for 5 min. The tissue was blocked for 30 min, within a humidified chamber, at room temperature with approximately 100 µl of 1% horse serum (Vectastain® ABC kit; Vector Laboratories Inc, CA, USA) diluted in TBS. Alternatively, the Envision™ System (Dako Australia Pty Ltd) was used with 100 µl of Dual Endogenous Enzyme Block (DEEB: Dako Australia Pty Ltd) solution added to each slide before incubation at room temperature for 10 min. The DEEB solution was rinsed from the sections using TBS.

Antibody and control solutions were prepared according to the kit instructions. To remove any immune complexes from the antisera, the primary antibody was centrifuged with a force of 5,590 *xg* for 5 min at 4°C. The working concentration of the ovine Notch-1 polyclonal antibody was 1.4 µg/ml in blocking solution. Negative controls were incubated in rabbit IgG or normal rabbit serum diluted at the same concentration as the antibody.

Blocking reagent was drained from the sections and approximately 100 µl of the primary antibody or control solution was added to each slide. The slides were returned to the chamber and incubated for 16 hr at 4°C.

The antibody and control sera were washed from the tissue with three 5 min washes of TBS. The sections were then incubated with the Vectastain® biotinylated secondary antibody in 2% horse serum for 30 min at room temperature. For the Envision™ System, 80 µl of the Envision™ Dual Link System Peroxidase (HRP, rabbit/mouse; Dako Australia Pty Ltd) was added to the sections.

The Vectastain® reagent mixture was prepared at least 30 min prior to use. The mixture contained 2 drops of reagent A, diluted in 5 ml of TBS, and 2 drops of reagent B. The slides were washed in TBS for 5 min before the tissue was incubated with the reagent mixture for 30 min.

The slides were washed thrice with TBS for 5 min before they were incubated with the DAB substrate (peroxidase substrate kit DAB; Vector Laboratories Inc.) as advised by the manufacturer. The substrate was set up within a 15 ml centrifuge tube (Greiner Bio-One); 5 ml Milli-Q water, 2 drops of buffer stock solution, 4 drops of DAB and 2 drops of hydrogen peroxide. The solution was mixed after the addition of each solution and immediately added to the sections. The tissue was visually monitored for colour development (2-10 min). The slides were rinsed in Milli-Q water to stop the reaction, counterstained with haematoxylin and coverslips were mounted as described in Section 2.2.6.

5.3 RESULTS

5.3.1 DELTA-1 EXPRESSION

5.3.1.1 Delta-1 protein expression in embryonic mouse skin

Delta-1 protein expression was investigated initially in murine tissues using immunofluorescence. In whisker follicles on 15 dpc, Delta-1 protein was detected in the epithelium and muscle underlying the mesenchyme. Negligible expression was detected in the mesenchyme, dermal condensate and epithelial plug (Figure 5.1).

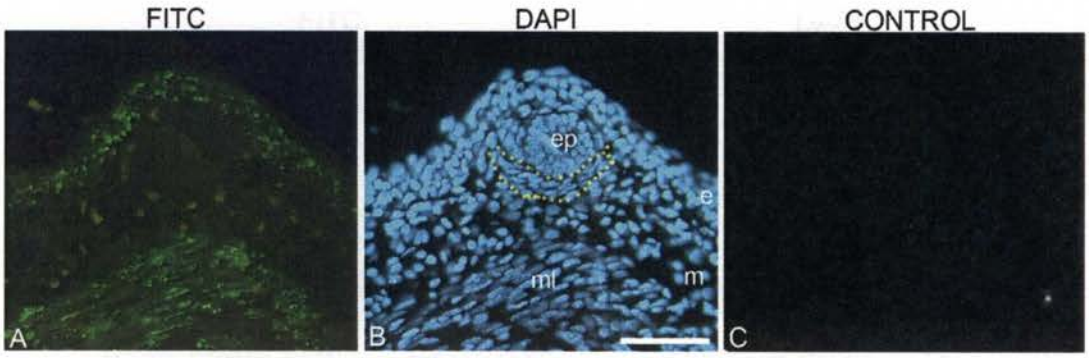

Figure 5.1: Delta-1 protein expression in a developing 15 dpc murine vibrissa follicle. Delta-1 was localised to the epithelium (e) and muscle layer (ml). Low levels of expression were detected in the mesenchyme (m), epithelial plug (ep) and dermal condensate (outlined in yellow). Autofluorescence was detected in blood vessels within the m. A, FITC fluorescence; B, DAPI nuclear counterstain. No fluorescence was detected in control-treated tissue (C). Scale represents 50 μm.

5.3.1.2 Delta-1 protein expression in adult sheep skin

Delta-1 protein expression was investigated in adult ovine skin. Protein expression appeared similar in adult Merino and Tukidale skin. In adult Merino skin, Delta-1 protein was detected in the epidermis and dermis. Expression appeared particularly strong in some areas of the follicle (Figure 5.2). On closer inspection of the follicles (Figure 5.3), Delta-1 protein expression was confirmed to be in the outer root sheath. It was evident that some cells (in the outer root sheath) expressed the protein, while others did not.

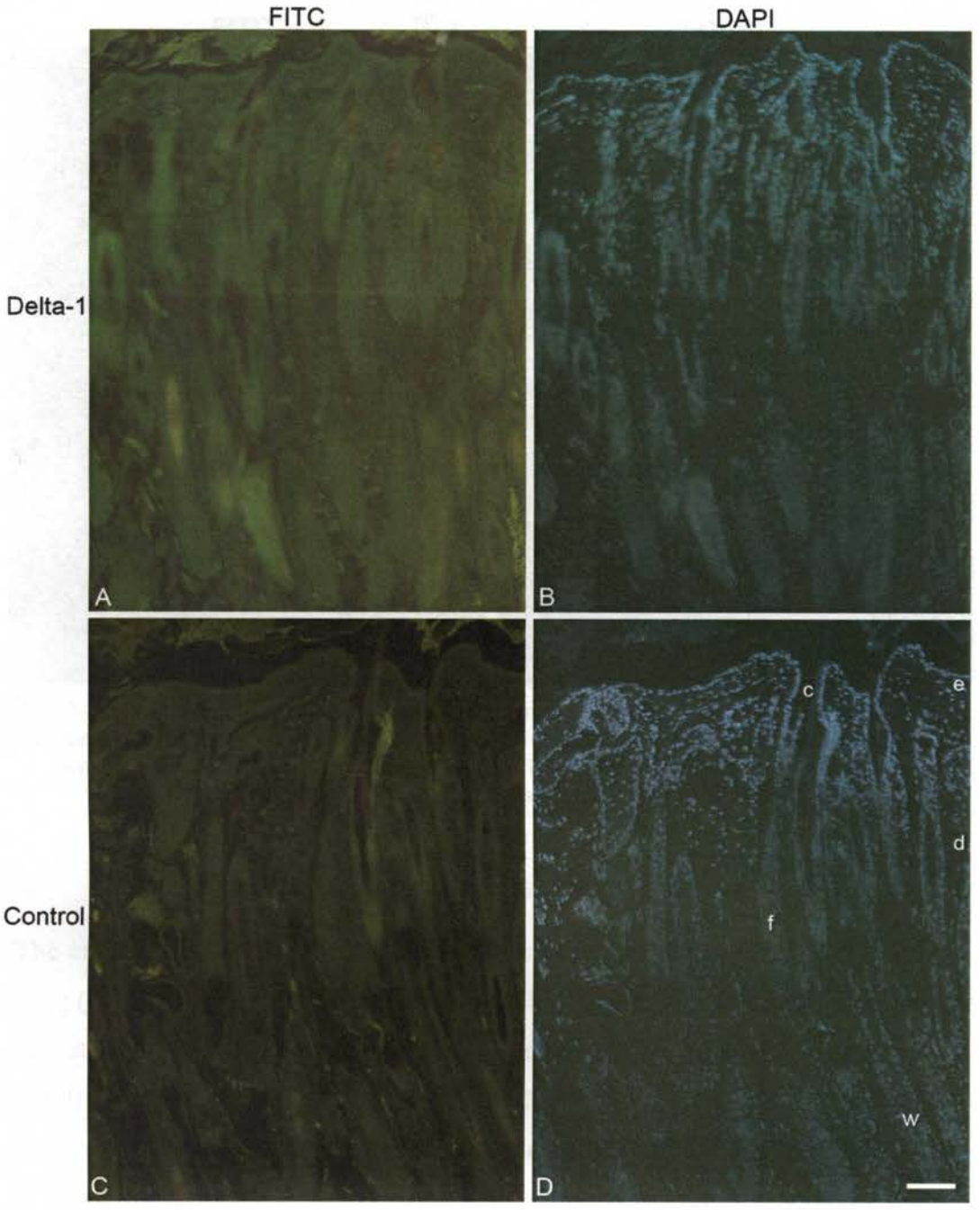

Figure 5.2: Delta-1 protein expression in adult sheep skin. Expression was similar in the Merino (pictured) and Tukidale skin samples (not shown). A; Delta-1 was detected in the epithelium (e) and dermis (d). Strong fluorescence was detected in areas of the follicle (f), thought to be the outer root sheath. Some autofluorescence was detected in the canal (c) and wool fibre (w). DAPI image of same field of view (B). Control tissue (C) showed no fluorescence, DAPI images of field (D). Scale represents 100 μm.

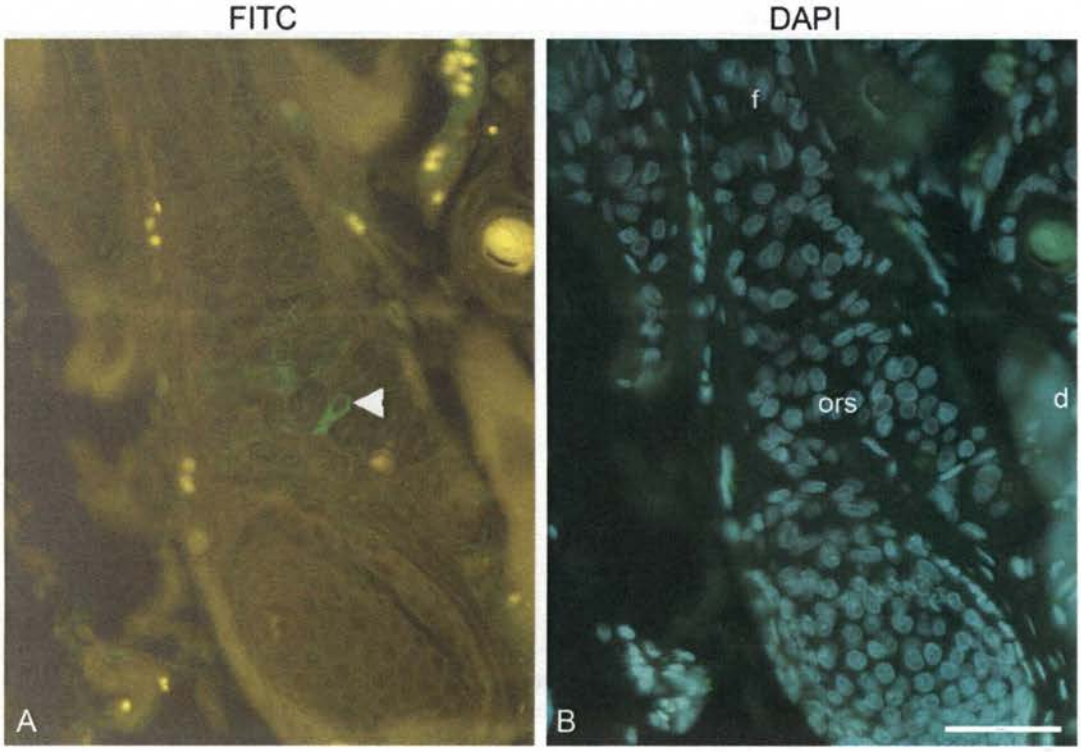

Figure 5.3: A closer inspection of Delta-1 protein expression in an adult Merino wool follicle. Fluorescence was detected in some cells of the outer root sheath (ors; white arrowhead), within a follicle (f). Minimal fluorescence was detected in the dermis (d). No fluorescence was detected in the controls (not shown). Scale represents 50 μm.

5.3.1.3 Delta-1 protein expression in foetal sheep skin

The expression of Delta-1 protein was investigated in foetal sheep skin prior to (d 56) and during (d 70) the initiation of primary wool follicles. Foetal Merino skin collected on d 56 showed that Delta-1 protein was expressed in the epithelium, particularly in the basal layer (Figure 5.4). Some mesenchymal cells were labelled with the antibody. The protein appeared to be expressed in the nucleus of the mesenchymal cells. In foetal Tukidale skin collected on d 56 of gestation Delta-1 protein expression appeared negligible in the epithelium (Figure 5.5). A few cells within the mesenchyme showed fluorescence.

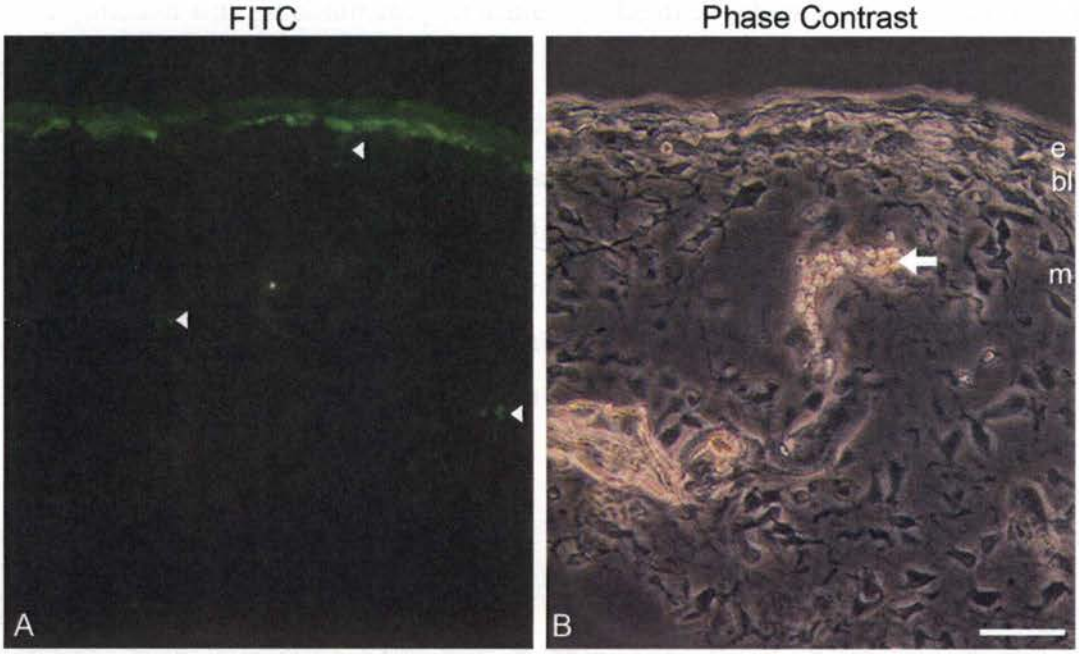

Figure 5.4: Delta-1 protein expression in Merino skin sampled prior to follicle initiation (d 56). A; Fluorescence was detected in the epithelium (e), particularly in the basal layer (bl), and in scattered cells (white arrowheads) within the mesenchyme (m). Some autofluorescence was detected in blood vessels (white arrow). No fluorescence was detected in the control tissue (not shown). B; Phase contrast image of same field of view. Photos courtesy of Hugh Graham. Scale represents 30 µm.

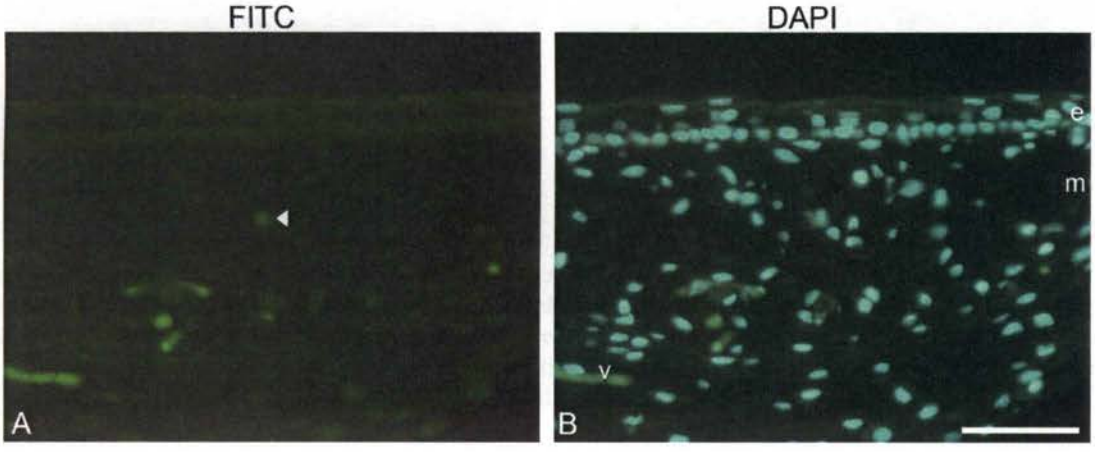

Figure 5.5: Delta-1 protein expression in Tukidale skin sampled prior to follicle initiation (d 56). A; Protein expression appeared negligible in the epithelium (e), a few cells showed fluorescence within the mesenchyme (m; white arrowhead). Some autofluorescence was detected in the blood vessels (v). No fluorescence was detected in the controls (not shown). B; DAPI stained image of the same field of view. Scale represents 50 µm.

Delta-1 protein expression was investigated in foetal skin collected during follicle initiation. In the d 70 Merino skin, fluorescence was detected in the upper layers of the epithelium, with the basal layer also showing immunoreactivity (Figure 5.6). No immunoreactivity was detected in the epithelial plug. After careful examination (of 3 slides from 4 foetuses) using FITC fluorescence and phase contrast microscopy or a filter for DAPI fluorescence, it was tentatively concluded that the immunoreactivity adjacent to the dermal-

epidermal junction was predominantly confined to the mesenchymal cells. Expression in the mesenchyme appeared particularly strong directly below the basement membrane. Fluorescence was detected in the mesenchyme, with some cells expressing the protein whilst others did not. Cells within the dermal condensate also showed fluorescence.

In d 70 Tukidale skin samples, Delta-1 protein expression appeared less widespread than in the Merino (Figure 5.7). Negligible levels of fluorescence were detected in the epithelium, basal layer and dermal condensate. Similarly, no protein was detected in the epithelial plug. A few cells within the mesenchyme appeared to express the protein.

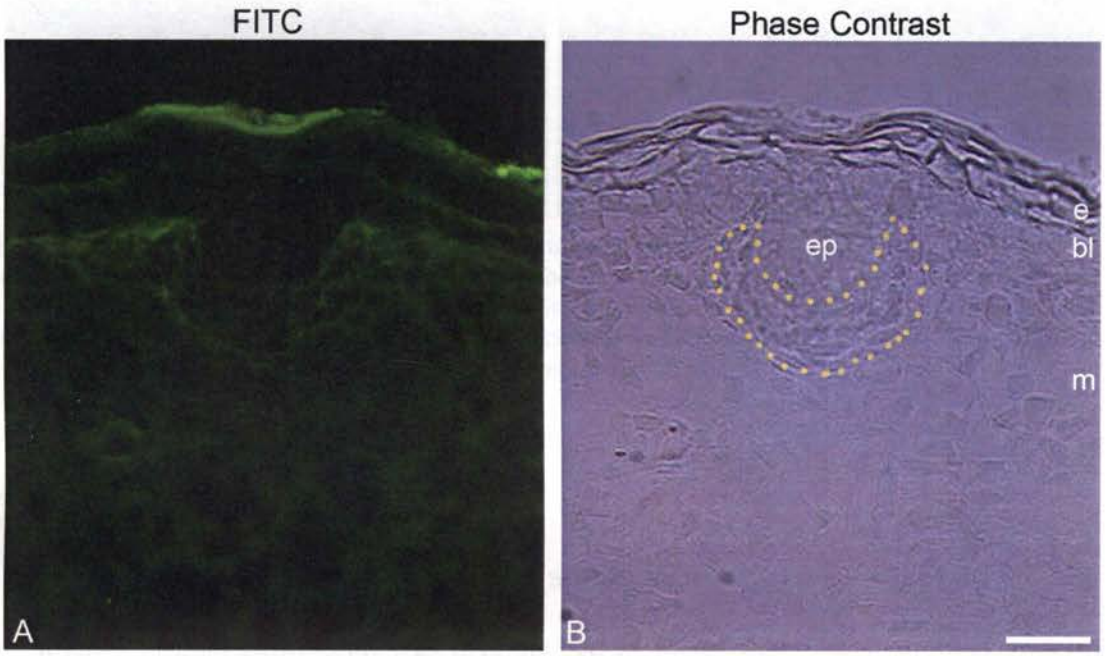

Figure 5.6: Delta-1 protein expression in foetal Merino skin sampled during primary follicle initiation (d 70). A; Fluorescence was detected in the upper layers of the epidermis (e), in the basal layer (bl), mesenchyme (m) and dermal condensate (outlined in yellow). No reactivity was detected in the epithelial plug (ep). No fluorescence was detected in the controls (not shown). B; Phase contrast image of the same field of view. Images courtesy of Hugh Graham. Scale represents 30 μm.

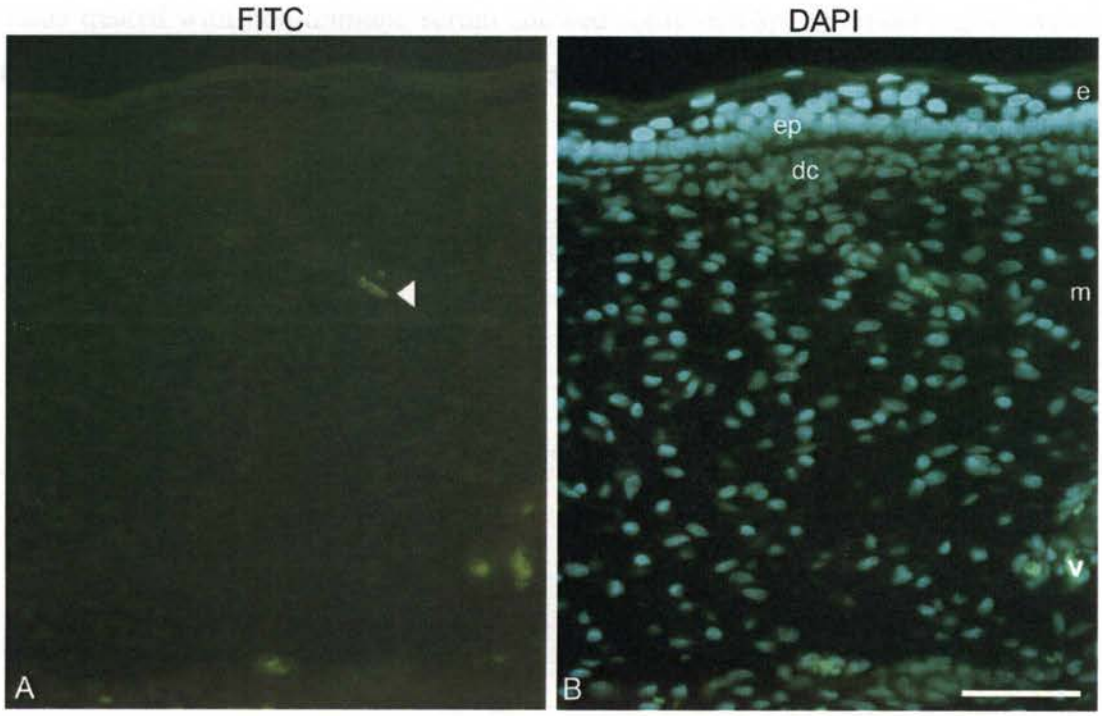

Figure 5.7: Delta-1 protein expression in Tukidale skin sampled during primary follicle initiation (d 70). A; Fluorescence was negligible in the epithelium (e), epithelial plug (ep) and dermal condensate (dc). A few cells within the mesenchyme (m) expressed the protein (white arrowhead). Blood vessels (v) displayed autofluorescence. No fluorescence was detected in the control tissue (not shown). B; DAPI image of same field of view. Scale represents 50 μm.

5.3.2 NOTCH-1 EXPRESSION

5.3.2.1 Notch-1 expression in foetal sheep skin

Notch-1 protein expression was investigated in foetal sheep skin sampled prior to and during primary follicle initiation using a polyclonal antibody developed to ovine Notch-1. Distribution of immunoreactivity was similar in the Merino and Tukidale skin. In the d 56 samples Notch-1 was detected in the epithelium, the basal layer of the epithelium, and throughout the mesenchyme (Figure 5.8). Within the mesenchyme some cells showed strong immunoreactivity to the Notch-1 antibody and others were not labelled. Non-specific staining in the control tissue incubated with non-immune serum was light relative to the succinct staining of a sub-population of cells in the antibody-treated sections. In the d 70 samples, Notch-1 protein was detected in the epithelium, the basal layer, epithelial plug and dermal condensate (Figure 5.9). As in the d 56 skin, the d 70 mesenchyme showed strong immunoreactivity to the Notch-1 antibody in some mesenchymal cells, while other cells had not stained. The Tukidale samples appeared to stain darker than the Merino, possibly due to the denser cell population in the mesenchyme of the Tukidale. Similar to the d 56 skin, the d

70 tissue treated with non-immune serum showed some non-specific staining. However, the controls stained to a lesser extent than the antibody-treated tissue.

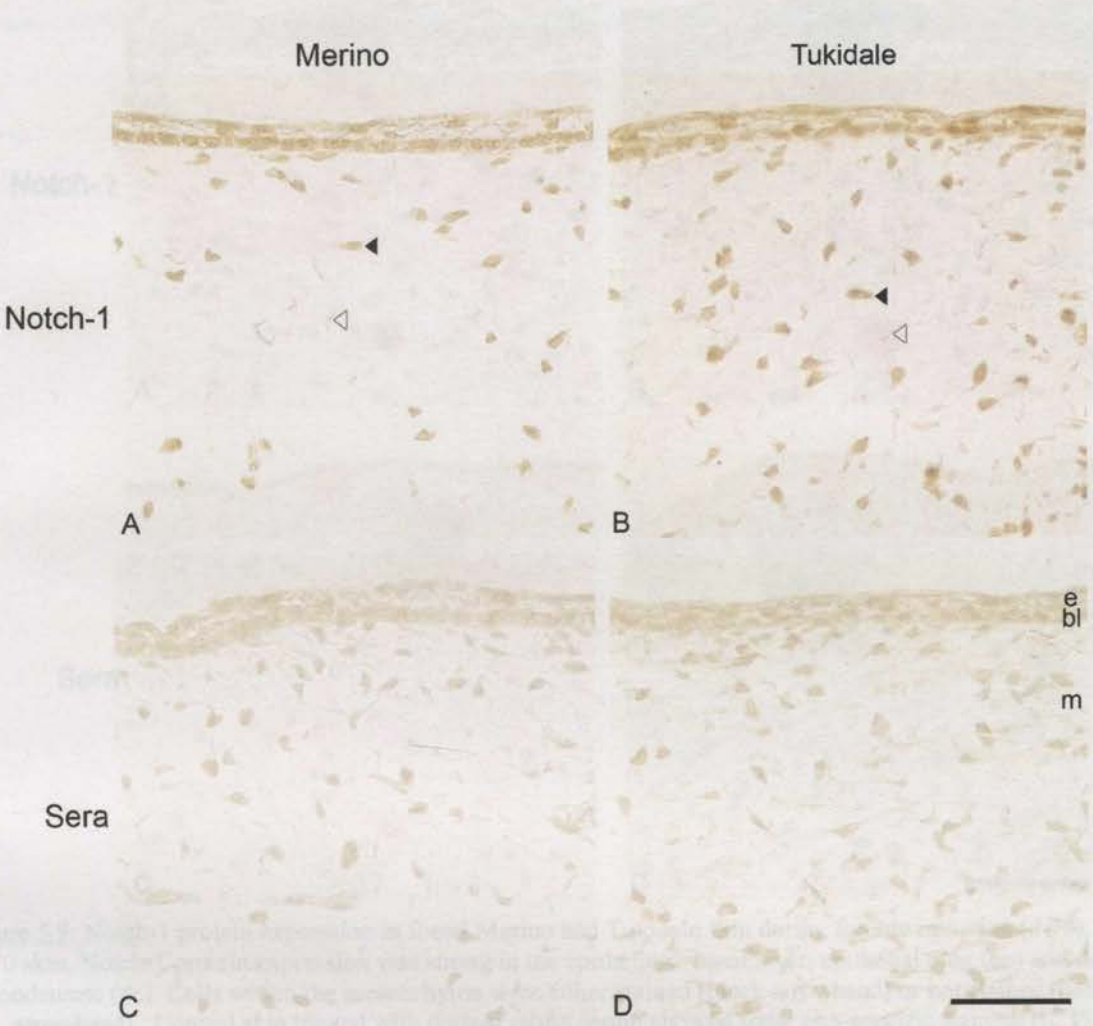

Figure 5.8: Notch-1 protein expression in foetal Merino and Tukidale skin prior to follicle initiation (d 56). In the d 56 skin (A, B) Notch-1 was detected in the epithelium (e), particularly in the basal layer (bl), and in the mesenchyme (m). Within the mesenchyme, some cells were stained (black arrowhead) whilst others had not stained (hollow arrowhead). Control skin treated with normal rabbit serum showed some non-specific staining (C, D). Scale represents 50 μm.

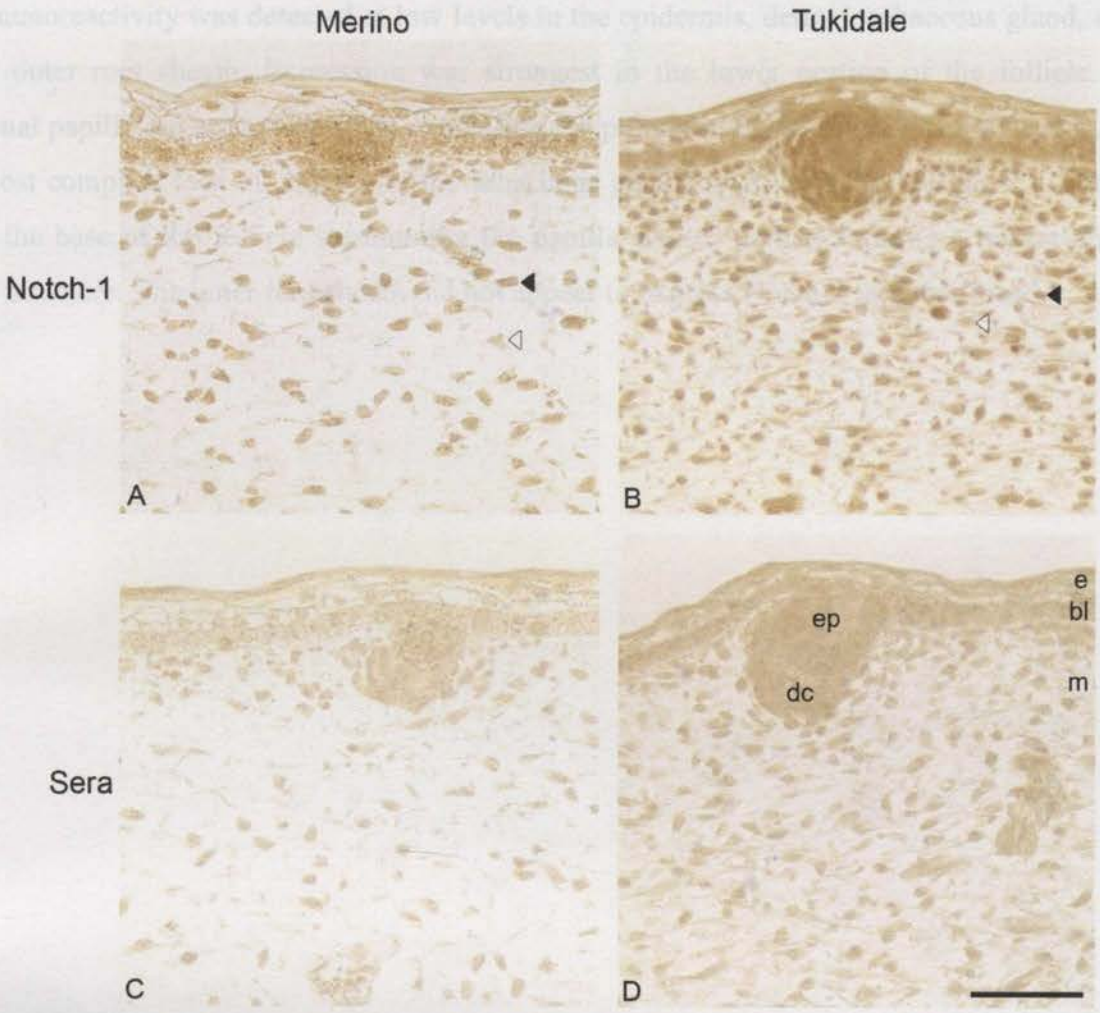

Figure 5.9: Notch-1 protein expression in foetal Merino and Tukidale skin during follicle initiation (d 70). In the d 70 skin, Notch-1 protein expression was strong in the epithelium, basal layer, epithelial plug (ep) and dermal condensate (dc). Cells within the mesenchyme were either stained (black arrowhead) or not stained (hollow arrowhead). Control skin treated with normal rabbit serum showed some non-specific staining (C, D). Scale represents 50 μm.

5.3.2.2 Notch-1 protein expression in adult sheep skin

Notch-1 protein expression was investigated in Merino and Tukidale adult skin samples. It was observed that immunoreactivity to the Notch-1 antibody appeared stronger in the Merino skin than in the Tukidale (Figure 5.10). Interestingly, this was the reverse of what was observed in the foetal skin samples, where the Tukidale appeared to be expressing higher levels of Notch-1 protein. However, this observation may be primarily due to the increased follicular density within the adult Merino skin. In the Merino, immunoreactivity to the Notch-1 antibody appeared to be strong throughout the tissue. High levels of Notch-1 protein were detected in the epidermis, sebaceous glands and outer root sheath. In the Tukidale, Notch-1 appeared to be expressed to a lesser degree in the upper section of the skin and wool follicles.

Immunoreactivity was detected at low levels in the epidermis, dermis, sebaceous gland, canal and outer root sheath. Expression was strongest in the lower portion of the follicle. The dermal papilla did not appear to be expressing the protein in the Merino or Tukidale skin. The almost complete lack of staining in the sebaceous glands relative to the Merino is of interest but the base of the follicle surrounding the papilla stained darker, forming a border around this structure. The inner root sheath did not appear to express Notch-1 in either breed.

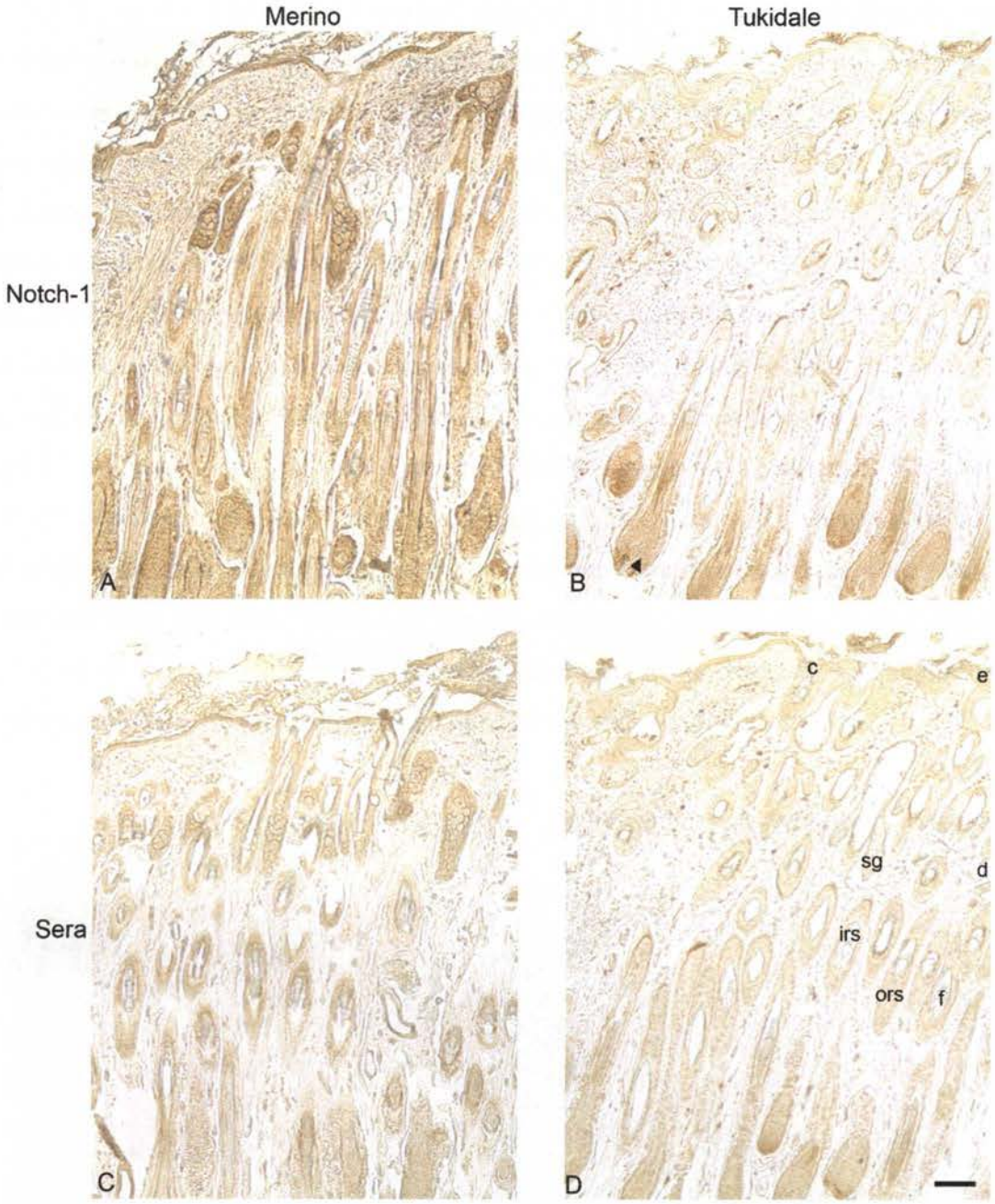

Figure 5.10: Notch-1 protein expression in adult sheep skin. Notch-1 antibody immunoreactivity appeared stronger in the Merino (A) than in the Tukidale (B) skin. Immunoreactivity was strong throughout the epidermis (e). The sebaceous gland (sg) and outer root sheath (ors) of the wool follicle appeared to express strong immunoreactivity. Protein was detected to a lesser extent in the dermis (d) and canal (c). In the Tukidale, immunoreactivity appeared to be stronger in the lower portion of the wool follicles. Protein was detected in the e, d, sg, c and ors but to a lesser extent than in the Merino. In both breeds the inner root sheath (irs), dermal papilla (black arrowhead) and wool fibre (f) had not stained. Control skin treated with normal rabbit serum showed some non-specific staining (Merino, C; Tukidale, D). Scale represents 100 μm.

5.3.3 ACTIVATED NOTCH-1 EXPRESSION

An antiserum to the activated form of human and murine Notch-1 was tested on foetal sheep skin during primary follicle initiation.

Following the fluorescence method (Section 2.2.9.1) the activated Notch-1 antibody was initially tested at a concentration of 200 µg/ml (Figure 5.11) on d 70 Merino skin. Strong immunoreactivity was seen in the basal layer and epithelial plug of the epidermis. Some immunofluorescence was detected in the dermal condensate and mesenchyme. The dermal condensate appeared to express slightly higher levels of the protein than mesenchyme, possibly as a result of the higher density of cells within the condensate. In general, mesenchymal cells appeared to express negligible amounts of the activated protein. However, some cells did show immunofluorescence suggesting that these cells were expressing the activated Notch-1 protein. Of interest, immunoreactivity in the mesenchymal cells appeared polarised to one side of the labelled cells, suggesting activated Notch-1 was compartmentalised in the cell cytoplasm (Figure 5.11; A, white arrowhead). Due to a high level of staining observed in the negative (non-immune serum) control tissues we cannot draw conclusions from this study because of the lack of specific staining. When the concentration of antibody was reduced, however, the level of fluorescence detected was negligible. The Vectastain colorimetric method of immunohistochemistry was therefore used.

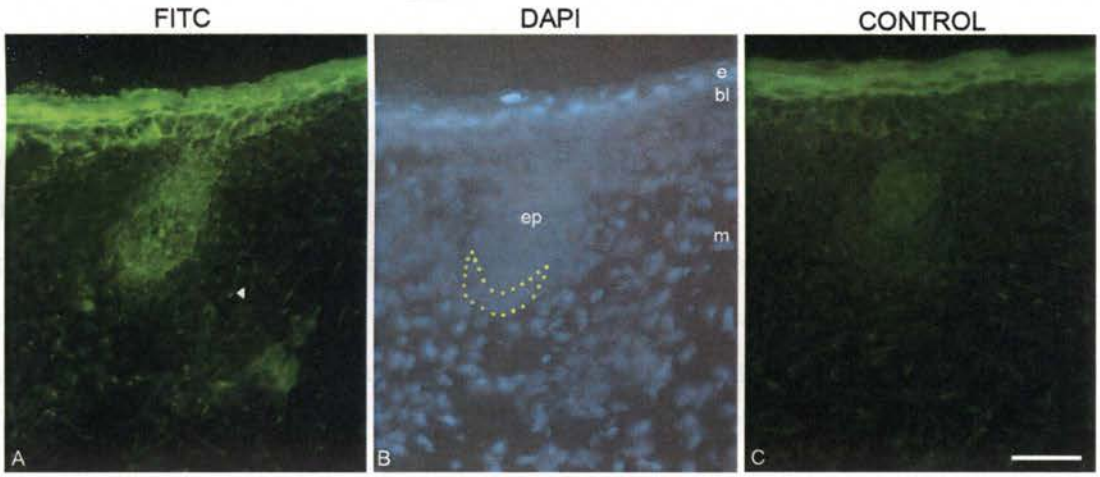

Figure 5.11: Activated Notch-1 protein expression in Merino skin sampled during primary follicle initiation (d 70). A; Immunofluorescence was strong in the epithelial components of the skin and developing follicle. Fluorescence was detected in the epidermis (e), basal layer (bl) and epithelial plug. Staining was detected in some cells of the mesenchyme (m) localised in areas of the cytoplasm in the mesenchymal cells (white arrowhead), and in the dermal condensate (outlined in yellow). B; Nuclei of section in A counterstained with DAPI. Control skin treated with normal rabbit serum also showed non-specific fluorescence (C). Images courtesy of Lisa Tomkins. Scale represents 30 µm.

The expression of activated Notch-1 protein was investigated further using the Vectastain methodology. The antibody was tested at working concentrations of 40 and 80 µg/ml. Protein was detected in the antibody-treated skin sections at both concentrations

(Figure 5.12). However, the skin treated with 80 µg/ml of antibody produced a more consistent staining pattern when the experiment was repeated.

Activated Notch-1 protein was detected most notably in a sub-population of cells in the mesenchyme. It was noted that protein expression appeared somewhat weaker in the uppermost layer of the mesenchyme, in those mesenchymal cells in closer proximity to the epidermis. Some protein was detected in the epithelial plug and dermal condensate. However, this staining could not be attributed to specific binding due to the similar staining seen in the controls. Staining was detected in the method control skin sections treated with normal rabbit serum at the same concentrations as the antibody. No stain was detected in the control sections that received no serum. This suggested that the rabbit serum was cross-reacting with the secondary antibody, producing non-specific staining. Unfortunately this problem could not be rectified.

Expression of activated Notch-1 protein was clearly detected in d 70 Merino skin counterstained with haematoxylin following immunohistochemistry using the Dako Envision™ System (Figure 5.13). The cells expressing the activated Notch-1 protein appeared brown-black in colour while those that were not expressing the protein appeared blue. Activated Notch-1 was detected throughout the epithelium, with the basal layer of the epithelium and epithelial plug staining particularly darkly. The mesenchyme contained cells that were expressing the protein and others that were not. A band of mesenchymal cells located directly below the epidermis did not express the activated Notch-1 protein. Below this layer of non-expressing cells, the mesenchymal cells displayed a differential level of activated Notch-1 expression. However, few cells were detected that did not express the protein. Immunoreactivity to the activated Notch-1 antibody was detected in few cells within the dermal condensate.

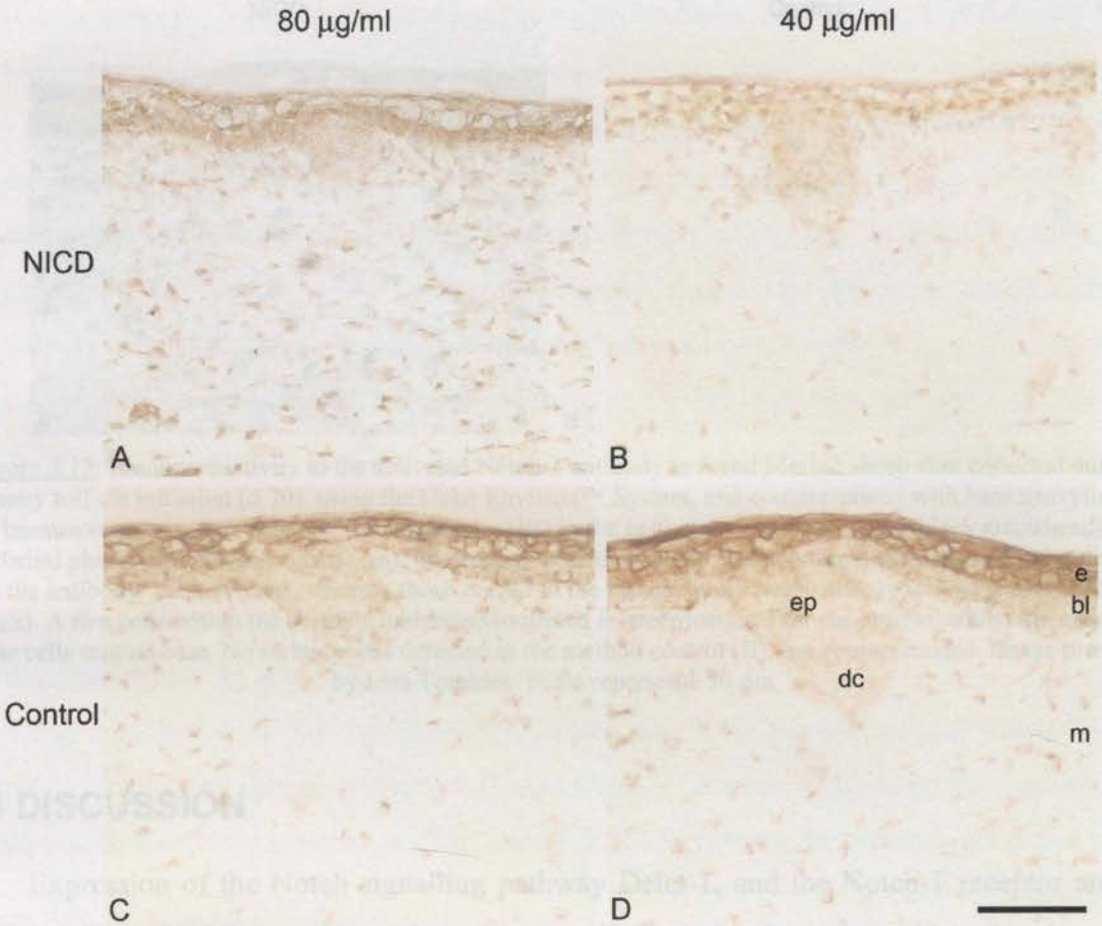

Figure 5.12: Immunoreactivity to the activated Notch-1 antibody in Merino skin sampled during primary follicle initiation (d 70), using the Vectastain method. Activated Notch-1 (NICD) antibody was tested at concentrations of 80 µg/ml (A) and 40 µg/ml (B). The higher concentration (A) gave a clearer, more consistent result. Immunoreactivity was detected in the epithelium (e), and was strongest in the basal layer (bl). However, the epithelial staining was inconclusive as similar staining was observed in the control tissue (C). Immunoreactivity in the mesenchyme (m) appeared weaker in the mesenchymal cells located beneath the epithelium, but was stronger in the deeper layers of the mesenchyme. Some protein was also visualised in the epithelial plug (ep) and dermal condensate (dc). Skin treated with the normal rabbit serum control also showed non-specific staining at 80 µg/ml (C) and 40 µg/ml (D). Strong staining was detected in the e and bl, and detected in the m, ep and dc. Scale represents 50 µm.

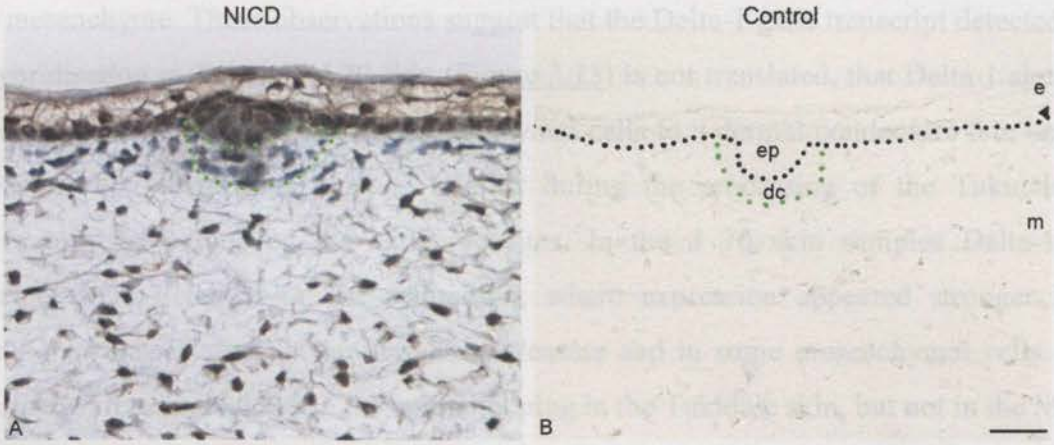

Figure 5.13: Immunoreactivity to the activated Notch-1 antibody in foetal Merino sheep skin collected during primary follicle initiation (d 70), using the Dako Envision™ System, and counterstained with haematoxylin. A; Immunoreactivity was detected (brown-black cells) in the epithelium (e), basal layer (black arrowhead), epithelial plug (ep) and mesenchyme (m). Mesenchymal cells below the epithelium did not appear to be stained with the antibody (stained blue), whereas those deeper in the mesenchyme were strongly stained for NICD (blue-black). A few cells within the dermal condensate (outlined in green) stained for the protein, whilst the majority of the cells stained blue. No staining was detected in the method control (B), not counterstained. Image provided by Lisa Tomkins. Scale represents 50 μm.

5.4 DISCUSSION

Expression of the Notch signalling pathway Delta-1, and the Notch-1 receptor and its activated form (NICD) were investigated in foetal sheep skin by immunohistochemistry. All results reported were reproduced a number of times. However, the inconsistency of staining in the d 56 and d 70 sections was believed to be a result of the antigenic sites within the tissue not being receptive to the antibodies. Unfortunately, this problem was not overcome.

Differences in Delta-1 expression were observed prior to and during follicle initiation in the Merino and Tukidale foetal skin. In the Merino skin at d 56, immunoreactivity to the Delta-1 antibody was observed in the epithelium, including the basal layer, and in nuclei of some mesenchymal cells. Whereas in Tukidale skin, negligible immunoreactivity was detected in the epithelium and only a few mesenchymal cells were immunoreactive, suggesting that lower levels of Delta-1 protein were expressed in the Tukidale foetal skin, compared to that in the Merino. In the d 70 Merino skin, Delta-1 protein appeared to be expressed in the epithelium including the basal layer, and higher levels of expression were apparent in the cells in the upper layer of the mesenchyme. Some immunofluorescence was also detected in the mesenchymal cells in the deeper regions of the mesenchyme, and in the dermal condensate. Delta-1 immunoreactivity was negligible in the epithelial plug. Immunoreactivity was negligible in sections of the Tukidale skin at d 70, suggesting that Delta-1 protein was not expressed in the Tukidale skin at d 70, except for a few cells scattered

in the mesenchyme. These observations suggest that the Delta-1 gene transcript detected by *in situ* hybridisation in Tukidale d 70 skin (Figure 3.13) is not translated, that Delta-1 signalling was no longer required to direct the mesenchymal cells to a dermal condensate fate once the condensates had formed, or that an artefact during the processing of the Tukidale skin samples may have blocked the antigenic sites. In the d 70 skin samples Delta-1 gene transcripts were detected in the epithelium, where expression appeared stronger in the interfollicular basal layer, in the dermal condensate and in some mesenchymal cells. Some transcripts were also detected in the epithelial plug in the Tukidale skin, but not in the Merino. Delta-1 protein expression appeared similar in adult skin of the Merino and Tukidale, where immunofluorescence was detected in the epidermis and dermis of the skin as well as in some cells of the outer root sheath of the wool follicles, thereby suggesting that Delta-1 had a similar role in adult sheep skin and follicles from sheep with markedly different wool follicle characteristics (refer to Appendices 2 and 3).

The localisation of Notch-1 protein appeared similar in the Merino and Tukidale skin sampled prior to and during primary follicle initiation. Protein expression corresponded to Notch-1 gene transcript expression (Section 4.3.3.2), suggesting the Notch-1 gene was being translated into the protein in the skin. In the d 56 samples, protein was detected in the epithelium, basal layer, and in scattered cells throughout the mesenchyme. In the d 70 samples, Notch-1 protein was detected in the epithelium, including the basal layer, epithelial plug, dermal condensate, and in the mesenchyme where higher levels of protein were observed in some cells. Interestingly, immunoreactivity to the Notch-1 antibody was stronger in the Tukidale than the Merino skin sampled on d 56 and d 70 of development, suggesting that there are higher levels of protein in the Tukidale skin. Notch-1 may play a greater role in wool follicle development in the Tukidale compared to the Merino (where Delta-1 appeared to be expressed to a greater extent). However, in the adult skin samples protein expression appeared to be increased in the Merino than Tukidale. These results highlight the possibility of a greater requirement for Notch-1 during follicle development in the Tukidale as a cell-sorting mechanism, and in the adult skin of the Merino where it may play a role in the maintenance of the wool follicle population.

Activated Notch-1 protein expression was investigated in Merino skin sampled during follicle initiation. Protein was detected in the epithelium, including the basal layer, the epithelial plug, the dermal condensate, and in some cells within the mesenchyme. Interestingly, expression of the activated receptor was not detected in a layer of mesenchymal cells located directly below the epidermis. Although non-specific staining was observed in the

controls treated with non-immune serum, the tissue was uniformly stained. Whereas, in the tissue treated with the antibody, differential staining was observed, with strong immunoreactivity in the lower layers of the mesenchyme, and weak to negligible immunoreactivity in the mesenchymal cells in the upper layers close to the epidermis.

The non-specific staining seen in the controls for the activated Notch-1 and to a lesser extent the Notch-1 immunohistochemistry experiments was not successfully eliminated from the tissue. Thereby, only tentative interpretations of these results could be made from these studies and this limited the conclusions that could be drawn.

Delta-1 and Notch-1 protein expression was detected throughout the epithelium prior to and during follicle initiation. Strong immunoreactivity to the antisera to Delta-1 and the Notch-1 receptor were detected in the basal layer of the epithelium on d 56 and d 70. This finding was in agreement with other research, and it has been suggested that this layer of cells is where the epithelial stem cells reside (Lowell *et al.*, 2000). In the d 70 samples, Notch-1 protein and its activated form were detected in the epithelial plug of the developing follicles. However, due to the staining similarities of the tissues treated with the non-immune serum (method control) and antibody, no conclusions could be made. Delta-1 protein was not detected in the epithelial plug, suggesting that Delta-1 protein was not involved in the development of the epithelial plug. If Notch-1 protein is expressed in this structure, it was assumed that another ligand, such as Jagged-1, may have been binding to the receptor within the plug (Gordon-Thomson *et al.*, 2008). Alternatively, reciprocal signalling and the interactions between the receptor and ligand (Jahoda *et al.*, 2001) may be orchestrated by Notch-1 cells and Delta-1 expressed in neighbouring epithelial plug and dermal condensate cells respectively: these interactions may play a role in the development of the wool follicle since Schmidt-Ulrich and Paus (2005) showed that communication between the dermal condensate and epithelial plug drives proliferation in both structures, shaping the dermal papilla and beginning the down-growth of the ectodermal placode.

Within the mesenchyme of foetal sheep skin, the cells expressing the Notch receptor and those expressing the Delta-1 ligand were most likely signalling to one another. On d 56, Delta-1 and Notch-1 protein appeared to be expressed in the mesenchymal cells. Lateral inhibition (Chitnis, 2006) may be a possible mechanism that specifies the dermal papilla cell population, with signalling of the Delta-1 or Notch-1 protein being upregulated in certain cells, which in turn signal to their surrounding cells instructing them not to take on the same (follicular) cell fate. In other systems, where cells express elevated levels of Delta-1 and Notch-1 it has been suggested that these cells bind to one another, either by Notch-Delta or

Delta-Delta interactions (Fehon *et al.*, 1990; Rebay *et al.*, 1991). This may also provide a mechanism prior to follicle initiation for creating cell-cell attachments that initiate the formation of dermal condensates. If these cells were clumping together to form the dermal condensates, as is visible in the d 70 samples, these attached cells would then migrate upwards through the mesenchyme, to form the condensates at regularly spaced intervals directly below the basement membrane. In the d 70 samples, Delta-1 expression appeared to be stronger below the basement membrane, suggesting that the ligand may be responsible for keeping the cells within the dermal condensate in close proximity to one another through inter-cellular interactions. As Delta-1 was also expressed in the condensates, the ligand may be involved in distinguishing these prepapilla cells from the rest of the mesenchymal cell population. Notch-1 protein appeared to be expressed in cells scattered throughout the mesenchyme as well as in the dermal condensate. Activated Notch protein was detected in cells scattered in the mesenchyme, below a distinct band where no active protein was detected, as well as in the dermal condensate. Interestingly, the localisation of activated Notch-1 protein expression appeared to be different to that of Delta in the mesenchyme, and the localisation of the activated form of the protein differed from that of the non-activated protein. Notch-1 may have a role in the preparation of cells to form the dermal condensate, but then be involved in maintaining cells as undifferentiated mesenchymal cells. From these studies, where Delta-1 and Notch-1 were shown to be upregulated in foetal sheep skin prior to follicle morphogenesis, and from earlier research (Moore *et al.*, 1998), it was believed that the cells in the dermal condensate most likely became committed to a follicle lineage prior to follicle initiation. In this study, we provide some evidence to suggest that the Delta-Notch interaction may be involved in the specification and the initial aggregation of this highly specialised cell population.

CHAPTER 6: BLOCKING THE NOTCH SIGNALLING PATHWAY *IN VITRO*

6.1 INTRODUCTION

Prior to the appearance of follicles, foetal skin consists of a thin epithelium overlying a mesenchyme. As the foetus develops, the epithelium becomes increasingly stratified and the mesenchyme more populated with mesenchymal cells. In the Merino, primary follicle development has been divided into different stages (refer to Section 1.6.1 and Figure 1.4) based on morphological criteria, beginning at around d 70 of gestation.

The extracellular matrix is comprised of collagens, glycoproteins, glycosaminoglycans and non-collagenous adhesion proteins. Different matricies contain different sets of these components. Together these matrix proteins contribute to the unique physical and biological characteristics of different tissues (Kleinman *et al.*, 1986). It is the complex interactions between these three main classes of macromolecules and cells that regulate cell movement, migration and aggregation (Moore and Moore, 2001). Various extracellular matrix compounds have been used in cell culture systems in an attempt to develop a model in which papilla cells aggregate *in vitro*.

The Notch signalling pathway is an evolutionarily conserved mechanism used for establishing differentiated cell populations within a vast array of organisms. Developing animals use Notch signalling to magnify and consolidate molecular differences between neighbouring cells, as discussed in Section 1.8.1. Differential expression is characterised by the interaction of Notch receptors and their ligands, such as Delta. Signalling does not require the intervention of secondary messenger pathways. Notch signals directly to the cell nucleus after activation by one of its ligands at the plasma membrane (Kopan, 2002). The molecules that influence the interaction between Notch and its ligands may be able to stimulate or inhibit Notch signalling depending on the pattern and level of ligand binding (Panin and Irvine, 1998). The ratio of Notch and Delta molecules on a cell is thought to be an important parameter in the Notch signalling system. For example, few Notch receptor molecules and an abundance of Delta ligand molecules would cause an over expression of Delta, by positive feedback, and would block the Notch receptors from signalling (Pourquié, 2000). Such interactions are thought to be non-productive (Chitnis, 2007).

The third cleavage of Notch is a constitutive intramembranous cleavage event, mediated by presenilin-dependent γ-secretase activity (Baron *et al.*, 2002). The γ-secretase enzyme complex is composed of presenilin, the transmembrane proteins nicastrin and anterior pharynx defective-1 (Aph-1) that stabilise the presenilin holoprotein, and presenilin enhancer-2 (Pen-2), a two-pass transmembrane protein that induces proteolysis of presenilin and maturation of the γ-secretase complex (Koo and Kopan, 2004; Bray, 2006). In mammals, Presenilin-1 and 2 are associated with a large complex of proteins that are responsible for the activity of γ-secretase. This complex cleaves the amyloid precursor protein within the transmembrane domain of the Notch receptor (Baron, 2003). New γ-secretase substrates and compounds interacting with presenilin have been identified, linking presenilin to a wide range of cellular processes, including signal transduction, cell adhesion, protein trafficking, tau phosphorylation and calcium regulation (Parks and Curtis, 2007).

It has been demonstrated that murine Delta-1 undergoes the same sequence of cleavages as Notch (Section 1.8.1.2.1), in an apparently signal-independent manner. It is thought that γ-secretase cleavage of Delta-1 depends on prior ectodomain shedding, making Delta-1 a substrate for regulated intramembrane proteolysis (Six *et al.*, 2003).

Previous research using γ-secretase inhibitors discovered that they effectively blocked the production of the Notch intracellular domain (NICD) in a variety of cell types, resulting in a range of effects. The γ-secretase inhibitor significantly blocked TNFα-induced synoviocyte proliferation in rheumatoid arthritis. Notch-1 was believed to be involved in TNFα-induced synoviocyte production (Nakazawa *et al.*, 2001). Treatment with the γ-secretase inhibitor has also been used to inactivate Notch signalling in retinal progenitors, leading to premature differentiation of stage-appropriate cell types. They discovered that 6 hr was the critical time for Notch inactivation to commit progenitors to differentiate in chick retinas, but that Notch activity was reduced after 3 hr of treatment (Nelson *et al.*, 2007). The Notch signalling pathway has also been found to be required to maintain the viability of the early murine melanoblast population. Apoptosis of melanoblasts in embryonic mouse skin (13.5 dpc) occurred after 24 hr of treatment with an inhibitor of Notch signalling, known as γ-secretase inhibitor IX or N-[N-(3,5-Difluorophenacetyl-L-alanyl)]-S-phenylglycine *t*-butyl ester (DAPT). Hair derived from the DAPT-treated skin was not pigmented and a complete absence of melanoblasts was revealed upon histological analysis. From this study, it appeared likely that Notch signalling was involved in inhibiting apoptosis (Pinnix and Herlyn, 2007).

Dermal papillae dissected from adult whisker follicles are widely used to study the behaviour of papilla cells *in vitro*. It is recognised that a major limitation of cell culture

experiments is the difficulty of establishing whether cells being grown *in vitro* behave and function in the same manner as their counterparts *in vivo* (Messenger *et al.*, 1986). However, the behaviour of early passage cells, their proliferative rates and responses to a range of growth factors in culture have shown that particular differentiated states are expressed *in vitro*, reflecting aspects of their functions in their natural environment *in vivo* (Pisansarakit *et al.*, 1991).

An *in vitro* model where dermal papilla cells isolated from vibrissae aggregated when cultured on Matrigel™-coated dishes was developed. Cell aggregation is a behaviour attributed to dermal papillae. Having an aggregating cell model enabled us to observe the behaviour of the papilla cells in culture and to investigate whether the Notch signalling pathway was involved in the formation of papilla cell aggregations. The role of Notch signalling during the aggreation of papilla cells was tested by treating the cell cultures with the γ-secretase inhibitor DAPT over a 30 day period. DAPT was employed to test the effect of blocking the third cleavage of the Notch receptor and preventing the activated form of the receptor from translocating the Notch signal from the cell surface to the nucleus.

The next step was to investigate whether the process of follicle formation, during foetal development, could be manipulated by treatment with DAPT. The Notch signalling pathway was studied in organ culture since the option of treating foetuses *in utero* was achievable but presented difficulties with surgery, interpretation of results and animal ethics.

Studies using skin cultures have been reported in the past (Paus *et al.*, 1999; Stenn and Paus, 2001). In these studies, small pieces of freshly harvested skin were placed on top of collagen-coated polycarbonate membranes and transferred to tissue culture dishes containing culture medium (DMEM + 10% FBS) and cultured for 4 days. Studies investigating whether treatment with DAPT affected the number of follicles were performed on foetal Tukidale and Merino skin. The numbers of follicles in the skin samples were counted on day 0 (prior to being placed on the membranes) and day 4 (following removal from the membranes). The effect of DAPT treatment on follicle diameter in Merino skin harvested on d 70 of foetal development was also investigated.

The expression patterns of the Notch-1 receptor and Delta-1 transcripts in foetal skin organ cultures, and the presence of Delta-1 protein expression in dermal papilla cell cultures are reported in this chapter.

6.2 MATERIALS AND METHODS

6.2.1 GENERAL TISSUE CULTURE

All tissue culture work was conducted aseptically within a biohazard hood (Ultima 120, Class II. Clyde-Apac, SA, Australia), unless otherwise stated. The hood was irradiated with ultraviolet light for 10 min and wiped out with 70% ethanol using gauze swabs (BSN Medical Australia Pty Ltd, Mount Waverley, VIC, Australia) before and after use.

A carbon dioxide incubator with SafeCell™ (MCO-20AIC, Sanyo North America Corp, Ontario, Canada) was sterilised with hot water and Rocca II 10% disinfectant (National Laboratories L&F products, NJ, USA) followed by wiping all surfaces with 70% ethanol before each experiment. The water tray was filled with sterile tap water and the incubator was set at 37°C with 5% carbon dioxide (Coregas Pty Ltd, Yennora, NSW, Australia) injection.

All solutions added to the cultured cells and skin biopsies were preheated to 37°C within a water bath (WB14; Ratek Instruments Pty Ltd, Boronia, VIC, Australia). Solutions were measured and dispensed using a BioMate Finnipipette® (Thermo Electron Corp). Any solutions added to the cells were filter sterilised using a 20 ml syringe attached to an Acrodisc® 0.22 µm syringe filter (Pall Life Sciences, Surry Hills, NSW, Australia) before use. All waste solutions were treated with Kerr Cavicide® (Bacto Laboratories Pty Ltd, Liverpool, NSW, Australia) overnight before disposal.

All cells and explants were cultured in Dulbecco's modified Eagles medium (DMEM) (MultiCel™; Thermo Electron Corp) with 10% foetal bovine serum (FBS; JRH Biosciences, a CSL Company, KS, USA) [heat inactivated at 60°C for 1 hr], 23mM Hepes buffer (MultiCel™), 10mM $NaHCO_3$ and 2% Penicillin/Streptomycin (MultiCel™) added. The culture medium (pH 7.4) was filter sterilised within a biohazard hood (BH2000; Gelman Sceinces, MI, USA) using a Nalgene® bottle-top filter (75 mm, 500 ml; ©Nalge Nunc International Corp, NY, USA) screwed on to a Schott bottle using a HydroTech vacuum pump (BioRad Laboratories Inc) and will be referred to hereafter as DMEM with 10% FBS.

6.2.1.1 Examining and photographing cell and skin cultures

Cultures were examined and images captured using phase contrast optics on an inverted microscope (TMS-F, Nikon Corp), connected to a camera (DS-L1, Nikon Digital Sight), and live imaging screen (C-0.6x; Nikon Corp).

6.2.2 DERMAL PAPILLA AND DERMAL FIBROBLAST CULTURES

6.2.2.1 Collection of dermal papillae and dermal fibroblasts

Skin was harvested from ewes euthanased (Section 2.2.3.3.2) for the experiments described in Chapters 3 and 4. The lips were wiped with 70% ethanol and a 3 × 1 cm section of the labium superius oris excised using a sterile scalpel blade (size 24; Swann-Morton®) and forceps. This area was used as a higher density of anagen follicles were collected from this site at an earlier time. The tissue was placed into a 70 ml specimen jar (Techno-Plas Pty Ltd) containing sterile Dulbecco's phosphate buffered saline (D-PBS: [2.67mM KCl; 1.47mM KH_2PO_4; 137.93mM NaCl; 8.1mM Na_2HPO_4] Multicel™; Thermo Electron Corp), and stored at 4°C.

Whisker follicles were isolated with the aid of a stereomicroscope, set up in a laminar flow hood under aseptic conditions (Cohen, 1965; Messenger, 1984; Pisansarakit and Moore, 1986; Inamatsu *et al.*, 1998). The lip tissue was washed in D-PBS to remove residual blood and transferred to a glass plate. The orientation of the whisker follicles was determined and individual follicles were isolated using a scalpel (Figure 6.1; A). The whisker capsules were then removed from the surrounding tissue using a scalpel and Watchmaker's forceps (Figure 6.1; B). Follicles that appeared to be in anagen were transferred to a fresh dish containing D-PBS with 10% Penicillin/Streptomycin (5000 IU/ml; Multicel™) and stored at 4°C overnight.

Individual capsules were placed on a glass plate and immersed in a drop of D-PBS. Using two pairs of Watchmaker forceps, the capsule was held firmly near the fibre and pierced with the lower tine of the second pair of forceps, halfway down the length of the capsule, releasing the blood. The bottom half of the capsule was then pulled away, exposing the rounded base of the follicle (Figure 6.1; C). The follicle was entirely freed of its surrounding capsule, then placed on a fresh glass plate in a drop of D-PBS containing 10% Penicillin/Streptomycin. The cutting edge of a 30 G insulin needle (Becton Dickinson and Co, NJ, USA) was used to slice the bulb of the follicle open at an obtuse angle to the follicle, releasing the dermal papilla (Figure 6.1; D). Any cells adhering to the base of the papilla were gently removed using the needle. The tip of the needle was used as a spoon to transfer the papilla to a 35 mm tissue culture dish (Cellstar) containing 3 ml DMEM with 10% FBS.

Rat whisker dermal papillae were collected and cultured using similar procedures. Dermal fibroblasts were collected from the interfollicular space. The dermal fibroblasts were amplified in culture using the same procedures as for the dermal papillae.

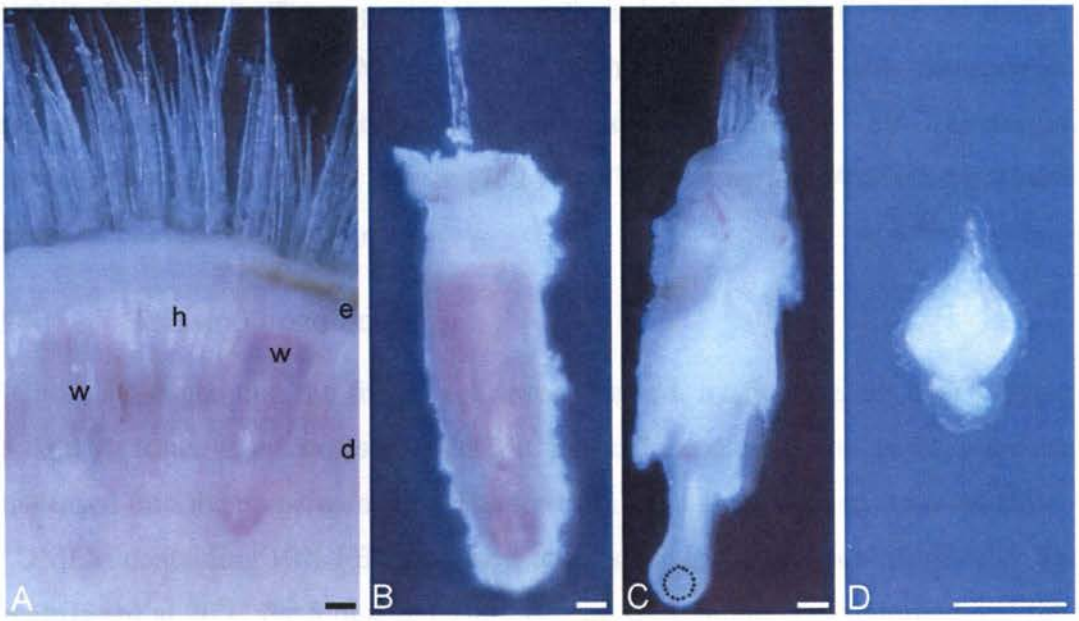

Figure 6.1: Steps followed in harvesting dermal papillae from ovine lip tissue. A; whisker capsules (w) within the tissue. Hair follicles (h), epidermis (e) and dermis (d) were visible. B; an isolated blood-filled capsule. C; capsule removed and base of follicle exposed with the dermal papilla visible (outlined). D; an isolated dermal papilla. Scale bars represent 250 μm.

6.2.2.2 Culturing dermal papillae and dermal fibroblasts

Five or six papillae were placed in each culture dish, and anchored to the base with the aid of the dissection needle. Pieces of dermal tissue were treated in the same manner. The dish was then placed into the incubator and the explants were incubated for 7 d without being disturbed. After 7 d the medium was replaced, and every 3 d thereafter. The dishes were examined under an inverted microscope (TMS-F, Nikon Corp) for cells growing out from the explants.

6.2.2.3 Trypsinising and freezing down cell cultures

Approximately 21 d after harvest, the cells growing from the explants appeared confluent. The media was aspirated from the dishes before 1 ml of trypsin solution [0.02% ethylenediamenetetra-acetic acid, dihydrate; 0.1% glucose; 0.04% KCl; 0.8% NaCl; 0.58% sodium bicarbonate; 0.1% trypsin] was added to each dish, for 3 min. The solution was then aspirated from each dish, and replaced with a further 2 ml trypsin and the cultures examined for detached cells. The cultures were incubated for a total of 3 min in trypsin, by which time the cells appeared as small, round, floating bodies. The cells from each dish were aspirated and deposited in 2 ml DMEM with 10% FBS. An additional 1 ml of media was added, picking up any remaining cells. The suspension was centrifuged at 20°C for 5 min, at 1,200

×*g* (5804R; Eppendorf). The supernatant was discarded and 2 ml of freezing media [20% FBS; 20% glycerol; 60% DMEM] was added to the pellet and the cells resuspended. The suspension was dispensed into two 1 ml cryogenic vials, stored at –80°C overnight, then transferred to a liquid nitrogen Dewar (750-RS; Taylor-Wharton, AL, USA). These were designated as Passage (P) 0 cultures.

6.2.2.4 Thawing frozen cells

Cryovials containing the frozen cells were thawed, by floating, on a 37°C water bath (Ratek WB14; Ratek Instruments Pty Ltd, VIC). The thawed cells, now in P1, were aspirated and dispensed into the prepared media. The freezing media was washed from the cells with 5 ml of DMEM containing 10% FBS, and filter sterilised into a 50 ml centrifuge tube. The tube was centrifuged at 20°C for 5 min at 1,200 ×*g*. The supernatant was discarded and the pellet resuspended in 1 ml of media. Medium (5ml aliquots composed of DMEM, FBS and 10 µg/ml FGF-2 [basic, human]) was dispensed into eight (60 mm) tissue culture dishes. Into the middle of each dish, 125 µl of the cell suspension was dispensed and the dishes swirled to ensure an even coverage of cells. Each dish was assessed for the presence of cells and incubated overnight.

6.2.2.5 Feeding cell cultures

The following day (d 1), the dishes were examined and photographed using a TV-lens (C-0.6x, Nikon Corp) connected to the inverted microscope and screen (DS-L1, Nikon Digital Sight). The cells were fed on d 3, 6, and 8 with 5 ml DMEM containing 10% FBS and 10 µg/ml of FGF-2. The dishes were returned to the incubator. On d 10, the cultures appeared confluent. The cells were trypsinised and seeded into new dishes (as P2) or frozen.

6.2.3 INVESTIGATING THE EFFECT OF EXTRACELLULAR MATRIX ON THE BEHAVIOUR OF DERMAL PAPILLA AND DERMAL FIBROBLAST CELLS

The effect of extracellular matrix material on the behaviour of rat dermal papilla and fibroblast cells, at P4, was studied. Collagen S (Roche Diagnostics) and BD Matrigel™ Matrix Basement Membrane (BD Biosciences, MA, USA) were tested. Collagen S, sourced from calf skin, contained collagen types I, II and III. Matrigel™, sourced from mouse sarcoma, is a solubilized tissue basement membrane containing; laminin, collagen type IV, heparan sulphate proteoglycan and entactin.

To coat dishes with Collagen S, 12 µl of solution was pipetted in a line down the middle of a 35 mm tissue culture dish, and spread over half the dish using a disposable cell scraper (Greiner Bio-one). The dishes were left to dry in the laminar flow hood for 1 hr.

The Matrigel™-treated dishes and equipment were chilled to 4°C before 25 µl of solution was pipetted in a line down the middle of the 35 mm tissue culture dish and spread over half the dish using a cell scraper. The Matrigel™ in the dishes was left to set for 15 min at room temperature.

Within each dish 2 ml of DMEM with 10% FBS was dispensed, before the dishes were stored in the incubator. The papilla and fibroblast cell cultures were trypsinised (Section 6.6.2.3) and a cell suspension of ~1 x 10^5 cells (determined using a haemocytometer) was added to each dish and cultured for 15 d. Fresh medium was administered every second day.

6.2.4 BLOCKING THE NOTCH SIGNALLING PATHWAY IN VITRO

To block Notch signalling and investigate the role of the Notch signalling pathway in dermal papilla cell aggregation and follicle formation in foetal sheep skin, the γ-secretase inhibitor IX or DAPT ($C_{23}H_{26}F_2N_2O_4$; Calbiochem®, a brand of EMD BioSciences Inc, CA, USA) was utilised (Figure 6.2).

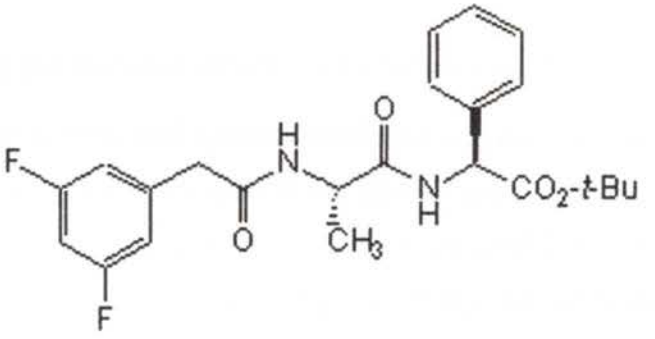

Figure 6.2: Structure of the cell permeable dipeptide inhibitor of γ-secretase, DAPT. DAPT specifically targets the C-terminal fragment of presenilin and is a γ-secretase specific inhibitor (Morohashi *et al.*, 2006). Image from product specification sheet, Calbiochem®.

Dovey *et al.* (2001) characterised DAPT and found it to be a highly specific γ-secretase inhibitor. Timmerman *et al.* (2004) found DAPT to have a dose-dependent negative effect on the number of transformed mesenchymal cells when 10µM and 50µM DAPT was administered to embryonic mouse explants. In this study, we tested DAPT at 25µM, 50µM and 100µM. The optimum concentration of 50µM was chosen for the experimental studies.

Three experimental groups were set up within each trial: untreated controls received DMEM with 10% FBS; functional controls received 0.1% dimethyl sulphoxide (DMSO) (Hybri-Max®; Sigma Aldrich Inc) in DMEM with 10% FBS; the treated cultures received DMEM with 10% FBS and 50μM DAPT (stock solution dissolved for a final concentration of 0.1% DMSO). For each trial, equal numbers of replicates (n=15) were included for each treatment group.

6.2.5 SETTING UP THE DERMAL PAPILLA NOTCH PATHWAY INHIBITOR TRIALS

6.2.5.1 Coating Dishes with Matrigel™

The dishes were coated with Matrigel™ as described in Section 6.2.3. To coat the entire base of the 60 mm tissue culture dish, 50 μl of Matrigel™ was used to coat each half of the tissue culture dish.

6.2.5.2 Preparing dermal papilla cells for the trials

The cell cultures were fed as described in Section 6.2.2.5 before they were trypsinised (Section 6.2.2.3). Approximately 1×10^5 of the dermal papilla cell suspension in passage 2 (P2) was seeded into each Matrigel™-coated dish for these studies.

6.2.5.3 Testing the effect of DAPT on dermal papilla cells

Sterile DMEM with 10% FBS (growth medium) was made up as described in Section 6.2.4. For each treatment group (untreated, 0.1% DMSO and 50μM DAPT), growth medium was dispensed into a 50 ml centrifuge tube to which the DAPT or DMSO was added. The cultures were replenished with growth media containing the treatments freshly prepared, every second or third day until d 28. The cultures were routinely examined and photographed over this period.

6.2.5.4 Quantifying the effects of DAPT on dermal papilla cells

To facilitate counting of the condensations of cells and aggregates in the sheep whisker dermal papilla cell cultures, the cultures were fixed with 2% paraformaldehyde in 1x PBS for 20 min. The fixative was discarded and the cells washed thrice with 5 ml of 1x PBS for 5 min.

The cells were stained for 5 min using Dako® Nuclear Fast Red (Kernechtrot) histological staining reagent (Dako Cytomation). The stain was aspirated and the cells washed twice in 5 ml Milli-Q water for 5 min and dried within the fume hood for 1 hr.

6.2.5.5 Counting structures within the fixed dermal papilla cultures

To eliminate bias when counting structures, random number tables were generated in Microsoft Office Excel 2003. Each dish was allocated a random number, concealing the treatment group until the dishes were examined and structures counted.

The stained cell cultures were observed under a Leica WILD M420 stereomicroscope (Leica Microsystems GmbH). The dishes were systematically scanned for the presence of cell aggregations and concentrated groups of cells. The cell aggregations were defined as a multi-layered, rounded ball of cells where a clear outline of the boundary of the aggregation was visualised due to cytoplasmic projections of the involved cells wrapping around the other cells. These structures stained dark in comparison to the other cells and concentrated groups. The concentrated groups were defined as single or multi-layered areas of cells in which the cells appeared very tightly packed together. However, they did not have a clear border. These areas were recognised as areas of cells that stained darker than the surrounding monolayer of cells. The numbers of these structures were recorded in an Excel spreadsheet. Images of the cells were taken using the Leica compound microscope under brightfield optics and a SPOT camera as described in Section 2.2.7.

6.2.5.6 Delta-1 protein expression in rat dermal papilla cultures

The localisation of Delta-1 protein was investigated in aggregating and non-aggregating rat dermal papilla cell cultures with immunocytochemistry using a goat polyclonal antibody to Delta-1, as described in Section 2.2.9.1. The secondary antibody used was anti-rabbit IgG conjugated to Alexafluor-488 (Molecular Probes, Invitrogen Australia Pty Ltd, Mount Waverley, VIC, Australia) at 10 µg/ml diluted in PBS with 0.1% BSA. Immunofluorescence was observed with a Leica fluorescence DMRBE Microscope using a green filter for FITC fluorescence (Section 2.2.7).

6.2.6 SKIN CULTURE STUDIES

Preparation of Merino and Tukidale animals for these studies included oestrus synchronisation and mating procedures as described in Sections 2.2.2. Euthanasia was carried out as described in Section 2.2.3.3.2.

6.2.6.1 Harvesting foetal sheep skin

The foetus was aseptically removed from the exteriorised uterus before skin (20 × 25mm) was collected from anterior, midside and posterior sites. Anterior samples were

excised from the shoulder region, ventral to the top of the shoulder and anterior to the foreflank. Midside samples were excised posterior to the foreflank, dorsal to the belly region and anterior to the last rib. Posterior skin samples were excised from the rump region, posterior to the rear flank, anterior to the dock and dorsal to the stifle.

The skins were placed within labelled 70 ml specimen jars containing D-PBS and stored at 4°C. Crown-rump length and weight measurements were taken for each foetus and recorded as described in Section 2.2.3.3.2.1.

6.2.6.2 Setting up the floating skin culture system

Within the biohazard hood, 8.0 μm, 19 × 42 mm membranes (GE Osmonics Inc, MN, USA) were prepared. The membranes were cut in half and individually soaked in 1 ml of 1 mg/ml collagen (type 1; from calf skin, Sigma Cell Culture) within a 35 mm tissue culture dish for 1 min, then air-dried for 10 min. In a separate 35 mm tissue culture dish, 2 ml of DMEM with 10% FBS was dispensed. Each membrane was placed on the surface of the growth medium in the dish, with the shiny side down, so that it floated and the upper surface remained dry. The dishes were stored within the incubator until required.

The skin samples were individually transferred with Watchmaker forceps, to a sterile glass plate within a 90 mm bacteriological dish containing ~5 ml of D-PBS. Muscle adhering to the dermis was removed and the sample cut into ~25 × 2 mm strips with a scalpel along its dorsoventral axis. Long, thin pieces of skin appeared to curl off their membranes at a slower rate compared to short, wide pieces. If the epidermis and dermis were detached, the strip was discarded.

Each strip of skin was transferred to a fresh dish, dermis uppermost, and a drop of D-PBS was added. An overlapping sequence of photographs of the strip was captured using a digital camera attached to an inverted microscope (Section 6.2.1.1).

The skin was transferred to the floating membrane, with the dermis in contact with the membrane, as illustrated in Figure 6.3. It was important that the uppermost surface of the membrane remained dry.

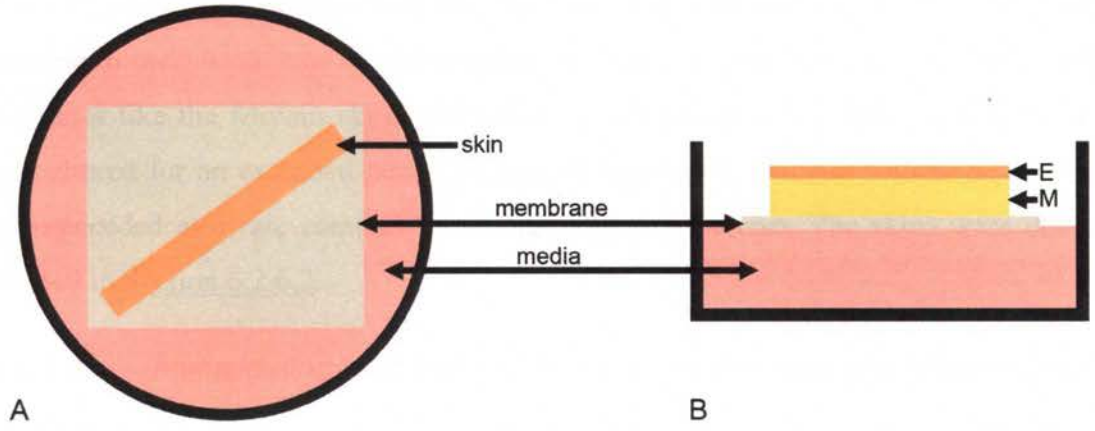

Figure 6.3: Schematic of the floating foetal skin culture system used for the trials. A; the skin was positioned diagonally across the middle of the collagen-coated membrane, floating on the media within the tissue culture dish. B; the skin was placed with the epithelium (E) uppermost and the mesenchyme (M) in contact with the membrane.

The growth medium was changed every 24 hr on the first 3 days (d 1-3) of the trial, unless otherwise specified. Care was taken to ensure the upper surface of the membrane remained dry.

On d 4, fine needles were used to detach the skins from their membranes. To do this, the needles were used to sink the membrane before gently sliding one needle under the skin and lifting it away from the membrane. The skins were transferred to a dry tissue culture dish, with the dermis uppermost and images of the skin recorded photographically as described in Section 6.2.1.1.

The skins were fixed in 4% paraformaldehyde in PBS for 4 hr at 4°C and processed into wax using the method described in Section 2.2.4.1.

6.2.6.3 Investigating the effect of DAPT on follicle development

To investigate the effect of blocking the Notch signalling pathway on follicle formation in foetal sheep skin, three treatment groups (untreated, 0.1% DMSO and 50μM DAPT) were set up within each trial (Section 6.2.4). The media was changed and the skins were treated every 24 hr on d 1-3 of the trials.

6.2.6.4 Trials conducted using the floating skin culture model

6.2.6.4.1 Pilot studies

Midside flank skin was collected from 3 Merino foetuses and 3 Tukidale foetuses on d 56 of development. Two pieces of skin were cultured from each foetus. The Merino skins

were cultured for 10 d and the Tukidale skins for 21 d. The skins were cultured for different times due to their behaviour on the membranes. The Tukidale skins had not curled off their membranes like the Merino skins and follicle development was evident so that those skins were cultured for an extended period of time to investigate whether follicle development *in vitro* proceeded at a rate comparable to that occurring *in vivo*. The skins were cultured as described in Section 6.2.6.2.

6.2.6.4.2 *Investigating follicle development in frozen-thawed and fresh skins*

Midside skin flank samples from d 70 Tukidale animals were collected. The 3 samples were sliced into 5 × 3 mm strips before freezing in freezing media [20% FBS; 20% glycerol; 60% DMEM] within 1 ml cryogenic vials, stored at –80°C overnight, then transferred to a liquid nitrogen Dewar.

The skin strips were thawed rapidly by floating the cryovials containing the skins on a 37°C water bath before working under aseptical conditions in a laminar flow hood. The skins were quickly processed through five washes in 5 ml of DMEM. Each tube was gently swirled before the media was aspirated and the skins transferred to the next wash, minimising the time they were exposed to glycerol. The contents of the final wash were tipped into a (60 mm) tissue culture dish.

6.2.6.4.3 *Investigating the effect of DAPT on follicle development*

The effect of DAPT on follicle development was investigated *in vitro* in 3 separate experiments using the culture system described in Section 6.2.6.2, following the treatment procedure described in Section 6.2.6.3:

i. Midside d 70 skin from 6 Tukidale foetuses (n=6).

ii. Skin was collected from anterior, midside and posterior sites on d 70 of gestation, from 4 Merino foetuses. From each foetus, 6 skins were included in each treatment group (n = 24).

iii. Merino skin samples were collected from the anterior, midside and posterior regions on d 54 (2 foetuses), d 63 (2 foetuses) and d 84 (1 foetus). From the d 54 samples, 3 skins from each foetus were included in each treatment group (n=6). From the d 63 skins, 6 samples were included from each foetus in each treatment group (n=12). From the d 84 skins, 6 samples were included in each treatment group (n=6).

6.2.7 INVESTIGATING CHANGES IN FOLLICLE NUMBER OVER THE TRIAL PERIOD

Serial photographs of the skins captured on d 0 and d 4 of the trials were assembled into complete images using Adobe Photoshop. Follicle numbers were recorded within five areas (Ø 1,250 μm) using the Cell Counter Plugin in ImageJ. The area of each skin was measured, on d 0 and d 4, to permit calculation of the degree of shrinkage.

The data from the DAPT trials were analysed with Genstat, using Linear Mixed Models.

6.2.8 INVESTIGATIONS INTO NOTCH-1 TRANSCRIPT AND DELTA-1 PROTEIN EXPRESSION IN THE CULTURED SKINS

The paraffin-embedded skins were sectioned as described in Section 2.2.5.1, before *in situ* hybridisation experiments using the Notch-1 cDNA probe (Section 2.2.8 and Section 4.2.2.4) and immunohistochemistry experiments (Section 2.2.9) using the anti-Delta-1 antibody were conducted.

6.3. RESULTS

6.3.1 DEVELOPMENT OF AN AGGREGATING CELL MODEL

Dermal papilla cells cultured on Matrigel™ formed papilla-like aggregations irrespective of whether the cells originated from rat or sheep (Tukidale or Merino) whiskers (Figure 6.4). Papilla cultures grown on Collagen S and uncoated tissue culture dishes did not form aggregations. Cultured fibroblasts did not aggregate in our experiments. Therefore, the experimental trials were conducted with dermal papilla cells grown on Matrigel™.

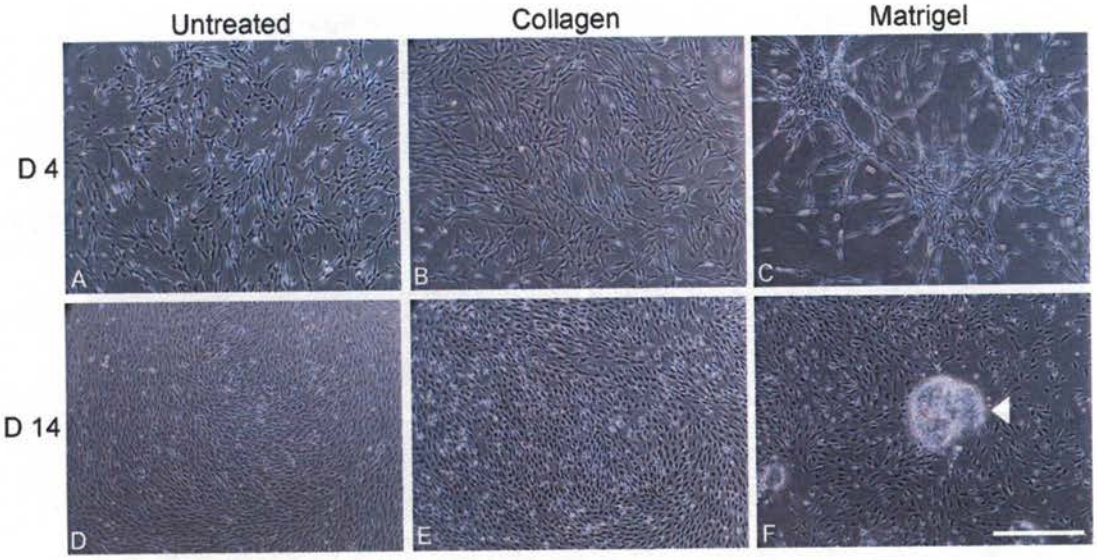

Figure 6.4: Rat dermal papilla cells grown on uncoated tissue culture dishes, Collagen or Matrigel™ for 14 d. Cells grown on uncoated tissue culture dishes became confluent but did not aggregate (A, D). Cells grown on Collagen S did not aggregate (B, E). Cells grown on Matrigel™ grew in star-like formations by d 4 (C) and formed aggregations (white arrowhead) by d 14 (F). Scale represents 50 µm. Photos courtesy of Lisa Tomkins.

6.3.2 DELTA-1 PROTEIN EXPRESSION IN RAT DERMAL PAPILLA CELL CULTURES

Immunocytochemical studies on rat papilla cultures showed that Delta-1 protein expression was concentrated in the cells that formed dermal papilla-like aggregations (Figure 6.5; A). Non-aggregating, but confluent cells in adjacent areas of the culture dish contained fewer stained cells (Figure 6.5; B) expressing lower levels of the protein. These results suggested Delta-1 was involved in the aggregative process.

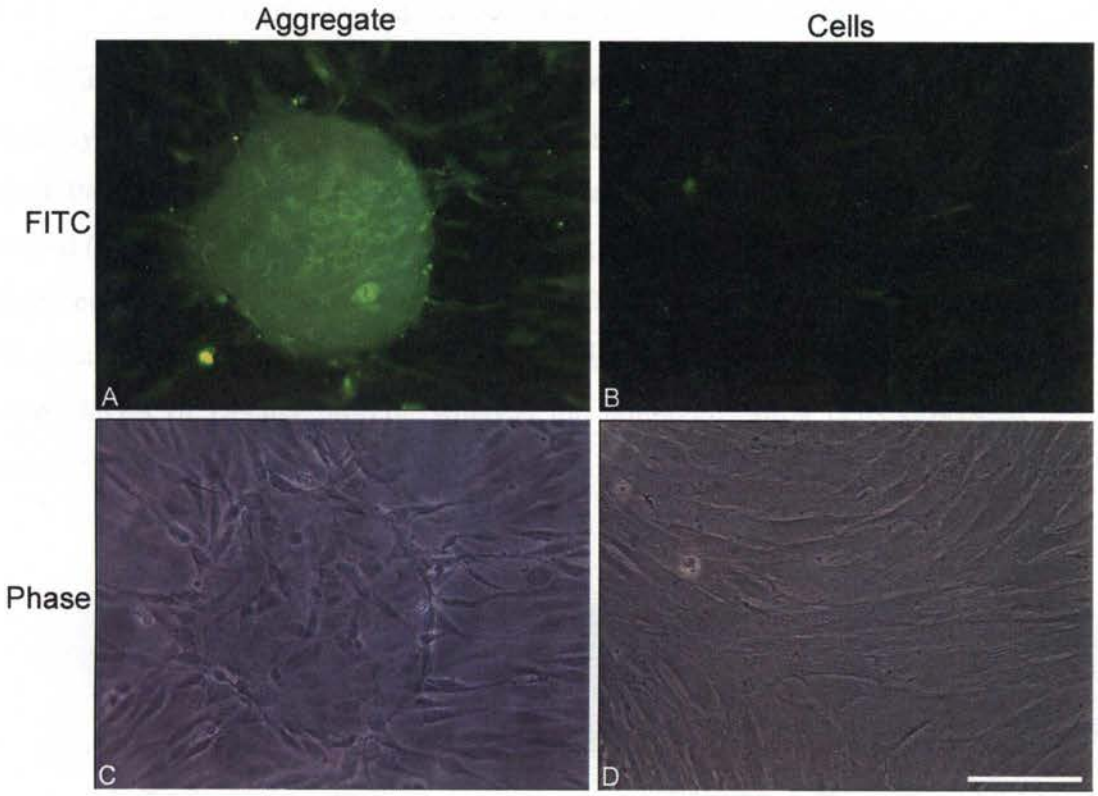

Figure 6.5: Rat dermal papilla cell cultures following treatment with Delta-1 antiserum. A; aggregations and surrounding cells showed strong anti-Delta-like-1 (FITC) fluorescence. B; non-aggregated, confluent areas of the culture dish contained fewer stained cells with lower levels of immunoreactivity. C and D; Phase contrast images of the same fields of view. Scale represents 100 μm. Cultures provided by Lisa Tomkins.

6.3.3 THE EFFECT OF DAPT ON RAT DERMAL PAPILLA CULTURES

Initially, DAPT was tested at concentrations of 25, 50, and 100μM on rat dermal papilla cultures grown on Matrigel™ to observe its effect on cell aggregation over a 30 d period. Untreated and 0.1% DMSO control cultures formed numerous aggregations (Figure 6.6; D and E respectively). The cells that received 25μM DAPT appeared to grow in a disorganised manner (not shown) compared to the untreated controls, and appeared to have a larger cytoplasm. A few aggregation-like structures did form in areas where the cells were highly condensed. Cultures that received 50μM DAPT (Figure 6.6; F) appeared to grow in a disorganised manner. These cells grew at a higher density than the 25μM cultures, with the individual cells appearing smaller. No aggregations were identified. The cultures that received 100μM DAPT grew in a similar manner to the other DAPT-treated cultures, with no aggregations observed (not shown). Some crystal-like structures were observed at this concentration. A higher rate of cell mortality was seen in these cultures, possibly indicating that treatment with DAPT at high concentrations was toxic for the cells.

6.3.3.1 Delta-1 protein expression in DAPT-treated cultures

To investigate whether blocking aggregation affected the expression of Delta-1 protein, immunocytochemistry was performed on fixed rat dermal papilla cultures from the DAPT trial. Delta-1 fluorescence was strongly expressed in the cellular aggregations found in the untreated (Figure 6.6; A) and DMSO (Figure 6.6; B) control groups, but was negligible in the non-aggregating cells in these dishes and in the DAPT-treated cultures (Figure 6.6; C). These findings are in accordance with earlier results (Figure 6.5) where aggregating cells expressed elevated levels of Delta-1 protein, whereas the non-aggregating cells expressed negligible amounts.

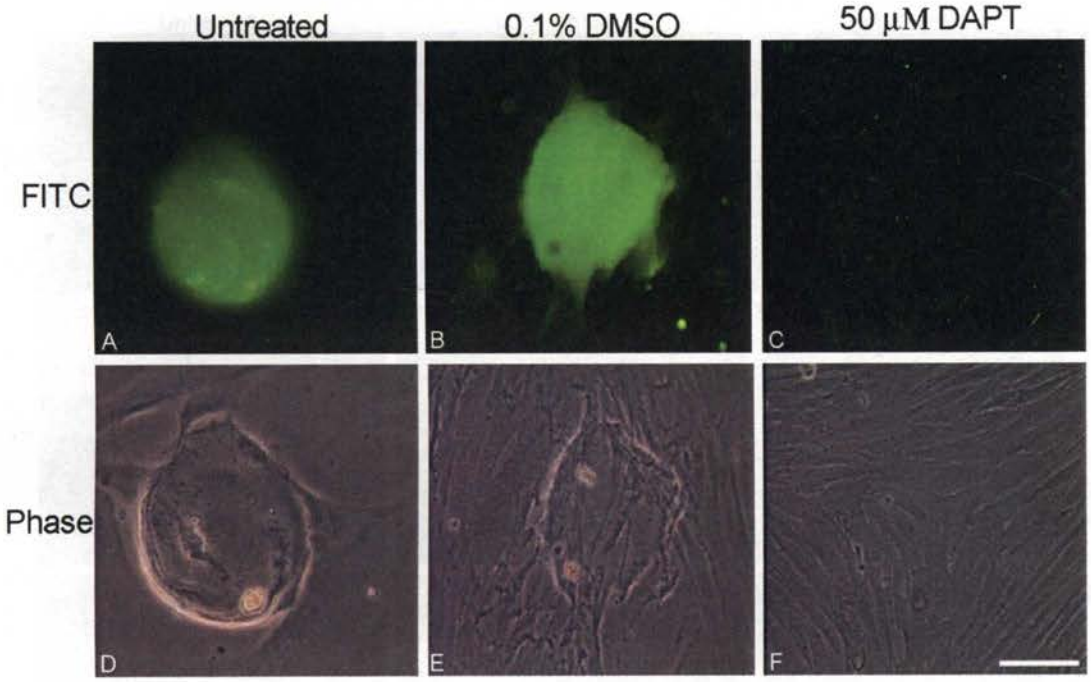

Figure 6.6: A preliminary DAPT trial was performed on rat dermal papilla cells and cells probed for Delta-1 expression. The untreated (A) and 0.1% DMSO control (B) cultures formed numerous aggregations, which strongly expressed Delta-1 protein. No aggregations formed in the 50µM DAPT-treated cultures, and a low level of Delta-1 protein was detected in these cells (C). Phase contrast D, E, F. Scale represents 100 µm. Cultures kindly provided by Lisa Tomkins.

6.3.4 THE EFFECT OF DAPT ON SHEEP DERMAL PAPILLA CULTURES

A trial utilising DAPT was conducted using papilla cell cultures isolated from Tukidale whiskers, cultured for 31 d. In this trial, 9 dishes were seeded with P2 cells so that each treatment group (untreated, 0.1% DMSO and 50µM DAPT) contained 3 replicates. The results were similar to those obtained with the rat cultures, with DAPT blocking cell

aggregation. DMSO did not appear to inhibit cell aggregation, compared to the untreated cultures (data not shown).

Two large-scale trials were set up using papilla cells isolated from Merino vibrissae. For each trial, P2 cells were seeded into 15 dishes for each treatment group (untreated, 0.1% DMSO and 50μM DAPT), each with 5 replicates. These cultures were treated and observed over a period of 31 d. The untreated (Figure 6.7; A, D, G) and DMSO (Figure 6.7; B, E, H) cultures produced a number of cellular aggregations over the trial period. The cultures that received DAPT (Figure 6.7; C, F, I) grew in a similar manner to the other two treatment groups, yet no aggregations formed.

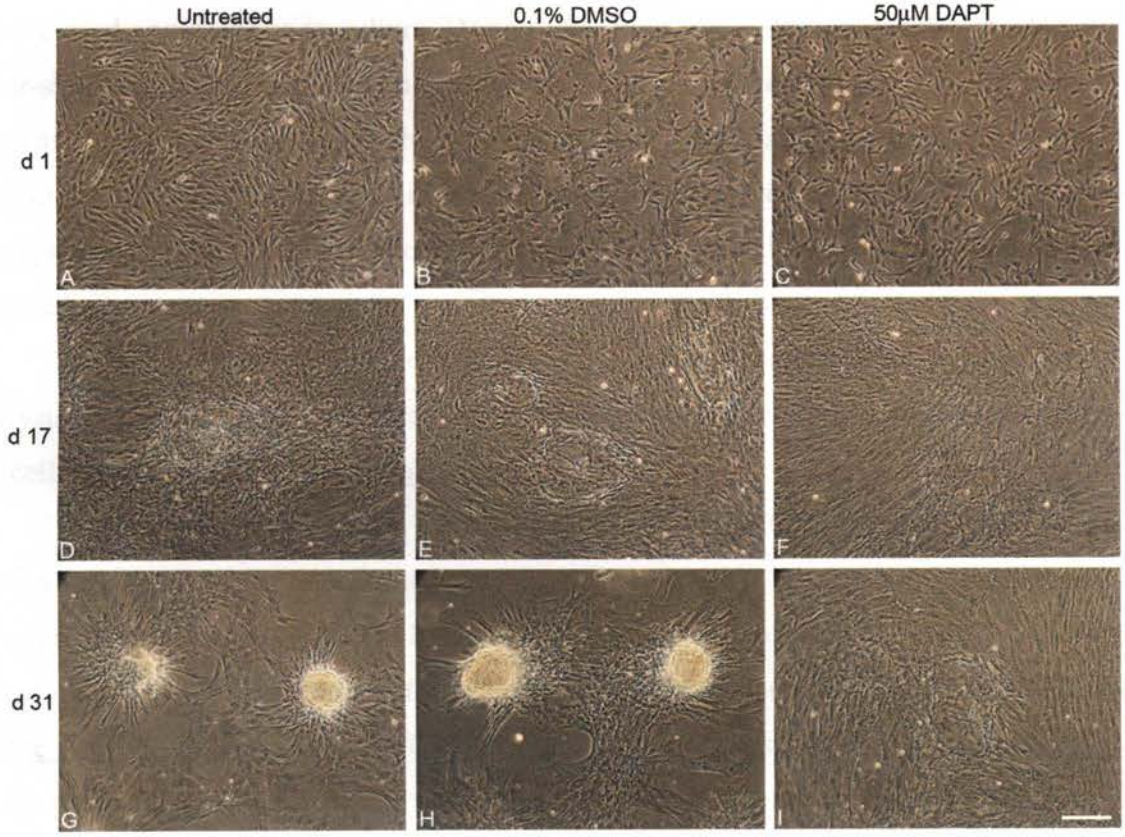

Figure 6.7: Dermal papillae isolated from Merino whiskers were grown *in vitro* for 31 d on Matrigel™. All cultures appeared similar on d 1 (A, B, C). The untreated and DMSO-treated cultured cells were observed to be forming groups of cells by d 17 (D, E) which further developed forming numerous cellular aggregations by the end of the trial (G, H). No groups of cells (F) or aggregations were observed in the DAPT-treated cell cultures (I). Scale represents 200 μm.

On d 31 the trials were concluded and the cells fixed and stained in preparation for counting. All cultures were systematically scanned under a microscope and the numbers of concentrated groups (Figure 6.8; A) and aggregations (Figure 6.8; B) recorded.

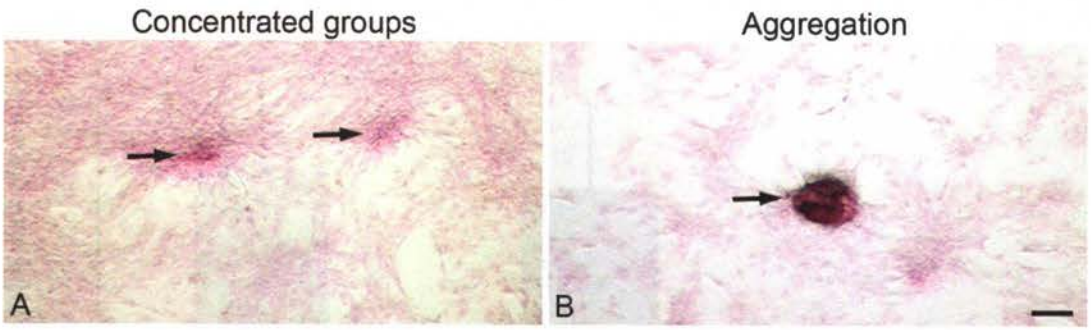

Figure 6.8: Stained cellular structures visualised in the sheep dermal papilla cell cultures counted at the end of the trial (d 31). A, concentrated groups of cells; B, cellular aggregations. Cell cultures were fixed with 2% paraformaldehyde prior to staining with nuclear fast red. Structures represented by black arrows. Scale represents 200 μm.

Concentrated groups of cells were thought to be the means by which the dermal papilla cells formed aggregations in culture. During formation, these groups of cells developed from a star-shaped radiating mass with a central focus. This suggested that the cells were migrating towards a common point using their cytoplasmic projections (Figure 6.4; C). Further, the formation of these condensed groups of cells appeared to influence the formation of aggregations, as only a few of these structures were detected in the DAPT-treated cultures (Figure 6.9).

The data from the counts were analysed using a generalised linear mixed model. The analysis revealed a highly significant interaction ($p<0.001$) between the treatment group and the cellular structures observed (Table A8.1).

Treatment was found to have a significant effect ($p<0.001$) on the number of dermal papilla cell aggregations that formed after 31 d (Figure 6.10). The principle finding was that no aggregations formed in the DAPT-treated cultures over the 31 d trial period. Significantly higher numbers of aggregations formed in the untreated compared to the DAPT cultures (Table A8.2). Similarly, the DMSO-control cultures formed significantly more aggregations compared to the DAPT-treated cultures. There was no significant difference in the number of cell aggregations counted in the untreated and DMSO cultures. These results suggested DAPT prevented the papilla cells from condensing to form aggregations, and that DMSO had no effect on aggregation.

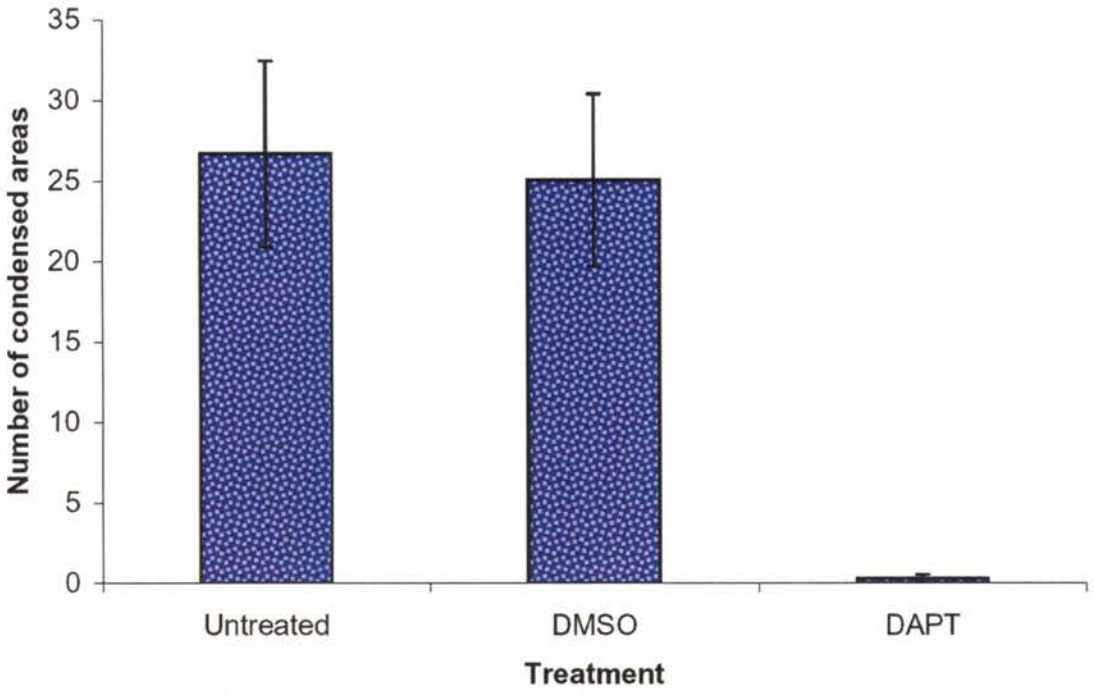

Figure 6.9: The mean number of concentrated groups of dermal papilla cells counted on d 31 of the trial for each treatment group. The number of concentrated groups was similar in the untreated and DMSO cultures, but markedly reduced in the DAPT cultures ($p<0.001$). Error bars represent standard error of the mean.

The formation of concentrated groups of dermal papilla cells was monitored over the 31 d trial. Treatment was found to have a significant effect on the number of concentrated groups counted in the cell cultures ($p<0.001$; Figure 6.9). The number of concentrated groups was not significantly different in the untreated and DMSO cultures. Significantly more concentrated groups formed in the untreated cultures compared to the DAPT cultures, and DMSO cultures compared to the DAPT cultures. These findings suggested that DMSO did not affect the formation of concentrated groups of cells, whereas DAPT appeared to prevent their formation. The condensed groups of cells appeared to develop into aggregations, with similar numbers to those of the aggregations observed. It was thought that the formation of concentrated groups of cells was the means by which dermal papilla cells aggregated *in vitro*.

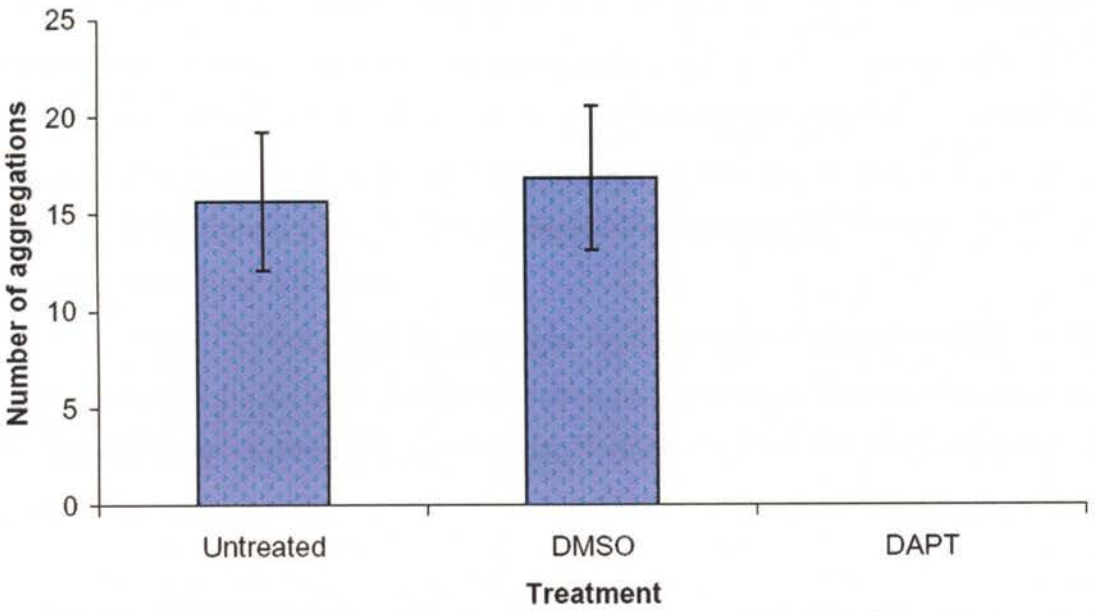

Figure 6.10: The mean number of dermal papilla cell aggregations counted on d 31 for each treatment group. Similar numbers of aggregations developed in the untreated and DMSO groups, none formed in the DAPT-treated cultures ($p<0.001$). Error bars represent standard error of the mean.

6.3.5 DEVELOPING THE FLOATING CULTURE SYSTEM FOR OVINE SKIN

6.3.5.1 Pilot studies using the floating skin culture model

Merino skin collected on d 56 of gestation, from 3 foetuses, was cultured to observe follicle development. No follicles were evident in the skins on d 0, as expected. One skin developed follicles by d 7 and was cultured for another 3 d. The other 5 skins had curled by d 7 and no follicles were visible.

Tukidale skin collected on d 56 of gestation, from 3 foetuses, was cultured for 21 d to compare follicle development *in vitro* to that which occurred *in vivo*. On d 7, the skins were removed from their membranes and follicles could be seen in 4 out of the 6 samples. These skins were placed back on their membranes. By d 21, some skins had curled. However, follicles were visible in all these skins. When compared to skins harvested on d 70, the cultured skins contained a dramatically reduced number of follicles.

Follicle development *in vitro* occurred at a reduced rate. However, these experiments were successful as the d 56 skin, which contained no follicles, produced follicles in culture, albeit at a highly variable rate and continued to do so over a 3 week period.

6.3.5.2 Follicle development in fresh and frozen-thawed skins

The development of follicles in d 70 Tukidale skin samples that were cultured directly following harvest were compared to skins that were frozen and thawed prior to culturing.

The Tukidale skin samples collected on d 70 of gestation and cultured fresh (Figure 6.11; A) or frozen and thawed prior to culturing (Figure 6.12; A) possessed numerous follicle buds. After 4 d in culture, the follicles within the fresh (Figure 6.11; B) and frozen-thawed (Figure 6.12; B) skins were counted. The number of follicles in the 3 fresh skins had increased by 359% from d 0 to d 4. In the 3 frozen-thawed skins, the number of follicles had increased by 116% from d 0 to d 4.

The process of freezing and thawing was found to have a negative effect on follicle development, with follicles in the frozen-thawed skins appearing different to those in the fresh skins. Therefore, the experiments investigating follicle development were conducted using fresh skins.

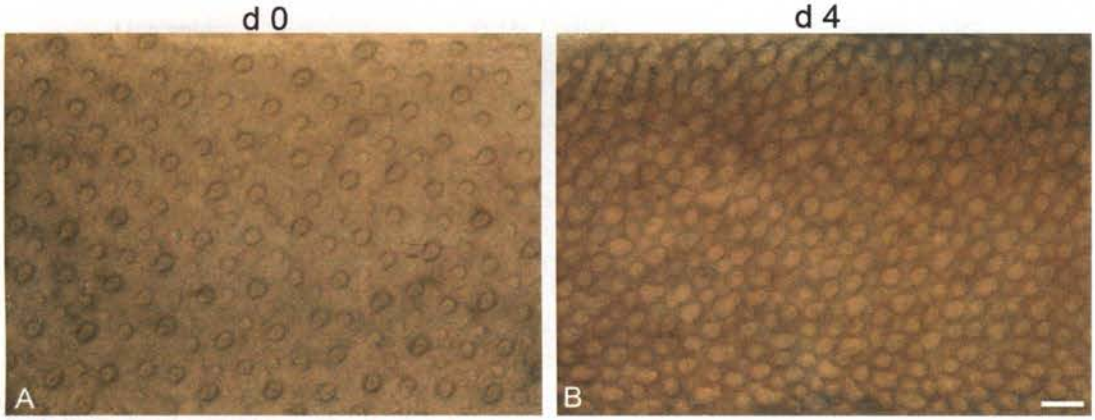

Figure 6.11: Fresh d 70 Tukidale midside skin before and after culturing on a collagen-coated membrane for 4 d. A; skin prior to placement on membrane, on d 0 of the trial. B; skin removed from the membrane at the end of the trial (d 4). Scale represents 200 μm.

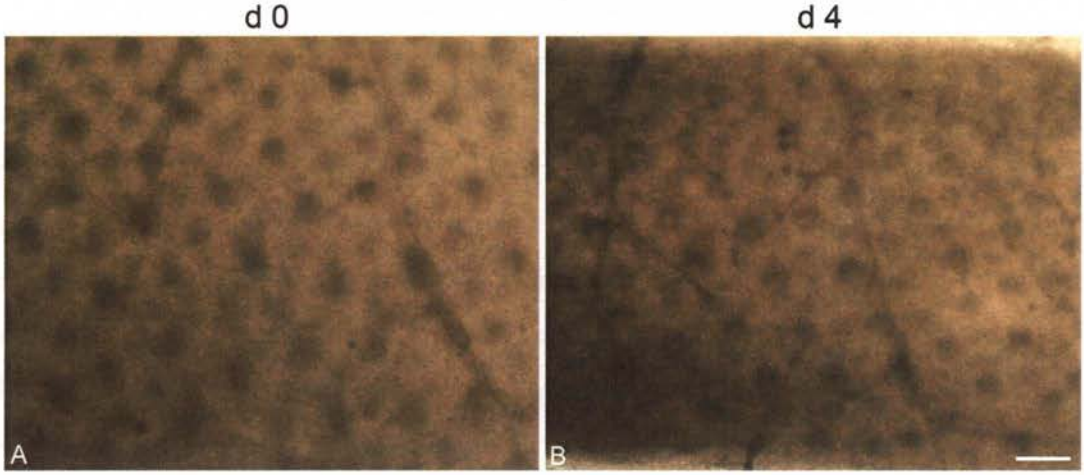

Figure 6.12: Frozen-thawed d 70 Tukidale midside skin was cultured on collagen-coated membranes for 4 d. Follicles were distinguished as dark, round areas within the tissue. A; follicles were evident in the skin on d 0 of trial, before being placed on membrane. B; follicles were observed in skin removed from membrane on d 4 of the trial. Scale represents 200 μm.

6.3.6 THE IMPACT OF BLOCKING NOTCH SIGNALLING IN TUKIDALE SKIN

Tukidale midside skin (n=6) was collected from 6 foetuses on d 70 of gestation, as described in Section 6.2.6.4.3; i, and cultured for 4 d. Follicle buds were visualised on d 0 and d 4 of the trial, as circular areas that were lighter in colour than the surrounding tissue. The untreated skin (Figure 6.13; A) had round follicles, with smaller follicles visible between larger follicles. The larger follicles were thought to be at a more advanced stage of development. Skin in the 0.1% DMSO control group (Figure 6.13; B) appeared similar to the untreated skin. Follicles within the skin treated with 50μM DAPT (Figure 6.13; C) appeared irregularly spaced and unevenly arranged compared to the skins in the two control groups. These follicles were harder to distinguish than those in the other 2 treatment groups.

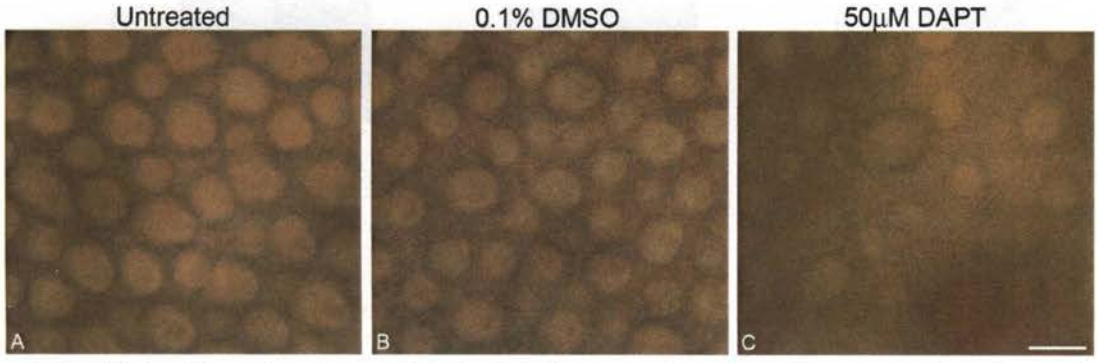

Figure 6.13: Midside skin collected from d 70 Tukidale foetuses cultured on collagen-coated membranes for 4 d. Similar follicle development was observed in all skins on d 0 (not shown). Follicles were visible as round, light areas within the skin. Untreated (A) and 0.1% DMSO (B) skin had numerous follicles that appeared regularly spaced throughout the sample. Skins treated with 50μM DAPT (C) contained irregularly spaced follicles. Scale represents 50 μm.

Follicle counts were performed on the d 70 Tukidale midside skins on d 0 and d 4 of the trial (Figure 6.14), with follicles counted in five random circles placed over each skin, each with a diameter of 1,250 μm. Fewer follicles were present in the DAPT-treated skins compared to the two control groups. A linear mixed model analysis produced a significant interaction between treatment and day of trial (p=0.017), refer to Table A9.1. No significant differences were found in the numbers of follicles counted in the 3 treatment groups on d 0. The number of follicles had significantly increased from d 0 to d 4, for all treatment groups. On d 4, no significant differences in follicle numbers were found between the untreated and DMSO skins, suggesting DMSO did not affect follicle development. Significantly more follicles had developed in the untreated skins compared to the DAPT-treated skins. Similarly, significantly more follicles had developed in the DMSO control skins compared to the DAPT-

treated skins. DAPT was therefore found to inhibit follicle development in Tukidale skin sampled during follicle initiation, while DMSO *per se* did not affect follicle development.

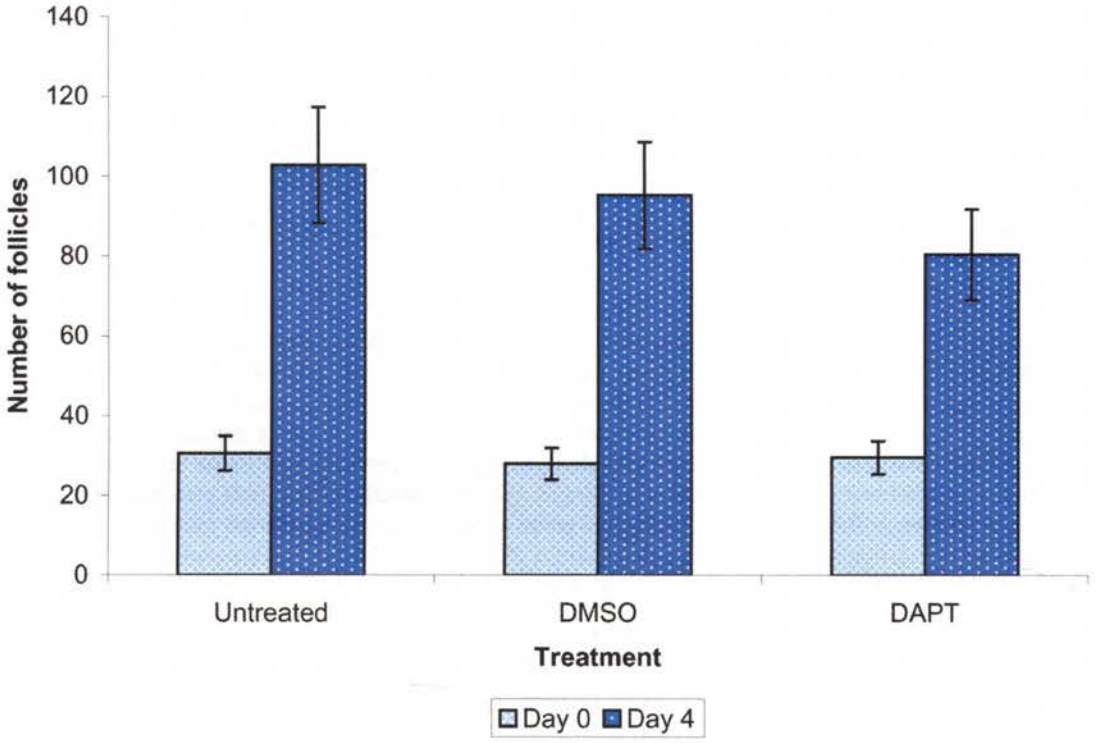

Figure 6.14: The interaction between treatment and day of trial had a significant effect (p=0.017) on follicle number in d 70 Tukidale skin. On d 0, no significant differences in follicle numbers between the 3 treatment groups were detected. The number of follicles was significantly higher on d 4 than d 0 for all treatment groups. A significantly higher number of follicles was counted in the untreated skins compared to the DAPT skins, and in the DMSO skins compared to the DAPT skins on d 4. There was no significant difference in follicle numbers between the untreated and DMSO skins on d 4. Error bars represent standard error of the mean.

6.3.7 THE IMPACT OF BLOCKING NOTCH SIGNALLING IN MERINO SKIN

6.3.7.1 During primary follicle initiation

Skin was collected from 4 Merino d 70 foetuses (n=24) as described in Section 6.2.6.4.3; ii. The skin was observed on d 0 and d 4 of the trial. On d 0 (Figure 6.15; A), numerous follicles were visible throughout the sample. On d 4, the follicles in the untreated skins (Figure 6.15; B) maintained their regular appearance. The follicles in the DMSO (Figure 6.15; C) and DAPT (Figure 6.15; D) skins appeared regular but were packed more tightly together. This suggested that DMSO and DAPT may have caused larger follicles to develop. Twenty follicle diameters were measured randomly for skins from each sample site and treatment group. A linear mixed model analysis revealed a significant interaction between treatment and site ($p<0.001$), and this was further investigated in Table 6.1. No significant differences in follicle diameter were detected for each site that received the same treatment.

There was no significant difference in follicle diameters in the untreated anterior skins compared to those that received DMSO. Significant differences in follicle diameter were seen for the posterior and midside skins that were untreated and DMSO-treated. Significant differences in follicle diameters were detected between the anterior, midside and posterior skin samples when untreated skins were compared with those that received DMSO and DAPT, and in those that were treated with DMSO compared to those treated with DAPT. These results suggested that DMSO and DAPT had an affect on follicle diameter in d 70 Merino skin. However, DMSO did not affect follicle diameter in anterior skin samples.

Table 6.1: The interaction between treatment and sample site had a significant effect ($p<0.001$) on follicle diameter (μm) in d 70 Merino skin. No significant differences were detected between the different sample sites for all treatment groups (A, B, C). Significant differences in follicle diameters were detected between all treatment groups and sample sites (D, E, F), accept for the untreated and DMSO anterior samples. There was one exception, where no significant difference between follicle diameters in the untreated and DMSO skins was detected for the anterior skin samples (noted with D). Significant differences were investigated between terms with the superscript letter corresponding to the terms being compared. Significant differences were denoted by a red letter superscript, non-significant differences were represented by a blue letter superscript. Least Significant Difference (LSD treatment 22.6; LSD site 17.2). Standard Error (SE).

Treatment	Collection Site	Mean	SE
Untreated	Anterior	112.7^{ADE}	18.4
	Midside	99.1^{ADE}	10.8
	Posterior	95.8^{ADE}	10.6
DMSO	Anterior	130.2^{BDF}	18.3
	Midside	109.4^{BDF}	10.8
	Posterior	113.3^{BDF}	13.7
DAPT	Anterior	119.6^{CEF}	10.6
	Midside	137.1^{CEF}	10.8
	Posterior	124.1^{CEF}	6.3

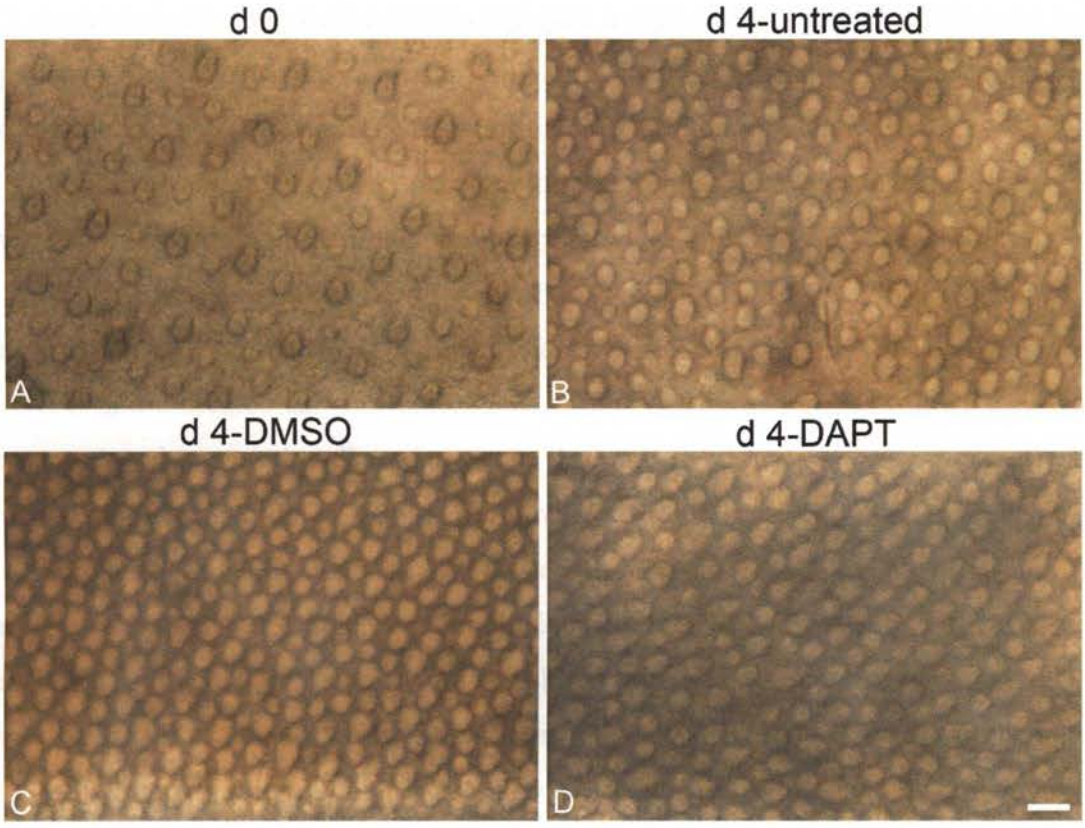

Figure 6.15: Merino skin collected on d 70 of gestation and cultured on collagen-coated membranes for 4 d. On d 0 of the trial (A) the follicles were regularly spaced. On d 4, the follicles in the untreated (B), DMSO (C) and DAPT (D) skins appeared to be similar. Scale represents 200 μm.

The numbers of follicles in each skin sample for each treatment (n=24) were counted on d 0 and d 4 of the trial. The data were analysed using a linear mixed model. The 4-way interaction of treatment × day of trial × side sampled × site was highly significant ($p<0.001$). This was not possible to interpret biologically and no conclusions could be drawn so this interaction was removed from the model. All 3-way interactions were found to be significant. The interaction of day of trial × treatment × sample site ($p=0.003$) was further investigated (Figure 6.16 and Table A9.2). This interaction was of interest, as follicle morphogenesis is known to occur in waves along the anterior-posterior axis of the foetus (Carter and Hardy, 1947).

The numbers of follicles in the skins collected from the 3 sample sites and allocated to the 3 treatment groups were not significantly different from one another on d 0. The number of follicles significantly increased from d 0 to d 4 for all sample sites and treatment groups. On d 4, follicle numbers were significantly different for some groups when comparisons between the sample sites within each treatment group were made. For the untreated controls, the midside skins contained significantly more follicles than the anterior and posterior skins and the posterior skins contained significantly more follicles than the anterior skins. For the

DAPT treated skins, the anterior skins displayed a significantly higher number of follicles compared to the midside and posterior skins. No other significant differences between the follicle numbers in the other sample sites within each treatment group existed.

Comparisons were also made between the different sample sites and treatments on d 4. In the anterior skin samples, follicle number was not significantly different in the untreated and DMSO treated skins suggesting that DMSO did not affect follicle development. A significantly higher number of follicles had formed in the DAPT-treated skins compared to the DMSO and untreated skins. This suggested that DAPT encouraged follicle development in the anterior skin samples. By contrast, in the midside skin samples significantly higher numbers of follicles had developed in the untreated skins compared to the DMSO and DAPT treated skins. The DMSO skins had developed significantly more follicles than the DAPT skins. These results demonstrated that in midside skin DMSO had a negative effect on follicle development, but that DAPT significantly inhibited follicle development compared to DMSO. In skin obtained from the posterior region, more follicles appeared to develop in the untreated and DMSO-treated skins compared to those incubated with DAPT. However these observations were not significant.

This experiment demonstrated that Merino skin collected on d 70 of gestation developed a significant number of follicles during a 4 d period *in vitro*. Although all skins had similar numbers of follicles on d 0, the different sample sites provided variable responses to DAPT and to adaptation to culture conditions over the 4 d period of the trial.

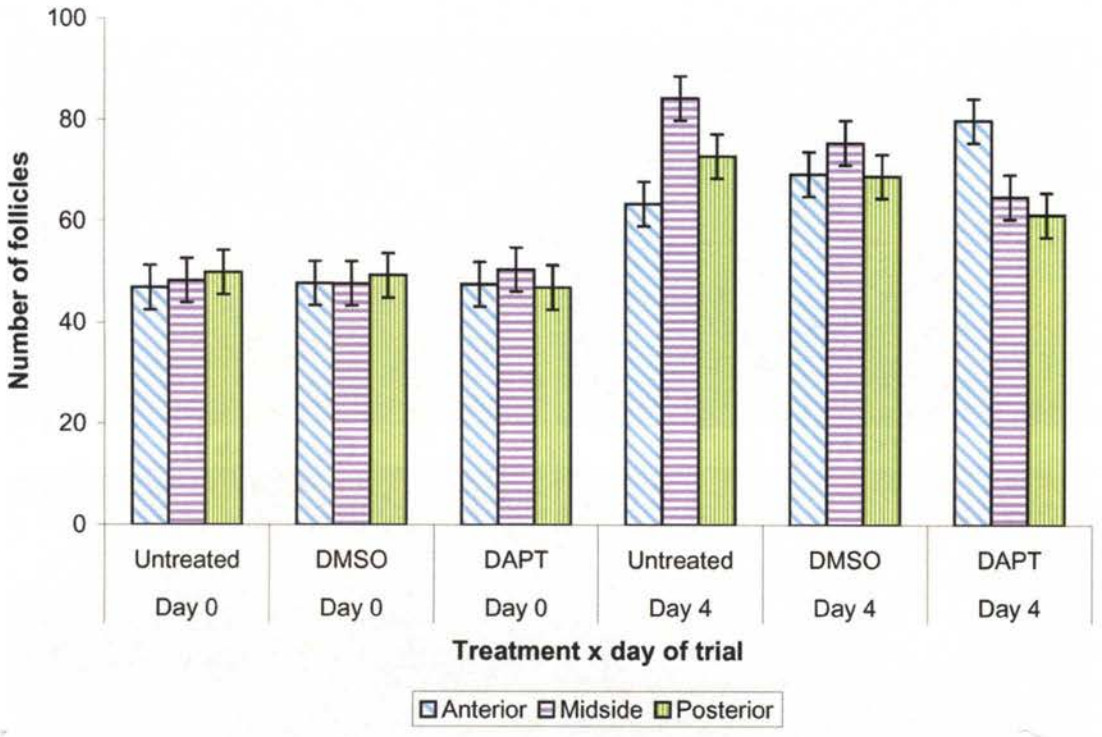

Figure 6.16: The mean number of follicles counted in d 70 Merino skins on d 0 and d 4 from anterior, midside and posterior sites for each treatment group (untreated, 0.1% DMSO, 50 μM DAPT). The 3-way interaction between day of trial, treatment and sample site was significant (p=0.003). Error bars represent standard error of the mean.

6.3.7.2 Effect of time of gestational stage on follicle development *in vitro*.

Skin was collected from Merino foetuses on d 54, d 63 and d 84, as described in Section 6.2.6.4.3; iii. Skin sampled prior to primary follicle initiation (d 54; n=6) had no follicles visible on d 0 (Figure 6.17; A), but a few follicle-like structures were observed on d 4 (Figure 6.17; B, C, D). Skin sampled during primary follicle initiation (d 63; n=12) had numerous follicles visible on d 0 (Figure 6.18; A) and d 4 of the trial (Figure 6.18; B, C, D). At the end of the trial, some areas of the skin samples appeared to be darker: this was artifactual resulting from the sample uplifting, shrinking and curling, creating thicker areas within the skin. It was difficult to count the number of follicles in these thickened areas. Skin collected during the development of secondary original follicles (d 84; n=6) was relatively more complex than that collected from younger foetuses. On d 0 (Figure 6. 19; A) the follicles were observed as distinct structures within the skin, while on d 4, it was difficult to distinguish follicles from one another, as they were packed so closely (Figure 6. 19; B, C, D). Areas within a number of these skin samples had thickened to an extent that no additional follicles could be observed.

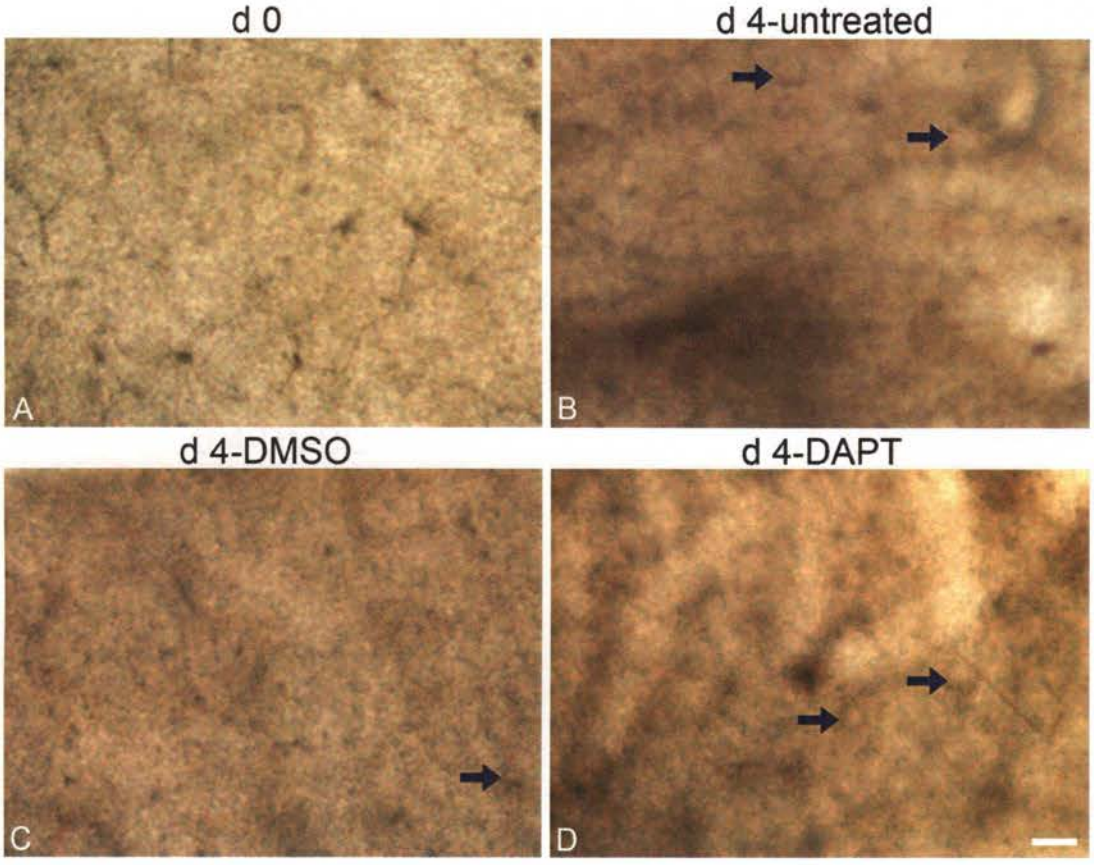

Figure 6.17: Foetal Merino skin collected on d 54 of gestation and cultured on collagen-coated membranes for 4 d. No follicles were detected in skin collected on d 0 (A) of the trial. On d 4, a few follicle-like structures were visible in the three treatment groups (B, C, D), denoted by black arrows. Scale represents 200 μm.

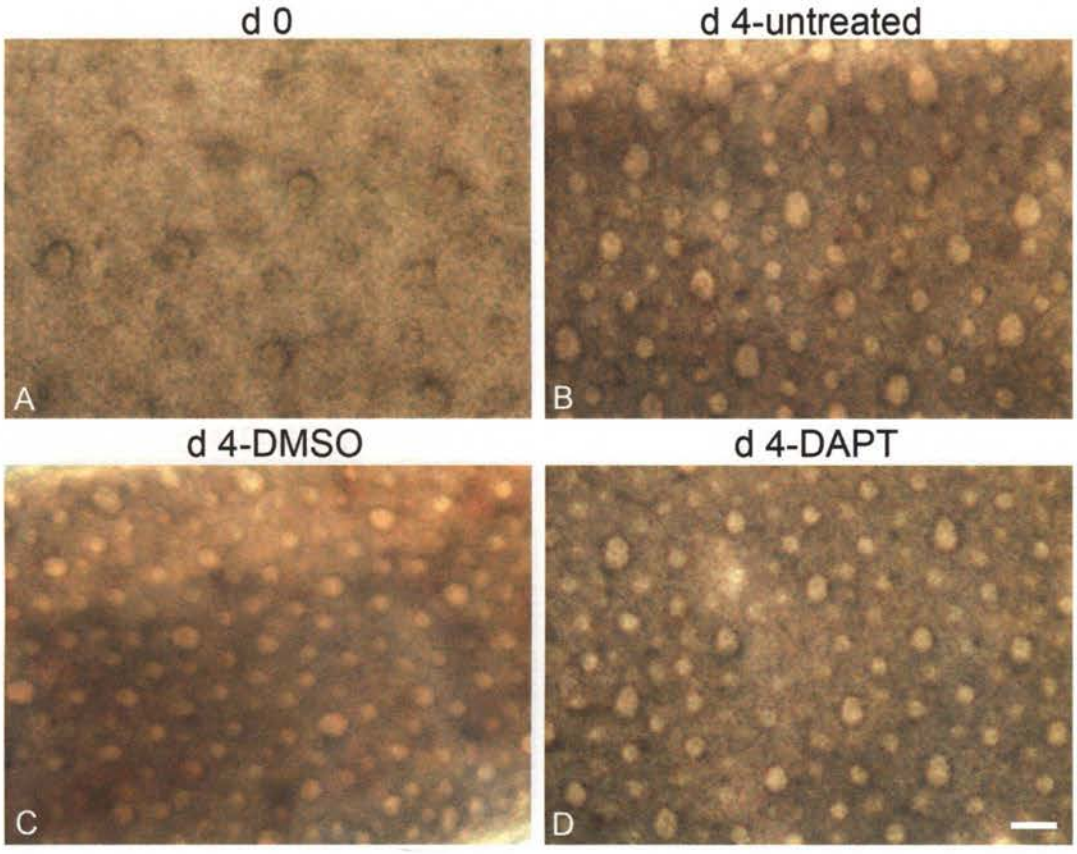

Figure 6.18: Foetal Merino skin collected on d 63 of gestation and cultured on collagen-coated membranes for 4 d. Primary follicle development was visible in the skin on d 0 (A). On 4 d, follicle development had progressed further. A larger number of follicles were observed in all treatment groups (B, C, D). Scale represents 200 μm.

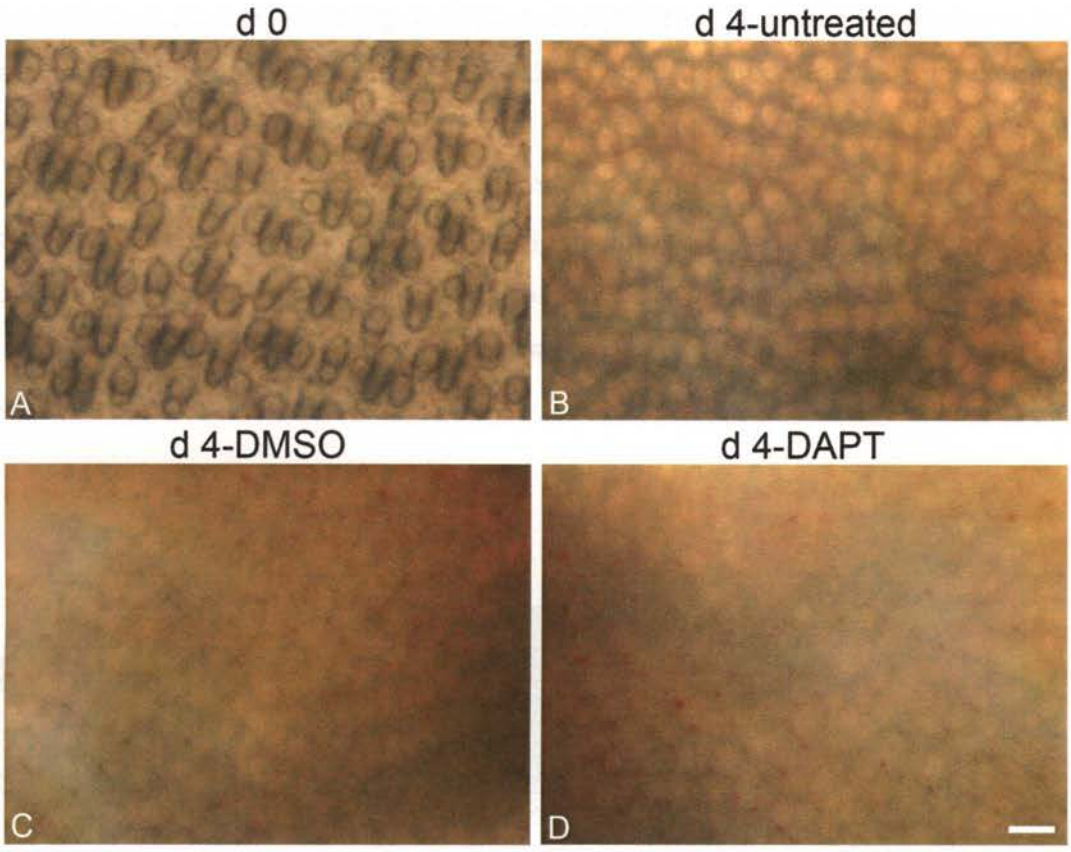

Figure 6.19: Foetal Merino skin collected on d 84 of gestation and cultured on collagen-coated membranes for 4 d. Numerous follicles were evident in the skin on d 0 (A). On d 4, the follicles were crowded together (B, C, D) and were difficult to distinguish from one another.
Scale represents 200 μm.

Follicles were counted on d 0 and d 4 of the trial and analysed using a linear mixed model. The 5 and 4-way interactions were dropped from the model as they were not possible to interpret biologically. The 3-way interaction day of trial × foetal age × sample site was highly significant ($p<0.001$). However, this interaction was of no interest as it did not investigate the effect of treatment on the numbers of follicles. The interaction of day of trial × treatment × foetal age was not significant ($p=0.183$). However, we were interested in the effect of treatment on the number of follicles from skin at different stages of follicle development so this non-significant interaction was investigated further (Figure 6.20 and Table A9.3). The 3 different foetal ages showed significant differences in follicle number, as expected. On d 0 and d 4 of the trial, the d 84 skins contained significantly more follicles than the d 63 skins, which in turn contained significantly more follicles than the d 54 skins. The number of follicles in the d 54 and d 63 skins did not increase significantly from d 0 to d 4. This was an unexpected finding, as in the earlier trials the number of follicles did significantly increase over the 4 day trial period. The number of follicles in the d 84 skins had decreased significantly from d 0 to d 4. This could be explained by the poor visibility of follicles after 4

days in culture, most likely leading to a gross underestimation of follicle numbers. *In vivo* a decrease in follicle numbers would not occur during development. In analysing the impact of the treatments the interaction of day of trial × treatment × foetal age was not significant (p=0.183). On d 0 of the trial, when the different age samples were looked at collectively, no significant differences between numbers of follicles in the 3 treatment groups were detected. However, on d 4 of the trial no significant differences between follicle numbers in the 3 treatment groups were found. Although the tissue at the end of the trial appeared to be viable, our results here suggest otherwise.

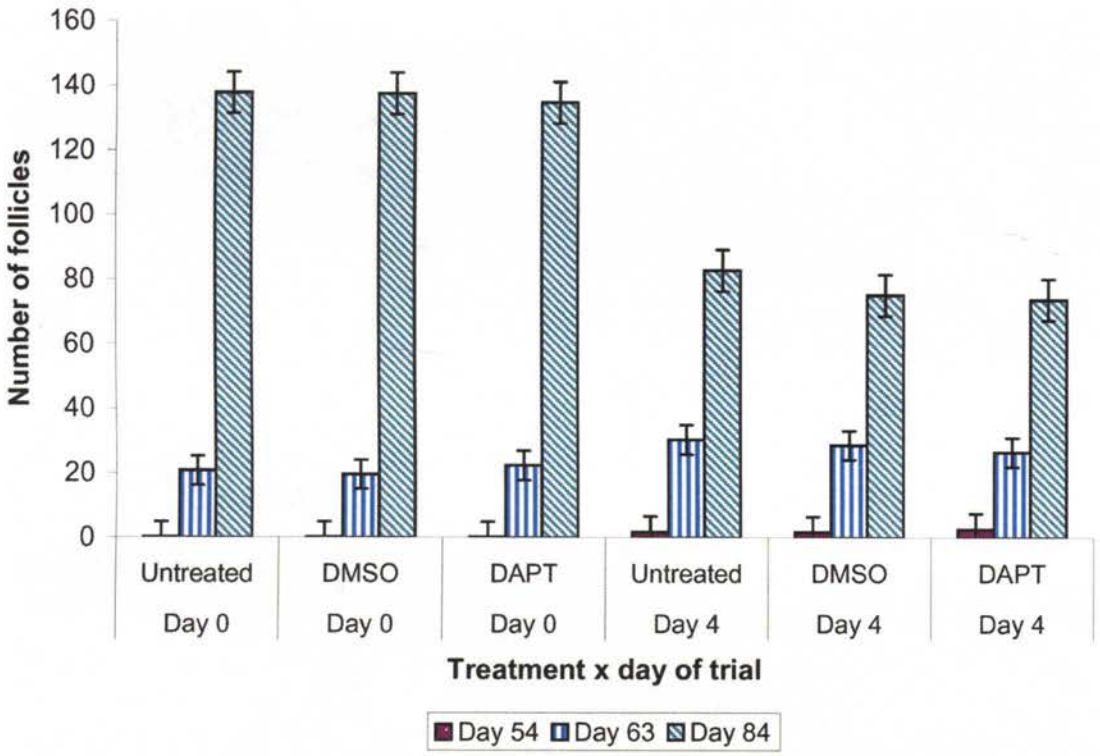

Figure 6.20: The effect of gestational age of donor skin and culture in the presence of the γ-secretase inhibitor DAPT and its solvent 0.1% DMSO on follicle development in foetal Merino skin. The interaction between the day of the trial, foetal age and treatment was investigated (p=0.183). The number of follicles in the different aged samples were significantly different from each other throughout the trial. The numbers of follicles increased from d 0 to d 4 of the trial in the d 54 and 63 samples but decreased in the d 84 skins. Treatment did not appear to affect the number of follicles that developed during the trial. Error bars represent standard error of the mean.

6.3.8 NOTCH-1 TRANSCRIPT EXPRESSION IN CULTURED SKIN

Localisation of gene transcripts for Notch-1 was studied in the d 70 Merino skin samples cultured for 4 days by performing *in situ* hybridisation experiments on the sectioned, wax-embedded tissue. The expression of Notch-1 in the skin changed over the 4 d period in culture. It was expressed strongly in the basal layer on d 0 of the trial, but no transcripts were

detected on d 4. On d 0 no transcripts were detected in the epithelial plug, but by d 4 Notch-1 was expressed within some cells of this structure (Figure 6.21). In the mesenchyme some cells were stained for the transcript on d 0 while others were not. On d 4 a higher level of staining was visualised, with fewer unstained cells observed. The level of staining in the mesenchyme appeared particularly strong in the DAPT treated skin (Figure 6.21; D), with very few unstained cells detected. Transcript expression in the dermal condensate appeared the same at the start and end of the trial.

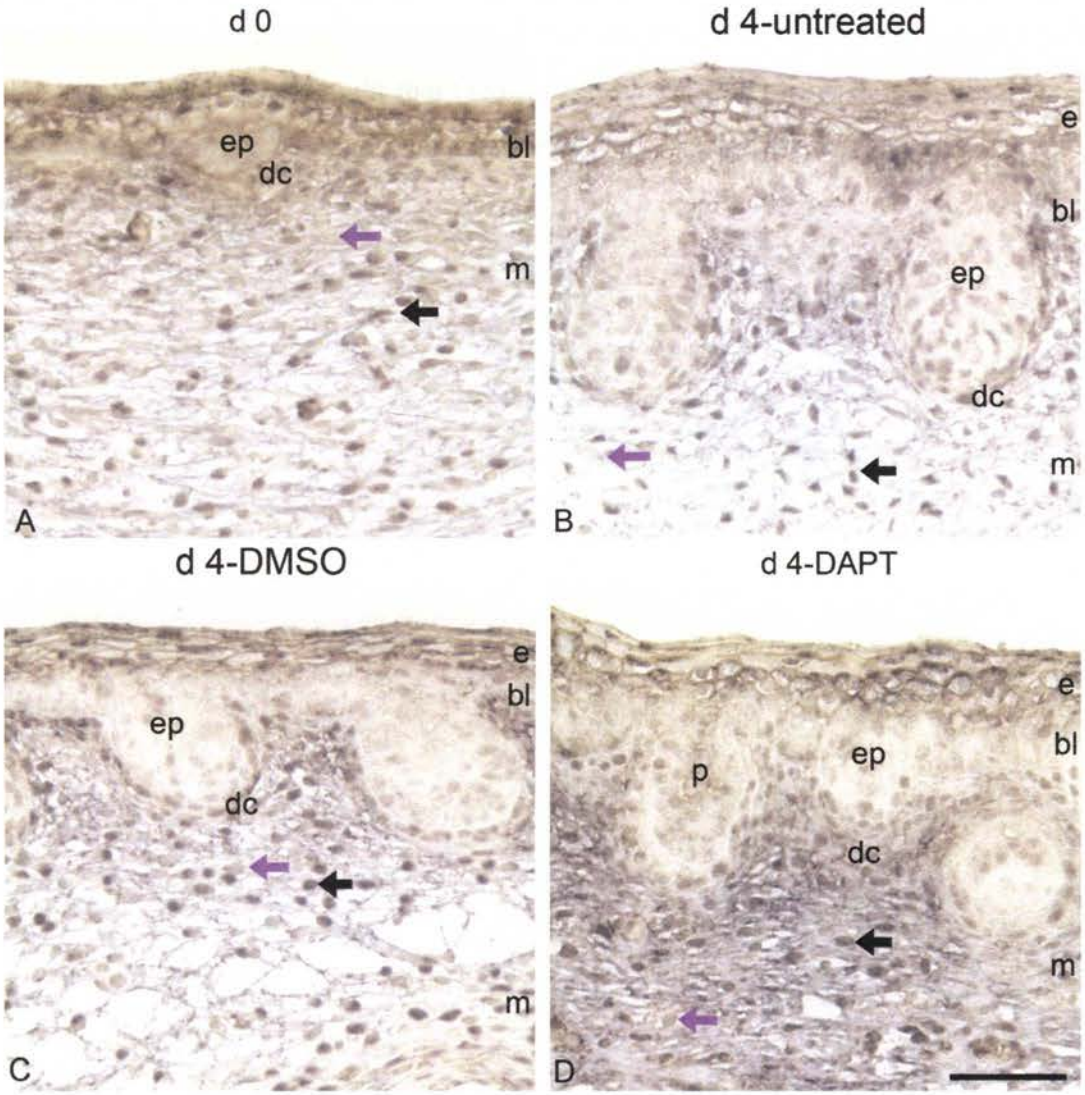

Figure 6.21: Investigation into Notch-1 transcript expression in d 70 Merino skin cultured for 4 d in the presence and absence of DAPT. (A) On d 0 Notch-1 transcripts were detected in the epidermal basal layer (bl), the dermal condensates (dc), and in a scattered subpopulation of cells in the mesenchyme (m). No transcripts were detected in the epithelial plug (ep). On d 4, follicle development had progressed with the epithelial plugs growing downward through the dermis. Notch-1 transcript expression was similar in all experimental groups (B, C, D). Transcripts were detected in the upper layers of the epithelium (e), scattered in some cells within the ep, in the dc with the cells bordering the ep being particularly strong and a relatively constant level of expression throughout the m. Transcripts were detected in the developing core of the plug (p), (D). No transcripts were detected in the bl at this stage. Unlabelled cells denoted by purple arrow, Notch-1 labelled cells denoted by black arrow. Scale represents 50 μm.

6.3.9 DELTA-1 PROTEIN EXPRESSION IN CULTURED SKIN

Delta-1 protein was localised in d 70 Merino skin cultured for 4 days using immunohistochemistry, as described in Section 2.2.9.1. In all skin sections studied, only small areas of the tissue appeared to be expressing the protein (Figure 6.22). No protein was detected in the upper layers of the epithelium, the epithelial plug or dermal condensate. No large differences in distribution were detected in the skins fixed on d 0 when compared to those after 4 d of culture. Similarly, skins that were cultured in the presence of DMSO or DAPT showed few differences in the distribution of staining. Cells expressing the Delta-1 protein appeared to be restricted to areas of the basal layer of the epithelium and to a few mesenchymal cells. It was thought that the process of culturing the skins or storing them in D-PBS prior to fixing may have had a negative effect on the expression of antigenic sites in the tissue.

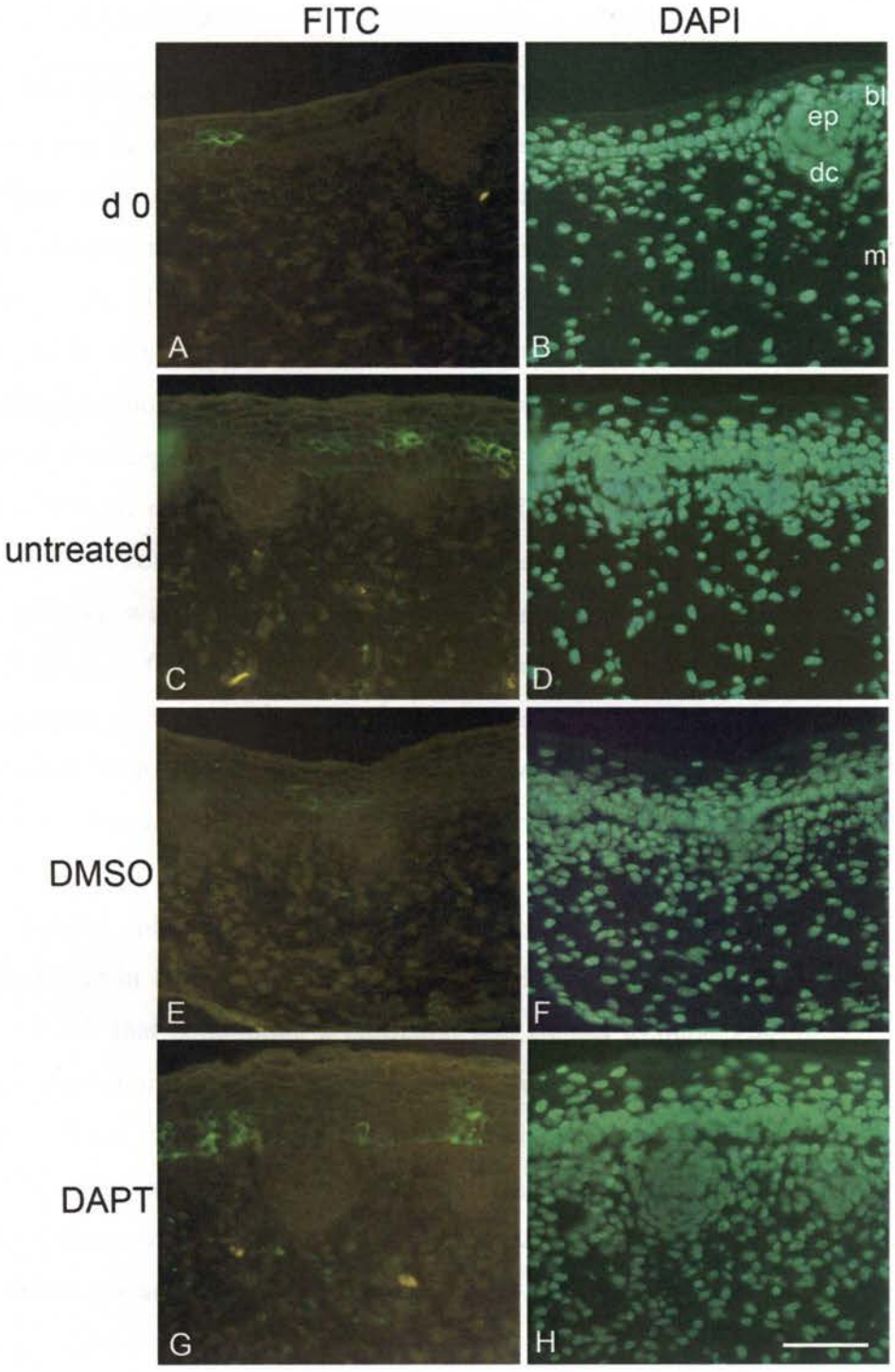

Figure 6.22: Investigation into Delta-1 protein expression in d 70 Merino skin cultured for 4 d in the presence and absence of DAPT. A and B at d 0; C-H at d 4. Immunofluorescence with the antibody to Delta-1and visualised with a donkey anti-goat IgG conjugated to FITC (A, C, E, G). DAPI fluorescence in nuclei was included to view the tissue morphology (B, D, F, H). Immunoreactivity to the Delta-1 antibody was detected in a few cells in all samples. The protein was localised to areas of the basal layer (bl) of the epithelium. The protein was also detected in a few mesenchymal cells (m). Scale represents 50 µm.

6.4. DISCUSSION

The collection of dermal papillae from rat and sheep whiskers facilitated a number of experiments in which the aggregative behaviour of these cells was investigated *in vitro*. Whiskers were chosen for investigation as they are a well-recognised model for dermal papilla culture studies. They are comparatively large in size and easy to isolate. Studies conducted by Messenger *et al.* (1986) showed dermal papilla cells grown on collagen gels were more likely to aggregate, compared to those grown on a plastic substrate. An experimental model in which papilla cells aggregated, irrespective of whether they originated from rat or sheep whiskers, was developed by coating the base of a tissue culture dish with Matrigel™. In contrast, dermal fibroblasts did not aggregate in culture, remaining as a monolayer of cells until confluence was reached, regardless of the extracellular matrix used. The cultures were allowed to continue to aggregate for a 31 day period to allow the aggregations to fully develop. The cells in the untreated and DMSO control dishes had begun to aggregate prior to reaching confluence, on approximately day 16. These findings were in agreement with earlier investigations in which cultured papilla cells, unlike dermal fibroblasts, formed multi-layered aggregates prior to reaching confluence (Jahoda and Oliver, 1984).

Lateral inhibition may be responsible for the formation of dermal papilla-like aggregations in culture. Notch signalling facilitates competitive interactions between cells, where a cell that is adopting a particular fate signals to neighbouring cells, inhibiting them from assuming that same fate. This mechanism allows adjacent cells with similar potential to adopt different fates, thereby regulating cell diversity in a developing tissue (Chitnis, 2006). Cells that express Notch do not bind to one-another. Therefore, Notch-Notch associations are likely to occur within a single cell and not between cells. In contrast, cells that express Delta do bind to one another, suggesting that Notch and Delta can compete for binding to Delta at the cell surface as both Delta-Delta and Delta-Notch associations can occur (Fehon *et al.*, 1990; Rebay *et al.*, 1991). It is thought that Notch and Delta may function *in vivo* to mediate adhesive interactions between cells (Fehon *et al.*, 1990). It was believed that only the extracellular domain of Notch was involved in the Notch-Delta interaction, since a deletion of most of the intracellular region did not affect aggregation with Delta-expressing cells (Rebay *et al.*, 1991).

A common feature of the Notch signalling pathway is that its various components often interact in ways that produce negative feedback loops. Such interactions lead to changes in

gene expression that result in specific patterns of cell differentiation (Weinmaster and Kintner, 2003). This feature may provide a mechanism by which some papilla cells are able to aggregate to form dermal papilla structures whereas other cells in the general mesenchymal cell population are prevented from aggregating. Thus, even cells that differentiated to form papillae within whiskers *in vivo*, when placed in culture, where all cells were given an equal opportunity to aggregate, were not all able to form papilla-like aggregations. This observation suggested that in culture, the dermal papilla cell population contained some selective intrinsic factor that instructed which cells could aggregate and where these aggregations formed. We hypothesise that without this instructive factor in cultures of differentiated dermal papilla cells, the entire cell population would aggregate. The results from these studies agree with previous findings that a cell destined for primary differentiation often expresses elevated levels of the ligand, in this case Delta-1, and signals to the surrounding receptor-expressing cells, instructing them not to take on the same cell fate (Hansson *et al.*, 2004).

Dermal papilla culture studies, using cells isolated from rat and sheep whisker follicles, demonstrated that inhibiting Notch signalling blocked cell aggregation. Rat and sheep dermal papilla cultures behaved in the same manner *in vitro*. The untreated and 0.1% DMSO control cell culture groups, grown on Matrigel™, formed numerous aggregations. DMSO did not appear to affect the aggregative behaviour of dermal papilla cells, with these cultures forming a similar number of aggregations to those observed in the untreated cultures. DAPT abolished papilla cell aggregation *in vitro*, presumably by blocking the S3 cleavage of Notch and Delta (Six *et al.*, 2003), mediated by γ-secretase. The aggregations seen in these studies had begun to form prior to the cells becoming confluent. No aggregations formed in any of the DAPT-treated dishes, no matter how confluent the dishes became. The aggregations that formed took on a dermal papillae-like appearance.

By preventing the dermal papilla cells from aggregating, it appeared that Notch signalling played a role in this process. It was therefore assumed that the aggregating cells were binding via Delta-Notch associations or Delta-Delta homotypic interactions. If only the extracellular domain of Notch was involved in cell adhesion between Notch and Delta expressing cells it would be expected that the formation of aggregations would not be affected by the loss of Notch signalling to the cell nucleus. However, as shown in the rat and sheep dermal papilla cell cultures, blocking Notch signalling also blocked cell aggregation. Therefore, activation of the Notch receptor appeared to be important for dermal papilla cell aggregation. These experiments demonstrated that DAPT inhibited follicle growth and the aggregation of dermal papilla cells originating from adult animals, thereby indicating that

DAPT effects follicle growth after cell fate has been determined in the foetus and Founder cells are established

From the Merino dermal papilla cultures, analysis of the numbers of aggregations and concentrated groups of cells suggested that aggregations developed following the formation of concentrated groups of cells. The function of Notch in this situation is to repress differentiation of cells carrying the Notch receptor. Therefore the failure of dermal papilla cells to aggregate in culture may be a result of all cells remaining equipotent, with none being capable of influencing the development of others.

The effect of DAPT on rat papilla cell cultures was tested for Delta-1 protein expression. This was uniformly strong in aggregating cells of the untreated and DMSO culture groups. It was interesting that cellular aggregations expressed high levels of Delta-1 protein, whereas neighbouring non-aggregating cells expressed minimal levels of protein. The relatively uniform expression of Delta amongst interacting cells suggested that Delta was mediating the cell-cell interactions and adherence. There are a couple of possible explanations for the enhanced level of Delta-1 protein within aggregations of cells. Firstly, neighbouring papilla cells expressing high levels of Delta may be binding to one another, forming Delta-Delta bonds, which may promote the process of aggregation. Secondly, the cells within an aggregation may collectively up-regulate their expression of Delta-1 to maintain the cells in close proximity to one another (Rebay *et al.*, 1991). Over-expression of Delta is believed to result in the cell-autonomous activation or inhibition of Notch signalling (Pourquié, 2000). It is possible that the increased level of Delta-1 protein expression seen in the rat papilla cell aggregations may be characteristic of aggregating papilla cells. Although not investigated, it could be assumed that the level of Notch-1 protein expression in the papilla cell aggregations would also have been elevated, compared to the non-aggregating cells, as a result of the Delta-Notch cell associations in these structures.

Organ culture is clearly useful for investigating developmental processes but a limitation is the difficulty in establishing whether events in culture mimic those *in vivo* (Messenger *et al.*, 1986). Here, a floating culture system was developed for foetal ovine skin using collagen-coated polycarbonate membranes.

The floating organ culture system is still in the early stages of testing with ovine skin. The procedure appeared to work, however some refinement may be necessary to allow the skins to be cultured for longer periods of time. Skins were sampled and included in these studies that had been collected from anterior, midside and posterior locations so as to increase the number of skin samples that could be included. Thereby, it was used as a practical way in

which to increase the number of replicates in each treatment group and trial. Some biological effects were seen to occur between the different sample sites but these were taken into account within the statistical analysis of the results.

Following 4 d in culture, all skin samples shrank, regardless of the age of the skin when collected or the time they were cultured. This was a disadvantage as the skins became thicker and the numbers of follicles was often difficult to determine. However, they did maintain a follicle-like appearance, with the different layers within the skins maintaining their morphological integrity, as was evident in the sectioned specimens. No viable option for preventing the skins from shrinking was found.

Skin collected prior to primary follicle initiation developed a few relatively large and irregularly spaced follicles after 14 d in culture. However, skin harvested during follicle initiation (d 63 and d 70) showed significant increases in follicle density after 4 d in culture, with new follicle buds forming at a rapid rate. Therefore, follicle development resumed in culture, with more follicle buds forming after the skin was harvested. In skin collected on d 70 it appeared that new follicle buds formed between those that were already present, as smaller follicles were seen between more advanced, larger follicles. This suggested that primary follicle initiation was occurring in stages, as occurs *in vivo*.

It may be expected that DAPT had a relatively small effect on follicle development over the 4 d trial period, and that a larger effect may have been seen had the studies been conducted for a longer period in culture. It was thought that repeated DAPT administration was crucial to its effect on follicle development. Although its half-life in the culture medium was unknown, DAPT treatment appeared to be effective when administered every 24 hr, as the number of follicle buds that formed was altered using this treatment regimen. It would also be worthwhile to administer DAPT to skins at other time points around follicle initiation, to test DAPT at different concentrations, or to treat the skins more regularly. Alternatively, pregnant ewes or the whole foetus could be treated with DAPT. However, this was not believed to be a viable experimental approach due to the broad range of roles Notch signalling is responsible for during foetal development, as other systems would most likely be affected.

In the skin cultures, DMSO appeared to have some inhibitory effect on the development of follicle buds, but this was an inconsistent result as in some cases it had a significant effect while in others it did not. DMSO is widely used as a solvent and readily penetrates the skin. It is used in veterinary practice to carry anti-inflammatory and antibiotic drugs through the skin, to a target area (Thomas, 2006). DMSO itself has anti-inflammatory properties. These properties may have caused a decrease in follicle number, as it may have reduced the follicle-

generative activity of the cells within the skin. In future experiments it may be useful to reduce the concentration of DMSO in order to reduce any effects it may be having on follicle development.

Research has shown that γ-secretase functions through Notch signalling in embryonic mouse skin and its epithelial appendages. Notch receptors were found to be redundant in controlling epithelial proliferation and differentiation and tissue homeostasis. Loss of γ-secretase and Notch signalling in the epithelial component of skin, did not affect skin patterning, cell fate selection, or early differentiation within the follicle (Pan *et al.*, 2004). In their studies Notch-1-deficient epithelial placode cells prematurely invaded the dermis suggesting that Notch-1 signalling was involved in regulating the onset of this process. Loss of Notch-1 signalling was found to lead to a gradual loss of follicles shortly after parturition, cyst formation and premature onset of catagen in remaining follicles.

Blocking Notch signalling in d 70 Tukidale skin caused fewer follicles to form compared to skin treated with DMSO alone. This suggested that DAPT inhibited follicle development. Blocking of Notch signalling in d 70 Merino anterior skin samples resulted in an increase in follicle numbers and an increase in follicle size, compared to the DMSO control skin. The larger follicle size would presumably produce a thicker fibre. This finding was in agreement with the Founder Cell Theory, in which it is believed that an inverse relationship between follicle density and fibre size exists (Moore *et al.*, 1989).

Foetal Merino skin collected from midside and posterior sample sites on d 70 did not respond to DAPT in the same manner as the anterior skin samples. This suggested that the skin from these sites was more sensitive to DAPT treatment than the anterior skin, even though no initial difference in follicle number was detected. Investigating, harvesting and treating skin with DAPT at different developmental stages in the Merino suggested that around d 70 was the optimal time to begin treatment as DAPT had a more profound influence on follicle numbers at this time point. Although dermal papilla cell aggregation and therefore follicle development was not abolished, DAPT did have a negative effect on follicle development in skins. Therefore, Notch signalling appeared to play a role in both dermal papilla cell aggregation (in the rat and sheep) and the formation of follicle buds in foetal sheep skin (Merino and Tukidale) *in vitro*.

No differences were detected in Delta-1 protein expression in d 70 Merino skin organ cultures on d 0 compared to the skin after 4 d of treatment, or between the different treatment groups on d 4. However, few cells stained in any of these samples and the staining pattern appeared highly irregular. As a result of this patchy expression throughout each of the

samples, no real conclusions could be made on whether DAPT had any effect on Delta-1 protein expression, though we have previously demonstrated this effect in dermal papilla cultures.

The Notch-1 cDNA probe used for the *in situ* hybridisations, would have bound to Notch-1 RNA irrespective of Notch-1 being cleaved at the S3 site (Figure 4.1) by DAPT. There are a couple of possible explanations for the increased level of Notch detected in the mesenchyme of the d 70 Merino DAPT-treated skin. Firstly, the cells may have responded to the blockade of Notch signalling by producing more Notch receptor in an attempt to activate the downstream Notch targets. Secondly, the Notch-1 receptor may have accumulated on the cell membrane due to the failure of the receptor to undergo S3 cleavage, thereby leaving Notch in its membrane-bound form. As more receptors were produced by the cell and processed up to the S3 cleavage stage, there may have been an accumulation of membrane-bound Notch receptors, compared to a cell that had not been treated with DAPT. Overall, these results suggested that DAPT increased the level of Notch-1 transcripts in the mesenchymal cells by inhibiting activation of the Notch receptor. Alternatively, these results may have been due to a backlog of unprocessed Notch-1 receptor and not increased transcription of Notch, as we know that the cDNA probe did not differentiate between membrane-tethered Notch-1 and Notch-1 that had undergone S3 cleavage. Therefore no radical morphological differences may have been expected in the skin on d 0 and d 4 of the trial. Proteolytic cleavage of Notch is an irreversible process whereby each Notch receptor molecule signals once, so that the intensity and duration of the signal cannot be regulated through desensitisation of the receptor (Schweisguth, 2004). Up-regulation of Notch-1 in the mesenchyme may have had effects on the tissue and follicle morphogenesis at a later stage of development. However, 4 d in culture was not sufficiently long to visualise any long-term effects that blocking Notch signalling may have had on follicle development. From previous research it could be presumed that the major effect of inhibiting Notch-1 signalling in skin would be evident in the mesenchyme as Cre-lox studies have shown that a Notch signal was not required for placode formation in embryonic mouse skin. The Notch-deficient epidermis appeared significantly thickened (Rangarajan *et al.*, 2001; Vauclair *et al.*, 2005), suggesting Notch was involved in regulating the proliferation of epidermal cells.

In the skin cultures, Notch appeared to play a role in the initiation and development of follicles. In the absence of Notch signalling, cells may have been recruited to the existing follicle buds, increasing their size. If the function of Notch in the skin was to repress cell differentiation, blocking Notch would encourage cell differentiation. These results suggested

that Notch signalling was involved in the initiation of new follicles. In the absence of Notch signalling existing follicles appeared to increase in size in preference to forming new follicles. Therefore it was possible that follicles in the skin required Notch-Delta heterotypic associations for new follicles to develop. When Notch was unavailable, due to DAPT-treatment, Delta-bearing cells may have associated with the existing follicles. This study and others (Rangarajan *et al.*, 2001; Pan *et al.*, 2004; Vauclair *et al.*, 2005) have shown that the major site of expression of Notch and its ligands is the epidermis. This makes the finding of the effects of DAPT on dermal papilla cells interesting but complicates the interpretation of results in the whole skin because one might expect that, despite the cited transgenic mouse studies, there may be residual effects within the epithelial compartment of developing follicles.

CHAPTER 7: GENERAL DISCUSSION AND CONCLUSIONS

In this investigation, foetal sheep skin collected from Merino and Tukidale animals was sampled prior to and during follicle initiation. The process of primary follicle initiation had commenced in all foetal skins sampled on d 70 of gestation.

Merinos and Tukidales are breeds of sheep with markedly different follicle characteristics yet counts of the proportions of mesenchymal cells (reported in Chapters 3 and 4) during wool follicle initiation are similar. During follicle initiation at d 70, a similar proportion of mesenchymal cells aggregated to form the dermal condensate in the Merino and Tukidale skin samples, a finding that was in disagreement with both the Founder Cell Theory (Moore *et al.*, 1989) and Reaction-Diffusion theory (Nagorcka, 1995a) of follicle development. The Founder Cell theory describes a developmental mechanism that was proposed to control both follicle diameter and fibre size. However, the breed differences and vastly different wool characteristics of the Merino and Tukidale skin were not evident in the foetal skin samples investigated in this project. No significant differences in the proportions of Notch-1 or Delta-1 labelled or unlabelled cells within the dermal condensates were detected between these two breeds. The possibility that a select subpopulation of mesenchymal cells may participate in primary wool follicle initiation (Moore *et al.*, 1989) cannot be discounted from these studies, as differential labelling for Notch-1 and Delta-1 was evident in the mesenchyme of Merino and Tukidale skins both prior to and during follicle initiation. In disagreement with the Founder Cell theory, the findings of this study suggest that the dimensions of the wool fibre are not specified during follicle morphogenesis. These theories do not take into account differences in the mitotic potential of the dermal condensate, following follicle initiation that might explain the differences in follicle size and fibre diameter seen in the mature animal. Adelson *et al.* (2002) found no correlation between foetal primary wool follicle rudiment diameter (d 81) and adult wool fibre diameter, and showed that the bulk of dermal condensate proliferation occurred in a 5 day window towards the end of primary follicle development. Their results along with those obtained from this study indicate that the genes that determine fibre diameter are expressed after follicle initiation and that follicle density and fibre diameter are specified separately during development. Therefore, it would be possible to influence one without necessarily affecting the other. Cell proliferation in the dermal condensate could account for the increase in cell number as a function of the developmental stage. While the initial formation of the dermal condensate may

involve cell migration, the increase in cell number during dermal papilla growth could be explained solely on the basis of cell proliferation (Adelson *et al.*, 1992).

In this study, no significant differences in cell number within the dermal condensate were detected between Merino and Tukidale skin sampled on d 70. The mitotic potential of cells within the condensate of these different breeds must differ, with the dermal condensate in the Tukidale having a higher level of proliferation compared to the Merino. An alternative explanation for the larger fibre diameter in the Tukidale is that the dermal condensate recruits cells from the mesenchymal cell population or the connective tissue sheath (Jahoda, 2003) into the prepapilla following follicle initiation and that the rate of migration of cells into the condensate occurs at a higher rate in the Tukidale than in the Merino. This recruitment may be from an innate mesenchymal cell population specified before follicle initiation. Thus, studies need to be targeted at the dermal condensate following follicle initiation, to determine the factors responsible for creating the differences seen in the adult fibre characteristics of the Merino and Tukidale sheep skin.

The results of this study have led to the development of an alternative hypothesis for the morphogenesis of primary wool follicles. As no differences were detected in the numbers of cells within the dermal condensates of primary wool follicles in Merino and Tukidale, it is suggested that wool follicle initiation occurs by similar mechanisms in all sheep, regardless of their differing adult fleece characteristics. However, following follicle initiation, different signalling molecules may be expressed in such different breeds so as to control the rate of cell proliferation within the dermal prepapilla. Alternatively, the dermal condensate may not act entirely as a separate structure from the other mesenchymal cells and may recruit cells from the connective tissue sheath (Jahoda, 2003) or mesenchymal cell population. This would offer an alternative or additional method to the postulated cell proliferation within the condensate (Adelson *et al.*, 1992). Such methods would provide the dermal prepapilla with ways to rapidly increase its cell number and would allow the prepapilla within the Tukidale skin to rapidly increase in cell number in comparison to the fine-woolled Merino. Thereby, other signalling molecules than those investigated in this study are likely involved in development of the dermal prepapilla following follicle initiation. The Notch signalling pathway may well be involved in the later development and expansion of the prepapilla cell population. However, it is beyond the scope of this study to speculate on the roles of the Notch signalling pathway, and in particular Notch-1 and Delta-1, in such development of the wool follicle.

In situ hybridisation studies showed that transcripts to Notch-1 and Delta-1 were expressed in foetal sheep skin prior to and during follicle initiation, suggesting the

involvement of these genes in follicle initiation. The localisation of these transcripts appeared to be similar in Merino and Tukidale samples, suggesting a common developmental pathway of wool follicle development in the two breeds. Northern hybridisations of the Delta-1 probe, and that conducted previously of the Notch-1 probe (Gordon-Thomson *et al.*, 2008) confirmed the probes used were binding to mRNA in sheep skin that corresponded with other known mammalian Delta-1 and Notch-1 homologs.

Prior to and during follicle initiation, Delta-1 and Notch-1 staining was strong in the epithelium and appeared to be concentrated in the basal layer, where stem cells are known to reside (Lavker *et al.*, 1993; Watt, 2001; Alonso and Fuchs, 2003). Negligible Delta-1 staining was detected in the epithelial plug. Notch-1 transcripts were detected in some cells within the epithelial plug, suggesting Notch-1 may be preventing those cells from differentiating. This finding agrees with other research suggesting Notch signalling maintains cells in an undifferentiated state (Arias *et al.*, 2002). Significantly fewer mesenchymal cells were labelled with Delta-1 and Notch-1, relative to the remaining mesenchymal cell population. This finding suggested these genes may be used as a sorting mechanism, by which some cells can be distinguished from the remainder of the mesenchymal cell population. The cells expressing Delta-1 and Notch-1 in the mesenchyme may be signalling to their neighbouring mesenchymal cells using the Nocth signalling mechanism of lateral inhibition to prevent the surrounding cells from taking on the same dermal condensate fate. It is likely that Notch signalling is interacting with other cytokine signalling pathways (including WNT, Bone Morphogenetic Protein, Fibroblast Growth Factor, Sonic Hedgehog and Transforming Growth Factor-β) that are known to regulate skin and follicle development.

Within the d 70 mesenchyme differential staining of Delta-1 and Notch-1 was observed. A significantly lower proportion of mesenchymal cells expressing the transcripts were found compared to the remaining non-stained mesenchymal cells. In contrast, the majority of cells within the dermal condensate expressed Delta-1, and a small proportion of cells in the dermal condensate, located along the dermal condensate – mesenchymal junction expressed Notch-1. Thus, Delta-1 and Notch-1 labelling may be used during wool follicle development as a mechanism for selecting cells to adopt a follicular fate and so be incorporated into the dermal condensate. Those cells expressing Delta-1 and Notch-1 may be signalling to their neighbouring cells, instructing them not to take on a similar cell fate, most likely by lateral inhibition, similar to that described in development of the nervous system in *Drosophila* by Pourquié (2000). The significantly higher proportion of Delta-1 labelled cells in the dermal condensate compared to unlabelled cells suggested that Delta-1 may be used during wool

follicle development to maintain the tightly-packed association of cells within the condensate. The proportion of Notch-1 expressing cells in the dermal condensate was significantly lower than the proportion of unlabelled cells. Interestingly, the cells bordering the condensate appeared to be expressing high levels of the Notch-1 transcript, highlighting a possible role for Notch-1 in distinguishing the dermal condensate from the surrounding undifferentiated mesenchyme. Thus, Delta-1 and Notch-1 signalling may be required for communication with mesenchymal cells prior to and during follicle formation, and recruitment of cells for aggregation to form the dermal condensate. Delta-1, but not Notch-1 may be responsible for maintaining the cells in close proximity to each other. This is likely as cells expressing Notch-1 will not bind to one another (Fehon *et al.*, 1990; Rebay *et al.*, 1991). However, Notch-Delta and Delta-Delta interactions would likely be working simultaneously within the cell populations of the mesenchyme and dermal condensate with both molecules detected in these studies.

Immunohistochemistry studies demonstrate that Notch pathway proteins are expressed in foetal sheep skin prior to and during follicle initiation, and the localisation of the proteins in the tissue was similar to that observed for the respective transcripts. Thus, the mRNA sequences for Delta-1 and Notch-1 were transcribed into protein within the cells. In the d 56 Merino samples, Delta-1 was expressed in the Merino epithelium, with high levels observed in the basal layer, and in a few mesenchymal cells. In the d 56 Tukidale samples, no Delta-1 protein was detected in the epithelium, and low levels of protein were detected in some mesenchymal cells. In the d 70 Merino samples, Delta-1 protein was detected in the epithelium, with negligible levels in the epithelial plug, in the mesenchyme with higher levels observed in mesenchymal cells lying beneath the epithelium, and in the dermal condensate. In the d 70 Tukidale skin, Delta-1 protein was detected in only a few mesenchymal cells. The differences in Delta-1 protein expression in the Merino and Tukidale samples were believed to be a result of problems exposing the antigenic sites for Delta-1 in the Tukidale samples, most likely an artefact of processing those samples.

Notch-1 protein expression was similar in Merino and Tukidale samples collected on d 56 and d 70 of gestation, and corresponded to the results obtained from the Notch-1 *in situ* hybridisation studies. In the d 56 samples, Notch-1 protein was detected in the epithelium, particularly in the basal layer, and in some mesenchymal cells. In the d 70 samples, protein was detected in the epithelium, particularly in the basal layer, in the epithelial plug, the dermal condensate, and some cells of the mesenchyme. Activated Notch-1 protein was detected in the epithelium, basal layer, epithelial plug and dermal condensate. Interestingly,

activated Notch protein was not detected in the superficial layer of the mesenchyme immediately below the epithelium indicating that Notch-1 was not signalling in those cells. Due to the inconsistency of this antibody and the high level of non-specific staining in the serum controls this antibody was not tested on d 56 skin samples. Therefore, whether Notch-1 was actively signalling in the superficial layer of the mesenchyme prior to follicle initiation cannot be commented on.

Due to Delta-1 immunoreactivity being negligible or absent in the epithelial plug it was most likely not involved in the formation of epithelial plugs. As Notch-1 expression was detected in the plug, it was assumed that the receptor was binding to another ligand, such as Jagged-1 that is expressed in these cells (Gordon-Thomson *et al.*, 2008). It is possible that other elements of the Notch signalling mechanism, involving the other three Notch receptors and four ligands, may operate in ovine skin during development.

Cell culture studies were used to investigate the role of the Notch signalling pathway on dermal papilla cells *in vitro*. First, an aggregating dermal papilla cell model was developed whereby rat and sheep cells were cultured on Matrigel™-coated dishes, in DMEM and 10% FBS. The effect of inhibiting Notch signalling was then explored using DAPT. In these studies, untreated cells and those treated with the diluent only, containing 0.1% DMSO (controls) when cultured for 31 d, produced similar numbers of condensed groups of cells and aggregations. It was presumed that the cell aggregations arose from condensed groups of cells that formed in the cultures. In the DAPT-treated cultures, the number of condensed groups of cells was significantly reduced and cell aggregation was abolished. Therefore, it was determined that by blocking S3 cleavage of Notch, dermal papilla cell aggregation was inhibited, clearly demonstrating the necessity of Notch signalling in the process of dermal papilla cell aggregation.

Delta-1 protein expression was investigated in aggregating and non-aggregating rat dermal papilla cultures. Delta-1 appeared to be upregulated in the aggregating papilla cells, with negligible expression observed in the non-aggregating cells. No Delta-1 protein was detected in cultures that had been treated with DAPT. These results suggested that Delta-1 played a role in maintaining the dermal papilla cells in close proximity with one another. As blocking Notch signalling also blocked cell aggregation, it was deduced that the papilla cells were binding via Delta-Notch, and possibly Delta-Delta, interactions.

A floating culture system in which foetal sheep skin was cultured on collagen-coated polycarbonate membranes was used to test the effect of DAPT treatment on the formation of wool follicle buds in intact skin over 4 d. Although the skins shrank and curled during the

culture period, the follicles maintained their appearance and the skin its morphological integrity, as shown in sectioned cultured skin on d 4. Importantly, it was demonstrated that follicle development resumed in culture, as follicle counts adjusted for skin shrinkage showed that the number of follicles in a skin increased during the 4 d trial. Culturing of skin collected prior to follicle initiation (d 56) was not as successful as d 70 skin, as only a few large, irregularly-spaced follicles developed. This suggested that distortion of the mesenchymal/epidermal cell interface through skin collection and during the initial period of culture altered the pattern of follicle initiation at this critical time point. In contrast, skin collected during primary follicle initiation showed a significant increase in follicle numbers after 4 d in culture, with new follicles forming at a rapid rate between those follicles already visible. Clearly the pattern of initiation sites had been established by the time the d 70 foetal skin had been harvested for the study.

DAPT had a small effect on follicle development over the culture period, when treatment was administered daily over the 4 day trials. The 0.1% DMSO control skins appeared to form fewer follicle buds in some cases, suggesting that DMSO also had some inhibitory effect on follicle initiation.

Treatment with DAPT appeared to have a negative effect on follicle formation in skins harvested during primary follicle initiation. In the d 70 Tukidale skin, DAPT treatment reduced the number of follicles that formed, and those follicles were larger than those observed in the control skins. In d 70 Merino skin samples originating from the anterior collection site, the number of follicles formed increased with DAPT treatment and those follicles were larger than those observed in the control skins. It was presumed that if these follicles continued to develop to maturity and produced a fibre, they would have produced a larger follicle and thicker fibre. Interestingly, the comparison of sampling sites demonstrated that the different sites possessed variable sensitivity to DAPT treatment, with the anterior skin being less responsive. This observation could be explained by the antero-posterior gradient of wool follicle development known to occur over the foetus during primary follicle initiation (Carter and Hardy, 1947). As the skin was sampled from anterior, midside and posterior sites, the follicles in the anterior skins would have been slightly more advanced than at the other two sites. Thereby, Notch signalling may no longer have been essential in the anterior skins as the cells may have already received a Notch signal, instructing the cells to form new follicles at the regularly-spaced initiation sites. In contrast, the midside and posterior skins may not have yet received a Notch signal and thereby the cells in those skins were not instructed to

form a new follicle, so that the cells that would normally form a new follicle were instead incorporated into the already-existing follicles making them larger.

The expression of Notch-1 transcripts and Delta-1 protein were investigated in d 70 cultured skins. Notch signalling was deemed to have a role in the formation of follicle buds in foetal sheep skin. No differences were detected in Delta-1 protein expression between skins at the start (d 0) and end (d 4) of the trial following treatment. The expression of the antigenic sites in the tissue may have been affected as a result of the tissue processing and culturing process. Notch-1 transcript expression had increased from d 0 to d 4 in the mesenchyme of the d 70 Merino skin following treatment using DAPT, suggesting that blocking Notch signalling either increased Notch-1 transcription or led to its accumulation through lack of degradation.

The expression of Delta-1 and Notch-1 transcripts and protein prior to and during wool follicle development suggests that the Notch signalling pathway has an integral role in follicle development. Labelling of a small proportion of mesenchymal cells for Delta-1 and Notch-1 in the skin prior to follicle initiation was suggestive of these genes and protein providing a means by which these cells were able to differentiate from the rest of the mesenchymal cell population. It was thought that the signalling mechanism of lateral inhibition may be responsible for the up-regulation of Delta-1 and Notch-1 in the small subpopulation of mesenchymal cells observed to be signalling. Those cells that were expressing the Notch-1 or Delta-1 signal were believed to be instructing their neighbouring mesenchymal cells not to take on the same fate. Once those cells had signalled to their neighbouring cells, it was suggested that they migrated to evenly-spaced positions below the basal layer of the epidermis, as instructed by signalling of Notch or Delta, or another molecule, where they formed aggregations with one another and a dermal condensate was created. The elevated level of Delta-1 in the dermal condensate and apparent bordering of Notch-1 expressing cells in the dermal condensate suggest a role for these genes in maintaining the condensate as a separate population of cells. In addition, Delta-1 protein expression was shown to be elevated in aggregating dermal papilla cells. Cell culture studies demonstrated that Notch signalling was required for cell aggregation to occur, and that by blocking the Notch pathway aggregation was abolished and Delta-1 protein expression was abolished. Thus, the dermal papilla-like aggregations that formed *in vitro* were dependent on Delta-Notch and Delta-Delta interactions. Further, treatment of foetal skin with DAPT caused a delay in the formation of new follicle buds and those follicles that formed following DAPT treatment were larger.

These results are suggestive of Notch playing a role in follicle initiation and in the regulation of the recruitment of mesenchymal cells to form the dermal condensate.

The cell culture studies established a role for Notch signalling in the aggregation of dermal papilla cells. These results taken together with the gene expression studies show that Notch-1 and Delta-1 are intimately involved in establishing the dermal condensates during wool follicle differentiation. However, due to the lack of differences in the number of cells expressing Delta-1 or Notch-1 transcripts in the condensates of Merino and Tukidale foetal skin, it was believed that these genes may not be of use as a source of genetic markers for identifying breed-specific differences in the dermal prepapilla cell population. However, the studies are limited by our inability to monitor changes in expression of Notch-related genes in real time for the duration of the critical period of follicle initiation: transient expression of these genes may be all that is required to specify mesenchymal cells as potential prepapilla cells which then aggregate through Notch receptor-ligand interactions. Subsequent proliferative activity within this cell population may then determine fibre diameter, although follicle pattern formation is more difficult to accommodate through Notch-ligand interactions.

Taken together, results from the *in situ* hybridisation, immunohistochemistry, cell and organ culture studies all point to the Notch signalling pathway being involved in primary wool follicle initiation in Merino and Tukidales. Some differences between gene transcript and protein expression were observed. One interesting finding was that Delta-1 protein in the d 70 Merino samples appeared to be more strongly expressed in mesenchymal cells below the epithelium. This observation was not detected in the d 70 Tukidale samples, suggesting the Delta-1 transcript was not translated into protein in the Tukidale. Notch-1 transcript and protein expression was similar in the d 56 samples of both breeds. In the d 70 samples, Notch-1 protein expression was found to be similar in the Merino and Tukidale tissue and corresponded to Notch-1 transcript expression, suggesting the transcript was being translated into the protein. Notch-1 protein expression appeared to be stronger in the d 70 Tukidale when compared to the Merino. However, limited conclusions could be drawn from the Notch-1 immunohistochemistry studies due to the presence of non-specific staining in the controls. Another interesting finding was that no activated Notch-1 protein was detected in a band of mesenchymal cells below the epithelium in d 70 Merino skin. However, the non-specific staining in the activated Notch-1 controls limited any conclusions that could be drawn from these experiments. Culturing dermal papilla cells demonstrated that Notch signalling was required for the papilla cells to aggregate, and that Delta-1 signalling was extremely strong within the aggregations. The results from the d 70 Merino skin culture trials demonstrated that

Notch-1 gene transcripts were expressed in the skin prior to and following the 4 day culture period, and that the localisation of transcripts was similar to that seen in the d 70 skins, as discussed earlier. Unfortunately, Delta-1 protein expression in the skins appeared to be affected by the process of preparing and culturing the skin. There was no consistency in the localisation of the protein within the cultured skins. This was possibly a result of the antigenic sites within the tissue being affected by D-PBS.

Neither the Reaction-Diffusion or Founder Cell hypotheses were able to predict the similarities in the number of cells within the dermal condensates during Merino and Tukidale follicle initiation as seen in these studies. However, the theory of cell proliferation in the dermal condensate following follicle initiation is consistent with the predictions of the Reaction-Diffusion system. Another possibility is that cells from the connective tissue sheath move into the dermal prepapilla. Use of both Notch-1 and Delta-1 as mesenchymal cell markers showed that there is expression of each in cells of the dermal condensate and surrounding mesenchyme. Further, while we have shown that there are no differences between the proportions of cells in the dermal condensates of the developing Merino and Tukidale sheep wool primary follicles, the number of Notch-1 and Delta-1 expressing cells is different, with one-third expressing Notch-1 and two-thirds expressing Delta-1. Whether the respective Notch-1-expressing and Delta-1-expressing cells are strictly different populations or whether some cells of the dermal condensate express each of these markers, and some express neither, is yet to be determined. Clearly further investigations of a larger range of candidate molecules in different experimental models are required to characterise the biological control of this important developmental mechanism for the benefit of the wool grower.

Further studies are needed to improve the floating skin culture technique so that clear and unequivocal results can be obtained. It would be desirable to minimise tissue shrinkage to prevent the separation of the skin from its supporting membrane in the culture medium. This would facilitate accurate counting of the number of follicle buds at the end of the experimental period. If shrinkage of the skins could be eliminated or reduced, the skins could be cultured for periods longer than 4 days. It would be advantageous to repeat the experiments using skin collected during primary follicle initiation from Merino and Tukidale foetuses. This would allow between breed comparisons of the formation of follicle buds in skin collected at comparable times and from the same anatomical sites.

The immunohistochemistry and *in situ* hybridisation studies to localise the Notch receptor and its ligands require further investigation. Additional immunohistochemistry

studies using the activated Notch antibody would be of benefit if unambiguous results could be obtained by eliminating the non-specific staining in the negative control tissue. Expression of the activated protein in sheep skin prior to follicle initiation would be of interest, as well as in the cultured skins following treatment with DAPT. It would also be beneficial to conduct *in situ* hybridisation studies using double staining with Notch-1 and Delta-1 so that the expression patterns of both transcripts could be studied simultaneously in skin collected prior to and during follicle initiation. Further studies of this family of receptors and ligands within the context of other developmental processes and signalling systems will assist us in determining their relative importance to wool follicle development.

Once the ovine Notch signalling pathway genes are completely sequenced, it would be beneficial to conduct *in situ* hybridisation experiments using ovine probes on ovine tissue. This may serve as a means to eliminate the non-specific staining seen in the DIG-labelled sense controls. Other experimental approaches that would be worthwhile exploring in order to investigate the genes being expressed in the foetal sheep mesenchyme of skin collected from Merino and Tukidale animals would be real-time PCR. Another, more specific approach could be to concentrate on the signalling molecules unique to the dermal prepapilla cell population by using laser capture techniques in combination with real-time PCR. Such techniques would give further weight to the studies conducted here.

REFERENCE LIST

Adelson, D. L., Kelley, B. A., and Nagorcka, B. N. (1992). Increase in dermal papilla cells by proliferation during development of the primary wool follicle. *Australian Journal of Agricultural Research* **43,** 843-856.

Adelson, D. L., Hollis, D. E., and Brown, G. (2002). Wool fibre diameter and follicle density are not specified simultaneously during wool follicle initiation. *Australian Journal of Agricultural Research* **53,** 1003-1009.

Adelson, D. L., Cam, G. R., DeSilva, U., and Franklin, I. R. (2004). Gene expression in sheep skin and wool (hair). *Genomics* **83,** 95-105.

Alberts, B., Johnson, A., Lewis, J., Raff, M., Roberts, K., and Walter, P. (2002). "Molecular Biology of the Cell." Taylor and Francis Group.

Alonso, L., and Fuchs, E. (2003). Stem cells of the skin epithelium. *Proceedings of the National Academy of Sciences USA* **100 (Suppl.),** 11830-11835.

Andl, T., Ressy, S. T., Gaddapara, T., and Millar, S. E. (2002). WNT signals are required for the initiation of hair follicle development. *Developmental Cell* **2,** 643-653.

Arias, A. M., Zecchini, V., and Brennan, K. (2002). CSL-independent Notch signalling: a checkpoint in cell fate decisions during development. *Current Opinion in Genetics & Development* **12,** 524-533.

Artavanis-Tsakonas, S., and Simpson, P. (1991). Choosing a cell fate: a view from the *Notch* locus. *Trends in Genetics* **7,** 403-408.

Artavanis-Tsakonas, S., Matsuno, K., and Fortini, M. E. (1995). Notch signaling. *Science* **268,** 225-232.

Artavanis-Tsakonas, S., Rand, M. D., and Lake, R. J. (1999). Notch signalling: cell fate control and signal integration in development. *Science* **284,** 770-776.

Barker, N., Morin, P. J., and Clevers, H. (2000). The Yin-Yang of TCF/beta-catenin signalling. *Advanced Cancer Research* **77,** 1-24.

Baron, M., Aslam, H., Flasza, M., Fostier, M., Higgs, J. E., Mazaleyrat, S. L., and Wilkin, M. B. (2002). Multiple levels of Notch signal reduction (Review). *Molecular Membrane Biology* **19,** 27-38.

Baron, M. (2003). An overview of the Notch signalling pathway. *Seminars in Cell & Developmental Biology* **14,** 113-119.

Behrens, J., von Kries, J. P., Kuhl, M., Bruhn, L., Wedlich, D., Grosschedl, R., and Birchmeier, W. (1996). Functional interaction of β-catenin with the transcription factor LEF-1. *Nature* **382,** 638-642.

Bernardos, R. L., Lentz, S. I., Wolfe, M. S., and Raymond, P. A. (2005). Notch-Delta signaling is required for spatial patterning and Müller glia differentiation in the zebrafish retina. *Developmental Biology* **278,** 381-395.

Bianchi, S., Dotti, M. T., and Federico, A. (2006). Physiology and pathology of notch signalling system. *Journal of Cellular Physiology* **207,** 300-308.

Billingham, R. E., and Silvers, W. K. (1965). Some Unsolved Problems in the Biology of the Skin. *In* "Biology of the Skin and Hair Growth" (A. G. Lyne and B. F. Short, Eds.), pp. 1-24. Angus & Robertson, Australia.

Blanpain, C., Lowry, W. E., Geoghegan, A., Polak, L., and Fuchs, E. (2004). Self-renewal, multipotency, and the existence of two cell populations within an epithelial stem cell niche. *Cell* **118,** 635-648.

Bonifacino, J. S., and Weissman, A. M. (1998). Ubiquitin and the control of protein fate in the secretory and endocytic pathways. *Annual Reviews in Cell Developmental Biology* **14,** 19-57.

Boras-Granic, K., Chang, H., Grosschedl, R., and Hamel, P. A. (2006). Lef1 is required for the transition of Wnt signalling from mesenchymal to epithelial cells in the mouse embryonic mammary gland. *Developmental Biology* **295,** 219-231.

Botto, S. A. (2000). The Notch pathway in ovine skin and wool follicle development. *In* "School of Science". The University of Western Sydney, Nepean.

Boulianne, G. L., de la Concha, A., Campos-Ortega, J. A., Jan, L. Y., and Jan, Y. N. (1993). The *Drosophila* neurogenic gene neuralized encodes a novel protein and is expressed in precursors of larval and adult neurons. *The EMBO Journal* **12,** 2586.

Bray, S. (1998). Notch signalling in *Drosophila*: three ways to use a pathway. *Seminars in Cell & Developmental Biology* **9,** 591-597.

Bray, S. (2006). Notch signalling: a simple pathway becomes complex. *Nature Reviews Molecular Cell Biology* **7,** 675-689.

Brown, G. H., Turner, H. N., Young, S. S. Y., and Dolling, C. H. S. (1966). Vital statistics for an experimental flock of Merino sheep. 3. Factors affecting wool and body characteristics, including the effect of age of ewe and its possible integration with method of selection. *Australian Journal of Agricultural Research* **17,** 577-581.

Bruckner, K., Perez, L., Clausen, H., and Cohen, S. (2000). Glycosyltransferase activity of Fringe modulates Notch-Delta interactions. *Nature* **406,** 411-415.

Buono, K. D., Robinson, G. W., Martin, C., Shi, S., Stanley, P., Tanigaki, K., Honjo, T., and Hennighasuen, L. (2006). The canonical Notch/RBP-J signaling pathway controls the balance of cell lineages in mammary epithelium during pregnancy. *Developmental Biology* **293,** 565-580.

Carson, C., Murdoch, B., and Roskams, A. J. (2006). Notch 2 and notch 1/3 segregate to neuronal and glial lineages of the developing olfactory epithelium. *Developmental Dynamics* **235,** 1678-1688.

Carter, H. B., and Hardy, M. H. (1947). Studies in the biology of the skin and fleece of sheep. IV. The hair follicle group and its topographical variations in the skin of the Merino foetus. *Bulletin of the Council for Scientific and Industrial Research, Australia* **215.**

Carter, H. B., and Clarke, W. H. (1957). The hair follicle group and skin follicle population of some non-Merino breeds of sheep. *Australian Journal of Agricultural Research* **8,** 109-119.

Celli, G., Larochelle, W. J., Mackem, S., Sharp, R., and Merlino, G. (1998). Soluble dominant-negative receptor uncovers essential roles for fibroblast growth factors in multi-organ induction and patterning. *European Molecular Biology Organization Journal* **17,** 642-655.

Champion, S. C., and Robards, G. E. (2000). Follicle characteristics, seasonal changes in fibre cross-sectional area and ellipticity in Australasian speciality carpet wool sheep, Romneys and Merinos. *Small Ruminant Research* **38,** 71-82.

Chang, C. H., Jiang, T. X., Lin, C. M., Burrus, L. W., Chuong, C. M., and Widelitz, R. (2004). Distinct Wnt members regulate the hierarchical morphogenesis of skin regions (spinal tract) and individual feathers. *Mechanisms of Development* **121,** 157-71.

Chapman, R. E. (1965). The Ovine Arrector Pili Musculature and Crimp Formation in Wool. *In* "Biology of the Skin and Hair Growth" (A. G. Lyne and B. F. Short, Eds.), pp. 201-232. Angus & Robertson, Australia.

Chiba, S. (2006). Concise review: Notch signaling in stem cell systems. *Stem Cells* **24,** 2437-2447.

Chitnis, A. (2006). Why is Delta endocytosis required for effective activation of Notch? *Developmental Dynamics* **235,** 886-894.

Chitnis, A. B. (2007). Notch signaling: a versatile tool for the fine patterning of cell fate in development. *In* "Principles of Developmental Genetics" (S. A. Moody, Ed.), pp. 316-339. Academic Press, Massachusetts, USA.

Chuong, C. M., Widelitz, R. B., Ting-Berreth, S. A., and Jiang, T. X. (1996). Early events during avian skin appendage regeneration: dependence on epithelial-mesenchymal interaction and order of molecular reappearance. *Journal of Investigative Dermatology* **107,** 639-646.

Claudinot, S., Nicolas, M., Oshima, H., Rochat, A., and Barrandon, Y. (2005). Long-term renewal of hair follicles from clonogenic multipotent stem cells. *Developmental Biology* **102,** 14677-14682.

Cohen, J. (1965). The Dermal Papilla. *In* "Biology of the Skin and Hair Growth" (A. G. Lyne and B. F. Short, Eds.), pp. 183-199. Angus & Robertson, Australia.

Crowe, R., Henrique, D., Ish-Horowicz, D., and Niswander, L. (1998). A new role for Notch and Delta in cell fate decisions: patterning the feather array. *Development* **125,** 767-775.

Dahlqvist, C., Blokzijl, A., Chapman, G., Falk, A., Dannaeus, K., Ibâñez, C. F., and Lendahl, U. (2003). Functional Notch signaling is required for BMP4-induced inhibition of myogenic differentiation. *Development* **130,** 6089-6099.

Dale, J. K., Maroto, M., Dequeant, M.-L., Malapert, P., McGrew, M., and Pourquié, O. (2003). Periodic Notch inhibition by Lunatic Fringe underlies the chick segmentation clock. *Nature* **421,** 275-278.

De Moerlooze, L., Spencer-Dene, B., Revest, J., Hajhosseini, M., Rosewell, L., and Dickson, C. (2000). An important role for the IIIb isoform of fibroblast growth factor receptor 2 (FGFR2) in mesenchymal-epithelial signaling during mouse organogenesis. *Development* **127,** 483-492.

De Strooper, B., Annaert, W., Cupers, P., Saftig, P., Craessaerts, K., Mumm, J. S., Schroeter, E. H., Schrijvers, V., Wolfe, M. S., Ray, W. J., Goate, A., and Kopan, R. (1999). A presenilin-1-dependent γ-secretase-like protease mediates release of Notch intracellular domain. *Nature* **398,** 518-522.

Dovey, H. F., John, V., Anderson, J. P., Chen, L. Z., de Sant Andrieu, P., Fang, L. Y., Freedman, S. B., Folmer, B., Goldbach, E., Holsztynska, E. J., Hu, K. L., Johnson-Wood, K. L., Kennedy, S. L., Kholodenkp, D., Knops, J. E., Latimer, L. H., Lee, M., Liao, Z., Lieberburg, I. M., Motter, R. N., Mutter, L. C., Nietz, J., Quinn, K. P., Sacchi, K. L., Seubert, P. A., Shopp, G. M., Thorsett, E. D., Tung, J. S., Wu, J., Yang, S., Yin, C. T., Schenk, D. B., May, P. C., Altstiel, L. D., Bender, M. H., Boggs, L. N., Britton, T. C., Clemens, J. C., Czilli, D. L., Dieckman-McGinty, D. K., Droste, J. J., Fuson, K. S., Gitter, B. D., Hyslop, P. A., Johnstone, E. M., Li, W. Y., Little, S. P., Mabry, T. E., Miller, F. D., and Audia, J. E. (2001). Functional gamma secretase inhibitors reduce beta-amyloid peptide levels in brain. *Journal of Neurochemistry* **76,** 173-181.

Dunwoodie, S. L., Henrique, D., Harrison, S. M., and Beddington, S. P. (1997). Mouse *Dll3*: a novel divergent *Delta* gene which may compelement the function of other *Delta* homologues during early pattern formation in the mouse embryo. *Development* **124,** 3065-3076.

Eames, B. F., and Schneider, R. A. (2005). Quail-duck chimeras reveal spatiotemporal plasticity in molecular and histogenic programs of cranial feather development. *Development* **132,** 1499-1509.

Ellisen, L. W., Bird, J., West, D. C., Soreng, A. L., Reynolds, T. C., Smith, S. D., and al, e. (1991). TAN-1, the human homologue of the Drosophila notch gene, is broken by chromosomal translocations in T lymphoblastic neoplasm. *Cell* **66,** 649-661.

Favier, B., Fliniaux, I., Thelu, J., Viallet, J. P., Demarchez, M., Jahoda, C. A. B., and Dhouailly, D. (2000). Localisation of members of the Notch system and the

differentiation of vibrissa hair follicles: receptors, ligands, and Fringe modulators. *Developmental Dynamics* **218,** 426-437.

Fehon, R. G., Kooh, P. J., Rebay, I., Regan, C. L., Xu, T., Muskavitch, M. A. T., and Artavanis-Tsakonas, S. (1990). Molecular interactions between the protein products of the neurogenic loci Notch and Delta, two EGF-homologous genes in Drosophila. *Cell* **61,** 523-534.

File, G. C. (1981). Highly fertile Merinos and their nutritional management through pregnancy and lactation. *Wool Technology and Sheep Breeding* **29,** 7-11.

Fleet, M. R., Forrest, J. W., Walker, S. K., and al, e. (2004). Foetal development of melanocyte populations in Merino wool-bearing skin. *Wool Technology and Sheep Breeding* **52,** 101-123.

Fleming, R. J., Gu, Y., and Hukriede, N. A. (1997). *Serrate*-mediated activation of Notch is specifically blocked by the product of the gene *fringe* in the dorsal compartment of the *Drosophila* wing imaginal disc. *Development* **124,** 2973-2981.

Fleming, R. J. (1998). Structural conservation of Notch receptors and ligands. *Seminars in Cell & Developmental Biology* **9,** 599-607.

Fuβ, B., and Hoch, M. (2002). Notch signaling controls cell fate specification along the dorsoventral axis of the *Drosophila* gut. *Current Biology* **12,** 171-179.

Fuchs, E. (2001). Beauty is skin deep: the fascinating biology of the epidermis and its appendages. *In* "The Harvey Lectures, Series 94", pp. 47-78.

Fuchs, E. (2007). Scratching the surface of skin development. *Nature* **445,** 834-842.

Fuchs, E. (2008). Skin stem cells: rising to the surface. *Journal of Cell Biology* **180,** 273-284.

Gat, U., DasGupta, R., Degenstein, L., and Fuchs, E. (1998). De novo hair follicle morphogenesis and hair tumors in mice expression a truncated β-catenin in skin. *Cell* **98,** 605-614.

Geling, A., Steiner, H., Willem, M., Bally-Cuif, L., and Haass, C. (2002). A γ-secretase inhibitor blocks Notch signaling *in vivo* and causes a severe neurogenic phenotype in zebrafish. *EMBO Reports* **3,** 688-694.

Gordon-Thomson, C., Botto, S. A., Cam, G. R., and Moore, G. P. M. (2008). Notch pathway gene expression and wool follicle cell fates. *Australian Journal of Experimental Agriculture* **48,** 648-656.

Gray-Schopfer, V., Wellbrock, C., and Marais, R. (2007). Melanoma biology and new targeted therapy. *Nature* **445,** 851-857.

Gritli-Linde, A., Hallberg, K., Harfe, B. D., Reyahi, A., Kannius-Janson, M., Nilsson, J., Cobourne, M. T., Sharpe, P. T., McMahon, A. P., and Linde, A. (2007). Abnormal hair development and apparent follicular transformation to mammary gland in the absence of Hedgehog signaling. *Developmental Cell* **12,** 99-112.

Guo, M., Jan, L. Y., and Jan, Y. N. (1996). Control of daughter cell fates during asymmetric cell division: interaction of Numb and Notch. *Neuron* **17,** 27-41.

Gupta-Rossi, N., Le Bail, N., Gonen, H., Brou, C., Lgeat, F., Six, E., Ciechanover, A., and Israel, A. (2001). Functional interaction between SEL-10, a F-box protein, and the nuclear form of activated Notch1 receptor. *Journal of Biological Chemistry* **276,** 34371-34378.

Haines, N., and Irvine, K. D. (2003). Glycosylation regulates Notch signalling. *Nature* **4,** 786-794.

Hamada, Y., Kadokawa, Y., Okabe, M., Ikawa, M., Coleman, J. R., and Tsujimoto, Y. (1999). Mutation in ankyrin repeats of the mouse Notch2 gene induces early embryonic lethality. *Development* **126,** 3415-3424.

Hammerschmidt, B., and Schlake, T. (2007). Localization of *Shh* expression by *Wnt* and *Eda* affects axial polarity and shape of hairs. *Developmental Biology* **305,** 246-261.

Han, G., Li, A. G., Liang, Y.-Y., Owens, P., He, W., Lu, S., Yoshimatsu, Y., Wang, D., ten Dijke, P., Lin, X., and Wang, X.-J. (2006). Smad7-induced β-catenin degradation alters epidermal appendage development. *Developmental Cell* **11,** 301-312.

Handjiski, B. K., Eichmüller, S., Hofmann, U., Czarnetzki, B. M., and Paus, R. (1994). Alkaline phosphatase activity and localization during the murine hair cycle. *British Journal of Dermatology* **131,** 303-310.

Hansson, E. M., Lendahl, U., and Chapman, G. (2004). Notch signaling in development and disease. *Seminars in Cancer Biology* **14,** 320-328.

Hardy, M. H. (1949). The development of mouse hair *in vitro* with some observations on pigmentation. *Journal of Anatomy* **83,** 364-384.

Hardy, M. H., and Lyne, A. G. (1956). The pre-natal development of wool follicles in the Merino sheep. *Australian Journal of Biological Science* **9,** 423-441.

Hardy, M. H. (1992). The secret life of the hair follicle. *Trends in Genetics* **8,** 55-61.

Heitzler, P., and Simpson, P. (1991). The choice of cell fate in the epidermis of Drosophila. *Cell* **34,** 1083-1092.

Henrique, D., Hirsinger, E., Adam, J., Le Roux, I., Pourquie, O., Ish-Horowicz, D., and Lewis, J. (1997). Maintenance of neuroepithelial progenitor cells by Delta-Notch signaling in the embryonic chick retina. *Current Biology* **7,** 661-670.

Herranz, H., Stamataki, E., Feiguin, F., and Milán, M. (2006). Self-refinement of Notch activity through the transmembrane protein Crumbs: modulation of γ-secretase activity. *EMBO Reports* **7,** 297-302.

Hershko, A., and Ciechanover, A. (1998). The ubiquitin system. *Annual Reviews in Biochemistry* **67,** 425-479.

Hicks, C., Johnston, S. H., di Sibio, G., Collazo, A., Vogt, T. F., and Weinmaster, G. (2000). Fringe differentially modulates Jagged1 and Delta1 signalling through Notch1 and Notch2. *Nature Cell Biology* **2,** 515-520.

Hocking Edwards, J. E., and Hynd, P. I. (1992). Cellular characteristics of wool follicles and fibres in finewool and strongwool Merinos. *Australian Journal of Agricultural Research* **43,** 355-365.

Hocking Edwards, J. E., Birtles, M. J., Harris, P. M., Parry, A. L., Paterson, E., Wickham, G. A., and McCutcheon, S. N. (1996). Pre- and post-natal wool follicle development and density in sheep of five genotypes. *Journal of Agricultural Science, Cambridge* **126,** 363-370.

Hocking Edwards, J. E. (1999). Reduction in wool follicles prior to birth in Merino sheep. *Reproduction, Fertility and Development* **11,** 229-234.

Hubbard, E. J., Wu, G., Kitajewski, J., and Greenwald, I. (1997). Sel-10, a negative regulator of lin-12 activity in *Caenorhabditis elegans*, encodes a member of the CDC4 family of proteins. *Genes & Development* **11,** 3182-3193.

Huelsken, J., Vogel, R., Erdmann, B., Cotsarelis, G., and Birchmeier, W. (2001). β-Catenin controls hair follicle morphogenesis and stem cell differentiation in the skin. *Cell* **105,** 533-545.

Ibrahim, L., and Wright, E. A. (1982). A quantitative study of hair growth using mouse and rat vibrissal follicles. I. Dermal papilla volume determines hair volume. *Journal of Embryological Experimental Morphology* **72,** 209-224.

Iino, M., Ehama, R., Nakazawa, Y., Iwabuchi, T., Ogo, M., Tajima, M., and Arase, S. (2007). Adensoine stimulates fibroblast growth factor-7 gene expression *via* adensosine A2b receptor signaling in dermal papilla cells. *Journal of Investigative Dermatology* **127,** 1318-1325.

Inamatsu, M., Matsuzaki, T., Iwanari, H., and Yoshizato, K. (1998). Establishment of rat dermal papilla cell lines that sustain the potency to induce hair follicles from afollicular skin. *Journal of Investigative Dermatology* **111,** 767-775.

Irvine, K. D. (1999). Fringe, Notch, and making developmental boundaries. *Current Opinion in Genetic Development* **9,** 434-441.

Irvine, K. D., and Rauskolb, C. (2001). Boundaries in development: Formation and function. *Annual Reviews in Cellular Developmental Biology* **17,** 189-214.

Ito, M., Yang, Z., Andl, T., Cui, C., Kim, N., Millar, S. E., and Cotsarelis, G. (2007). Wnt-dependent *de novo* hair follicle regeneration in adult mouse skin after wounding. *Nature* **447,** 316-321.

Jahoda, C. A. B., and Oliver, R. F. (1984). Vibrissa dermal papilla cell aggregative behaviour *in vivo* and *in vitro*. *Journal of Embryological Experimental Morphology* **79,** 211-224.

Jahoda, C. A. B. (2003). Cell movement in the hair follicle dermis - more than a two-way street? *The Journal of Investigative Dermatology* **121,** ix-xi.

Jahoda, C. A. B., Oliver, R. F., Reynolds, T. C., Forrester, J. C., Gillespie, J. W., Cserhalmi-Friedman, P. B., Christiano, A. M., and Horne, K. A. (2001). Trans-species hair growth induction by human hair follicle dermal papillae. *Experimental Dermatology* **10,** 229-237.

Jahoda, C. A. B., Whitehouse, C. J., Reynolds. A. J., Hole, N. (2003). Hair follicle dermal cells differentiate into adipogenic and osteogenic lineages. *Experimental Dermatology* **12,** 849-859.

Jenkinson, D. M., Montgomery, I., and Elder, H. Y. (1979). The ultrastructure of the sweat glands of the ox, sheep and goat during sweating and recovery. *Journal of Anatomy* **129,** 117-140.

Joutel, A., Corpechot, C., Ducros, A., Vahedi, K., Chabriat, H., Mouton, P., and al, e. (1996). Notch3 mutations in CADASIL, a hereditary adult-onset condition causing stroke and dementia. *Nature* **826,** 213-217.

Joutel, A., and Tournier-Lasserve, E. (1998). Notch signalling pathway and human disease. *Seminars in Cell & Developmental Biology* **9,** 619-625.

Kanwar, R., and Fortini, M. E. (2004). Notch signalling: a different sort makes the cut. *Current Biology* **14,** R1043-R1045.

Kaplan, E. D., and Holbrook, K. A. (1994). Dynamic expression patterns of tenascin, proteoglycans, and cell adhesion molecules during human hair follicle morphogenesis. *Developmental Dynamics* **199,** 141-155.

Kelly, R. W., Macleod, I., Hynd, P. I., and Greeff, J. (1996). Nutrition during fetal life alters annual wool production and quality in young Merino sheep. *Australian Journal of Experimental Agriculture* **36,** 259-67.

Kim, J., Irvine, K. D., and Carrol, S. B. (1995). Cell recognition, signal induction and symmetrical gene activation at the dorsal-ventral boundary of the developing *Drosophila* wing. *Cell* **82,** 795-802.

Kishimoto, J., Burgeson, R. E., and Morgan, B. A. (2000). Wnt signaling maintains hair-inducing activity of the dermal papilla. *Genes & Development* **14,** 1181-1185.

Kleinman, H. K., McGarvey, M. L., Hassell, J. R., Star, V. L., Cannon, F. B., Laurie, G. W., and Martin, G. R. (1986). Basement membrane complexes with biological activity. *Biochemistry* **25,** 312-318.

Kollar, E. J. (1966). An *in vitro* study of hair and vibrissae development in embryonic mouse skin. *The Journal of Investigative Dermatology* **46,** 254-262.

Koo, E. H., and Kopan, R. (2004). Potential role of presenilin-regulated signaling pathways in sporadic neurodegeneration. *Nature Medicine* **10 (suppl. 1),** S26-S33.

Kopan, R. (2002). Notch: a membrane-bound transcription factor. *Journal of Cell Science* **115,** 1095-1097.

Kratochwil, K., Dull, M., Farinas, I., Galceran, J., and Grosschedl, R. (1996). Lef1 expression is activated by BMP-4 and regulates inductive tissue interactions in tooth and hair development. *Genes & Development* **10,** 1382-1394.

Krebs, L. T., Xue, Y., Norton, C. R., Shutter, J. R., Maguire, M., Sundberg, J. P., Gallahan, D., Closson, V., Kitajewski, J., Callahan, R., Smith, G. H., Stark, K. L., and Gridley, T. (2000). Notch signaling is essential for vascular morphogenesis in mice. *Genes & Development* **14,** 1343-1352.

Krebs, L. T., Xue, Y., Norton, C. R., Sundberg, J. P., Beatus, P., Lendahl, U., Joutel, A., and Gridley, T. (2003). Characterization of *Notch3*-deficient mice: normal embryonic development and absence of genetic interactions with a *Notch1* muation. *Genesis* **37,** 139-143.

Larsson, C., Lardelli, M., White, I., and Lendahl, U. (1994). The human NOTCH1, 2, and 3 genes are located at chromosome positions 9q34, 1p13-11, and 19p13.2-p13.1 in regions of neoplasia-associated translocation. *Genomics* **24,** 253-258.

Lavker, R. M., Miller, S., Wilson, C., Cotsarelis, G., Wei, Z.-G., Yang, J.-S., and Sun, T.-T. (1993). Hair follicle stem cells: their location, role in hair cycle, and involvement in skin tumor formation. *The Journal of Investigative Dermatology* **101,** 16S-26S.

LaVoie, M. J., and Selkoe, D. J. (2003). The Notch ligands, Jagged and Delta, are sequentially processed by α-secretase and Presenilin/γ-secretase and release signaling fragments. *The Journal of Biological Chemistry* **278,** 34427-34437.

Le Borgne, R., and Schweisguth, F. (2003). Notch signalling: endocytosis makes Delta signalling better. *Current Biology* **13,** R273-R275.

Lei, L., Xu, A., Panin, V. M., and Irvine, K. D. (2003). An O-fucose site in the ligand binding domain inhibits Notch activation. *Development* **130,** 6411-6421.

Lewis, J. (1998). Notch signalling and the control of cell fate choices in vertebrates. *Seminars in Cell & Developmental Biology* **9,** 583-589.

Lin, J. Y., and Fisher, D. E. (2007). Melanocyte biology and skin pigmentation. *Nature* **445,** 843-850.

Lindner, G., Menrad, A., Gherardi, E., Merlino, G., Welker, P., and al., e. (2000). Involvement of hepatocyte growth factor/scatter factor and met receptor signaling in hair follicle morphogenesis and cycling. *The FASEB Journal* **14,** 319-332.

Lindsell, C. E., Shawber, C. J., Boulter, J., and Weinmaster, G. (1995). Jagged: a mammalian ligand that activates Notch1. *Cell* **80,** 909-917.

Lindsell, C. E., Boulter, J., di Sibio, G., Gossler, A., and Weinmaster, G. (1996). Expression patterns of *Jagged, Delta1, Notch1, Notch2,* and *Notch3* genes identify ligand-receptor pairs that may function in neural development. *Molecular and Cellular Neuroscience* **8,** 14-27.

Lowell, S., Jones, P., Le Roux, I., Dunne, J., and Watt, F. M. (2000). Stimulation of human epidermal differentiation by Delta-Notch signalling at the boundaries of stem-cell clusters. *Current Biology* **10,** 491-500.

Lumpkin, E. A., and Caterina, M. J. (2007). Mechanisms of sensory transduction in the skin. *Nature* **445,** 858-865.

Lyne, A. G. (1966). The development of hair follicles. *The Australian Journal of Science* **28,** 370-377.

Matsuzaki, T., and Yoshizato, K. (1998). Role of hair papilla cells on induction and regeneration processes of hair follicles. *Wound Repair and Regeneration* **6,** 524-530.

Messenger, A. G. (1984). The culture of dermal papilla cells from human hair follicles. *British Journal of Dermatology* **110,** 685-689.

Messenger, A. G., Senior, H. J., and Bleehen, S. S. (1986). The *in vitro* properties of dermal papilla cell lines established from human hair follicles. *British Journal of Dermatology* **114,** 425-430.

Miele, L., and Osborne, B. (1999). Arbiter of differentiation and death: Notch signaling meets apoptosis. *Journal of Cellular Physiology* **181,** 393-409.

Mill, P., Mo, R., Fu, H., Grachtouk, M., Kim, P. C., Dlugosz, A. A., and Hui, C.-C. (2003). Sonic hedgehog-dependent activation of Gli2 is essential for embryonic hair follicle development. *Genes & Development* **17,** 282-294.

Millar, S. E. (2002). Molecular mechanisms regulating hair follicle development. *Journal of Investigative Dermatology* **118,** 216-225.

Montagna, W., Chase, H. B., Malone, J. D., and Melarango, H. P. (1952). Cyclic changes in polysaccharides of the papilla of the hair follicle. *Quaterly Journal of Microscopic Science* **93,** 241.

Mooney, J. R., and Nagorcka, B. N. (1985). The role of a reaction-diffusion system in the initiation of skin organ primordia. I. The first wave of initiation. *Journal of Theoretical Biology* **114,** 243-272.

Moore, A. G., and Moore, G. P. M. (2001). Extracellular matrix molecules and follicle morphogenesis in ovine skin. *Reproduction, Fertility and Development* **13,** 143-149.

Moore, G. P. M., Jackson, N., and Isaacs, K. (1989). Evidence of a unique developmental mechanism specifying both wool follicle density and fibre size in sheep selected for single skin and fleece characters. *Genetic Research, Cambridge* **53,** 57-62.

Moore, G. P. M., Jackson, N., and Brown, G. (1995). Estimating densities of original and derived secondary wool follicles in the sheep. *Wool Technology and Sheep Breeding* **43,** 263-267.

Moore, G. P. M., Jackson, N., Isaacs, K., and Brown, G. (1996). Development and density of wool fibres in Merino sheep selected for single fibre characteristics. *Australian Journal of Agricultural Research* **47,** 1195-1201.

Moore, G. P. M., Jackson, N., Isaacs, K., and Brown, G. (1998). Pattern and Morphogenesis in Skin. *Journal of Theoretical Biology* **191,** 87-94.

Morel, V., and Le Borgne, R. (2003). Snail is required for Delta endocytosis and Notch-dependent activation of *single-minded* expression. *Development Genes and Evolution* **213,** 65-72.

Morohashi, Y., Kan, T., Tominari, Y., Fuwa, H., Okamura, Y., Watanabe, N., Sato, C., Natsugari, H., Fukuyama, T., Iwatsubo, T., and Tomita, T. (2006). C-terminal fragment of presenilin is the molecular target of a dipeptide γ-secretase-specific inhibitor DAPT (N-[N-(3,5-difluorophenacetyl)-L-alanyl]-S-phenylglycine *t*-butyl ester). *The Journal of Biological Chemistry* **281,** 14670-14676.

Muller-Rover, S., Peters, E. J., Botchkarev, V. A., Panteleyev, A., and Paus, R. (1998). Distinct patterns of NCAM expression are associated with defined stages of murine hair follicle morphogenesis and regression. *Journal of Histochemistry & Cytochemistry* **46,** 1401-1410.

Myat, A., Henrique, D., Ish-Horowicz, D., and Lewis, J. (1996). A chick homologue of *Serrate* and its relationship with *Notch* and *Delta* homologues during central neurogenesis. *Developmental Biology* **174,** 233-247.

Nagorcka, B. N. (1986). The role of the reaction-diffusion system in the initiation of skin organ primordia. I. The first wave of initiation. *Journal of Theoretical Biology* **121,** 449-475.

Nagorcka, B. N. (1995a). The reaction-diffusion (RD) theory of wool (hair) follicle initiation and development. I. Primary follicles. *Australian Journal of Agricultural Research* **46,** 333-355.

Nagorcka, B. N. (1995b). The reaction-diffusion (RD) theory of wool (hair) follicle initiation and development. II.* Original secondary follicles. *Australian Journal of Agricultural Research* **46,** 357-378.

Nakazawa, M., Ishii, H., Aono, H., Takai, M., Honda, T., Aratani, S., Fukamizu, A., Nakamura, H., Yoshino, S., Kobata, T., Nishioka, K., and Nakajima, T. (2001). Role of Notch-1 intracellular domain in activation of rheumatoid synoviocytes. *Arthritis & Rheumatism* **44,** 1545-1554.

Nelson, B. R., Hartman, B. H., Georgi, S. A., Lan, M. S., and Reh, T. A. (2007). Transient inactivation of Notch signaling synchronizes differentiation of neural progenitor cells. *Developmental Biology* **304,** 479-498.

Niimi, H., Pardali, K., Vanlandewijck, M., Heldin, C.-H., and Moustakas, A. (2007). Notch signaling is necessary for epithelial growth arrest by TGF-ß. *The Journal of Cell Biology* **176,** 695-707.

Noramly, S., and Morgan, B. A. (1998). BMP's mediate lateral inhibition at successive stage in the feather tract development. *Development* **125,** 3375-3787.

Noramly, S., Freeman, A., and Morgan, B. A. (1999). β-catenin signalling can initiate feather bud development. *Development* **126,** 3509-3521.

O'Connor-Giles, K. M., and Skeath, J. B. (2003). Numb inhibits membrane localization of Sanpodo, a four-pass transmembrane protein to promote asymmetric divisions in Drosophila. *Development of the Cell* **5,** 231-243.

Ohuchi, H., Hori, Y., Yamasaki, M., Harada, H., Sekine, K., Kato, S., and Itoh, N. (2000). FGF10 acts as a major ligand for FGF receptor 2 IIIb in mouse multi-organ development. *Biochemical and Biophysical Research Communications* **277,** 643-649.

Olivera-Martinez, I., Viallet, J. P., Michon, F., Pearton, D. J., and Dhouailly, D. (2004). The different steps of skin formation in vertebrates. *International Journal of Developmental Biology* **48,** 107-115.

Olivier, A., Lauret, E., Gonin, P., and Galy, A. (2008). The Notch ligand delta-1 is a hematopoietic development cofactor for plasmacytoid dendritic cells. *Blood* **107,** 2694-2701.

Ong, C.-T., Cheng, H.-T., Chang, L.-W., Ohtsuka, T., Kageyama, R., Stormo, G. D., and Kopan, R. (2006). Target selectivity of vertebrate Notch proteins. *The Journal of Biological Chemistry* **281,** 5106-5119.

Pan, Y., Lin, M.-H., Tian, X., Cheng, H.-T., Gridley, T., Shen, J., and Kopan, R. (2004). γ-Secretase functions through Notch signaling to maintain skin appendages but is not required for their patterning or initial morphogenesis. *Developmental Cell* **7,** 731-743.

Panin, V. M., Papayannopoulos, V., Wilson, R., and Irvine, K. D. (1997). Fringe modulates Notch ligand interactions. *Nature* **387,** 908-912.

Panin, V. M., and Irvine, K. D. (1998). Modulators of Notch signaling. *Seminars in Cell & Developmental Biology* **9,** 609-617.

Parks, A. L., and Curtis, D. (2007). Presenilin diversifies its portfolio. *Trends in Genetics* **23,** 140-150.

Paus, R., Müller-Röver, S., van der Veen, C., Maurer, M., Eichmüller, S., Ling, G., Hofmann, U., Foitzik, K., Mecklenburg, L. and Handjiski, B. (1999). A comprehensive guide for the recognition and classification of distict stages of hair follicle morphogenesis. *Journal of Investigative Dermatology* **113,** 523-532.

Peterson, R. E., and McClay, D. R. (2005). A Fringe-modified Notch signal affects specification of mesoderm and endoderm in the sea urchin embryo. *Developmental Biology* **282,** 126-137.

Pierard, G. E., and De La Brassinne, M. (1975). Modulation of dermal cell activity during hair growth in the rat. *Journal of Cutaneous Pathology* **2,** 35.

Pinnix, C. C., and Herlyn, M. (2007). The many faces of Notch signaling in skin-derived cells. *Pigment Cell Research* **20,** 458-465.

Pisansarakit, P., and Moore, G. P. M. (1986). Induction of hair follicles in mouse skin by rat vibrissa dermal papilla. *Journal of Embryological Experimental Morphology* **94,** 113-119.

Pisansarakit, P., du Cros, D. L., and Moore, G. P. M. (1991). Cultivation of mesenchymal cells derived from the skin and hair follicles of the sheep: The involvement of peptide factors in growth regulation. *Archives of Dermatological Research* **283,** 321-327.

Pispa, J., and Thesleff, I. (2003). Mechanisms of ectodermal organogenesis. *Developmental Biology* **262,** 195-205.

Plowman, J. E., Paton, L. N., and Bryson, W. G. (2007). The differential expression of proteins in the cortical cells of wool and hair fibres. *Experimental Dermatology* **16,** 707-714.

Pourquié, O. (2000). Skin development: Delta laid bare. *Current Biology* **10,** R425-R428.

Powell, B. C., Passmore, E. A., Nesci, A., and Dunn, S. M. (1998). The Notch signalling pathway in hair growth. *Mechanisms of Development* **78,** 189-192.

Purvis, I. W., and Franklin, I. R. (2005). Major genes and QTL influencing wool production and quality: a review. *Genetics Selection Evolution* **37,** S97-S107.

Qi, H., Rand, M. D., Wu, X., Sestan, N., Wang, W., Rakic, P., Xu, T., and Artavanis-Tsakonas, S. (1999). Processing of the Notch ligand Delta by the metalloprotease Kuzbanian. *Science* **283,** 91-94.

Rand, M. D., Grimm, L. M., Artavanis-Tsakonas, S., Patriub, V., Blacklow, S. C., Sklar, J., and Aster, J. C. (2000). Calcium depletion dissociates and activates heterodimeric Notch receptors. *Molecular Cell Biology* **20,** 1825-1835.

Rangarajan, A., Talora, C., Okuyama, R., Nicolas, M., Mammucari, C., Oh, H., Aster, J. C., Krishna, S., Metzger, D., Chambon, P., Miele, L., Aguet, M., Radtke, F., and Dotto, G. P. (2001). Notch signaling is a direct determinant of keratinocyte grwoth arrest and entry into differentiation. *The EMBO Journal* **20,** 3427-3436.

Rao, P., and Kadesch, T. (2003). The intracellular form of Notch blocks transforming growth factor beta-mediated growth arrest in Mv1Lu epithelial cells. *Molecular Cell Biology* **23,** 6694-6701.

Rebay, I., Fleming, R. J., Fehon, R. G., Cherbas, L., Cherbas, P., and Artavanis-Tsakonas, S. (1991). Specific EGF repeats of Notch mediate interactions with Delta and Serrate: Implications for Notch as a multifunctional receptor. *Cell* **67,** 687-699.

Rendel, J. M., and Nay, T. (1978). Selection for high and low ratio and high and low primary density in Merino sheep. *Australian Journal of Agricultural Research* **29,** 1077-1086.

Rendl, M., Lewis, L., and Fuchs, E. (2005). Molecular dissection of mesenchymal-epithelial interactions in the hair follicle. *PLoS Biology* **3,** 1-15.

Robbins, J., Blondel, B. J., Gallahan, D., and Callahan, R. (1992). Mouse mammary tumor gene int-3: a member of the notch gene family transforms mammary epithelial cells. *Journal of Virology* **66,** 2594-2609.

Roche. (2002). "Roche applied science DIG-application manual for non-radioactive in situ hybridisation."

Roegiers, F., and Jan, Y. N. (2004). Asymmetric cell division. *Current Opinion in Cell Biology* **16,** 195-205.

Rogers, G. E. (2006). Biology of the wool follicle: an excursion into a unique tissue interaction system waiting to be rediscovered. *Experimental Dermatology* **15,** 931-949.

Rohn, J. L., Lauring, A. S., Linenberger, M. L., and Overbaugh, J. (1996). Transduction of Notch2 in feline leukemia virus-induced thymic lymphoma. *Journal of Virology* **70,** 8071-8080.

Roth, S. I. (1965). The Cytology of the Murine Resting (Telogen) Hair Follicle. *In* "Biology of the Skin and Hair Growth" (A. G. Lyne and B. F. Short, Eds.), pp. 233-249. Angus & Robertson, Australia.

Roy, M., Pear, W. S., and Aster, J. C. (2007). The multifaceted role of Notch in cancer. *Current Opinion in Genetics & Development* **17,** 52-59.

Sakata, T., Sakaguchi, H., Tsuda, L., Higashitani, A., Aigaki, T., Matsuno, K., and Hayashi, S. (2004). Nedd4 regulates endocytosis of Notch and suppresses its ligand-independent activation. *Current Biology* **14,** look up.

Sato, K., Kang, W. H., Saga, K., and Sato, K. T. (1989). Biology of sweat glands and their disorders. I. Normal sweat gland function. *Journal of the American Academy of Dermatology* **20,** 537-63.

Schmidt-Ullrich, R., and Paus, R. (2005). Molecular principles of hair follicle induction and morphogenesis. *BioEssays* **27,** 247-261.

Schweisguth, F. (2004). Regulation of Notch signalling activity. *Current Biology* **14,** R129-R138.

Sick, S., Reinker, S., Timmer, J., and Schlake, T. (2006). WNT and DKK determine hair follicle spacing through a reaction-diffusion mechanism. *Science* **134,** 1447-1450.

Simpson, P. (1998). Introduction: Notch signalling and choice of cell fates in development. *Seminars in Cell & Developmental Biology* **9,** 581-582.

Six, E., Ndiaye, D., Laâbi, Y., Brou, C., Gupta-Rossi, N., Israël, A., and Logeat, F. (2003). The Notch ligand Delta1 is sequentially cleaved by an ADAM protease and γ-secretase. *Proceedings of the National Academy of Science* **100,** 7638-7643.

Skeath, J. B., and Doe, C. Q. (1998). Sanpodo and Notch act in opposition to Numb to distinguish sibling neuron fates in the *Drosophila* CNS. *Development* **125,** 1857-1865.

Slominski, A., Tobin, D. J., Shibahara, S., and Wortsman, J. (2004). Melanin pigmentation in mammalian skin and its hormonal regulation. *Physiological Reviews* **84,** 1155-1228.

Song, H., Wang, Y., and Goetinck, P. F. (1996). Fibroblast growth factor 2 can replace ectodermal signaling for feather development. *Proceedings of the National Academy of Science USA* **93,** 10246-10249.

Sparrow, D. B., Chapman, G., Wouters, M. A., Whittock, N. V., Ellard, S., Fatkin, D., Turnpenny, P. D., Kusumi, K., Sillence, D., and Dunwoodie, S. L. (2006). Mutation of the *Lunatic Fringe* gene in humans causes Spondylocostal Dystosis with a severe vertebral phenotype. *The American Journal of Human Genetics* **78,** 28-37.

Stark, J., Andl, T., and Millar, S. E. (2007). Hairy math: insights into hair-follicle spacing and orientation. *Cell* **128,** 17-20.

Stenn, K. S., and Paus, R. (2001). Controls of hair follicle cycling. *Physiological Reviews* **81,** 449-494.

Stephenson, S. K. (1957). Wool follicle development in the New Zealand Romney and N-type sheep. I. The relationships of development to age in the New-Zealand Romney and N-type sheep foetuses and a comparison with results obtained from the Merino. *Australian Journal of Agricultural Research* **8,** 371-384.

St-Jacques, B., Dassule, H. R., Karanova, I., Botchkarev, V. A., Li, J., Danielian, P. S., McMahon, J. A., Lewis, P. M., Paus, R., and McMahon, A. P. (1998). Sonic hedgehog signaling is essential for hair development. *Current Biology* **8,** 1058-1068.

Straile, W. E. (1965). Root Sheath-Dermal Papilla Relationships and the Control of Hair Growth. *In* "Biology of the Skin and Hair Growth" (A. G. Lyne and B. F. Short, Eds.), pp. 35-57. Angus & Robertson, Australia.

Swiatek, P. J., Lindsell, C. E., Franco del Amo, F., Weinmaster, G., and Gridley, T. (1994). Notch1 is essential for postimplantation development in mice. *Genes & Development* **8,** 707-719.

Tanii, H., Jiang, J., Fukumori, A., Tagami, S., Okazaki, Y., Okochi, M., and Takeda, M. (2006). Effect of Valine on the efficiency and precision at S4 cleavage of the Notch-1 transmembrane domain. *Journal of Neuroscience Research* **84,** 918-925.

Thomas, H. S. (2006). DMSO: a multifaceted medication. *California Thoroughbred* **July,** 48-49.

Tiede, S., Kloepper, J. E., Bodò, E., Tiwari, S., Kruse, C., and Paus, R. (2007). Hair follicle stem cells: walking the maze. *European Journal of Cell Biology* **86,** 355-376.

Timmerman, L. A., Grego-Bessa, J., Raya, Á., Bertrán, E., Pérez-Pomares, J., Diez, J., Aranda, S., Palomo, S., McCormick, F., Izpisúa-Belmonte, J. C., and de la Pompa, J. L. (2004). Notch promotes epithelial-mesenchymal transition during cardiac development and oncogenic transformation. *Genes & Development* **18,** 99-115.

Tobin, D. J., Gunin, A., Magerl, M., Handijski, B., and Paus, R. (2003a). Plasticity and cytokinetic dynamics of the hair follicle mesenchyme: implications for hair growth control. *Journal of Investigative Dermatology* **120,** 895-904.

Tobin, D. J., Gunin, A., Magerl, M., and Paus, R. (2003b). Plasticity and cytokinetic dynamics of the hair follicle mesenchyme during the hair growth cycle: implications for growth control and hair follicle transformations. *Journal of Investigative Dermatology Symposium Proceedings* **8,** 80-86.

Turner, H. N. (1961). Relationships among clean wool weight and its components. II. The effect of maternal handicap and its influence on selection. *Australian Journal of Agricultural Research* **12,** 974-991.

Turner, H. N., Brown, G. H., and Ford, G. H. (1968). The influence of age structure on total productivity in breeding flocks of Merino sheep. I. Flocks with a fixed number of breeding ewes, producing their own replacements. *Australian Journal of Agricultural Research* **19,** 443-475.

van Genderen, C., Okamura, R. M., Farinas, I., Quo, R. G., Parslow, T. G., Bruhn, L., and Grosschedl, R. (1994). Development of several organs that require inductive epithelial-mesenchymal interactions is impaired in LEF-1-deficient mice. *Genes & Development* **8,** 2691-2703.

Van Scott, E. J., and Ekel, T. M. (1958). Geometric relationships between the matrix of the hair bulb and its dermal papilla in normal alopecic scalp. *Journal of Investigative Dermatology* **31,** 281-287.

Vauclair, S., Nicholas, M., Barrandon, Y., and Radtke, F. (2005). Notch1 is essential for postnatal hair follicle development and homeostasis. *Developmental Biology* **284,** 184-193.

Viallet, J. P., Prin, F., Olivera-Martinez, I., Hirsinger, E., Pourquié, O., and Dhouailly, D. (1998). Chick *Delta-1* gene expression and the formation of the feather primordia. *Mechanisms of Development* **72,** 159-168.

Ward, E. J., Shcherbata, H. R., Reynolds, S. H., Fischer, K. A., Hatfield, S. D., and Ruohola-Baker, H. (2006). Stem cells signal to the niche through the Notch pathway in the *Drosophila* ovary. *Current Biology* **16,** 2352-2358.

Watt, F. M. (2001). Stem cell fate and patterning in mammalian epidermis. *Current Opinion in Genetics & Development* **11,** 410-417.

Weinmaster, G., and Kintner, C. (2003). Modulation of Notch signalling during somitogenesis. *Annual Reviews in Cell Developmental Biology* **19,** 367-395.

Wesley, C. S. (1999). Notch and Wingless regulate expression of cuticle patterning genes. *Molecular Cell Biology* **19,** 5743-5758.

Wesley, C. S., and Saez, L. (2000). Notch responds differently to Delta and Wingless in cultured *Drosophila* cells. *Journal of Biological Chemistry* **275,** 9099-9101.

Widelitz, R. B., Jiang, T. X., Noveen, A., Cheng, C. W., and Chuong, C. M. (1996). FGF induces new feather buds from developing avian skin. *Journal of Investigative Dermatology* **107,** 797-803.

Wilkin, M. B., Carbery, A.-M., Fostier, M., Aslam, H., Mazaleyrat, S. L., Higgs, J. E., Myat, A., Evans, D. A. P., Cornell, M., and Baron, M. (2004). Regulation of Notch endosomal sorting and signalling by *Drosophila* Nedd4 family proteins. *Current Biology* **14,** look up.

Williams, D., Profeta, K., and Stenn, K. S. (1994). Isolation and culture of follicular papillae from murine vibrissae: an introductory approach. *British Journal of Dermatology* **130,** 290-297.

Winkelman, R. K. (1965). *In* "Biology of the Skin and Hair Growth" (A. G. Lyne and B. F. Short, Eds.). Angus and Robertson, Sydney.

Wodarz, A., and Nusse, R. (1998). Mechanisms of Wnt signalling in development. *Annual Reviews in Cell Developmental Biology* **14,** 59-88.

Woods, J. L., and Orwin, D. F. G. (1982). The cytology of cuticle scale pattern formation in the wool follicle. *Journal of Ultrastructure Research* **80**, 230-242.

Wu, W., Glinka, A., Delius, H., and Niehrs, C. (2000). Mutual antagonism between *dickkopf1* and *dickkopf2* regulates Wnt/β-catenin signalling. *Current Biology* **10,** 1611-1614.

Yamamoto, N., Tanigaki, K., Han, H., Hiai, H., and Honjo, T. (2003). Notch/RBP-J signaling regulates epidermal/hair fate determination of hair follicle stem cells. *Current Biology* **13,** 333-338.

Yi, R., O'Carrol, D., Pasolli, H. A., Zhang, Z., Dietrich, F. S., Tarakhovsky, A., and Fuchs, E. (2006). Morphogenesis in skin is governed by discrete sets of differentially expressed microRNAs. *Nature Genetics* **38,** 356-362.

Young, S. S. Y., and Chapman, R. E. (1958). Fleece characters and their influence on wool production per unit area of skin in Merino sheep. *Australian Journal of Agricultural Research* **9,** 363-372.

Zheng, Y., Du, X., Wang, W., Boucher, M., Parimoo, S., and Stenn, K. S. (2005). Organogenesis from dissociated cells: generation of mature cycling hair follicles from skin-derived cells. *Journal of Investigative Dermatology* **124,** 867-876.

Zhou, J., Jia, L., W., L., Miao, C., Liu, S., Cao, Y., and Duan, E. (2006). Role of sonic hedgehog in maintaining a pool of proliferating stem cells in the human fetal epidermis. *Human Reproduction* **21,** 1698-1704.

Zhou, P., Byrne, C., Jacobs, J., and Fuchs, E. (1995). Lymphoid enhancer factor 1 directs hair follicle patterning and epithelial cell fate. *Genes & Development* **9,** 700-713.

APPENDIX 0: PHAGEMID VECTORS

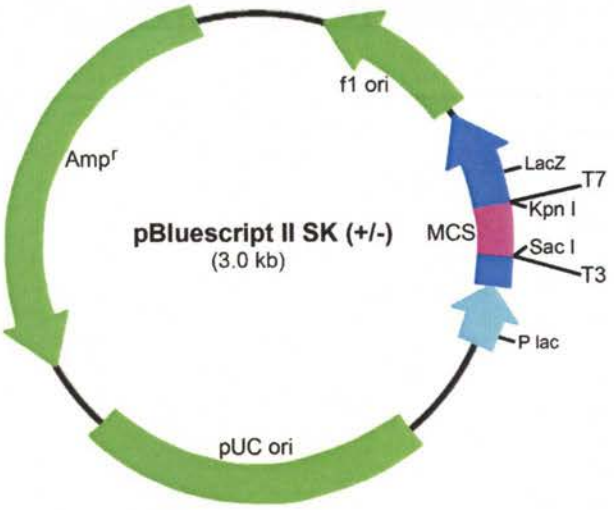

Figure A0.1: The structure of the 3 kb pBluescript II SK (+/–) phagemid vector. Inclusion of the ampicillin resistance gene (Amp^r), origin of replication (ori), multiple cloning site (MCS) and disrupted LacZ gene are shown. The MCS region is located in the region 598-826, and is flanked by the restriction enzymes KpnI and SacI at the T7 and T3 promoter sites respectively. Image adapted from the pBluescript® II phagemid vectors instruction manual (2003), Stratagene.

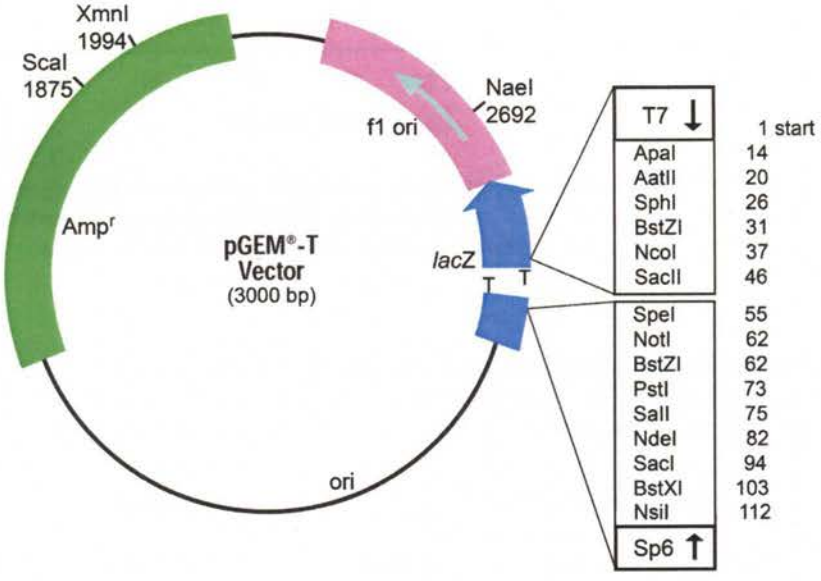

Figure A0.2: Schematic of the structure of the 3 kb pGEM®-T Vector system. The T7 RNA polymerase transcription initiation site is located at 1, the Sp6 RNA polymerase transcription initiation site is located at 126. The T7 RNA polymerase promoter site (-17 to +3) runs from 2984-3. The Sp6 RNA polymerase promoter site (-17 to +3) runs from 124-143. The multiple cloning region for the vector is located between 10-113. The *lacZ* start codon is at position 165, the *lac* operon sequences are found from 2821-2981 and 151-380, and the *lac* operator region is located at 185-201. An uninterrupted *lacZ* gene allows the plasmid to utilize β-galactosidase. The β-lactamase coding region runs 1322-2182 and confers resistance to ampicillin (Amp^r). The phage f1 region (f1 ori) is located between 2365-2820, there is a second origin or replication (ori) within the vector. The binding site of pUC/M13 forward sequencing primer is 2941-2957, and the reverse sequencing primer 161-177. Image adapted from Promega Technical Manual (revised May, 1997).

APPENDIX 1: FOETAL CROWN-RUMP LENGTH AND WEIGHT MEASUREMENTS

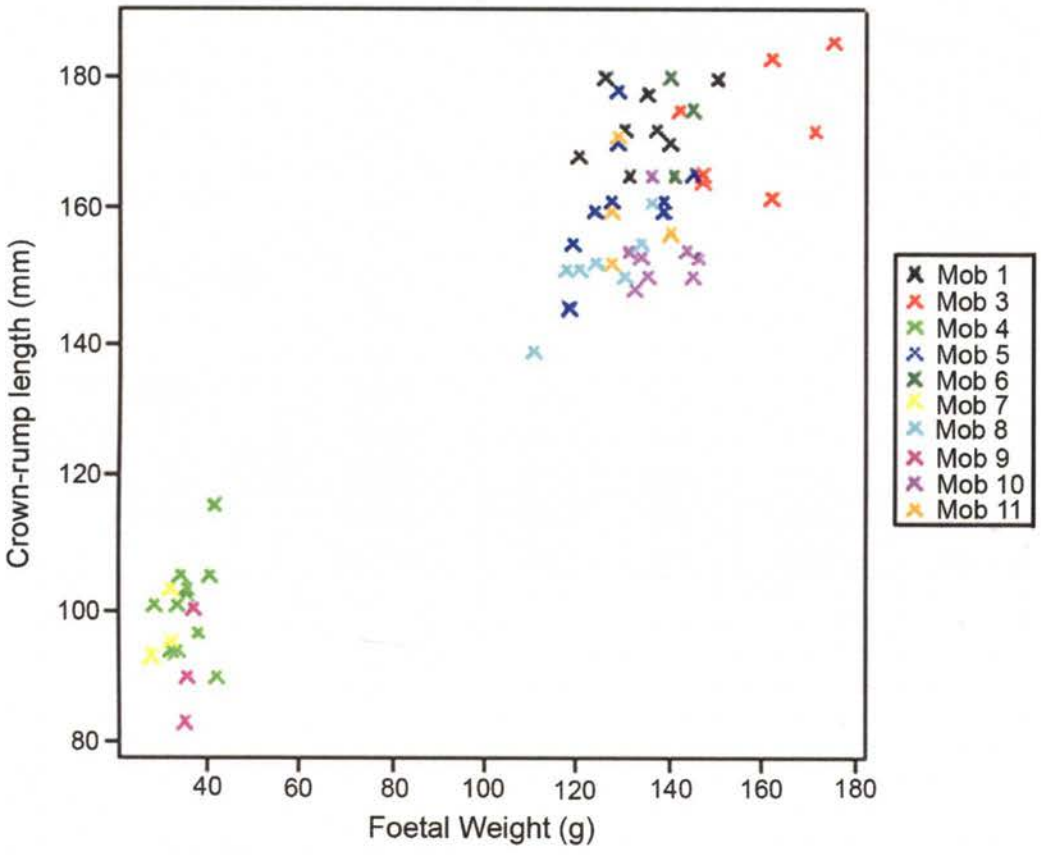

Figure A1.1: Foetal weight and crown-rump length measurements from sampled foetuses following euthanasia. The cluster in the bottom left corner corresponds to d 56 samples, those in the upper right correspond to those sampled on d 70 of gestation. Mobs 1-8 Merino, 9-11 Tukidale.

Table A1.1: Separate univariate linear mixed model analyses were conducted for foetal crown-rump and weight data. Similar results were obtained, with gender, foetal age and the number of foetuses having a significant effect on the crown-rump length and weights of the foetuses. Year of sampling and breed were not significant.

Fixed effect	Crown-rump length	Foetal Weight
Gender	<0.001	0.003
Foetal age	<0.001	<0.001
Number of foetuses	0.006	0.035
Year	0.271	0.291
Breed	0.861	0.246

Table A1.2: The predicted means and standard errors (SE) produced from the linear mixed model analyses of crown-rump lenth and foetal weight. The significant fixed effects (gender, foetal age and number of foetuses) were investigated further. Means that were not significantly different for each effect (>0.05) share the same letter superscript. Interestingly, male foetuses were significantly longer and heavier than their female counterparts. Not suprisingly, the d 70 foetuses were significantly longer and heavier than the d 56 foetuses. Singletons, twins and triplets did not have significantly different crown-rump lengths. However, for foetal weight singletons and twins were not significantly different from each other but both were significantly heavier than their triplet counterparts.

Fixed effect		Crown-rump length		Foetal Weight	
		Mean	SE	Mean	SE
Gender	Male	131.3^{A}	5.9	87.22^{A}	6.7
	Female	124.8^{B}	6.1	81.07^{B}	7.0
Foetal Age	d 56	96.1^{A}	8.6	33.42^{A}	9.8
	d 70	160.0^{B}	5.0	134.87^{B}	5.6
Number of foetuses	Singleton	127.9^{A}	5.9	88.41^{A}	6.7
	Twin	124.2^{A}	7.6	89.09^{A}	6.6
	Triplet	132.0^{A}	5.8	74.94^{B}	8.5
Year	2005	137.3	8.8	94.4	10.0
	2006	125.6	3.8	81.0	4.3
	2007	121.3	11.3	77.0	12.8
Breed	Merino	127.4	5.3	79.2	6.0
	Tukidale	128.7	8.4	89.0	9.5

APPENDIX 2: S:P FOLLICLE RATIO ANALYSIS

Table A2.1: The data for the secondary to primary (S:P) follicle ratios were analysed on the log scale using a linear mixed model. Breed had a highly significant effect ($p<0.001$) on the S:P follicle ratio, with the adult Merino skin having a significantly higher S:P ratio than the Tukidale skin samples. Significantly different means have different letter superscripts.

S:P follicle ratio		Mean	SE
Breed	Merino	2.894^{A}	0.054
	Tukidale	1.663^{B}	0.055

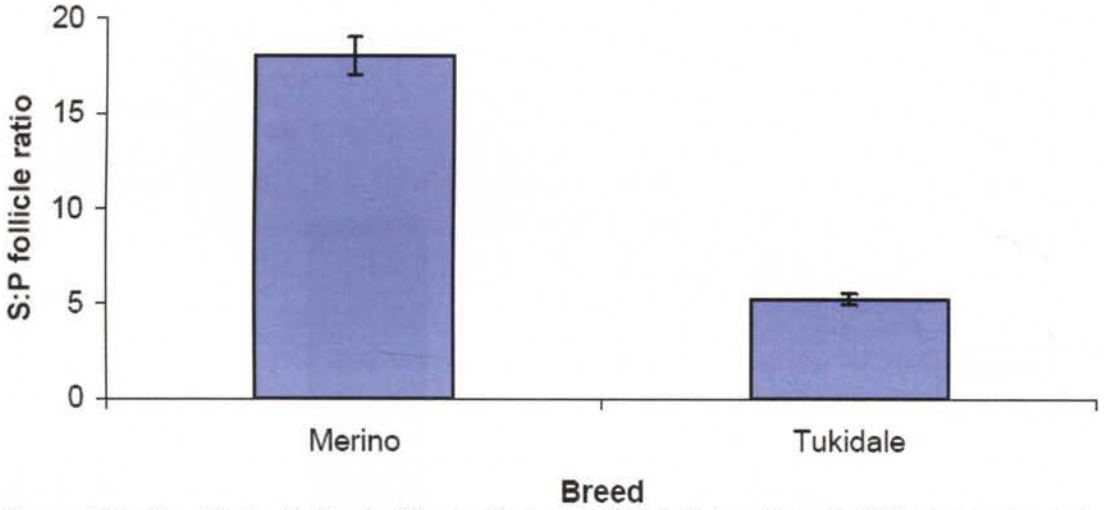

Figure A2.1: Breed had a highly significant effect on the S:P follicle ratio ($p<0.001$). The Merino had a significantly higher S:P follicle ratio compared to the Tukidale. By backtransforming the means it was found that the Merino skin comprised of ~18 secondary follicles for each primary follicle and the Tukidale skin contained ~5 secondary follicles for each primary follicle.

APPENDIX 3: WOOL FIBRE DIAMETER ANALYSIS

Table A3.1: The fibre diameter data were analysed on the log scale using a linear mixed model, and the interaction between breed and follicle type was highly significant ($p<0.001$). The mean fibre diameter was significantly larger for the Tukidale primary than the Merino primary, and Tukidale secondary than Merino secondary. The primary fibre in the Tukidale was significantly wider than the secondary. The primary and secondary fibres in the Merino were not significantly different. Means that were not significantly different share the same letter superscripts.

	Follicle type	Primary		Secondary	
		Mean	SE	Mean	SE
Breed	Merino	2.792^{AC}	0.047	2.778^{AC}	0.047
	Tukidale	3.874^{BD}	0.047	3.152^{BE}	0.047

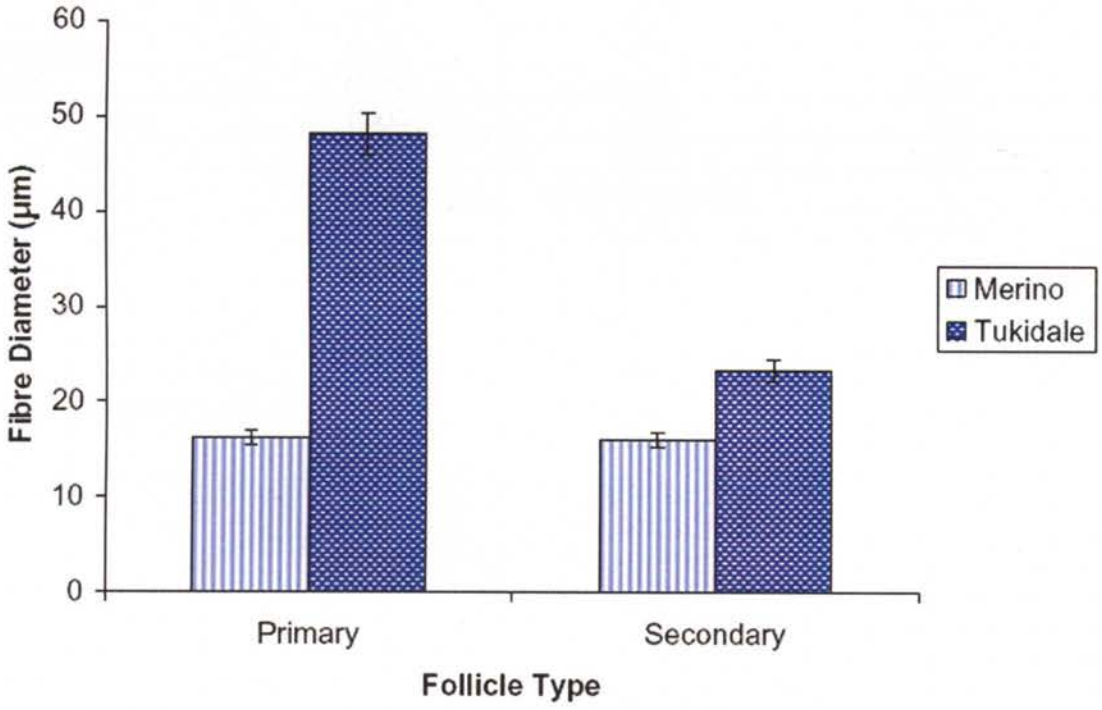

Figure A3.1: The fibre diameters for the adult ewes used in this study were investigated. The interaction between breed and follicle type was highly significant ($p<0.001$) for wool fibre diameter. In the Merino, the primary and secondary fibre diameters were not significantly different, with both follicle types having a fibre diameter of ~16 µm. In the Tukidale, the primary fibres were of a significantly higher micron than the secondary fibres (~48 µm and ~23 µm respectively). The Tukidale fibres were significantly thicker than their Merino counterparts.

APPENDIX 4: SPOT CAMERA PARAMETERS

Table A4.1: The parameters specified for capturing brightfield and fluorescence images using the SPOT camera and software.

	Fluorescence Blue	Fluorescence Green	Lightfield
Pixel bit depth	24 (RGB)	24 (RGB)	24 (RGB)
Exposure	Auto	Auto	Auto
Use:			
Red	Y	Y	Y
Green	Y	Y	Y
Blue	Y	Y	Y
Image type	fluorescence	fluorescence	brightfield-transmitted light
White balance:			
Red	1.655	1.000	1.500
Green	1.000	3.000	1.000
Blue	2.229	1.500	3.500
Colour order	RGB	RGB	RGB
Binning	None	None	None
Adjustment factor	1.000	1.000	1.000
Auto-gain limit	1.600	1.600	1.600
Minimum exposure	1000 milliseconds	1000 milliseconds	x
Chip imaging area	full chip	full chip	full chip
Post processing:			
Colour enhancement	Y	Y	Y
Chip defect correction	Y	Y	Y
Noise filter	x	x	Y
Gamma adjustment 1.50	HSV	HSV	x

APPENDIX 5: NUCLEOTIDE SEQUENCES

5.1 DELTA-1

5.1.1 SEQUENCING RESULTS FROM T3 PROMOTER

```
3′  1   GGGGGTCNCCGCGGGGGCGGCCNCTCTAGAACTAGTGGATCCCCNGGGCTGCANGAATTC
   61   ATGTCTTACGGTCAAGGGTTCATTATATTTATTTTGGAAAAATATTTTTAAAATGAATTT
  121   CTTCATTAACAAAACAGTAAAAAACTCAAATAACATTTGCACAATATTCCATAAATACAT
  181   TTATATACAAAAAAATATAGTCACATAGACCCGAAGTGCCTTTGTACATATTTACCAAAA
  241   TTTAAATTATAAAAAAATGAACGTCACAAAATACTCAAGCTTTACAGATATCATGAAAAA
  301   TATTTTTACAAATCCCAAAAAAATAACACACGTTTTCTTTTTCCCGTCTAGGAAAAAAAA
  361   AAACACATCTCAGTATCAAAAAGGACAATAAAGGCAGTTGTGTTTCTAGTTCAAGGAAAG
  421   ACTGGCTCATAGTAATCCAAGATAGACGTGTGGGCAGTGCGTGCTTCCTATATGAATCAA
  481   GTCACTCGTCCATTTAAATATATACTCTTCAAAGCAACTGTCCATAGTGCAATGGGAACA
  541   ACCAGCAGGCAGTCCAGCGGCAGCCAAAGCCTAGGCTGGCAGTGTCGGGCGCCTCTGCTA
  601   ACTCTGAGAGAACCAGCTTCGCCTGAACCTGGGTTCTCAGCAGCAGTCCCTGGGTTTCCT
  661   CTCCCTTCCTCTCTCAGCAGCATTCATCGGGGCTATATCCTTGGAATTTTATTTGAGAGN
  721   AATGGGAATTTTGCCCCATCGCTTCCATCTTANCCTCAGTCGCTATACNCNCTCCTCCTT
  781   TTCTGCGNACAGAACATACNCCGACNGGNACTGGGGGNCCTTGGANGNAANANAAAAGAC
  841   NCNGGCCNTTTTCGGNCNGGANNCCCCCCCCCCTAAGGGNGGGGNGATCTTCNNTTCCCN
  901   GNANANCCTGGGACGGGCCNTGGGGGCCCGTTNGGNGGGGN 5′
```

5.1.2 SEQUENCING RESULTS FROM T7 PROMOTER

```
5′  1   ANGGGTNCGGGCCCCCCTCGAGGTCNAGGTATCGATAAGCTTGATATCGAATTCATGTCT
   61   TACGGTCAAGGCCATGGCACCTGCCAGCAACCCTGGCAGTGTAACTGGCAGGAAGGCTGG
  121   GGGGGCCTTTTCTGCAACCAAGACCTGAACTACTGTACTCACCATAAGCCGTGCAGGAAT
  181   GGAGCCACCTGCACCAACACGGGCCAGGGGAGCTACACATGTTCCTGCCGACCTGGGTAT
  241   ACAGGTGCCAACTGTGAGCTGGAAGTAGATGAGTGTGCTCCTAGCCCCTGCAAGAACGGA
  301   GCGAGCTGCACGGACCTTGAGGACAGCTTCTCTTGCACCTGCCCTCCCGGCTTCTATGGC
  361   AAGGTCTGTGAGCTGAGCGCCATGACCTGTGCAGATGGCCCTTGCTTCAATGGAGGACGA
  421   TGTTCAGATAACCCTGACGGAGGCTACACCTGCCATTGCCCCTTGGGCTTCTCTGGCTTC
  481   AACTGTGAGAAGAAGATGGATCTCTGCGGCTCTTCCCCTTGTTCTAACGGTGCCAAGTGT
  541   GTGGACCTCGGCAACTCTTACCTGTGCCGGTGCCAGGCTGGCTTCTCCGGGAGGTACTGC
  601   GAGGACAATGTGGATGACTGTGCCTCCTCCCCGTGTGCAAATGGGGGCACCTGCCGGGAC
  661   AGTGTGAACGACTTCTCCTGTACCTGCCCACCTGGCTACACGGGCAGAACTGCAGCGCCC
  721   CTGTCAGCAGGTGTGANCATGCACCCTGCCATAATGGGGNCNCCTGCCACCAGANGGNCN
  781   ACCGCTACATGTGTGANTGCCCCCAGGGCTANGGNGGCCCAACTGCCANTTTTGCTCCTG
  841   AACCNCCCNAGGGCCATGGNGGNGAACCCANTGAAAGNCTNTGGANACCCGGGNGGCCCT
  901   NCCCTGGNGNCCGGTTTCCGGGNGGGCTNTCCCNGCNCTCTGGNTN 3′
```

5.2 DELTA-3

5.2.1 SEQUENCING RESULTS FROM T3 PROMOTER

```
3′  1   GGNNCTCNCGCGGTGGCGGCCGCTCTAGAACTAGTGGATCCCCCGGGCTGCAGGAATTCA
   61   TGTCTTACGGTCAAGGGTCTCCCCCATCCCAGGTCTCTGGCATGTCCTAGAGATTCTTAC
  121   CCACCTTCGGCTGCCACTGATTTCCGTTCACTCACAAGGCCCTCTACCTGGTCTCCATAC
  181   TCCTGAGACTATTTCCCCATCCTGTCCCCCAAAGCAATGGTCTCTCTGCAGGTGTCTCCG
  241   CTTTCCCAGACGCTGATCCTGGCTTTTCTTCTTCCTCAGGCACTGCCAGCTGGTGTCTTC
  301   GAGCTACAAATTCATTCTTTCGGGCCAGGCCCAGGCCTCGGGACCCCACGCTCCCCCTGC
  361   AACGCCCGAGGCCCTTGCCGCCTCTTCTTCAGGGTCTGCCTGAAGCCCGGAGTCTCCCAG
  421   GAGGCCACCGAGTCCCTGTGCGCCCTGGGCGCAGCACTGAGCACGAGCGTCCCGGTCTAT
  481   ACGGAGCACCCCGGAGAGTCAGCGGCTGCCCTGCCGCTGCCTGATGGCCTCGTACGTGTG
  541   CCCTTCCGCGATGCTTGGCCGGGCACCTTCTCCCTCGTCATTGAAACCTGGAGAGAGCAG
  601   CTGGGAGAGCATGCTGGAGGGCCCGCCTGGAAACTGCTAGCACGTGTGGTCGGCCGTANA
  661   NGCCTGGCGGCTGGGGGCCCGTGGGCCCGCGATGTGCAGCGCACAGGCACATGGGANTTG
  721   CACTTNTCCTAACGCGCGCGGTGCGANCCNCCCGCCGTCGGGGCCGCCTGCGCGCGCCTG
  781   TGCCGCTAACCAATGCCCCTCNNGGGGNGGCCGGGAATGNAACCTGNANGCAATTCCAAA
  841   AAAATGNAAACCCCGTTTGGGGTCAAAAAGTTGAACCCCAAANNGGTTATGGNAAAAACT
  901   GANA 5′
```

5.2.2 SEQUENCING RESULTS FROM T7 PROMOTER

```
5′  1   CNNNNNCNNNNNNNNNNNNTGGGTCCGGGCCCCCCCTCGAGGTCNACGGTATCGATAAGCT
   61   TGATATCGAATTCATGTCTTACGGTCAAGGTTTTTTTTTGGTTGAGCAAAATAAGAACCT
  121   TTATAGATGTCTCTGGGGAGATGAGAAAAACTAGGTTATAAATAAGCAATATGTACAATA
  181   AAGCCCTTTCAAAGAGTCTCCAGTCGGTAGGGGGAGGTAGAGATTGGACACCACAAAGTA
  241   AATAAAATCATTCAGGCTCCATCTCCAGGCGATGATAGAGAAGGGACAAGATAGAGAAGG
  301   GGCAGGATCAGGCCTCTCGTGCATAAATGGAAGGGGCTGGTATGACATAAATGGATCTAG
  361   AGTCTCCATCTTCAGGATGATTCCAGTCAGCCGACGAACTGGGGCCATCCCCAGCACCGT
  421   CTTGTAACCTCAGGTTGTTGAGTGCATCCGGGAGCGTGTGGACCGAAGGCTCCCGGGTCC
  481   CAGAAAGCAGGCGAGTCCCGGTATCCTGGCCAGGACCTCGGCGGCGAACGTGGATGACCA
  541   AGAGTGCGGCGCCAGCCAAACCGGCGGCCACCAGCAGCCCCAAGGCGGGAGGCAGAAGAA
  601   AGCGCTGTGGATCCGCCTGCCTCANGCCCCGCGGGGCGGCGGGCACCGCGTCCGCGCCGT
  661   CCCGGGCGCACAGCGAACTCGCATCTCACGCCCATGTAGCCGGCGCGCANGCGCAAACAG
  721   GCCAGAGAATGGGCGTAGCACGGCCTCNTGCCCNCAGGGCGGGAAGCNCAGGGTCGCNCG
  781   TTCTCGGCAGTCNCGCCCCCCAAACCCACNCCNAGGAACACGGGCCGAGCCCCCCCCTCC
  841   CNCNNTGCCCCTTTGGCCAGGCCGGCCCGGNCCATCTTCCAGTNTGTTNCCACCNGGCCG
  901   GGAANNCNCCGAAAGGGGACNAACGGG 3′
```

5.3 LUNATIC FRINGE

5.3.1 SEQUENCING RESULTS FROM T3 PROMOTER

```
3′  1   GAGAGAAACCAAARATRYTGGAGCTCCACCGYGGTGGGGCYGYTCTAASAMKRRGTGGAT
   61   CCCCCGGGCTGCCGAATTCATGTCTTCGGTCAAGGATTMCCAGATACTGGAAGGCATAAA
  121   TACAGTACTARGGCACTCATTGTCCAGCTTTCCAAAGACCAAGCCTGTCTGGSTTCCACT
  181   TTTTTCTGATCCACMGAAAAGATAAAATAAGACCCTCTCCAGCCCACCCCAGAAAACARC
  241   CACCCCCCACCTCCTTTCACACCCACCCCTCCCCTTTCAAGAAAGAGCACAGTAAAAAAA
  301   TACTGTCACAATATGTACAGGCACACCCACTATGGGCGACTTTCTCTCTACTTTGGAGAG
  361   GAGATAAAATTCATAGSTCWGAACCCCACTTGGTGTGGGAGACAAAGATAMGGMATCAGA
  421   GGGTGGGGCTGAAGACTTCGCCTCCACCCTGGAGGGCAGGGGGGTGGGGGAGCATTGTTC
  481   ACCAGAATGGCACCAGGCAGCGCCCCGGGCCAGAGCTCACAAGGGGTCCAGGCCTTTACT
  541   ACCCAATYCACMTCCCTAGGACTGGGCACAGCTCAGCTGACAGGAAAGCTCCAGATAGTG
  601   CTAGCACCCACATARARACTGCTAMATCAGCACCACGGACCCTGAGKGGAGCCCAAGGCC
  661   TCMCCCACCCCCACTGCAARATCCAAACACAGATCCMMAAACTGCCTCGGGTGGTGCTCA
  721   RAGGTATAGGGAMARACTGCCMTCCTGAAAACMGACTGCCAGGGTYGAACGGGGGCCGCC
  781   AAAACMCAAWTRACMACCCCATAACARGCCTGAAAAKCCGGACCAGGCGGCTC 5′
```

5.3.2 SEQUENCING RESULTS FROM T7 PROMOTER

```
5′  1   NNNNNNNNNGATGGGTNCGGGCCCCCCTCGAGGTCTAGGTATCGATAAGCTTGATATCGA
   61   ATTCATGTCTTACGGTCAAGGGCTGGCACTGGGATAGATATTACGTGCGGCCGCCGGCCA
  121   CCATGCTCCAGCGGTGCGGCCGGCGCCTGCTGCTGGCGCTGGTGGGCGCGCTGTTGGCTT
  181   GTCTCCTGGTGCTCACGGCCGACCCGCCACCGACTCCGATGCCCGCTGAGCGCGGACGGC
  241   GCGCGCTGCGTAGCCTGGCGGGCTCCTCTGGAGGAGCTCCGGCTTCAGGGTCCAGGGCGG
  301   CTGTGGATCCCGGAGTCCTCACCCGCGAGGTGCATAGCCTCTCCGAGTACTTCAGTCTAC
  361   TCACCCGCGCGCGCAGAGACGCGGATCCACCGCCCGGGGTCGCTTCTCGCCAGGGCGACG
  421   GCCATCCGCGTCCCCCCGCCGAAGTTCTGTCCCCTCGCGACGTCTTCATCGCCGTCAAGA
  481   CCACCANAAAGTTTCACCGCGCGCGGCTCGATCTGCTGTTCGAGACCTGGATCTCGCGCC
  541   AACAAGGAAATGAAAGTTCATCTTCACTGATGGGGAAGAAGAAACTCTGGCCAANCTCAC
  601   ANGGCAATGTGGNGGCTCACCAAATTGNTTCTTCGGNCNAAAACCGCCAANNTCTTGTCC
  661   TGGAAANAATGGGNTNNGGAAANATAAAACNAATTNNTTNGAATNTGGNAAAAAAAATGG
  721   TTNTTNCCNCTGGAANAAAAAAAAAANAATTAAACCTNCGGGGGGTNTGNTTGGGGGTTN
  781   CTGGGCN 3′
```

5.4 OVINE NOTCH-1

5.4.1 PARTIAL SEQUENCE (ACCESSION NUMBER; EF999923)

```
5′  1   CCCTTTCTACCGCTGTCTATGCCCTGCCAAGTTCAACGGGCTGCTGTGCCACATCCTGGA
   61   CTACAGCTTCGGGGGCGGCGTGGGCCTCAACATCCCCCCGCCGCAGGTCGAGGAGACCTG
  121   CGAGCTCCCCGGCTGCCGCGAGGAGGCCGGCAACAAGGTCTGCAGCCTGCAGTGCAACAA
```

```
 181  CCACGCGTGCGGCTGGGACGGCGGCAACTGCTCCCTCAACTTCGACGACCCCTGGCAGAA
 241  CTGCACGCAGGCCCTGCAGTGCTGGAAGTACTTCAGCAACGGTCGCTGCGACAGCCAGTG
 301  CAACTCGGCCGGCTGCCTCTTCGACGGCTTCGACTGCCAGCGCGCAGAAGGCCAGTGCAA
 361  CCCCCTGTACGACCAGTACTGCAAGGACCACTTCAGGGACGGGCACTGCGACCAGGGCTG
 421  CAACAGCGCGGAGTGCGAGTGGGACGGGCTGGACTGCGCGGAGCACGTGCCTGAGCGGCT
 481  GGCGGCCGGCACGCTGGTGCTGGTGGTCCTCATGCCACCCGAGCAGCTACGCAACCGCTC
 541  CCTGCACTTCCTGCGCGAGGTCAGCCGCCTGCTGCACACCAATGTGGTTTTCAAGCGCGA
 601  TGCCAGCGGCCAGCAGATGATCTTCCCTTACTACGGCCGCGAAGAGGAGCTGCACAAGCA
 661  CCCCGTCAGGCGCTCCGTGGGTGGCGGGGCCCCGCTGCTCCCAGGCGGCGCCAGCAGACG
 721  CCAGCGCAGGGAGCTGGACCCCATGGACATCCGCGGGTCCATCGTCTACCTGGAGATCGA
 781  CAACCGGCAGTGCGTCCAGTCGTCCTCGCAGTGCTTCCAGAGCGCCACGGATGTGGCCGC
 841  CTTCCTGGGTGCGCTGGCCTCGCTGGGCAGCCTCAACATCCCCTACAAGATTGAGGCCGT
 901  GCAGAGTGAGACGGTGGAGCCGCCCCCGCCCCCGCCGCTGCACTTCATGTACGTGGCCGT
 961  GGTGGCCTTCGTGCTGCTGTTCTTCGTGGGCTGCGGGGTGCTGCTGTCGCGGAAGCGCCG
1021  GCGGCAGCATGGCCAGCTTTGGTTCCCCGAGGGCTTCAAGGTGTCGGAAGCCAGCAAGAA
1081  GAAGCGGCGCGAGCCCCTCGGCGAGGACTCCGTGGGCCTCAAACCCCTGAAGAACTTTTC
1141  GGACGGCGCCCTCATGGACGACAACCAGAATGAGTGGGGCGACGAGGGCCTGGAGGCCAA
1201  GAAGTTCCGGTTCGAGGAGCCCGTGGTCCTCCCTGACCTGGACGACCAGACAGACCACCG
1261  GCAGTGGACCCAGCAGCACCTGGACGCCGCCGACCTGCGCGTGTCTGCCATGGCCCCCAC
1321  GCCTCCCCAGGGCGAGGCGGATGCCGACTGCATGGACGTGAACGTCCGCGGGCCGGATGG
1381  CTTCACGCCCCTCATGATCGCCTCCTGCAGCGGAGGGGGCCTAGAGACAGGCAACAGTGA
1441  GGAAGAAGAAGAT 3′
```

5.4.2 SEQUENCING RESULTS FROM SP6 PROMOTER

```
3′  1  CTTGCATCCAACGCGTTGGGAAGCTCTCCCATATGGTCGACCTGCAGGCGGCCGCACTAG
  61   TGATTATCTTCTTATTCCTCACTGTTGCCTGTCTCTAGGCCCCCTCCGCTGCAGGAGGCG
 121   ATCATGAGGGGCGTGAAGCCATCCGGCCCGCGGACGTTCACGTCCATGCAGTCGGCATCC
 181   GCCTCGCCCTGGGGAGGCGTGGGGGCCATGGCAGACACGCGCAGGTCGGCGGCGTCCAGG
 241   TGCTGCTGGGTCCACTGCCGGTGGTCTGTCTGGTCGTCCAGGTCAGGGAGGACCACGGGC
 301   TCCTCGAACCGGAACTTCTTGGCCTCCAGGCCCTCGTCGCCCCACTCATTCTGGTTGTCG
 361   TCCATGAGGGCGCCGTCCGAAGAGTTCTTCAGGGGTTTGAGGCCCACGGAGTCCTCGCCG
 421   AGGGGCTCGCGCCGCTTCTTCTTGCTGGCTTCCGACACCTTGAAGCCCTCGGGGAACCAG
 481   AGCTGGCCATGCTGTCGCCGGCGCTTCCGCGGCAGCAGCACCCCGCAGCCCACGAAGAAC
 541   AGCAGCACGAAGGCCACCACGGCCACGTACATGAAGTGCAGCGGTGGGGGCGGGGGCGGC
 601   TCCACCGTCTCACTCTGCACGGCCTCAATCTTGTANGGGATGTTGAGGCTGCCCAGCGGG
 661   GCCAGCGCACCCAGGAANGCGGCCACATCCGTGGCGCTCTGGAAACACTGCGAGGACGAN
 721   TGGACGCACTGCCGGTTGTCGATCTCAGGTANACGATGGACCGCGGATGTCATGGGGTCA
 781   NCTCCCTGCGCTGGCGTCTGCTGGCGCCCCTGGGAACACGGGGCCCNCCACCANGAACNC
 841   TGANGGGTGNTGTGCACTCCNTNCCGNCGTATAAGGAAATATNTGCTGGCCTGGATCCCT
 901   TGAAANAATTGGTNNAAAGNGCTAACTCCCANAATCAGAANGTNCTAATTTCCGGTGAAA
 961   AAAAAAAA 5′
```

5.4.3 SEQUENCING RESULTS FROM T7 PROMOTER

```
5′  1  GAATGGGCCGAAGTCGCATGCTCCCGGCCGCCATGGCCGCGGGATTCCCTTTCTACCGCT
  61   GTCTATGCCCTGCCAAGTTCAACGGGCTGCTGTGCCACATCCTGGACTACAGCTTCGGGG
 121   GCGGCGTGGGCCTCGACATCCCCCCGCCGCAGGTCGAGGAGACCTGCGAGCTCCCCGGCT
 181   GCCGCGAGGAGGCCGGCAACAAGGTCTGCAGCCTGCAGTGCAACAACCACGCGTGCGGCT
 241   GGGACGGCGGCGACTGCTCCCTCAACTTCGACGACCCCTGGCAGAACTGCACGCAGGCCC
 301   TGCAGTGCTGGAAGTACTTCAGCAACGGTCGCTGCGACAGCCAGTGCAACTCGGCCGGCT
 361   GCCTCTTCGACGGCTTCGACTGCCAGCGCGCAGAAGGCCAGTGCAACCCCCTGTACGACC
 421   AGTACTGCAAGGACCACTTCAGGGACGGGCACTGCGACCAGGGCTGCAACAGCGCGGAGT
 481   GCGAGTGGGACGGGCTGGACTGCGCGGAGCACGTGCCTGAACGGCTGGCGGCCGGNACNC
 541   TGGTGCTGGTGGTCCTCATGCCACCCNANANNTANNCAANCGNTCCCTGNATTCNTGNNN
 601   NANNTCANNNNNCTGNTGNAANNAATGTGNNCTTTNANNANNAANNNNNN 3′
```

5.5 MURINE VS OVINE EST SEQUENCE ALIGNMENT

5.5.1 DELTA-1

5.5.1.1 *M.musculus* mRNA for Delta-like 1 protein (X80903.1) vs *Ovis aries* cDNA, mRNA sequence (EE862149.1)

(83% identity, E = 3e-72)

```
2370  GCCGCTGGACTGCCTGCT-GGTTGTTCCCATTGCACTATGGACAGTTGC-TTTGAAGAGT  2427
      |||||||  ||||||  ||  ||  ||||||||||||||||||||  ||  ||  |||  ||  |  |
229   GCCGCTGCTCTGCCT-CTAGGACGTTCCCATTGCACTATGGACGGTCGCTTTTAAAAAAT  287

2428  ATATATTTAAATGGACGAGT-GACTTGATTCA-TA--TAGGAAGCACGCACTGCCCACAC  2483
      ||||||||||||  ||   |  |  |||||||  |||  ||   ||  ||||||||||||  ||   |
288   ATATATTTAAAT-GA--A-TGGACTTGA-TCACTACGTAAGAAGCACGCACTG-CCTGAA  341

2484  GTCTAT-CT-TGGATTAC-TATGAGCCAGTCTTTC-CTTGAACTAGAA--ACACA-ACTG  2536
      ||  |||   |  ||||||  |  ||||||||||||  |||  ||||||  |||||   |||  |  ||||
342   GTGTATATTCTGGATT-CTTATGAGCCAGTC-TTCTCTTGAATTAGAATCACAAACACTG  399

2537  CCTTTATTGTCCTTTTTGATACTGAGATGTGttttttttttttCCTAGACG-GGAAAAAGA  2595
      |||||||||||||||||||||||  |  |||||        ||||  ||||   |  ||   ||  |
400   CCTTTATTGTCCTTTTTGATACTAAAATGTG-------TTTTTCTAG--GTGG---AA-A  446

2596  AAACGTGTGTTAttttttttGGGATTTGTAAAAATATTTTTCATGATATCTGTAAAGCTTG  2655
      |||  |||  ||||   |||||  |||  ||||||||||||||||||||||||||||||||||||||||
447   AAATGTGCGTTA--TTTTTTGGACTTGTAAAAATATTTTTCATGATATCTGTAAAGCTTG  504

2656  AGTATTTTGTGACGTTCAttttttttATAATTTAAATTTT-GGTAAATATGTACAAAGGCA  2714
      ||||||||||||  ||||||||||  ||||||||||||||  ||||||||||||||||||||
505   AGTATTTTGTGATGTTCATTTTTT-ATAATTTAAATTTTTGGTAAATATGTACAAAGGCA  563

2715  CTTCGGGTCTATGTGACTATAttttttttGTATATAAATGTATTTATGGAAT  2765
      |||||||||  ||||||||||||||||||||||||||||||||||||||||
564   CTTCGGGTCAATGTGACTATATTTTTTTGTATATAAATGTATTTATGGAAT  614
```

5.5.1.2 *M.musculus* mRNA for Delta-like 1 protein (X80903.1) vs *Ovis aries* cDNA, mRNA sequence (EE749368.1)

(88% homologous, E = 1e-46)

```
11   ACCATGGGCCGTCGGAGCGCGCTAGCCCTTGCCGTGGTCTCTGCCCTGCTGTGCCAGGTC  70
     ||||||||| | ||| |||| || ||||| |||||  |||| | ||||||||||||||||
699  ACCATGGGCGGGCGGTGCGCCCTGGCCCTCGCCGTACTCTC-GGCCTGCTGTGCCAGGTC  757

71   TGGAGCTCCGGCGTATTTGAGCTGAAGCTGCAGGAGTTCGTCAACAAGAAGGGGCTGCTG  130
     |||||||||||  ||  || ||||||||||||||||||||||||||||||||||||||||
758  TGGAGCTCCGGGGTGTTCGAGCTGAAGCTGCAGGAGTTCGTCAACAAGAAGGGGCTGCTG  817

131  GGGAACCGCAACTGCTGCC-GCGGGGGCTCTGGCCCGCC  168
     ||  |||  ||||||||||| ||||||||  | ||||||||
818  GG-AAC-GCAACTGCTGCCCGCGGGGGCGCGGGCCCGCC  854
```

5.5.1.3 *M.musculus* mRNA for Delta-like 1 protein (X80903.1) vs *Ovis aries* cDNA, mRNA sequence (EE853192.1)

(80% identity, E = 9e-38)

```
2370  GCCGCTGGACTGCCTGCT-GGTTGTTCCCATTGCACTATGGACAGTTGC-TTTGAAGAGT  2427
      |||||||  ||||||  ||  ||  ||||||||||||||||||||  ||  ||  |||  ||  |  |
44    GCCGCTGCTCTGCCT-CTAGGACGTTCCCATTGCACTATGGACGGTCGCTTTTAAAAAAT  102

2428  ATATATTTAAATGGACGAGT-GACTTGATTCA-TA--TAGGAAGCACGCACTGCCCACAC  2483
      ||||||||||||  ||   |  |  |||||||  |||  ||   ||  ||||||||||||  ||   |
103   ATATATTTAAAT-GA--A-TGGACTTGA-TCACTACGTAAGAAGCACGCACTG-CCTGAA  156

2484  GTCTAT-CT-TGGATTAC-TATGAGCCAGTCTTTC-CTTGAACTAGAA--ACACA-ACTG  2536
      ||  |||   |  ||||||  |  ||||||||||||  |||  ||||||  |||||   |||  |  ||||
157   GTGTATATTCTGGATT-CTTATGAGCCAGTC-TTCTCTTGAATTAGAATCACAAACACTG  214

2537  CCTTTATTGTCCTTTTTGATACTGAGATGTGttttttttttttCCTAGACG-GGAAAAAGA  2595
      |||||||||||||||||||||||  |  |||||        ||||  ||||   |  ||   ||  |
215   CCTTTATTGTCCTTTTTGATACTAAAATGTG-------TTTTTCTAG--GTGG---AA-A  261

2596  AAACGTGTGTTAttttttttGGGATTTGTAAAAATATTTTTCATGATATCTGTAAAGCTTG  2655
      |||  |||  ||||   |||||  |||  ||||||||||||||||||||||||||||||||||||
262   AAATGTGCGTTA--TTTTTTGGACTTGTAAAAATATTTTTCATGATATCTGTAAAGCTTG  319

2656  AGTATTTTGT  2665
      ||||||||||
320   AGTATTTTGT  329
```

5.5.2 DELTA-3

5.5.2.1 *Mus musculus* Delta-like 3 (Drosophila)(*Dll3*) mRNA (NM007866.2) vs *Ovine aries* cDNA, mRNA sequence (EE835675.1)

(79% identity, E = 3e-74)

```
1487  AGGCGGATCCACAGCGCTTTCTTCTGCCTCCCGCCTTGGGGCTGCTGGTGGCCGCCGGTT  1546
      ||| ||| |||||||||||| ||| |||| || || ||||| |||||||||||||| || |
24    AGGGGGACCCACAGCGCTTCCTTTTGCCGCCAGCTTTGGGACTGCTGGTGGCCGCGGGCT  83

1547  TGGCTGGCGCCGCACTCTTGGTCATCCACGTTCGCCGCCGAGGTCCTGGCCAGGATACCG  1606
      ||||  |||| || |||||| |  ||||||| || ||||| || ||| ||| |||||| |
84    TGGCCAGCGCTGCGCTCTTGCTGGTCCACGTGCGACGCCGTGGCCCTAGCCGGGATACTG  143

1607  GGACTCGCCTGCTTTCTGGGACCCGGGAGCCTTCGGTCCACACGCTCCCGGATGCACTCA  1666
      || ||||| || |  | ||||||| |||||| ||||||||| |||| || ||||||||||
144   GGCCTCGCTTGTTGGCGGGGACCCCGGAGCCATCGGTCCACGCGCTTCCTGATGCACTCA  203

1667  ACAACCTGAGGTTACAAGACGGTGCTGGGGATGGCCCCAGTTCGTCGGCTGACTGGAATC  1726
      ||||| |||||   || || ||| | ||||| ||||| ||  | ||  | ||||||| ||
204   ACAACATGAGGACGCAGGAAGGTCCCGGGGACGGCCCGAGCCCATCCTCAGACTGGAGTC  263

1727  ATCCTGAAGATGGAGACTCTAGATCCATTTATGTCATACCAGCCCCTTCCATTTATGCAC  1786
      | |||||||||||||| || | || ||||| |||||| | || |||||||| ||||| |
264   ACCCTGAAGATGGAGACGCTCGTTCGATTTACGTCATATCTGCTCCTTCCATCTATGCTC  323

1787  GAGAGGCCTGATCCTGCCCCTTCTCTAT  1814
      | ||||| ||| |||| |||||||| ||
324   GGGAGGCTTGA-CCTGGCCCTTCTCCAT  350
```

5.5.3 LUNATIC FRINGE

5.5.3.1 *Mus musculus* LFNG O-fucosylpeptide 3-beta-N acetylglucosaminyltransferase (Lfng), mRNA (NM_008494.3) vs *Ovis aries* cDNA, mRNA sequence (EE823094.1)

(85% identity, E = 2e-179)

```
712   CTGGCCAGCTATCCCCACACCCAAGACGTGTACATCGGCAAGCCCAGCCTGGACAGGCCC  771
      |||| ||| || || ||||| || ||||| ||| | |||||||||||||||||||||||
17    CTGGGCAGTTACCCGCACACACAGGACGTCTACCTGGGCAAGCCCAGCCTGGACAGGCCC  76

772   ATCCAGGCCACAGAACGGATCAGCGAGCACAAAGTGAGACCTGTCCACTTTTGGTTTGCC  831
      |||||||||||||| ||| ||||||| ||| ||| | |||||||||| |||||||||
77    ATCCAGGCCACAGAGCGGGTCAGCGAAAACACGGTGCGTCCTGTCCACTTCTGGTTTGCC  136

832   ACCGGAGGAGCTGGCTTCTGCATCAGCCGAGGGCTGGCCCTAAAGATGGGCCCATGGGCC  891
      ||||| || |||||||||||||||||||||||||| ||||| |||||| |||| ||||||
137   ACCGGCGGGGCTGGCTTCTGCATCAGCCGAGGGCTAGCCCTGAAGATGAGCCCCTGGGCC  196

892   AGTGGAGGACACTTCATGAGCACGGCAGAGCGCATCCGGCTCCCCGATGACTGCACCATT  951
      || ||||| |||||||||||||||| ||||| |||||||| || || ||||||||||
197   AGCGGAGGCCACTTCATGAGCACGGCCGAGCGGATCCGGCTGCCTGACGACTGCACCATC  256
```

```
952   GGCTACATTGTAGAGGCTCTGCTGGGTGTACCCCTCATCCGGAGCGGCCTCTTCCACTCC  1011
      |||||||| || ||||| |||||||| || |||||| | ||  | || ||||||||||||
257   GGCTACATCGTGGAGGCGCTGCTGGGCGTGCCCCTCGTGCGCTGTGGGCTCTTCCACTCC  316

1012  CACCTAGAGAACCTGCAGCAGGTGCCCACCACCGAGCTTCATGAGCAGGTGACCCTGAGC  1071
      ||||| ||||| |||||||| |||||  || ||||||| || ||||||||||||||||||
317   CACCTGGAGAATCTGCAGCAAGTGCCTGCCTCCGAGCTCCACGAGCAGGTGACCCTGAGC  376

1072  TATGGCATGTTTGAGAACAAGCGGAACGCAGTGCACATCAAGGGACCATTCTCTGTGGAA  1131
      || |||||||||| |||||||||||||| || ||||| ||||| || ||||| |||||
377   TACGGCATGTTTGAAAACAAGCGGAACGCCGTCCACATTAAGGGGCCCTTCTCGGTGGAG  436

1132  GCTGACCCATCCAGGTTCCGCTCTGTCCATTGCCACCTGTACCCAGACACACCCTGGTGT  1191
      |||||||| || |||||||||||||||| ||||| |||||||| ||||||||||||||
437   GCTGACCCGTCGAGGTTCCGCTCTGTCCACTGCCATCTGTACCCGGACACACCCTGGTGC  496

1192  CCTCGCTCCGCCATCTTCTAGCAGTCGTGGTTGAAACTCTGTCCCTGGGCGCCCCTGGTA  1251
      || ||| | ||||||||||||  | ||||| |||||| | ||||| ||||||||||||||
497   CCCCGCACTGCCATCTTCTAGTGGCCGTGGCTGAAACCCCGTCCCCGGGCGCCCCTGGTA  556
```

5.5.3.2 *Mus musculus* LFNG O-fucosylpeptide 3-beta-N-acetylglucosaminyltransferase (Lfng), mRNA (NM_008494.3) vs *Ovis aries* cDNA, mRNA sequence (EE828983.1)

(85% identity, E = 5e-129)

```
874   AAGATGGGCCCATGGGCCAGTGGAGGACACTTCATGAGCACGGCAGAGCGCATCCGGCTC  933
      |||||| |||| |||||||| ||||| |||||||||||||||| ||||| ||||||||
2     AAGATGAGCCCCTGGGCCAGCGGAGGCCACTTCATGAGCACGGCCGAGCGGATCCGGCTG  61

934   CCCGATGACTGCACCATTGGCTACATTGTAGAGGCTCTGCTGGGTGTACCCCTCATCCGG  993
      || || |||||||||| |||||||| || ||||| |||||||| || |||||| | ||
62    CCTGACGACTGCACCATCGGCTACATCGTGGAGGCGCTGCTGGGCGTGCCCCTCGTGCGC  121

994   AGCGGCCTCTTCCACTCCCACCTAGAGAACCTGCAGCAGGTGCCCACCACCGAGCTTCAT  1053
      | || |||||||||||||||| ||||| |||||||| |||||  || ||||||| ||
122   TGTGGGCTCTTCCACTCCCACCTGGAGAATCTGCAGCAAGTGCCTGCCTCCGAGCTCCAC  181

1054  GAGCAGGTGACCCTGAGCTATGGCATGTTTGAGAACAAGCGGAACGCAGTGCACATCAAG  1113
      |||||||||||||||||| |||||||||| |||||||||||||| || ||||| |||
182   GAGCAGGTGACCCTGAGCTACGGCATGTTTGAAAACAAGCGGAACGCCGTCCACATTAAG  241

1114  GGACCATTCTCTGTGGAAGCTGACCCATCCAGGTTCCGCTCTGTCCATTGCCACCTGTAC  1173
      || || ||||| ||||| |||||||| || |||||||||||||||| ||||| ||||||
242   GGGCCCTTCTCGGTGGAGGCTGACCCGTCGAGGTTCCGCTCTGTCCACTGCCATCTGTAC  301

1174  CCAGACACACCCTGGTGTCCTCGCTCCGCCATCTTCTAGCAGTCGTGGTTGAAACTCTGT  1233
      || |||||||||||||| || ||| | |||||||||||  | ||||| |||||| | ||
302   CCGGACACACCCTGGTGCCCCCGCACTGCCATCTTCTAGTGGCCGTGGCTGAAACCCCGT  361

1234  CCCTGGGCGCCCCTGGTATCCAAAGGGCCCAGGGACC  1270
      ||| |||||||||||||||||||||||||  |||||
362   CCCCGGGCGCCCCTGGTATCCAAAGGGCCCGAGGACC  398
```

APPENDIX 6: DELTA-1 ANALYSES

Table A6.1: The interaction of age × breed × Delta-1 had a highly significant effect (p=0.001) on the number of mesenchymal cells counted. There was no significant difference in the numbers of unlabelled or Delta-1 labelled cells counted when the 2 breeds and ages were compared. For the d 56 Merino samples and the d 70 Tukidale samples, there was no significant difference between the numbers of labelled and unlabelled cells. For the d 70 Merino and d 56 Tukidale samples, there were significantly more unlabelled than labelled mesenchymal cells. Means that were not significantly different share the same letter superscript. Standard error (SE).

Foetal Age	Breed	Delta Label	Mean	SE
d 56	Merino	Yes	3.579^{A}	0.055
		No	3.833^{A}	0.048
d 56	Tukidale	Yes	3.650^{A}	0.063
		No	4.056^{B}	0.052
d 70	Merino	Yes	4.286^{A}	0.039
		No	4.628^{B}	0.033
d 70	Tukidale	Yes	4.396^{A}	0.044
		No	4.548^{A}	0.040

Table A6.2: The main effect of labelling with Delta-1 had a highly significant effect (p<0.001) on the number of cells counted within the dermal condensate. Significantly more cells within the condensate were labelled with Delta-1 than cells that remained unlabelled. Breed did not have a significant effect on the number of cells within the structure (p=0.440) and was not investigated further. Means that were significantly different have different letter superscripts. Standard error (SE).

Delta label	Mean	SE
Yes	2.640^{A}	0.044
No	2.079^{B}	0.057

APPENDIX 7: NOTCH-1 ANALYSES

Table A7.1: The interaction breed × age × Notch label had a highly significant effect ($p=0.001$) on the number of cells counted within the mesenchyme. Significantly more unlabelled mesenchymal cells were counted than Notch-1 labelled cells for both breeds and ages investigated. Means that were significantly different had different letter superscripts. In addition, the d 56 Merino samples contained significantly more Notch-1 labelled than unlabelled mesenchymal cells compared to the Tukidale samples. However, this was reversed in the d 70 samples, with the Tukidale samples containing more labelled cells. The numbers of labelled and unlabelled cells was significantly higher in the d 70 samples than the d 56 samples. Standard error (SE).

Foetal age	Breed	Notch label	Mean	SE
d 56	Merino	Yes	3.523^{A}	0.058
		No	4.196^{B}	0.058
d 56	Tukidale	Yes	3.257^{A}	0.070
		No	4.229^{BC}	0.070
d 70	Merino	Yes	4.086^{A}	0.058
		No	4.871^{B}	0.058
d 70	Tukidale	Yes	4.258^{A}	0.070
		No	4.979^{B}	0.070

Table A7.2: The main effect of Notch labeling had a significant effect ($p<0.001$) on the number of cells counted in the dermal condensate. Significantly more unlabelled than Notch-1 labelled cells were counted within the dermal condensate. Means that were significantly different had different letter superscripts. Standard error (SE).

Notch label	Mean	SE
Yes	2.757^{A}	0.076
No	3.499^{B}	0.076

APPENDIX 8: SHEEP DERMAL PAPILLAE TRIALS

Table A8.1: The numbers of aggregations and condensed groups of cells within sheep dermal papilla cell cultures were counted at the end of the 31 d trials. The data were analysed using a linear mixed model analysis, on the log scale. The interaction of treatment × structure was not significant (p=0.136). However, this interaction was of interest and thereby was further investigated. The numbers of aggregations counted were similar for the untreated and DMSO control cultures. The DAPT cultures did not form any aggregations, and this treatment had a significantly lower number of aggregations compared to the other experimental groups. Similarly, the number of condensed areas counted in the untreated and DMSO cultures were similar, but the DAPT cultures contained significantly fewer structures compared to the untreated and DMSO control cultures. In addition, within each treatment group the numbers condensed areas were significantly higher than the number of aggregations. Means that were not significantly different share the same letter superscript. Standard error (SE).

Structure	Treatment	Mean	SE
Aggregations	Untreated	2.703^{A}	0.216
	DMSO	2.783^{A}	0.212
	DAPT	0.000^{B}	0.208
Condensed areas	Untreated	3.295^{A}	0.216
	DMSO	3.256^{A}	0.212
	DAPT	0.179^{B}	0.208

APPENDIX 9: DAPT SKIN CULTURE TRIALS

Table A9.1: The number of follicle buds within d 70 Tukidale skin were counted prior to (d 0) and after culturing (d 4) with different treatments. The count data was analysed on the log scale using a linear mixed model. The day of trial × treatment interaction was significant (p=0.017). On d 0, the number of follicles counted was similar for all 3 treatment groups. On d 4, the untreated and DMSO control skins contained similar numbers of follicles. There were significantly fewer follicle buds counted in the DAPT-treated skins compared to the untreated and DMSO-control skins. The mean number of follicle buds in each treatment group significantly increased from d 0 to d 4. Means that were not significantly different share the same letter superscript. Standard error (SE).

Day of trial	Treatment	Mean	SE
d 0	Untreated	3.421^{A}	0.141
d 0	DMSO	3.332^{A}	0.141
d 0	DAPT	3.388^{A}	0.141
d 4	Untreated	4.633^{A}	0.141
d 4	DMSO	4.557^{AB}	0.141
d 4	DAPT	4.388^{B}	0.141

Table A9.2: The number of follicle buds within d 70 Merino skins were counted prior to (d 0) and after culturing (d 4) with different treatments. The count data was analysed using a linear mixed model. The treatment × day of trial × collection site interaction was significant (p=0.003) and investigated further. On d 0 no significant differences in the numbers of follicle buds were detected between the untreated, DMSO or DAPT skins, or the different skin collection sites. The number of follicle buds had significantly increased from d 0 to 4 for all sites and treatment groups. On d 4, significant differences were detected in follicle numbers between some groups. There was no significant difference in follicle number between the anterior untreated and DMSO skins, but the DAPT-treated skins contained significantly more follicles than the 2 control groups. The midside skins were significantly different for each treatment, with the untreated skins containing significantly more follicles than the DMSO (and DAPT) skins, and the DMSO skins containing significantly more follicles than the DAPT skins. In the posterior skin samples, the number of follicles in the untreated and DMSO skins were not significantly different, the number of follicles in the DMSO and DAPT skins were not significantly different, significantly more follicles formed in the untreated skins compared to the DAPT skins. When comparing the effect of site it was found that no significant differences existed between the d 4 DMSO control skins. For the untreated skins, the number of follicles counted in the anterior samples was significantly less than that in the midside (and posterior) samples, and that significantly fewer follicles were counted in the posterior samples compared to the midside samples. For the DAPT-treated skins, no significant difference was detected between the anterior and midside samples, or the midside and posterior samples. However, significantly more follicles had formed in the anterior compared to the posterior samples. Means that were not significantly different share the same letter superscript; treatment (red) and site (blue). Standard error (SE).

Day of trial	Treatment	Collection site	Mean	SE
d 0	Untreated	Anterior	46.93^{A}	4.36
		Midside	48.33^{A}	4.36
		Posterior	49.95^{A}	4.36
d 0	DMSO	Anterior	47.80^{A}	4.36
		Midside	47.73^{A}	4.36
		Posterior	49.32^{A}	4.36
d 0	DAPT	Anterior	47.58^{A}	4.36
		Midside	50.52^{A}	4.36
		Posterior	47.00^{A}	4.36
d 4	Untreated	Anterior	63.55^{AH}	4.43
		Midside	84.37^{CI}	4.39
		Posterior	72.95^{FJ}	4.36
d 4	DMSO	Anterior	69.39^{A}	4.43
		Midside	75.58^{D}	4.36
		Posterior	68.97^{FG}	4.36
d 4	DAPT	Anterior	79.97^{BK}	4.36
		Midside	64.92^{EKL}	4.39
		Posterior	61.34^{GL}	4.43

Table A9.3: The number of follicle buds within Merino skin collected on d 54, 63 and 84 were counted prior to (d 0) and after culturing (d 4) with different treatments. The interaction of day of trial × foetal age × treatment was not statistically significant (p=0.183), but was of biological interest and was thereby investigated further. No significant difference was detected in the number of follicle buds in skins of the same foetal age on d 0 of the trial. Significantly different numbers of follicles were counted in skins from the different foetal ages (d 84>63>54). The number of follicles counted on d 0 and d 4 of the trial were not significantly different for the d 54 and 63 skins. The number of follicles in the d 84 skins significantly decreased from d 0 to 4. On d 4 of the trial, no significant differences were detected in follicle number between the different experimental groups. Standard error (SE).

Day of trial	Foetal age	Treatment	Mean	SE
d 0	d 54	Untreated	0.27	4.70
		DMSO	0.30	4.70
		DAPT	0.23	4.70
d 0	d 63	Untreated	20.77	4.55
		DMSO	19.53	4.55
		DAPT	22.33	4.55
d 0	d 84	Untreated	137.87	6.44
		DMSO	137.53	6.44
		DAPT	134.77	6.44
d 4	d 54	Untreated	1.83	4.76
		DMSO	1.71	4.78
		DAPT	2.63	4.79
d 4	d 63	Untreated	30.37	4.58
		DMSO	28.67	4.56
		DAPT	26.48	4.55
d 4	d 84	Untreated	82.77	6.44
		DMSO	75.13	6.44
		DAPT	73.74	6.44